FACULTY OF MEDICINE AND HEALTH SCIENCES

Novel molecular insights and targeted therapies in T-cell acute lymphoblastic leukemia

Sofie Peirs

Promotors: Prof. Dr. Bruce Poppe, Prof. Dr. Pieter Van Vlierberghe

Submitted to the Faculty of Medicine and Health Sciences of Ghent University, in fulfilment of the requirements for the degree of Doctor in Health Sciences

Academic year: 2016-2017

GHENT UNIVERSITY

.

Thesis submitted to fulfill the requirements for the degree of Doctor in Health Sciences

Promotors: prof. dr. Bruce Poppe
Ghent University, Belgium

prof. dr. Pieter Van Vlierberghe
Ghent University, Belgium

Members of the examination committee:

prof. dr. Triona Ni Chonghaile
Royal College of Surgeons in Ireland, Ireland

dr. Charles de Bock
KULeuven, Belgium

prof. dr. Nadine Van Roy
Ghent University, Belgium

prof. dr. Katleen De Preter
Ghent University, Belgium

prof. dr. Jan Philippé
Ghent University, Belgium

dr. Bram De Wilde
Ghent University, Belgium

The research described in this thesis was conducted at the Center for Medical Genetics, Ghent University, Ghent, Belgium.

This work was supported by the Fund for Scientific Research (FWO) Flanders (PhD grant to Sofie Peirs), Stand Up To Cancer (KOTK; PhD grant to Sofie Peirs) and project funding obtained from the Foundation Against Cancer (STK), the Children Cancer Fund Ghent (Kinderkankerfonds VZW), the Swiss Bridge Foundation and Worldwide Cancer Research.

Table of Contents

List of abbreviations

ABD	Absence of biallelic TCRγ locus deletion
ALL	Acute lymphoblastic leukemia
AML	Acute myeloid leukemia
AOD	Amine oxidase domain
APAF1	Apoptotic protease-activating factor 1
AR	Androgen receptor
ASO	Antisense oligonucleotide
ATRA	All-trans-retinoic acid
AUC	Area under the curve
AYA	Adolescents and young adults
BAALC	Brain and acute leukemia, cytoplasmic
BAD	BCL-2 associated agonist of cell death
BAK	BCL-2 homologous antagonist/killer
BAX	BCL-2 associated X
BCL11B	B-cell CLL/lymphoma 11B
BCL2	B-cell lymphoma 2
BCL2A1	BCL2 related protein A1
BCL2L1	BCL2-like 1
BCP	B cell precursor
BET	Bromodomain and extra-terminal family of proteins
BH	Blocks of sequence homology
BM	Bone marrow
BRD	Bromodomain
BTD	Breakthrough therapy designation
BTK	Bruton tyrosine kinase
CCND3	cyclin D3
CD	Cluster of differentiation
CDK	cyclin dependent kinase
CDKN2A	Cyclin-dependent kinase inhibitor 2A
ChIP	Chromatin immunoprecipitation
CI	Combination index
cIAP	Cellular inhibitor of apoptosis
CID	CtBP interacting domain
CLL	Chronic lymphocytic leukemia
CMJ	Corticomedullary junction
CML	Chronic myeloid leukemia
CMP	Common myeloid progenitor
CNOT3	CCR4-NOT transcription complex subunit 3
CNRQ	Calibrated normalized relative quantities
CREB	cAMP response element-binding protein
CREBBP	CREB binding protein
CSC	Cancer stem cell
CtBP	C-terminal binding protein
cTEC	Cortical thymic epithelial cell
Cyt c	Cytochrome c

DC	Dendritic cell
DLBCL	Diffuse large B-cell lymphoma
DMSO	Dimethylsulfoxide
DN	Double negative ($CD4^-$ $CD8^-$)
DNAi	DNA interference
DNMT1	DNA methyltransferase 1
DOT1L	DOT1-like histone lysine methyltransferase
DP	Double positive ($CD4^+$ $CD8^+$)
DR	Death receptor
ED	Effective dose
EED	Embryonic ectoderm development
eGFP	Enhanced green fluorescent protein
EGIL	European Group for the Immunological Characterization of Leukemias
eIF	Eukaryotic initiating factor
ELL	Elongation factor for RNA polymerase II
E_{max}	Maximal efficacy
EMT	Epithelial-mesenchymal transition
EMT-TF	EMT transcription factors
EP300	E1A binding protein p300
ER	Estrogen receptor
ERK	Extracellular signal-regulated kinase
ESC	Embryonic stem cell
ETP	Early thymic progenitor
ETP-ALL	Early T-cell precursor ALL
ETV6	ETS variant 6
EZH2	Enhancer of zeste 2 PRC2 subunit
FACS	Fluorescence-activated cell sorter
FAD	Flavin adenine dinucleotide
FADD	FAS-associated protein with death domain
FBS	Fetal bovine serum
FDA	U.S. Food and Drug Administration
FL	Follicular lymphoma
FLT	Fms related tyrosine kinase 3
FOXO	Forkhead box O
GATA3	GATA binding protein 3
GEO	Gene expression omnibus
GFI1	Growth factor independent 1
GFP	Green fluorescent protein
GMP	Granulocyte-monocyte progenitor
GSEA	Gene set enrichment analysis
GSI	γ-secretase inhibitor
GSK3B	Glycogen synthase kinase-3 beta
HAT	Histone acetyltransferase
hCD45	Human CD45
HD	Homeodomain
HDAC	Histone deacetylase
HES1	Hes family bHLH transcription factor 1
HOXA	Homeobox A cluster

HRK	Harakiri
HSC	Hematopoietic stem cell
HSCT	Hematopoietic stem cell transplantation
HSP90	Heat shock protein 90
IAP	Inhibitor of apoptosis
iBH3	Intracellular BH3 profiling
IC_{50}	Half maximal inhibitory concentration
ICN1	Intracellular NOTCH1
IDH	Isocitrate dehydrogenase
IGFBP7	Insulin like growth factor binding protein 7
IL7	Interleukin-7
IL7R	Interleukin-7 receptor
ISP	Immature single positive
ITGAM	Integrin subunit alpha M
JAK	Janus kinase
JARID1A	Jumonji/ARID domain-containing protein 1A
JMJD3	Jumonji domain containing 3
JNK1/2	c-Jun N-terminal kinase 1 or 2
KDM1A (LSD1)	Lysine demethylase 1A (Lysine-specific demethylase 1)
KDM5A	Lysine-specific demethylase 5A
LC-MS/MS	Liquid chromatography tandem mass spectrometry
LCS	Leukemic stem cell
LEF1	Lymphoid enhancer binding factor 1
LINCS	Library of integrated cellular signatures
LMO	LIM domain only
MACS	Magnetic activated cell sorting
MAO	Monoamine oxidase
MAPK	Mitogen-activated protein kinase 1
MCL-1	BCL-2 family apoptosis regulator
MDS	Myelodysplastic syndrome
MED1	Mediator complex subunit 1
MEF2C	Myocyte enhancer factor 2
MEK	Mitogen-extracellular signal-regulated kinase
MEP	Megakaryocyte-erythroid progenitor
MLL	Mixed lineage leukemia
MLLr	MLL-rearranged
MLP	Multilymphoid progenitor
MM	multiple myeloma
MN1	Meningioma 1
MOM	Mitochondrial outer membrane
MOMP	Mitochondrial outer membrane permeabilization
MPP	Multipotent progenitor
MRD	Minimal residual disease
MSC	Mesenchymal stromal cells
mTEC	Medullary thymic epithelial cell
mTOR	Mechanistic target of rapamycin
MYBBP1A	MYB binding protein 1A
MYPT1	Myosin phosphatase target subunit 1

NF1	Neurofibromin 1
NHL	Non-Hodgkin lymphoma
NKX2-1	NK2 homeobox 1
NKX2-2	NK2 homeobox 2
NSCLC	Non-small cell lung cancer
NSD	Nuclear receptor binding SET domain protein
NSG	Nonobese diabetic/severe combined immunodeficient gamma
NUMA1	Nuclear mitotic apparatus protein 1
NUP214	Nucleoporin 214
NuRD	Nucleosome remodeling/histone deacetylating
PCR	Polymerase chain reaction
PDX	Patient-derived xenograft
PI	Propidium iodide
PHF6	Plant homeodomain finger 6
PI3K	Phosphoinositide-3-kinase
PIP2	Phosphatidylinositol 4,5-bisphosphate
PIP3	Phosphatidylinositol 3,4,5-trisphosphate
PRC2	Polycomb repressive complex 2
P-TEFb	Positive transcription elongation factor b
PTEN	Phosphatase and tensin homolog
PTPN11	Protein tyrosine phosphatase non-receptor type 11
PUMA	p53 upregulated modulator of apoptosis
qPCR	Quantitative real-time PCR
qRT-PCR	Quantitative real-time reverse transcription PCR
RBP2	Retinoblastoma-binding protein 2
RIPA	Radioimmunoprecipitation assay
RUNX1	Runt related transcription factor 1
SBD	SMAD binding domain
SCLC	Small cell lung cancer
SCZ	Subcapsular zone
SERCA	Sarco/endoplasmic reticulum calcium ATPase
SETD2	SET domain containing 2
SLL	Small lymphocytic lymphoma
SMAC	Second mitochondria-derived activator of caspase
SNAIL2	Snail family transcriptional repressor 2
SP	Single positive ($CD4^+$ or $CD8^+$)
STAT	Signal transducer and activator of transcription
T-ALL	T-cell acute lymphoblastic leukemia
tBID	Truncated BID
TCR	T cell receptor
TET	Ten-Eleven Translocation protein family
T-LBL	T-cell lymphoblastic leukemia/lymphoma
TLS	Tumor lysis syndrome
TLX1	T-cell leukemia homeobox 1
TLX3	T-cell leukemia homeobox 3
TNF	Tumor necrosis factor
TNFR1	Type 1 tumor necrosis factor receptor
TRADD	TNFR1-accociated death domain protein

TRAILR	TNF-related apoptosis-inducing ligand receptor
TSP	Thymus seeding progenitor
TWIST1	Twist family bHLH transcription factor 1
TYK2	Tyrosine kinase 2
UTR	Untranslated region
UTX	Ubiquitously transcribed tetratricopeptide repeat, X chromosome
VIM	Vimentin
VSN	Variance stabilization and calibration
WT1	Wilms tumor 1
XIAP	X-linked inhibitor of apoptosis protein
ZEB2	Zinc finger E-box binding homeobox 2
ZF	Zinc finger

CHAPTER 1
Introduction

Outline of the introduction

The research performed as part of this doctoral thesis aimed to gain novel insights into the molecular mechanisms driving T-cell acute lymphoblastic leukemia (T-ALL) and to identify new therapeutic strategies for patients with T-ALL. In this first introductory chapter, the topics covered in the thesis are introduced. The state-of-the-art knowledge and broader context provided in Chapter 1 allow a critical reading of the results and discussion.

In part I, the disease T-ALL and its current treatment are described. The short-comings and side effects of the current treatment strategies indicate that there is still room for improvement. Within T-ALL, several subgroups can be distinguished. The main focus in this doctoral thesis was on the early immature subgroup, a subgroup associated with a poor prognosis. Searching new treatment strategies for these patients by investigating the molecular mechanisms that play a role in this subgroup was the goal of this work.

One way to find more effective and targeted therapies is increasing our knowledge on the genetic and epigenetic alterations present in T-ALL. In that way, druggable targets can be identified. Part II of the introduction discusses therefore the genetic and epigenetic factors that play a role in the pathogenesis of T-ALL and the opportunities for targeted therapies. A detailed description of ZEB2 (zinc finger E-box binding homeobox 2), KDM1A (lysine demethylase 1A) and BET (bromodomain and extraterminal) proteins is given since these were central to the research performed in this thesis. The transcription factor ZEB2 is an oncogenic driver of early immature T-ALL and the determination of its interaction partners was part of our objectives. One of the newly identified interaction partners, KDM1A, turned out to be druggable. Consequently, KDM1A inhibition was one of the treatment strategies evaluated in this thesis. BET bromodomain inhibitors were also studied in this work and are thus also discussed in detail in this part of the introduction.

Part III deals with the role of apoptosis, a form of programmed cell death, in cancer. The pathways of apoptosis are described and ways to exploit apoptosis in cancer therapy are given. The emphasis is on the intrinsic pathway of apoptosis, a pathway that is governed by the B-cell lymphoma 2 (BCL-2) family of proteins, since inhibition of the anti-apoptotic factor BCL-2 was the subject of two publications that are part of this PhD thesis.

PART I Description and contemporary treatment of T-cell acute lymphoblastic leukemia

1. What is T-cell acute lymphoblastic leukemia (T-ALL)?

Cancer is a genetic disease because the transformation of a healthy cell to a cancer cell is caused by changes in genetic material. This transformation is a multistep process during which the cells acquire capabilities that enable them to become malignant. The hallmark capabilities that allow cancer cells to survive, proliferate and disseminate are sustaining proliferative signaling, evading growth suppressors, resisting cell death, enabling replicative immortality, inducing angiogenesis and activating invasion and metastasis[1]. Leukemias are cancers of the white blood cells and depending on the type of cell that becomes malignant, several types of leukemias can be distinguished.

Blood cells are lifelong produced from hematopoietic stem cells (HSCs) residing in the bone marrow. These HSCs have the capacity of self-renewal and to differentiate in any type of blood cell. During this differentiation process, progenitor cell intermediates are formed (Figure 1)[2].

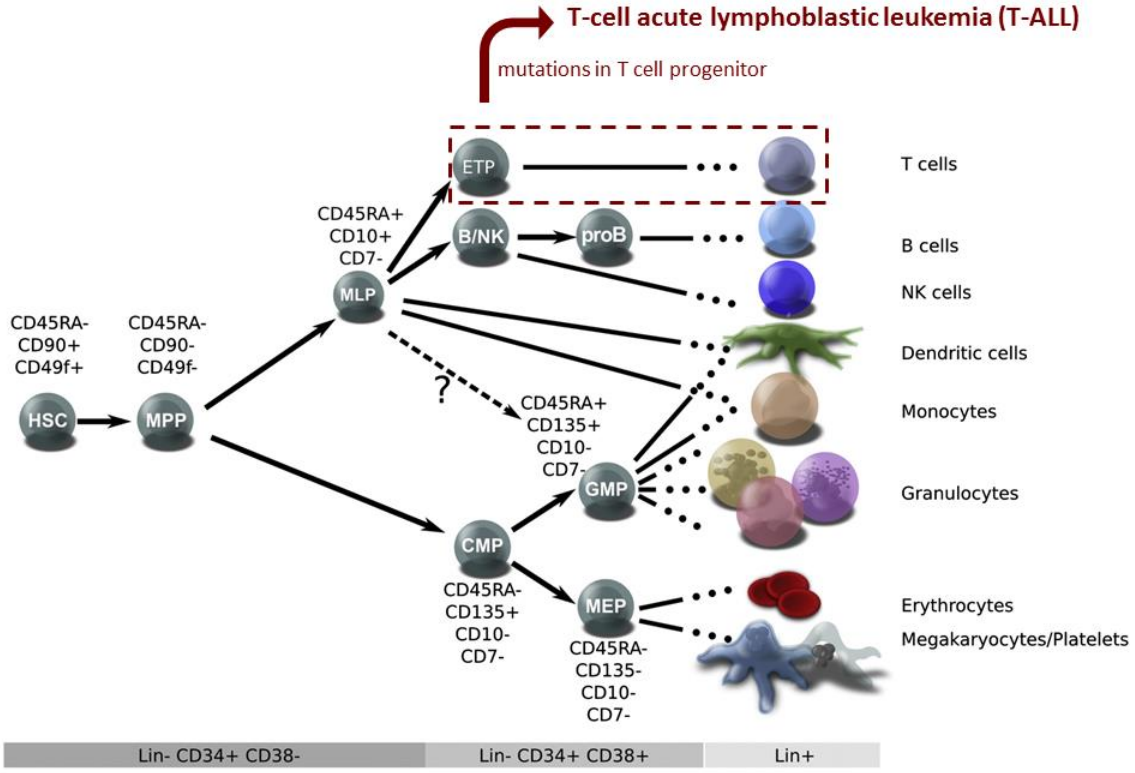

Figure 1. Schematic representation of human hematopoiesis. *HSCs in the bone marrow (left) can differentiate via several progenitor cell intermediates to terminally differentiated blood cells (right). Via the cluster of differentiation (CD) cell surface markers, a distinction between the different progenitors can be made. Multilymphoid progenitors (MLPs) also possess myeloid, but not erythroid and megakaryocytic potential. Accumulation of mutations in a T-cell progenitor can cause T-cell acute lymphoblastic leukemia (T-ALL). HSC: hematopoietic stem cell; MPP: multipotent progenitor; MLP: multilymphoid progenitor; ETP: early thymic progenitor, CMP: common myeloid progenitor; GMP: granulocyte-monocyte progenitor; MEP: megakaryocyte-erythroid progenitor; Lin: cocktail containing cell surface markers for all terminally differentiated populations. Adapted from Doulatov et al.[2].*

All the mature blood cells, with the exception of T cells, are formed in the bone marrow. For T cell development, bone marrow-derived thymus seeding progenitors (TSPs) home to the thymus. Within the thymus, the cells migrate via a defined pattern through several signaling microenvironments and differentiate to mature T cells (Figure 2)[3]. When during this differentiation process mutations occur in a lymphoid progenitor cell (lymphoblast), this cell can become malignant. The resulting cancer is called acute lymphoblastic leukemia (ALL) if more than 25% of the nucleated cells in the bone marrow are lymphoblasts[4, 5]. ALL arising from T cell progenitors is called T-ALL while transformation of B cell precursors (BCP) leads to BCP-ALL. Most symptoms in patients with these diseases are a result from the shortages of normal blood cells. Thrombocytopenia leads to bruising or bleeding, anemia causes fatigue and pallor while neutropenia can lead to infections. Leukemic cells may also infiltrate the liver, spleen, lymph nodes, mediastinum and central nervous system[6].

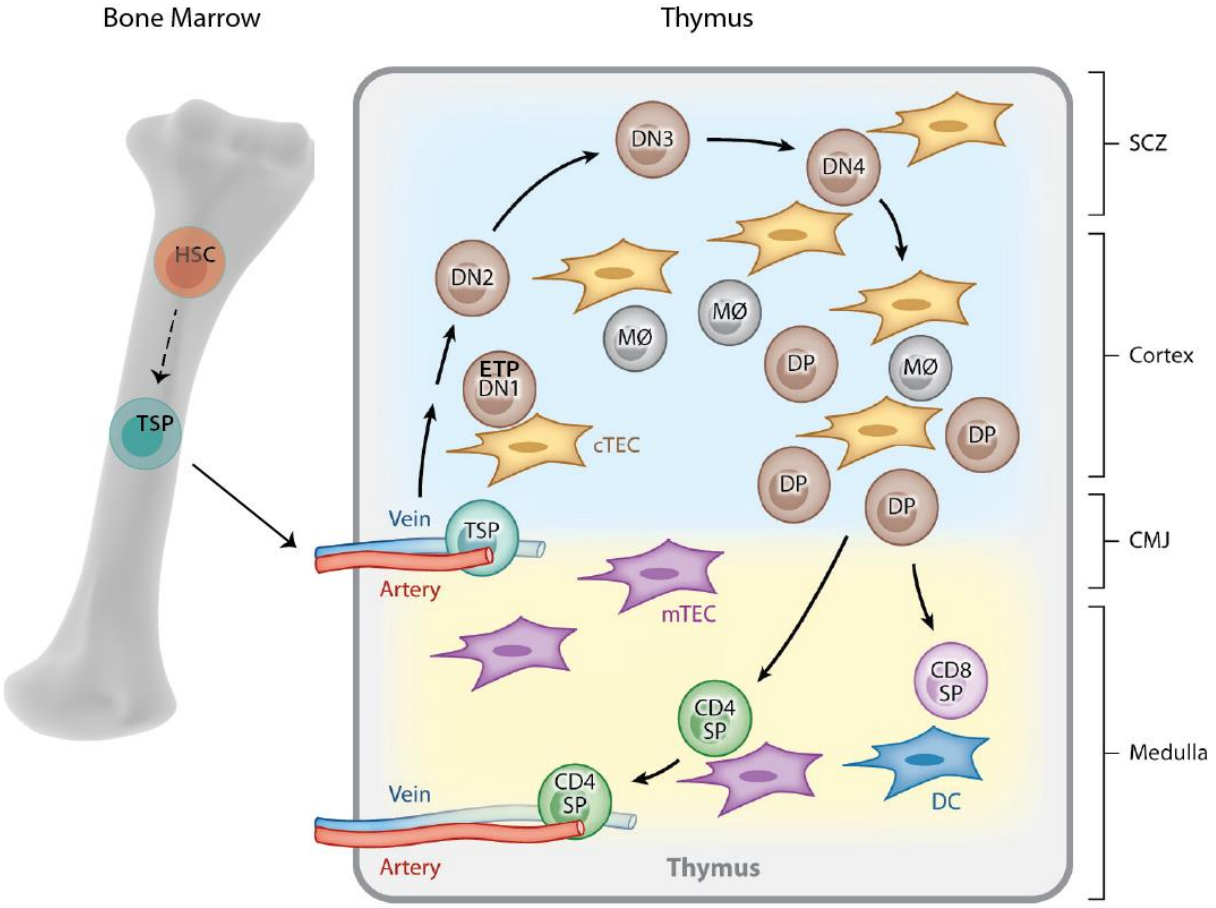

Figure 2. T cell development in the thymus. *The thymus provides the necessary microenvironment for the development of T cells. Four compartments can be distinguished in a thymus: the subcapsular zone (SCZ), the cortex (in blue), the corticomedullary junction (CMJ) and the medulla (in yellow). In the SCZ mainly cortical thymic epithelial cells (cTECs) are present. In the cortex a mix of cTECs, fibroblasts and macrophages (MΦ) can be found while the medulla is populated by medullary thymic epithelial cells (mTECs) and dendritic cells (DCs). TSPs, derived from HSC in the bone marrow, enter the thymus at the CMJ where a dense network of endothelial cells is present. They progress to the ETP stage upon contact with the cTECs and differentiate via progenitor cell intermediates to mature T cells while migrating through the thymus via a defined pattern. The progenitors are in the beginning negative for both the co-receptors CD4 (cluster of differentiation 4) and CD8 and are therefore called double negative (DN). Next, they mature to $CD4^+$ and $CD8^+$ double positive (DP) cells and finally to mature $CD4^+$ or $CD8^+$ single positive (SP) cells that leave the thymus via blood vessels. Adapted from Koch and Radtke[7].*

2. Incidence

Leukemia is the most common cancer type in children under 15 years old. 80% of the leukemia diagnoses in this age group are ALL[8]. The peak prevalence in children is between the ages of 2 to 5 years while most adults with ALL are older than 65[9, 10]. Moreover, ALL is more common in children than in adults with two-thirds of ALL cases being diagnosed in children[10]. T-ALL accounts for about 15% of childhood and 25% of adult ALL cases[11]. For Belgium this means that about 10-15 children (0-14 years) receive the diagnosis of T-ALL each year[12]. Remarkably, there is a gender bias in T-ALL with more boys than girls being affected[13].

3. T-ALL subgroups

T-ALL can be subdivided into subgroups based on several criteria, including gene expression profiles, genetic rearrangements and immunophenotype. Molecular-cytogenetic and gene expression profiling studies demonstrated the existence of 6 distinct molecular subgroups[13-17] (Figure 3): early immature, T-cell leukemia homeobox 1 (*TLX1)*, T-cell leukemia homeobox 3 (*TLX3*), *TAL*/LIM domain only (*LMO*), homeobox A cluster (*HOXA*) and the proliferative cluster.

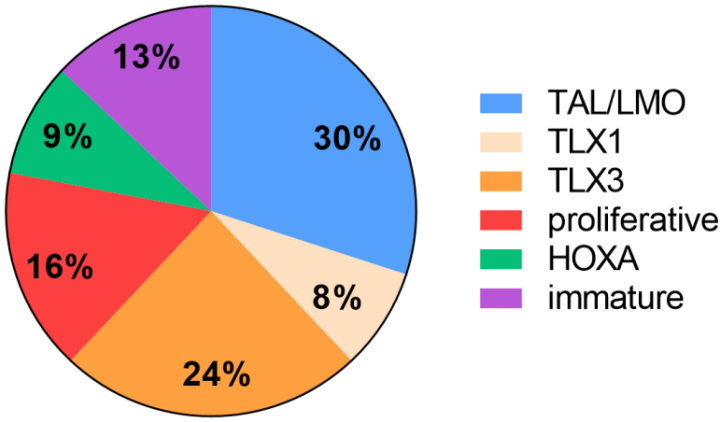

Figure 3. Frequencies of molecular subgroups in pediatric T-ALL. *Pie chart based on data presented in[14, 17].*

Each subgroup shows aberrant activation of specific T-ALL transcription factor oncogenes. Early immature T-ALLs are characterized by high levels of the transcription factors *LYL1*, *LMO2* and myocyte enhancer factor 2 (*MEF2C)* and high expression of genes expressed in early immature thymocytes. The *TLX1* and *TLX3* clusters have an aberrant expression of *TLX1* and *TLX3* respectively, often caused by genetic rearrangements. In the *TAL*/*LMO* subgroup, high expression of *LMO1*/*2*/*3* and/or the basic helix-loop-helix transcription factors *TAL1*/*2* is found, often as a result of translocations. Activation of *HOXA* genes is observed in cases with CALM-AF10, SET-NUP214 or mixed lineage leukemia (MLL)-fusions and in cases with rearrangements that directly activate *HOXA* genes. T-ALLs belonging to the proliferative cluster display strong expression of proliferation genes together with ectopic expression of NK2 homeobox 1 (*NKX2-1*) or NK2 homeobox 2 (*NKX2-2*), which is the result of rearrangements. The *NKX2-1*/*NKX2-2* rearranged T-ALL cases cluster together with *TLX1*-rearranged cases suggesting related pathogenic mechanisms.

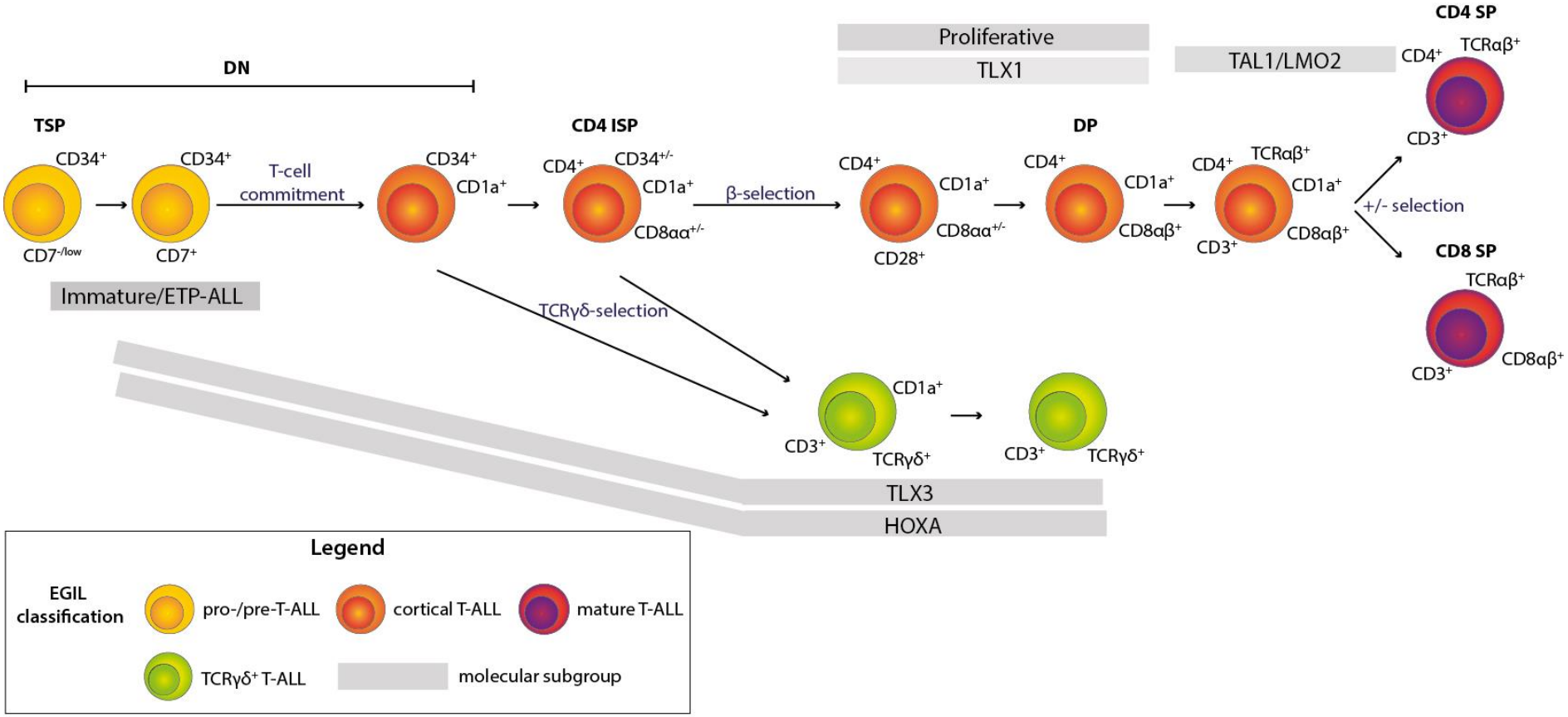

Figure 4. Schematic representation of T cell development and the association of T-ALL subgroups with the arrest at a particular developmental stage. *Multipotent progenitor cells travel from the bone marrow to the thymus (thymus seeding progenitors, TSPs) and differentiate via several progenitor cell intermediates to mature T cells. The cluster of differentiation (CD) cell surface markers can be used to distinguish between the different progenitors. In the beginning, T cell progenitors are negative for the glycoproteins CD4 and CD8 and are therefore called 'double negative (DN)'. Once CD1a is expressed, the cells are T cell committed which means that the potential to become another blood cell type is eliminated. TCR rearrangements at TCRD, TCRG,TCRB and TCRA loci take place during the differentiation process and result in the formation of either T cells with TCRαβ or TCRγδ. In the TCRαβ-lineage, cells become positive for both CD4 and CD8 (double positive, DP) and finally undergo a positive and negative selection that determines whether the cell matures into $CD4^+$ or $CD8^+$ single positive (SP) T cells. ISP: immature single positive ($CD4^+$). Figure based on data and figures presented in*[14, 15, 17, 18].

Interestingly, these genetic subtypes relate to an arrest at a particular stage of T cell development that can be recognized via immunophenotypic markers (Figure 4). The immunophenotypical classification of T-ALL is shown in Table 1 and indicated in Figure 4.

Table 1. Immunophenotypical classification of T-ALL based on the classification of the European Group for the Immunological Characterization of Leukemias (EGIL)[19, 20]. *TCR: T cell receptor.*

T-ALL CATEGORY	IMMUNOPHENOTYPIC PROFILE
PRO-T-ALL	only intracellular $CD3^+$ and $CD7^+$
PRE-T-ALL	≥ 1 of $CD2^+$,$CD5^+$, $CD8^+$
CORTICAL-T-ALL	$CD1a^+$
MATURE T-ALL	membrane $CD3^+$, $CD1a^-$
Α/Β$^+$ T-ALL (GROUP A)	anti-TCR α/β^+
Γ/Δ$^+$ T-ALL (GROUP B)	anti-TCR γ/δ^+

Several studies have described early immature T-ALLs based on different criteria. There is a large overlap between *LYL1*$^+$ signature cases[15], T-ALLs with absence of biallelic TCRγ locus deletion (ABD)[21], *MEF2C*-dysregulated T-ALLs[22] and the so-called early T-cell precursor ALLs (ETP-ALLs), which are immunophenotypically defined as $CD1a^-$, $CD8^-$, $CD5^{weak}$ with stem-cell/myeloid markers such as CD13, CD117, CD33 and CD34. Furthermore, ETP-ALLs have a transcriptional program related to early T cell precursors (ETPs)[23].

4. Treatment

The treatment for children with ALL consists of 3 phases of chemotherapy that take in total 2 to 3 years. First, induction therapy is given for 4 to 6 weeks. The drugs included in this phase are a glucocorticoid (prednisone or dexamethasone), vincristine, asparaginase and optionally an anthracycline. For patients with T-ALL, often cyclophosphamide is added to the regimen. The goal of this phase is to achieve remission, which is successful in 98% to 99% of children. However, stopping the treatment after this phase would lead to relapse. Therefore, the induction phase is followed by a consolidation/intensification phase in which intensive combination chemotherapy is given. The most widely used strategy is delayed intensification with asparaginase, vincristine and dexamethasone with or without anthracycline, mercaptopurine and methotrexate. For patients with T-ALL, repeated courses of extended intravenous infusion over 24 hours of high doses methotrexate are widely used. The last phase of treatment is the maintenance period taking 18 to 30 months. Daily oral mercaptopurine or thioguanine is combined with weekly low-dose methotrexate. Sometimes also pulses of glucocorticoids and vincristine are included[6, 9, 24]. An overview of the working mechanisms of the conventional chemotherapeutics is given in Table 2 and Figure 5. For all treatment phases, no real consensus exists on what the optimal regimen is[24]. Intrathecal chemotherapy (central nervous system directed therapy) is also given during the treatment in order to kill leukemic cells that might have spread to the brain and spinal cord. In the past, this was pursued via cranial irradiation, a practice that is now abandoned or limited in most protocols due to the adverse side effects[25].

Table 2. Overview of conventional chemotherapeutics used in the treatment of ALL and their working mechanism.

TYPE OF CHEMOTHERAPY	DRUGS USED IN ALL	WORKING MECHANISM
GLUCOCORTICOIDS	prednisone, dexamethasone	Bind to glucocorticoid receptor. This arrests growth and induces apoptosis in lymphoid tissue[26].
VINCA ALKALOIDS	vincristine	Bind to tubulin leading to the disruption of the mitotic spindle microtubules organization. Cell cycle is inhibited at metaphase of mitosis[27].
ENZYMES	L-asparaginase	Leukemic cells can't make their own asparagine. Asparaginase converts free asparagine to aspartic acid leading to starvation[28].
ANTHRACYCLINES	doxorubicin, daunorubicin	Intercalate with DNA and interfere with the function of Topoisomerase II. At high drug levels free radicals are formed that induce DNA damage[29].
ALKYLATING AGENTS	cyclophosphamide	Alkylate and crosslink DNA which induces DNA damage and apoptosis. Low doses promote antitumor immunity[30].
ANTIFOLATES	methotrexate	Inhibit DNA biosynthesis via the partial depletion of reduced folates and direct inhibition of folate dependent enzymes[31].
NUCLEOSIDE ANALOGUES	6-mercaptopurine, thioguanine, cytarabine, nelarabine, clofarabine	Incorporate into DNA resulting in synthesis inhibition and chain termination. Some also inhibit enzymes involved in the generation of nucleotides and RNA synthesis[32].

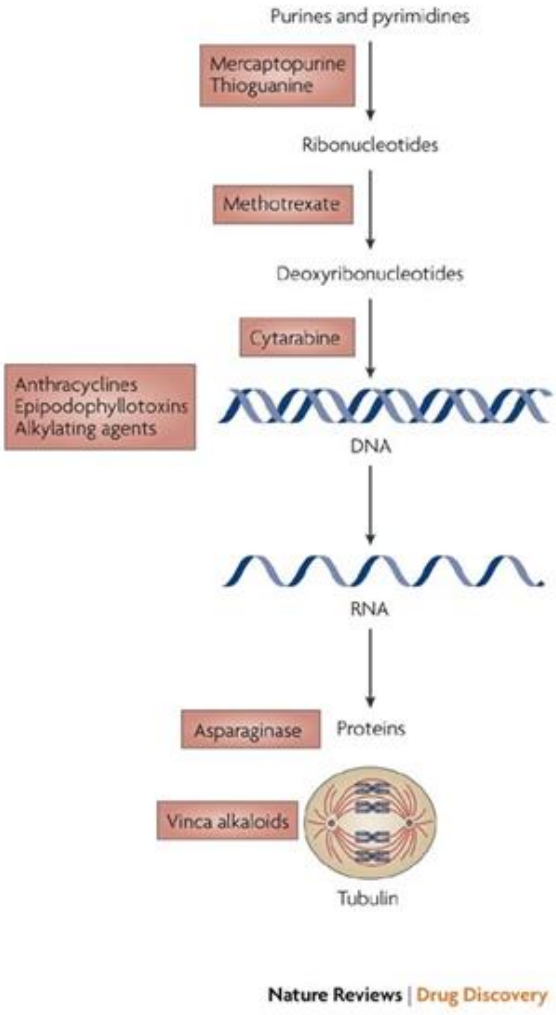

Figure 5. Conventional chemotherapeutics used in ALL[33].

Besides chemotherapy, an allogeneic hematopoietic stem cell transplantation (HSCT) belongs to the treatment options. HSCT is only used in 5 to 10% of children during primary therapy while more than half of the children that relapse receive a transplantation[6].

These pediatric intensive chemotherapy regimens are also recommended for adolescents and young adults (AYA) with T-ALL[34]. Older patients do not tolerate intensive chemotherapy as well as AYA. For them, optimized supportive care, targeted therapies, moderately intensified consolidation and reduced-intensity stem cell transplantation are the most promising approaches for the future. It will be important to discriminate between fit and unfit patients[35].

15% to 20% of childhood ALL patients and about 50% of adult ALL patients relapse[36, 37]. Relapses occur the most often during treatment or within the first two years after completing the treatment. The major site where relapse occurs is the bone marrow and this may or may not be combined with involvement of other sites such as the central nervous system or testes. Isolated central nervous system, testicular or other extramedullary relapses occur also but are less frequent[36]. Pediatric patients with an early marrow relapse or T-ALL are considered as high-risk relapse patients. Their treatment generally consists of multidrug chemotherapy followed by HSCT while low-risk or standard-risk relapse patients receive about 2 years of chemotherapy[38]. The chemotherapy that is currently used to treat relapsed ALL consists mostly of different combinations of the same agents used in frontline therapy[36]. The U.S. Food and Drug Administration (FDA) approved the use of the drugs nelarabine (Arranon) and clofarabine (Table 2) for treatment of ALL patients with refractory or relapsed disease after earlier chemotherapy. Nelarabine is only approved to use in T-ALL patients while clofarabine can only be used after at least two prior regimens[36, 39]. Patients with central nervous system relapse are treated with radiotherapy and systemic chemotherapy. Radiotherapy is often also used for the treatment of extramedullary relapse while an orchiectomy may be performed in case of testicular relapse[36, 38].

The contemporary treatment regimens are accompanied by acute and long-term side effects. Long-term toxicities associated with childhood ALL include cardiac dysfunction, osteonecrosis, neurocognitive impairment and second malignant neoplasms[40]. Still, 2-4% of pediatric patients die from treatment-related complications, which are mainly caused by infections, often preceded by chemotherapy-induced neutropenia, bleeding, thrombosis or tumor burden complications and organ toxicity[41]. Moreover, a high rate of illness due to chronic health conditions was found in survivors of childhood cancer[42].

All the chemotherapeutic agents used nowadays for the treatment of T-ALL are non-specific, affecting general mechanisms like DNA synthesis and cell division. Therefore, not only cancer cells are killed but often also normal healthy cells which causes side effects. A better understanding of the molecular mechanisms that cause T-ALL or contribute to the development of the disease can lead to the development of molecularly targeted therapies. These targeted therapies target specific molecules that are involved in the pathogenesis of the disease. By targeting cancer-specific molecules, targeted therapies may have less toxic effects on normal cells.

5. Prognosis

The cure rate for childhood ALL has gradually increased over the past decades thanks to the fine-tuning of combination chemotherapy and better understanding of the disease biology. Nowadays, the survival rates reach approximately 85%[24, 43, 44]. Although these numbers are high, the outcome for children that fail induction therapy or suffer from relapsed disease remains extremely poor with only 7-23% of relapsed T-ALL patients surviving beyond 3 to 5 years after the initial diagnosis[38]. Compared to childhood leukemia, the clinical picture for adult ALL is even worse with high relapse rates and 5-year overall survival rates of 35-48%[37, 45-48]. Minimal residual disease (MRD), i.e. the residual leukemic cells during or after treatment is an important prognostic indicator. MRD can be detected using immunophenotyping by flow cytometry (sensitivity of 10^{-3} to 10^{-4}) and/or quantitative real-time polymerase chain reaction (qPCR; sensitivity of 10^{-4} to 10^{-5}). Follow-up of MRD during treatment can identify patients at high risk of relapse and patients with a good response allowing less intensive chemotherapy[49]. In a large cohort of pediatric T-ALL patients, an MRD of more than 10^{-3} at day 78 was the most important predictor for relapse[50]. The survival chances of ALL patients after relapse are influenced by several factors. The outcome is especially poor if relapse happens less than 18 months from the initial diagnosis[51, 52].

Most publications describing ETP-ALL reported an inferior outcome with a high proportion of remission failure or hematological relapse when using standard intensive chemotherapy[23, 53-56]. Also research groups studying *LYL1*$^{+}$ early immature T-ALL[15], T-ALL with ABD[21] and early immature adult T-ALL defined on the basis of gene expression data[57] found an association between early immature T-ALLs and poor prognosis[15, 21, 57]. However, some studies question the prognostic relevance of early immature T-ALL[22, 58]. A recent study on a large cohort of T-ALL patients treated on a contemporary protocol failed to find significant differences in outcome between ETP-ALL and other T-ALL cases[58].

PART II The genetic and epigenetic landscape of T-ALL

1. T-ALL development is a multistep process

T-ALL arises from the malignant transformation of T cell progenitor cells. This transformation is a multistep process in which thymic progenitor cells gradually accumulate genetic and epigenetic changes[59]. A hierarchical model of T-ALL development has been proposed with the formation of pre-leukemic stem cells (pre-LSCs) as first step. Pre-LSCs are long-lived cells with self-renewal properties that allow clonal expansion. They harbor some but not all of the mutations present in the diagnostic clone. In contrast to fully transformed leukemic cells, pre-LSCs retain the ability to differentiate into the full spectrum of mature daughter cells. Pre-LSCs are often resistant to chemotherapy and can be the origin of relapse. The clonal expansion of these pre-LSCs allows the acquisition of oncogenic events leading eventually to cancer[59, 60]. For example, mutations in the DNA methyltransferase (DNMT) *DNMT3A* were found as an early event in acute myeloid leukemia (AML) leading to a clonally expanded pool of pre-LSCs from which AML evolves[61].

In T-ALL, the combined overexpression of *TAL1* and *LMO1* in DN3 mouse thymocytes, the double negative stage in T cell development where T lineage commitment driven by NOTCH1 takes place, reprograms the DN3 thymocytes into self-renewing pre-LSCs with retained differentiation capacity. For this reprogramming, high physiological levels of NOTCH1 were critically required. Moreover, overexpression of *LYL1* and *LMO1* results in a similar reprogramming[62]. Previously, McCormack et al.[63] already detected the formation of pre-LSCc upon overexpression of *Lmo2* in the thymus from mice. An essential factor in this reprogramming was LYL1[64]. Again, the self-renewal capacity was restricted to the DN3 population[63].

Altogether, activation of TAL1 or LYL1 together with LMO1 or LMO2 can drive oncogenic reprogramming of DN3 thymic precursors into self-renewing pre-LSCs. These proteins are all part of the basic helix-loop-helix transcription factor complex. The transcription factors LMO1 and LMO2 are recruited to DNA by the basic helix-loop-helix factor TAL1 or LYL1[59, 60]. Whether other T-ALL specific transcription factor oncogenes have the capacity to induce self-renewal remains to be established.

2. Genetic alterations and opportunities for targeted therapies in T-ALL

2.1. Overview of genetic alterations in T-ALL

T-ALL is a genetically heterogeneous disease in which multiple oncogenes and tumor suppressors cooperate to alter the normal mechanisms that control differentiation, growth and survival during thymocyte development.

Constitutive activation of NOTCH1 signaling is identified in over 50% of T-ALL patients[13]. Moreover, deletions of the *CDKN2A* (*cyclin-dependent kinase inhibitor 2A*) locus in chromosome band 9p21, which encompasses the *p16/INK4A* and *p14/ARF* suppressor genes, are present in more than 70% of all T-ALL cases[13]. Thus, constitutive activation of NOTCH1 signaling cooperates with loss of *p16/INK4A* and *p14/ARF* in T-cell transformation

and constitutes the core of the oncogenic program in the pathogenesis of T-ALL. Furthermore, aberrant expression of specific transcription factor oncogenes defines the distinct molecular-genetic subgroups in T-ALL as described in part I. In addition, whole-genome T-ALL profiling has provided a fairly complete and comprehensive list of additional genetic defects that are shared among the different genetic subclasses and activate a plethora of oncogenic signaling cascades, including interleukin-7 receptor (IL7R)/Janus kinase (JAK)/signal transducer and activator of transcription (STAT), phosphoinositide-3-kinase (PI3K)/AKT/mechanistic target of rapamycin (mTOR) and RAS/RAF/mitogen-extracellular signal-regulated kinase (MEK)/extracellular signal-regulated kinase (ERK) signaling[65]. Hyperactivation of mTOR explains, at least in part, the addiction of T-ALL cells to cap-dependent translation in which the eukaryotic initiating factors (eIF) eIF4E and eIF4A play an important role[66, 67].

The tyrosine kinase ABL1 is frequently activated via *ABL1* genomic rearrangements. Additionally, activation of the oncogenic transcription factors *MYC* and *MYB* is often found in T-ALL. *MYC* is a critical NOTCH1 direct target gene but can also be activated via rare translocations while *MYB* can be overexpressed in T-ALL via translocations or focal duplications. On the other hand, the transcription factor tumor suppressor genes *WT1* (Wilms tumor 1), *LEF1* (lymphoid enhancer binding factor 1) and *BCL11B* (B-cell CLL/lymphoma 11B) are often inactivated by mutations or deletions[13]. De Keersmaecker et al.[68] recently identified mutations in CCR4-NOT transcription complex subunit 3 (*CNOT3*), which is part of a complex that regulates gene transcription, and in the ribosomal genes *RPL5* and *RPL10*.

Genetic alterations in early immature T-ALL subtypes

Early immature T-ALLs are characterized by a high degree of genetic heterogeneity including genetic alterations in hematopoietic transcription factors such as *RUNX1* (runt related transcription factor 1), *GATA3* (GATA binding protein 3) and *ETV6* **(**ETS variant 6), activating mutations in critical mediators of cytokine receptor and RAS signaling and mutations in myeloid specific oncogenes and tumor suppressors[69, 70]. Given the myeloid mutational spectrum and gene expression signature of these tumors, myeloid-directed therapies have been suggested for poor prognostic early immature/ETP T-ALL[69].

Adults versus children

A recent genome-wide sequencing study[68] reported a correlation between age at diagnosis and number of somatic mutations in T-ALL and showed that particular genes are preferentially affected in adults versus children. For example, the newly identified mutations in *CNOT3* were mainly present in adults, whereas mutations affecting the ribosomal protein RPL10 were almost exclusively found in children[68]. Another example is the plant homeodomain finger 6 (*PHF6*) gene. Van Vlierberghe et al.[71] identified *PHF6* as an X-linked tumor suppressor in T-ALL carrying truncating or missense mutations in about 15% of pediatric and 40% of adult T-ALLs.

2.2. Opportunities to target genetic alterations in T-ALL

The NOTCH1 signaling pathway gains a lot of attention as a rational molecular target. NOTCH1 is a class I transmembrane receptor that regulates T cell development. Upon interaction between NOTCH1 and its ligands, the extracellular domains of the receptor are cleaved by the ADAM10 metalloprotease. Next, the γ-secretase complex cleaves the transmembrane region of the receptor releasing the intracellular portion of NOTCH1 (ICN1) which then translocates into the nucleus and activates gene expression of target genes[72]. Most of the NOTCH1 activating mutations identified in T-ALL result in ligand-independent receptor activation or stabilization of the cytoplasmic ICN1[72, 73]. Small molecule γ-secretase inhibitors (GSIs) block the proteolytic cleavage of NOTCH1 and inhibit the release of ICN1. Preclinical studies were promising and GSIs entered phase I clinical trials for patients with T-ALL[72]. However, dose-limiting gastrointestinal toxicities were observed and the responses in the clinic were limited and not durable[74, 75]. The use of GSIs in combination with chemotherapy or targeted therapies could increase the antileukemic effects of GSIs as exemplified by several preclinical studies[76-79]. In addition to GSIs, blocking NOTCH1 signaling with NOTCH1 inhibitory antibodies[80, 81], preventing the assembly of the ICN1 transcriptional complex by using the stapled peptide SAHM1[82] and inhibition of the sarco/endoplasmic reticulum calcium ATPase (SERCA) channels to impair the maturation of mutated NOTCH1 receptors[83], are possible therapeutic options to target oncogenic NOTCH1 signaling (Table 3).

As almost 50% of T-ALL patients carry activating mutations in the JAK/STAT, PI3K/AKT/mTOR or RAS/RAF/MEK/ERK signaling pathways[84], targeting these pathways might be an interesting therapeutic strategy. An overview of available inhibitors for these pathways and other opportunities for targeted therapies in T-ALL is given in Table 3.

Table 3. Opportunities to target genetic alterations in T-ALL.

PATHWAY	THERAPIES
NOTCH1	- NOTCH1 inhibitory antibodies and stapled peptides (e.g. SAHM1) - γ-secretase inhibitors (e.g. PF-03084014) - SERCA inhibitors (e.g. thapsigargin)
JAK/STAT	- JAK1/JAK2 inhibitors (e.g. ruxolitinib) - JAK3 inhibitors (e.g. tofacitinib)
PI3K/AKT/mTOR	- PI3K inhibitors (e.g. BKM120) - AKT inhibitors (e.g. MK-2206 dihydrochloride) - Dual PI3K/mTOR inhibitor (e.g. NVP-BEZ235 (dactolisib)) - mTOR inhibitors (e.g. rapamycin)
RAS/RAF/MEK/ERK	- MEK inhibitors (e.g. trametinib) - ERK inhibitors (e.g. GDC-0994)
ABL1 KINASE	- ABL1 inhibitors (e.g. imatinib)
CAP-DEPENDENT TRANSLATION	- eIF4A inhibitors (e.g. silvestrol) - eIF4E inhibitors (e.g. 4EGI-1)

2.3. The transcription factor ZEB2 as an oncogene in early immature T-ALL

ZEB2: a transcriptional repressor or activator ?

The zinc finger E-box binding homeobox 2 protein (ZEB2/SIP1) belongs to the ZEB family, consisting of the two highly homologous proteins ZEB1 and ZEB2. These molecules are large multidomain transcription factors that bind with their C-terminal and N-terminal clusters of zinc fingers to bipartite E-box motifs in the DNA. Depending on the cellular context and target gene, ZEB proteins can act as transcriptional repressors or activators. The availability and interactions with other transcription factors and cofactors play an important role in this. For ZEB2, interactions with receptor-activated SMADs, the nucleosome remodeling/histone deacetylating (NuRD) complex, the transcriptional co-repressor CtBP (C-terminal binding protein) and the histone acetyltransferases p300 and p/CAF have been described. Furthermore, SUMOylation by the polycomb group protein Pc2 can regulate the transcriptional activity of ZEB2[85, 86] (Figure 6). Additionally, export of the ZEB proteins to the cytoplasm in a temporal- and/or tissue-specific manner can also control their functionality[86].

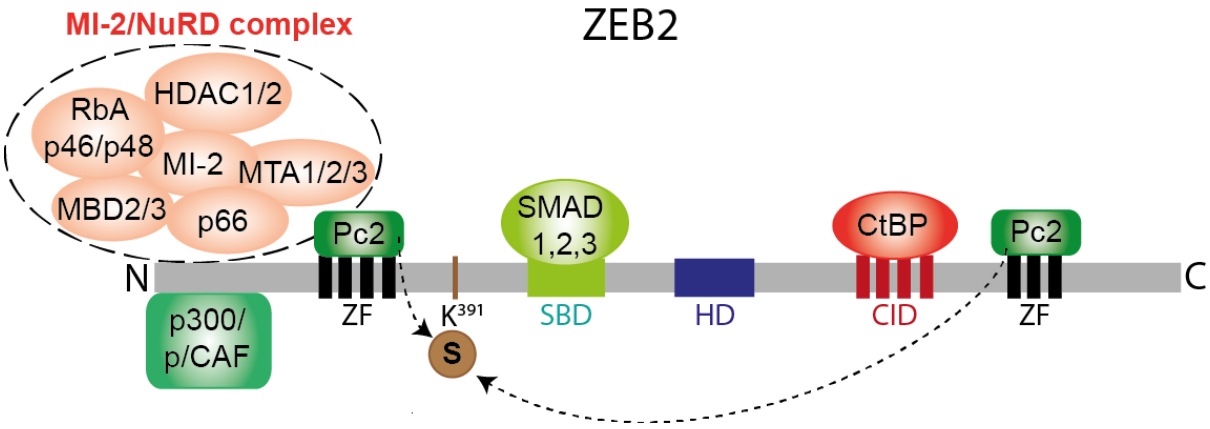

Figure 6. Schematic representation of the domains and known interaction partners of the ZEB2 transcription factor. *The N- and C-terminal clusters of zinc fingers (ZF) are important for DNA binding while the homeodomain (HD), CtBP interacting domain (CID) and Smad binding domain (SBD) are mainly used for protein-protein interactions with other transcription factors and cofactors with repressor or activator activities. The polycomb group protein Pc2 has SUMO E3 ligase activity and SUMOylates (indicated with S in the figure) ZEB2 at the 390-IKTE-393 sequence. Figure based on*[85-87].

A large intron with an internal ribosomal entry site is present in the 5' untranslated region (UTR) of *ZEB2*. When the natural antisense transcript *ZEB2-AS1* is transcribed, the splicing of this intron is blocked with a stronger expression of the ZEB2 protein as result[85].

ZEB2 in epithelial-mesenchymal transition

ZEB2 is one of the master regulators driving epithelial-mesenchymal transition (EMT). During EMT, epithelial cells lose their cell-cell junctions and apical-basal polarity, reorganize their cytoskeleton, change their shape and reprogram their gene expression profile to undergo a transition to mesenchymal cells. Mesenchymal cells are more motile and are able to degrade extracellular matrix proteins enabling them to invade tissues. This process is implicated in both normal embryonic development and tumorigenesis[88]. In several cancer types, such as glioma[89], colorectal cancer[90], renal cell carcinoma[91] and ovarian cancer[92], *ZEB2*

overexpression is an unfavorable factor that may promote migration and invasion. In melanoma, the situation is different. Normal melanocytes do not belong to the epithelial lineage and they express already the EMT-inducing transcription factors ZEB2 and SNAIL2 (snail family transcriptional repressor 2). These factors behave as tumor-suppressor proteins. A switch from ZEB2/SNAIL2 to ZEB1/TWIST1 (twist family bHLH transcription factor 1) expression was found as a major risk factor for poor outcome in melanoma and was associated with a gain in invasive properties[93].

ZEB2 in hematological malignancies

Zeb2 is abundantly expressed in the hematopoietic system and is essential for differentiation and mobilization of hematopoietic stem cells during murine embryonic development[94]. In addition, *Zeb2* inactivation in the adult murine hematopoietic system leads also to severe differentiation defects[95]. However, the role of ZEB2 in normal human T cell development and hematologic malignancies has not been thoroughly investigated.

Goossens et al.[96] identified the translocation t(2;14)(q22;q32) as a rare but recurrent genetic event in early immature T-ALL. Detailed cytogenetic analysis allowed mapping of the translocation breakpoint at 14q32 within the *BCL11B* locus and within close vicinity of the *ZEB2* gene at chromosomal band 2q22. Notably, juxtaposition of *BCL11B* near putative oncogenes has been previously reported for a number of T-ALL oncogenes including *TLX3*, *NKX2-5* and *PU.1*[97, 98]. Therefore, this work suggested that sustained expression of the EMT regulator ZEB2 could act as a molecular driver of immature T-ALL development. It is also interesting to note that *BCL11B* haploinsufficiency has also been implicated in T cell leukemogenesis, as exemplified by the loss-of-function *BCL11B* deletions and mutations identified in primary T-ALLs[99, 100]. Therefore, this particular chromosomal translocation might execute a dual function toward malignant T cell transformation with concomitant loss of *BCL11B* and gain of *ZEB2*, a concept that also applies for the other *BCL11B*-driven translocations mentioned above. Furthermore, *ZEB2* was higher expressed in human immature T-ALL patients than in other T-ALL patients. Using a conditional ROSA26-based *Zeb2* gain-of-function mouse model, Goossens et al.[96] showed that hematopoietic overexpression of *Zeb2* resulted in spontaneous thymic lymphoma development starting at 5 months of age, indicating that *Zeb2* can act as a bona fide oncogene in hematologic T cell malignancies. Furthermore, breeding of this tumor model in a tumor-prone p53 null background revealed that *Zeb2* overexpression shortens tumor latency and drives a gene expression profile that resembles early immature T-ALL, including the early T cell/stem-cell markers *c-Kit*, *Baalc* (brain and acute leukemia, cytoplasmic) and *Lyl1*. Similar activation of a stem-cell-like transcriptional program has previously been described in a *CD2-Lmo2*^{tg} mouse model[101], in which preleukemic thymocytes acquired *Lmo2*-driven self-renewal capacity as a prerequisite of full clonal T cell transformation[63]. Similarly, transplantation experiments using *Zeb2*-overexpressing lymphoblasts in immunodeficient mice showed that *Zeb2*-driven tumors contained a higher fraction of leukemia-initiating cells as compared with controls[96], suggesting some putative commonalities between the *Zeb2*- and *Lmo2*-driven tumor models as described above. Interestingly, ZEB proteins also bind tandem E-boxes[102], suggesting a potential overlap or competition for the same regulatory sequences with the above-described LYL1/LMO2 transcriptional regulatory complex[103]. *Zeb2* tumors were also characterized by enhanced JAK/STAT signaling through transcriptional activation of *IL7R*[96]. This association between ZEB2 and IL7R/JAK/STAT activation is in line with other recent studies that reported alternative *in vivo* models for early immature T-ALL. Indeed, bone marrow

transplantation of precursor cells expressing gain-of-function *IL7R*[104] or *JAK3*[105] mutations resulted in the development of a transplantable murine early immature T-ALL, reminiscent of the human disease. Altogether, this study[96] convincingly identified *ZEB2* as a novel oncogene implicated in early immature T-ALL, but the molecular mechanisms by which ZEB2 regulates leukemic stem cell activity, in addition to the spectrum of direct ZEB2 target genes that modulate disease initiation or progression, remains to be established.

Recently, the importance of ZEB2 in the development of acute myeloid leukemia (AML) was also identified using shRNA screens. *ZEB2* is highly expressed in AML and knockdown of ZEB2 in AML cells impaired their proliferation and resulted in aberrant differentiation[106].

3. Epigenetic alterations and opportunities for targeted therapies in T-ALL

3.1. Overview of epigenetic alterations in T-ALL

Changes in transcriptional regulation, which occur independent of the genomic DNA sequence, are studied in the field of epigenetics. The dynamic interplay between histone modifications and DNA methylation defines the chromatin structure of the human genome and serves as a conceptual framework to understand transcriptional regulation. In a recent landmark study, Huether et al.[107] sequenced 633 epigenetic regulatory genes in over 1000 pediatric tumors representing 21 different cancer subtypes and found T-ALL to be among the tumors with the highest frequency of mutations in genes that encode proteins involved in epigenetic regulation. Indeed, over the last 5 years, genome-wide and candidate-approach based studies have identified recurrent genomic lesions in a variety of genes involved in DNA methylation and post-translational histone modifications in T-ALL. Therefore, disruption of epigenetic homeostasis in normal T cells might act as a core component of hematopoietic T cell transformation[108].

An overview of epigenetic alterations detected in T-ALL is presented in Table 4.

Table 4. Epigenetic alterations in human T-ALL. *Table adapted from Peirs et al.*[108]

GENE	DEFECT	INCIDENCE IN T-ALL	REFERENCES
DNA METHYLATION			
DNMT3A[a]	mutation	4-19%	70, 109-112
DNMT3B	aberrant transcripts	NA	113
TET1	mutation	6-14%	68, 114
IDH1[a]	mutation	2-6%	70, 115
IDH2[a]	mutation	5-9%	70, 110
HISTONE METHYLATION			
EZH2	mutation/deletion	11-18%	57, 69, 116
SUZ12	mutation/deletion	6-11%	57, 69, 116
EED	mutation/deletion	10%	69
JARID2	mutation	1/11	110
UTX	mutation	5%	68, 107
JMJD3	overexpression	NA	117
MLL1	rearrangements	5%	118
MLL2	mutation	10% of ETP-ALL	111
DOT1L	mislocated	10%	119
SETD2	mutation/deletion	8% of ETP-ALL	69
HISTONE ACETYLATION			
CREBBP	mutation	NA	120
EP300	mutation	2%	107
HDACs	elevated expression	NA	121, 122
HDAC5	mutation	1%	107
HDAC7	mutation	4%	107

a Only detected in adults.
NA: not available

DNA methylation

DNA methylation is executed by the DNA methyltransferases DNMT1, DNMT3A and DNMT3B (Figure 7). This DNA modification controls transcription and chromatin structure, maintains genomic stability and regulates X chromosome inactivation[123]. Aberrant patterns of DNA methylation are a characteristic feature of human cancer. The cancer epigenome displays global DNA hypomethylation of CpG-poor regions in combination with local hypermethylation of CpG-rich promoter regions. The general DNA hypomethylation is thought to trigger chromosomal instability, whereas local DNA hypermethylation mediates repression of a specific set of tumor suppressor genes[124].

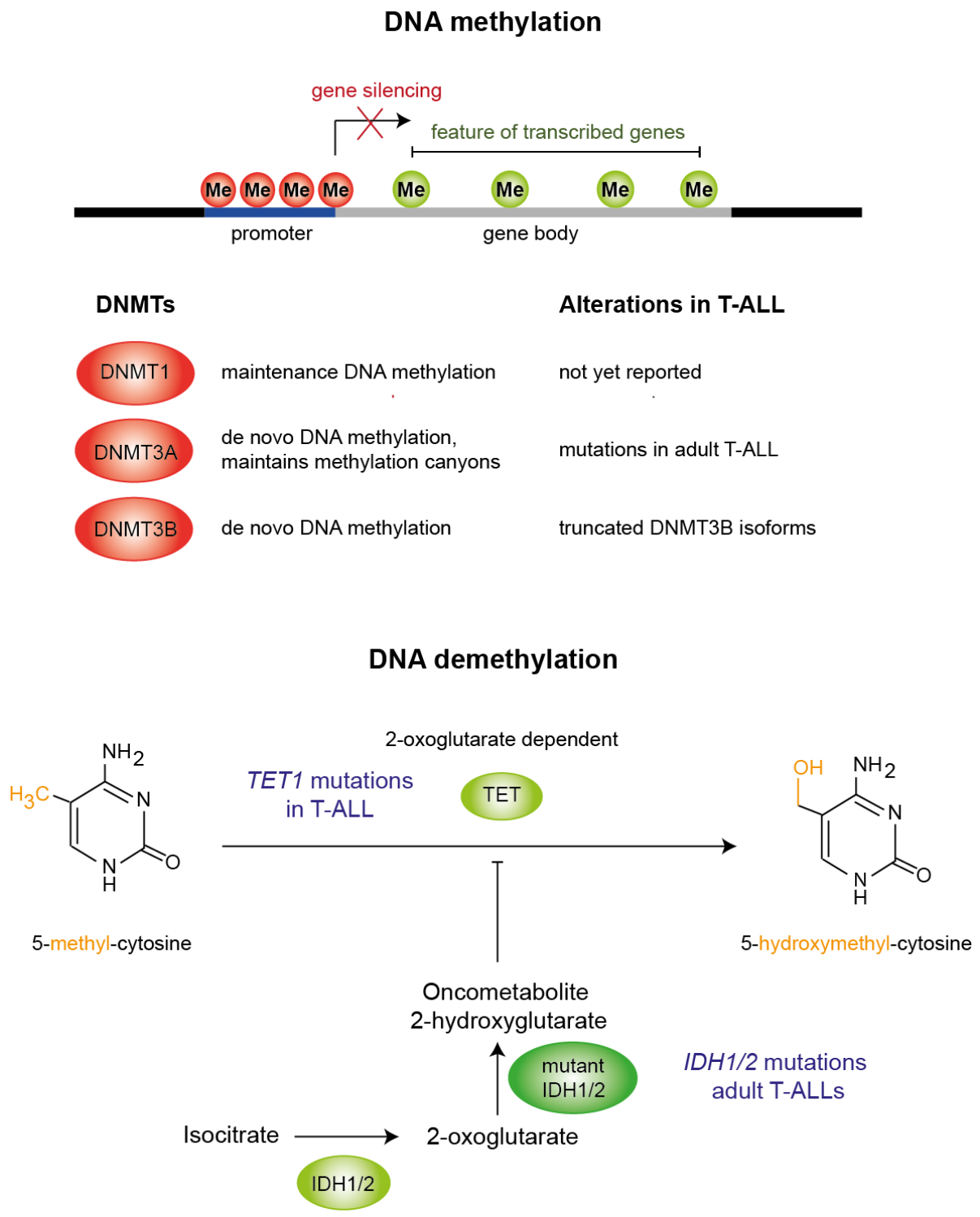

Figure 7. Schematic representation of DNA (de)methylation with indication of alterations found in T-ALL. *DNA methylation is carried out by DNA methyltransferases on a cytosine in the context of CpG dinucleotides. Methylation of CpG islands at transcriptional start sites is associated with gene silencing while gene body methylation was found to correlate with active transcription. DNMT1 is a maintenance DNMT while DNMT3A and DNMT3B are responsible for de novo DNA methylation. Furthermore, DNMT3A is needed for the maintenance of the methylation canyons which are enriched in genes dysregulated in leukemias. Enzymes from the Ten-Eleven Translocation (TET) protein family catalyze the conversion of methylated cytosine to 5-hydroxymethyl-cytosine, which promotes DNA demethylation. Neomorphic mutations in isocitrate dehydrogenases (IDH) inhibit the activity of TET enzymes via the production of the oncometabolite 2-hydroxyglutarate*[108].

Mutations targeting *DNMT3A* have been identified in up to 19% of human T-ALL and are mainly associated with immature T-ALL subtypes[57, 111]. Similar to what has been observed in AML[125, 126], *DNMT3A* mutations are associated with poor prognosis in the context of T-ALL[57, 109]. Interestingly, Kramer et al.[127] demonstrated with the help of mouse models that DNMT3A is required for normal T cell development and acts as a T-ALL tumor suppressor. *DNMT3B* produces several isoforms due to alternative splicing[123] and aberrant *DNMT3B* transcripts encoding truncated proteins have been observed in cancer cell lines including the T-ALL cell line JURKAT[113]. Notably, the oncogenic property of one particular isoform was firmly established in transgenic mice suggesting that DNMT3B mediated redistribution of DNA methylation might be involved in carcinogenesis[128].

It has been postulated that the initial steps of active DNA demethylation are promoted by the conversion of 5-methyl-cytosine to 5-hydroxymethyl-cytosine by dioxygenases of the Ten-Eleven Translocation (TET) protein family which includes TET1, TET2 and TET3[129, 130] (Figure 7). *TET1* mutations have been detected in a fraction of human T-ALLs[68, 114]. TET enzymes require 2-oxoglutarate that can be derived from several sources including isocitrate. Isocitrate dehydrogenases (IDH) catalyze the decarboxylation of isocitrate to 2-oxoglutarate[131] (Figure 7). *IDH1* and *IDH2* mutations have not been identified in pediatric T-ALL[132] but seem to occur exclusively in adult T-ALL[70, 110, 115]. Moreover, and similar to what has been observed for *DNMT3A* mutations, *IDH1* or *IDH2* mutant adult T-ALL patients show characteristic expression of myeloid antigens (CD13 and/or CD33) and a gene expression profile reminiscent of HSCs and myeloid progenitors[70].

Histone acetyltransferases and deacetylases

Histone acetyltransferases (HATs) and histone deacetylases (HDACs) regulate acetylation of both histone and non-histone proteins. These enzymes are part of multiprotein complexes that determine their substrate specificity and lysine preference. In general, histone acetylation releases the chromatin structure and acts as a molecular scaffold for transcription-related proteins to trigger active gene transcription[133]. CREBBP (CREB binding protein) and EP300 (E1A binding protein p300) are transcriptional coactivators with HAT activity that share significant amino acid homology and have established roles in hematopoiesis[134]. Deletions or loss-of-function mutations in the *CREBBP* gene have been identified in about 20% of relapsed ALL cases and included missense mutations targeting the HAT domain and frame-shift or nonsense mutations resulting in truncated CREBBP protein. Enrichment of *CREBBP* mutations at relapse suggests that loss of *CREBBP* is implicated in therapy resistance, possibly through impaired regulation of glucocorticoid responsive genes[120]. In this study, *CREBBP* mutations were also identified in 3 primary T-ALL samples and different T-ALL cell lines[120]. Notably, heterozygous *Crebbp* deficient mice show an increased incidence of hematopoietic tumors, further confirming the tumor suppressive properties of CREBBP in leukemia development[135]. Although *EP300* mutations in relapsed ALL were sparse[120], independent screening efforts did identify recurrent *EP300* mutations in about 5% of childhood ETP-ALLs[69]. Moreover, other studies also reported *EP300* mutations in a small fraction of pediatric[107] and adult[110] T-ALL.

Finally, the oncogenic or tumor suppressive potential of HDACs in the context of T-cell transformation remains controversial. Although some studies reported elevated expression levels[121, 122] or enhanced activity of particular HDACs[136] in primary T-ALL, Huether et al.[107] reported somatic mutations in *HDAC5* or *HDAC7* in about 5% of childhood T-ALL.

Histone methyltransferases and demethylases

The polycomb repressive complex 2 (PRC2) mediates transcriptional gene repression by writing the repressive H3K27me3 histone mark at specific loci throughout the genome. Loss-of-function mutations and deletions targeting the core components of this complex (*EZH2* (enhancer of zeste 2 PRC2 subunit), *SUZ12* and *EED* (embryonic ectoderm development)) have been identified in both pediatric[69] and adult[57, 116] T-ALL. The role of PRC2 as a tumor suppressor in the T cell lineage has been confirmed using xenografts of human T-ALL cell lines[116] and a conditional *Ezh2* knockout mouse model[110]. Although the H3K27 specific histone demethylase UTX (ubiquitously transcribed tetratricopeptide repeat, X chromosome) and the PRC2 complex seem to exert opposite functions on gene transcription, recent exome sequencing analysis unraveled recurrent loss-of-function mutations targeting *UTX* in about 5% of T-ALLs [68, 107], suggesting that both chromatin remodelers can exert tumor suppressive functions during T-cell transformation. In contrast, the H3K27 demethylase JMJD3 (jumonji domain containing 3) was shown to be overexpressed in primary T-ALL samples and in a mouse model of NOTCH1-induced T-ALL[117].

In T-ALL, rearrangements of the H3K4 methyltransferase *MLL1* are found in about 5% of patients[118] and most frequently result in the expression of *MLL1-AF4* or *MLL1-ENL* fusion transcripts[137]. The leukemic cells of these *MLL1*-rearranged T-ALLs are characterized by an increased level of *HOXA* expression and show an early arrest in thymocyte differentiation or commitment towards the γδ-lineage[16, 137]. Translocations directly targeting the *HOXA* locus[16, 138] or genetic rearrangements that result in *CALM-AF10* or *SET-NUP214* fusion transcripts show a similar activation of *HOXA* gene expression[16, 119, 137, 139]. Notably, MLL fusion proteins[140-143] as well as CALM-AF10[141, 144] and SET-NUP214[119] chimeric proteins recruit the H3K79 DOT1-like histone lysine methyltransferase (DOT1L) which results in elevated levels of H3K79 methylation at the *HOXA* locus and concomitant upregulation of *HOXA* gene expression. In addition, *MLL2* mutations have recently been identified in 10% of immature adult T-ALL[111].

Trimethylation of lysine 36 at histone H3 (H3K36me3) is generally associated with active gene transcription and is mainly detected in gene bodies of its target genes[145]. The enzymes NSD1 and NSD2 (nuclear receptor binding SET domain protein 1 and 2) act as H3K36 mono- and dimethylases, whereas SETD2 (SET domain containing 2) mediates H3K36 trimethylation. SETD2 functionally connects H3K36me3 with transcriptional elongation through binding with RNA polymerase II[145]. *SETD2* mutations and deletions were identified in 8% of childhood ETP-ALL cases, while no mutations were observed in mature subtypes of human T-ALL [69].

Noncoding RNAs

Both oncomirs and tumor suppressor miRNAs that negatively regulate the expression of respectively tumor suppressor genes and oncogenes have been identified in T-ALL. Moreover, the role of long noncoding RNAs in the context of T-ALL is starting to be explored. For more details, the reader is referred to an excellent review that was recently published[146].

3.2. Opportunities to target epigenetic alterations in T-ALL

The overwhelming evidence that inappropriate regulation of epigenetic factors serve as an intrinsic part of the molecular circuitry that is perturbed during malignant transformation, created an enormous interest in pharmacological intervention of epigenetic processes. Indeed, development of targeted therapies against epigenetic modifiers as new treatment modalities for human leukemia is currently ongoing and epigenetic opportunities for targeted therapy that might be relevant for the treatment of human T-ALL are summarized in Table 5.

Table 5. Putative epigenetic therapies for the treatment of human T-ALL. *Updated table from Peirs et al.[108] CTCL: cutaneous T-cell lymphoma; PTCL: peripheral T-cell lymphoma; MM: multiple myeloma; MDS: myelodysplastic syndromes.*

TARGET	RATIONALE FOR USE IN T-ALL	EXAMPLES OF INHIBITORS
HDACs	Increased expression levels and enhanced activity of HDACs in T-ALL. Several studies described the induction of apoptosis by HDAC inhibitors in T-ALL cell lines and T-ALL patient blasts [147-149].	- Vorinostat and Romidepsin (FDA approved for refractory CTCL) - Panobinostat (FDA approved for refractory MM) - Belinostat (FDA approved for relapsed or refractory PTCL)
DOT1L	*MLL*-rearranged, CALM-AF10-positive and SET-NUP214-positive leukemias recruit the DOT1L enzymatic activity to drive elevated expression of genes important in leukemogenesis.	- EPZ-5676 (phase I trial in AML and ALL with MLL rearrangements)
JMJD3	JMJD3 is overexpressed in primary T-ALL cells. Evidence supporting a role for JMJD3 in the maintenance of T-ALL has been obtained. GSKJ4 showed anti-tumorigenic activity in T-ALL cell lines and in primary T-ALL cells[117].	- GSKJ4 (dual JMJD3/UTX inhibitor)
DNMTs	The DNMT inhibitor decitabine enhances chemosensitivity of ETP-ALL patient-derived samples[150].	- Azacitidine and Decitabine (FDA approved for MDS)
IDH1/2	14% of immature adult T-ALLs carry a mutation in *IDH1* or *IDH2*.	- AG-120 and AG-221 (mutant IDH1/2 inhibitors; phase I in IDH1/2-mutated positive hematologic malignancies)

3.3. Inhibition of BRD4 to repress the transcription of oncogenes

.

BRD4 and super-enhancers

Bromodomains (BRDs) are protein interaction modules that recognize acetylation of lysine residues. The bromodomain and extra-terminal (BET) family of proteins are critically involved in transcriptional regulation and consist of BRD2, BRD3, BRD4 and BRDT[151].

BRD4 is an important BET family member that associates with positive transcription elongation factor b (P-TEFb) and Mediator in a transcriptional co-activator complex that recruits the transcriptional apparatus to acetylated chromatin. Recent studies identified

extreme large enhancers that are co-occupied by the transcriptional co-activators BRD4 and mediator complex subunit 1 (MED1) and drive expression of lineage identity genes[152, 153] or prominent proto-oncogenes in human cancer[154]. In addition, these so-called super-enhancers show broad binding of traditional enhancer associated histone marks including H3K27ac and H3K4me1[152, 153]. In the context of T-ALL, a fraction of functional NOTCH1 binding sites are located near super-enhancer regions in the vicinity of genes critically involved in normal and malignant T cell development including *MYC* and *IL7R* [155, 156]. Since super-enhancers are often associated with critical oncogenes, it has been postulated that the establishment of a super-enhancer catalogue of human cancer could trigger the discovery of novel oncogenes that are critically involved in tumor development[153, 154]. In that respect, recent work identified super-enhancer sequences in the T-ALL cell lines JURKAT, DND-41 and RPMI-8402. These analyses confirmed the presence of super-enhancer sequences near putative T-ALL oncogenes, including *MYB*, *MYC*, *ERG*, *GFI1* (growth factor independent 1), CCND3 (cyclin D3), *CDK6* (cyclin dependent kinase 6), *TAL1* and *NOTCH1*[153]. However and most notably, super-enhancers were also identified near genes with a well-established tumor suppressor function in the pathogenesis of T-ALL, including *ETV6*, *WT1*, *LEF1*, *GATA3* and *RUNX1*[153]. Therefore, identification of super-enhancers seems to provide a snapshot of critical mediators of normal T cell differentiation that can execute both oncogenic as well as tumor suppressive functions in the context of T cell neoplasms. Nevertheless, these analyses on human T-ALL cell lines should be further extended towards a more in-depth and comprehensive characterization of super-enhancers in molecular genetic subgroups of primary human T-ALL and refined subpopulations of normal T cells.

Small molecules targeting BET bromodomains

Over the last years, small molecules that target the binding of acetylated lysines to members of the BET family of proteins have been developed. These acetylated lysine mimetics competitively engage the bromodomain pocket and cause displacement of BRD2, BRD3, BRD4 and BRDT from chromatin. Notably, these pan-BET inhibitors have shown therapeutic effects in a variety of hematological malignancies including AML, multiple myeloma and lymphoma[157]. The anti-tumoral properties of these molecules are at least in part mediated by super-enhancer inhibition near genes that are critically involved in tumor maintenance, such as *MYC* or *BCL2* (B-cell lymphoma 2)[154]. Nevertheless, given the broad impact of BET inhibition on transcriptional regulation, concerns have been raised regarding tolerability and toxicity in humans. Therefore, selective inhibition of individual BET proteins could avoid adverse side effects when these molecules are moved into clinical trials[158]. Notably, elegant studies recently suggested that MYC regulates the leukemia initiating capacity of malignant T cells[156, 159]. Therefore, therapeutic targeting of MYC by BET inhibitors could represent a valuable strategy for targeted therapy in human T-ALL[156, 159, 160]. Indeed, King et al.[156] reported dose-dependent growth inhibition of T-ALL cell lines and primary human T-ALL samples upon treatment with the BET inhibitor JQ1. Moreover, treatment of NOTCH1-driven primary mouse T-ALL using CPI203, a JQ1 derivative with enhanced bioavailability, resulted in rapid reduction of leukemia burden confirming the therapeutic potential of this compound *in vivo*[156]. Importantly, the *in vivo* relevance of pharmacological BRD4 inhibition by JQ1 was further confirmed in immunodeficient mice xenografted with primary human T-ALL[160] and a *Tal1*/*Lmo2* driven murine T-ALL tumor model[159]. Moreover, relapsed or induction failure primary T-ALL cells responded *in vitro* to short-term JQ1 treatment, confirming that BET inhibition could also serve as a valuable therapeutic strategy for clinically challenging subtypes of human T-ALL[159, 161]. Obviously, BET inhibition not only results in *MYC* or *MYCN*

inactivation, but will also affect other prominent T-ALL oncogenes including *IL7R*, *MYB* and *BCL2*[162, 163]. Besides the use of small molecule BRD4 inhibitors as single agents, some studies have also evaluated potential synergisms with other therapeutic agents in the context of T-ALL. For example, the combination of γ-secretase inhibitors, which block NOTCH1 signaling, with JQ1 showed synergistic *in vivo* anti-tumor effects in mice xenografted with primary T-ALLs[164].

All validated BRD4 antagonists interact with one BRD while BET proteins have tandem BRDs. Therefore, bivalent inhibition could increase the potency of the inhibitors. Indeed, Tanaka et al.[165] developed the bivalent BET inhibitor MT1 which showed greater efficacy than JQ1 in leukemia mouse models. In 2015, a new innovative strategy to target the BET family of proteins was published in Science. Instead of inhibiting the BRDs of BET proteins, BET proteins can be targeted for degradation. The authors conjugated a phthalimide moiety to JQ1 and obtained the bifunctional dBET1. Similar to JQ1, dBET1 binds to BET BRDs. Next, the phthalimide moiety hijacks the cereblon E3 ubiquitin ligase and targets the BET protein for proteasomal degradation. Interestingly, dBET1 induced even more pronounced antileukemic effects in human AML cells than JQ1[166].

Several BET bromodomain inhibitors are evaluated in clinical trials for solid tumors and hematological malignancies (Table 6). For example, the small-molecule BRD2/3/4 inhibitor OTX015 is currently evaluated in a phase I dose-escalation clinical trial for acute leukemia. Some patients (3/41) achieved complete remission[167].

Table 6. Overview of BET bromodomain inhibitors in clinical trials. *Clinicaltrials.gov was consulted on 28th of December 2016.*

COMPOUND	CLINICAL TRIAL STAGE
FT-1101	Phase I in AML and myelodysplastic syndrome (MDS)
CPI-0610	Phase I in hematological malignancies Phase II in peripheral nerve sheath tumors
GSK525762 (I-BET762)	Phase I/II in hematological malignancies and solid tumors
ZEN003694	Phase I in prostate cancer
OTX015/MK-8628	Phase I in solid tumors and hematological malignancies Phase II in recurrent glioblastoma multiforme patients
BMS-986158	Phase I/II in solid tumors
GSK2820151	Phase I in solid tumors
TEN-010	Phase I in solid tumors, AML and MDS
BAY1238097	Phase I in solid tumors and lymphoma
INCB057643	Phase I/II in solid tumors and hematological malignancies
INCB054329	Phase I/II in solid tumors and hematological malignancies
RVX000222 (RVX-208, APABETALONE)	Phase III in high-risk type 2 diabetes mellitus subjects with coronary artery disease
GS-5829	Phase I/II in solid tumors and lymphoma
ABBV-075	Phase I in solid tumor and hematological malignancies

3.4. Targeting the lysine demethylase KDM1A as a therapeutic strategy in many cancers

The role of KDM1A in transcriptional regulation

Histone posttranslational modifications, including phosphorylation, acetylation, methylation and ubiquitination, regulate the chromatin structure and the binding of non-histone proteins to regulate gene expression[168]. Methylation of histones is carried out by methyltransferases while demethylases remove methyl groups. The lysine demethylase 1A (KDM1A, synonym LSD1) is an amino oxidase that oxidatively removes the methyl groups from mono- and dimethylated lysine 4 on histone 3 (H3K4me1 and H3K4me2) with the help of its cofactor flavin adenine dinucleotide (FAD). The amine oxidase domain (AOD) of the protein has two sites to bind the methylated substrate and FAD[169, 170]. H3K4 methylation is generally associated with transcriptional activation, with H3K4me3 located at active promoters and H3K4me1 at active enhancers[171]. Therefore, KDM1A acts as a co-repressor by demethylating H3K4 (Figure 8). Interestingly, KDM1A interacts via its Tower domain with interaction partners. Interaction with the CoREST and NuRD complex, which are involved in transcriptional repression, has been described. Remarkably, when KDM1A binds to the androgen (AR) or estrogen (ER) nuclear receptors, its substrate specificity changes to H3K9me1 and H3K9me2[169, 170]. Since methylation of H3K9 is mainly associated with transcriptional silencing[168], KDM1A acts here as a co-activator [169, 170] (Figure 8). Moreover, KDM1A can also be part of the ELL (elongation factor for RNA polymerase II) complex, containing the P-TEFb transcriptional elongation factor, and MLL super-complex[170].

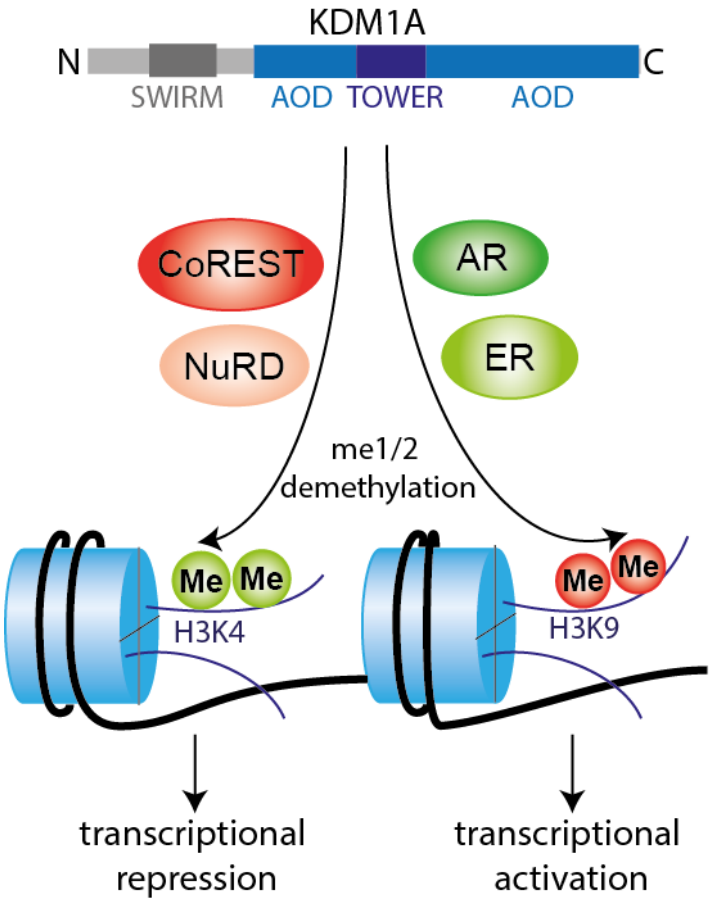

Figure 8. Structure and demethylating activity of KDM1A. *KDM1A contains three protein domains. The SWIRM domain and AOD are together responsible for the enzymatic activity while the TOWER domain is involved in protein interactions. KDM1A catalyzes the demethylation of mono- and dimethylated H3K4 and H3K9. Although H3K4me1 and me2 are the primary substrates, KDM1A can also demethylate H3K9me1 and me2 when it is bound to the androgen (AR) or estrogen receptor (ER). Therefore, KDM1A can act as a transcriptional co-repressor or co-activator depending on its substrate and interaction partners. Figure based on*[170].

Lysine residues at non-histone proteins can also be demethylated by KDM1A. Demethylation of the dimethylated K370 residue of tumor suppressor p53 by KDM1A inhibits the pro-apoptotic activity of p53. Another substrate of KDM1A is MYPT1 (myosin phosphatase target subunit 1), a phosphatase that regulates retinoblastoma protein 1. MYPT1 loses its stability upon demethylation by KDM1A. This may enhance the phosphorylation and consequent inactivation of retinoblastoma protein 1, allowing cell cycle progression. Furthermore, demethylation of DNMT1 by KDM1A protects it from degradation. Likewise, the protein stability of the E2F1 transcription factor increases after demethylation of K185[169, 170].

The activity and function of KDM1A can further be regulated through interactions with proteins, alternative splicing, non-coding RNAs and posttranslational modifications[172]. Phosphorylation[173-175], deacetylation[176] and deubiquitylation[174] of KDM1A have been reported.

KDM1A is also important in developmental processes[170]. The protein is highly expressed and plays a key role in human embryonic stem cells (ESCs). In these cells, KDM1A regulates the balance between self-renewal and differentiation by controlling H3K4 methylation levels of

bivalent domains in the promoters of a subset of developmental genes. KDM1A activity is essential to maintain the silencing of these genes and to keep the cells in an undifferentiated state. During differentiation, KDM1A expression is progressively downregulated[177]. An interesting role for KDM1A at enhancer sites during ESC differentiation was found in mouse ESCs. There, KDM1A binds active enhancers as part of the NuRD complex together with ESC master transcription factors that recruit histone acetyltransferases. However, no demethylation of H3K4 occurs because the activity of KDM1A is inhibited in the presence of acetylated histones. Only during differentiation, when the level of acetylated histones is decreased, KDM1A is able to demethylate H3K4me1 at enhancers of ESC-specific genes[178].

KDM1A is also involved in EMT-related epigenetic reprogramming[179]. Noteworthy, the EMT-inducing transcription factors SNAIL1 and ZEB1 can both recruit KDM1A[88].

Another essential function of KDM1A is controlling the differentiation of several cell types[170]. In the hematopoietic system, KDM1A can be recruited by the homologous transcriptional repressors GFI1 and GFI1B[180] or TAL1[181] to mediate transcriptional repression and to control hematopoietic differentiation. Conditional inactivation of *Kdm1a* in the hematopoietic system of mice fetuses resulted in pancytopenia in newborns while deletion of *Kdm1a* during adult hematopoiesis was associated with a lack of myeloid progenitor cells. Furthermore, a defect in HSC self-renewal and terminal differentiation of granulocytes and erythroid cells was detected in absence of *Kdm1a*[182].

KDM1A in cancer

KDM1A is overexpressed in various solid human cancers, including bladder cancer[183], small cell lung cancer (SCLC)[183], non-small cell lung cancer (NSCLC)[184], prostate cancer[185], ER-negative breast cancer[186], colorectal cancer[183], neuroblastoma[187, 188], oral cancer[189] and cervical cancer[190]. In many of these cancers, an association between high KDM1A expression and shorter survival was found[183-185, 187-189]. Knockdown or pharmacological inhibition of KDM1A decreased cell growth in several cancer cell lines indicating that KDM1A contributes to human carcinogenesis[183, 184, 186, 188, 189]. As mentioned before, KDM1A plays a role in EMT, which can also contribute to the aggressiveness of a cancer. Indeed, Liu et al.[190] observed EMT in cervical cancer upon ectopic expression of KDM1A, resulting in the promotion of invasion and metastasis.

In addition to the solid tumors, KDM1A overexpression was also identified in a substantial part of myeloproliferative neoplasms, myelodysplastic syndromes, AML, chronic myeloid leukemia (CML), ALL and lymphomas[191]. In human AML, translocations involving the methyltransferase *MLL* occur frequently. Harris et al.[192] identified KDM1A as an essential factor to sustain the oncogenic potential of MLL-AF9 AML cells. Knockdown of *Kdm1a* in AML cells from mice with MLL-AF9 leukemia resulted in the loss of their colony-forming cell and leukemic stem cell potential. Moreover, differentiation and apoptosis of the cells was induced. Their work supports a model in which KDM1A acts at genes bound by the MLL-AF9 fusion oncoprotein to maintain low levels of H3K4me2 relative to H3K4me3, allowing transcription required for oncogenic transformation. Upon knockdown of *Kdm1a*, a selective increase of H3K4me2 was observed that was associated with the downregulation of these genes[192]. Finally, inhibition of KDM1A does not only elicit anti-tumor responses in MLL-rearranged AML[192, 193], but also in other AML subtypes[194].

Since *KDM1A* is also strongly expressed in T-cell lymphoblastic leukemia/lymphoma (T-LBL), Wada et al.[195] studied the protein in this context. Of the four known KDM1A isoforms, two were detected in normal human and murine hematopoietic cells and primary T-LBL samples. Overexpression of the shortest human *KDM1A* isoform in mouse bone marrow cells induced the expression of the *HoxA* family and increased the self-renewal of HSCs *in vivo* and *in vitro*. Most notably, overexpression of the shortest human *KDM1A* isoform in a transgenic mouse model led to focal hyperplasia of T lymphocytes but not to hematological malignancies. Nevertheless, irradiation of *KDM1A*-overexpressing mice resulted in the accelerated development of T-LBL compared to control mice, indicating that KDM1A overexpression generates preleukemic HSCs[195]. Other elements pointing towards an important role for KDM1A in T cell leukemogenesis are the described interactions with NOTCH1[196] and TAL1[181, 197], two factors that are often aberrantly activated in T-ALL. KDM1A plays a dual role in NOTCH1 signaling. In the absence of NOTCH1, KDM1A is associated with the CSL-repressor complex and demethylates the activating H3K4me2 mark at NOTCH1-target genes. On the other hand, in the context of the NOTCH-activation complex, the catalytic activity of KDM1A changes to function as a NOTCH1 coactivator that triggers H3K9me2 demethylation[196].

Inhibitors of KDM1A

Plenty of irreversible and reversible KDM1A inhibitors with a wide variety in chemical structures have been developed[198, 199].

The first small molecules that were evaluated as KDM1A inhibitors, were inhibitors of the homologous monoamine oxidase (MAO). Tranylcypromine (2-PCPA) is the most representative one in this category. Tranylcypromine forms a covalent adduct with the FAD cofactor in the active cavity of KDM1A and irreversibly inhibits KDM1A activity. Interestingly, tranylcypromine is able to enhance all-trans-retinoic acid (ATRA)-induced differentiation in AML cells and the combination of these two drugs has a potent anti-leukemic effect *in vivo* and *in vitro*[200]. Later on, more potent and selective derivatives of MAO inactivator based inhibitors were developed[198, 201]. In the study of Harris et al.[192], tranylcypromine and two analogs induced loss of clonogenic potential and differentiation in MLL leukemia cells. Moreover, treatment of mice transplanted with mouse MLL-rearranged AML cells completely blocked the progression of the leukemia into the circulation. Oryzon Genomics and GlaxoSmithKline each have a tranylcypromine derivative, ORY-1001 and GSK2879552 respectively, that entered clinical trials. GSK2879552 was developed and tested on cell lines from different cancer types by Mohammad et al.[202]. Especially the proliferation of SCLC and AML cell lines was inhibited and *in vivo* treatment of SCLC xenografts was promising[202].

An overview of the KDM1A inhibitors that are currently evaluated in clinical trials is given in Table 7. Very recently, a novel irreversible KDM1A inhibitor T-3775440 was published[203]. T-3775440 achieves anti-leukemic and transdifferentiation activity in acute erythroleukemia and acute megakaryoblastic leukemia by disrupting the interaction between KDM1A and GFI1B[203].

Table 7. Overview of KDM1A inhibitors in clinical trials. *clinicaltrials.gov and EU Clinical Trials Register were consulted on 3th of January 2017.*

COMPOUND	WORKING MECHANISM	CLINICAL TRIAL STAGE
TRANYLCYPROMINE (2-PCPA)	MAO inhibitor, forms covalent adduct with FAD	Phase I/II in AML and MDS in combination with ATRA
GSK2879552	Tranylcypromine derivative	Phase I in AML and SCLC
ORY-1001 (RG-6016)	Tranylcypromine derivative	Phase I in acute leukemia
IMG-7289	Not reported	Phase I in AML and MDS in combination with and without ATRA
INCB059872	Not reported	Phase I/II in advanced malignancies

PART III Targeting apoptosis in cancer

1. Apoptosis: programmed cell death

A cell can die in many different ways and this may happen in a controlled or uncontrolled manner. Apoptosis is the major form of programmed cell death. It plays a crucial role in the formation and deletion of structures during development and in the regulation of cell numbers. In addition, apoptosis protects us against unwanted and potentially dangerous cells[204]. The process of apoptosis can be triggered by various stresses such as DNA damage, loss of growth factor signaling, energy stress and hypoxia. Cancer cells also suffer from various apoptosis-inducing stresses, including signaling imbalances resulting from elevated levels of oncogenic signaling, DNA damage linked to hyperproliferation and of course also stresses coming from chemotherapy during treatment. In spite of all these stresses, cancers can often still develop and even resist therapy. Resisting cell death is therefore one of the hallmarks of cancer as previously mentioned in part I. Cancer cells can develop mechanisms to escape apoptosis including upregulation of anti-apoptotic factors and downregulation of pro-apoptotic factors[1, 205].

Apoptosis is mediated by caspases, a class of cysteine proteases. Two distinct but congregating pathways, the intrinsic/mitochondrial pathway and the extrinsic/death receptor-mediated pathway of apoptosis can lead to the activation of caspases (Figure 9). Initiator caspases (caspase-8, -9, and -10) are first activated. In turn, executioner caspases (caspase-3, -6 and -7) are activated via an initiator caspase[206]. These proteases cleave numerous proteins, ultimately resulting in apoptosis characterized by cell shrinkage, nuclear fragmentation, chromatin condensation and membrane blebbing. The dying cell is recognized by phagocytes and cleared[207].

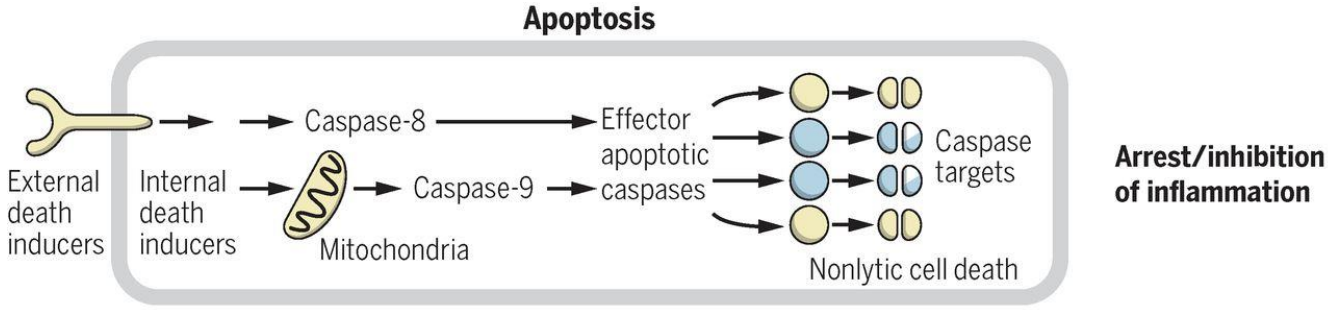

Figure 9. An intrinsic or extrinsic pathway can activate caspases resulting in apoptosis[206].

Since apoptosis is a nonlytic mode of cell death that causes minimal inflammation, it is an attractive target for cancer therapy[208].

2. Intrinsic pathway of apoptosis

2.1. BCL-2 family of proteins governs the intrinsic pathway of apoptosis

The B-cell lymphoma 2 (BCL-2) family of proteins regulates the intrinsic (mitochondrial) pathway of apoptosis and consists of both pro- and anti-apoptotic proteins. The balance between these members determines whether a cell goes into apoptosis or not[209]. All the proteins belonging to the BCL-2 family contain blocks of sequence homology (BH domains). The pro-survival proteins and the pro-apoptotic effectors share four of these BH domains (BH1, BH2, BH3, BH4) while the BH3-only pro-apoptotic family members only have the BH3 domain. The interactions between the family members occur mainly on the mitochondrial outer membrane (MOM). In response to cytotoxic stresses, BH3-only pro-apoptotic proteins are stimulated transcriptionally or post-translationally. Activator BH3-only proteins can directly activate the pro-apoptotic effectors BAX (BCL-2 associated X) and BAK (BCL-2 homologous antagonist/killer) leading to the initiation of apoptosis. The pro-survival proteins can however prevent apoptosis by binding the BH3 domains of the BH3-only proteins or by binding activated BAX or BAK. Furthermore, while sensitizer BH3-only proteins can not activate apoptosis directly, they are able to neutralize the pro-survival proteins (Figure 10). Moreover, there is some selectivity in these interactions. Not all the BH3-only proteins can bind to all the pro-survival proteins and not all the pro-survival proteins are able to interact with BAK[210, 211].

Upon activation, BAX and BAK undergo a conformational change from monomers into homo-oligomers that can permeabilize the MOM[211]. This process is called Mitochondrial Outer Membrane Permeabilization (MOMP) and is, in most cases, a point of no return for cell survival. Apoptogenic proteins are released from the intermembrane space into the cytosol. The binding of cytochrome c (cyt c) to apoptotic protease-activating factor 1 (APAF1) leads to conformational changes and oligomerization and eventually to the formation of the apoptosome. From here, the proteolytic cascade starts with the consecutive activation of initiator and effector caspases (Figure 10).

The well-known tumor suppressor p53 can regulate the expression and activity of BCL-2 family proteins. Stress-activated p53 directly induces transcription of pro-apoptotic factors such as *BAX*, *PUMA* (p53 upregulated modulator of apoptosis) and *NOXA* and represses transcription of anti-apoptotic BCL-2 family genes including *BCL2* and *BCL2-like 1* (*BCL2L1;* encoding BCL-X_L) in some settings. In addition, p53 can also have transcription-independent effects in the cytoplasm. In response to stress, p53 accumulates in the cytosol or mitochondria and interacts with members of the BCL-2 family. It has been suggested that p53 acts like a BH3-only protein. However, the relevance of these transcription-independent activities for p53-mediated apoptosis is under debate[212-215].

Posttranslational modifications add an extra layer of complexity to the regulation of the BCL-2 family members. Phosphorylation of BIM by ERK and AKT targets the protein for proteasomal degradation while phosphorylation by c-JUN enhances its pro-apoptotic activities[216]. MCL-1 (BCL-2 family apoptosis regulator) is stabilized through phosphorylation of the PEST domain by ERK1/2 but this phosphorylation primes MCL-1 for phosphorylation by glycogen synthase kinase-3 beta (GSK3B) which enhances the polyubiquitination and degradation of MCL-1[217]. BCL-2 itself can also be phosphorylated and this happens for

example during mitosis. Phosphorylated BCL-2 binds BIM and BAK with a higher affinity, which enhances its anti-apoptotic activity[218].

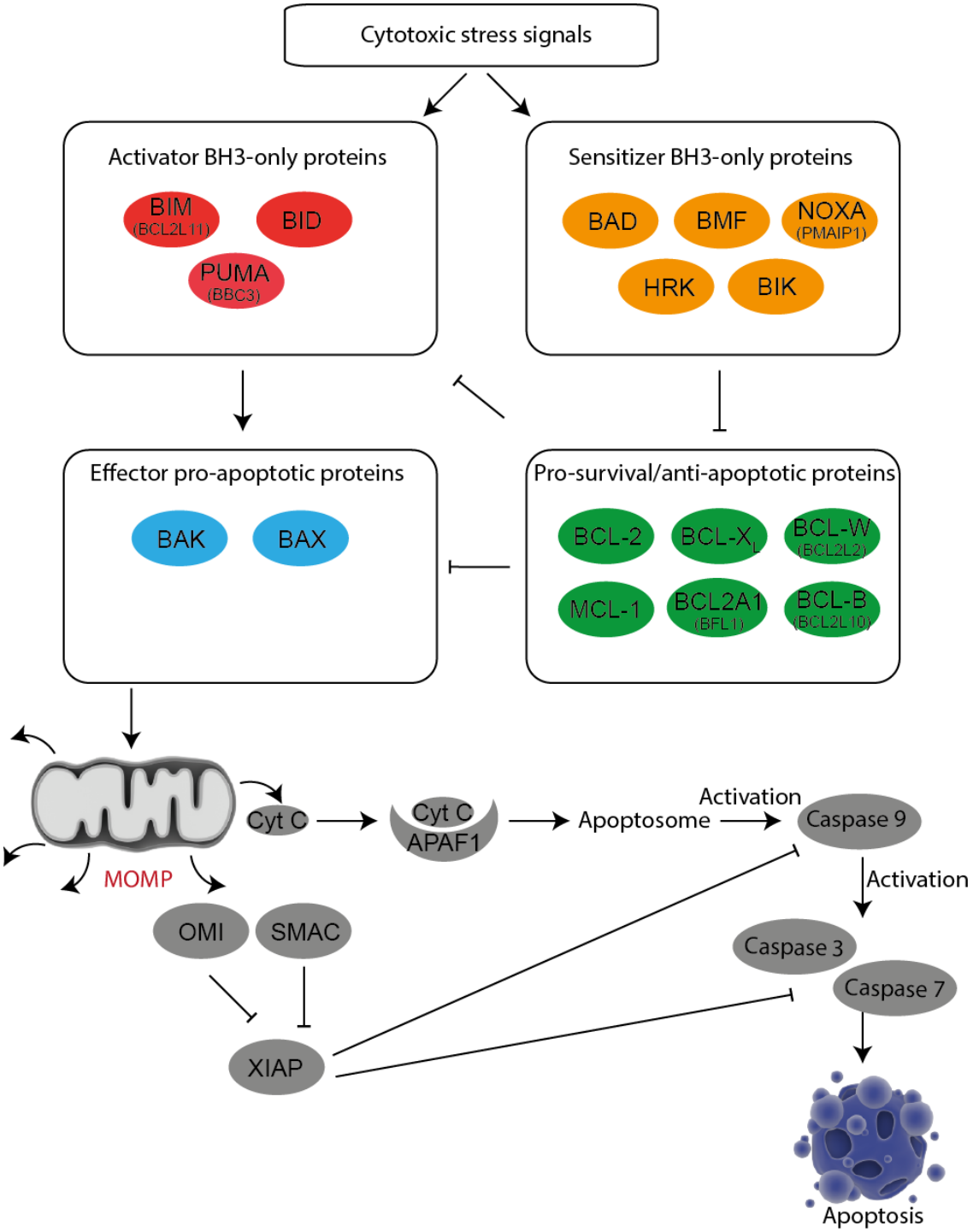

Figure 10. The BCL-2 family of proteins controls the intrinsic (mitochondrial) pathway of apoptosis. *Proteins belonging to the BCL-2 family can be divided into four groups that execute pro- or anti-apoptotic functions. Whether PUMA can function as a real activator, is still under debate. When the effector pro-apoptotic proteins BAX or BAK are activated, mitochondrial outer membrane permeabilization (MOMP) occurs. Apoptogenic factors such as cytochrome c (cyt c), second mitochondria-derived activator of caspase (SMAC) and OMI are released. Cyt c interacts with APAF1, resulting in the formation of the apoptosome and the activation of caspase 9. Caspase 9 activates on its turn the effector caspases 3 and 7, ultimately leading to apoptosis. The release of OMI and SMAC inhibits the caspase inhibitory function of X-linked inhibitor of apoptosis protein (XIAP). Figure is based on*[207, 210, 211].

2.2. BH3 profiling

The group of dr. Anthony Letai developed a technique, called BH3 profiling, that allows to determine how cancer cells evade the intrinsic pathway of apoptosis. The technique uses synthetic peptides that are derived from the BH3 domains of BH3-only proteins. Exposing mitochondria to these peptides and measuring the induction of MOMP gives information about the apoptotic blocks present in the cell[219, 220].

A first way to evade intrinsic apoptotic signaling is the loss of functional BAX and BAK. Cells without functional BAX and BAK are apoptotically incompetent and will not respond to both sensitizer and activator BH3 peptides. Secondly, cells that induce MOMP in response to the addition of activator peptides but not to the addition of sensitizer peptides, have an intact effector arm but are unprimed. This means that the anti-apoptotic proteins in these cells are not occupied by activator BH3-only proteins. Consequently, the binding of sensitizer peptides to the anti-apoptotic proteins will not release activator BH3-only proteins that can activate BAX/BAK. The upstream activation of BH3-only proteins might be inhibited in these cells. Lastly, cells that respond to both activator and sensitizer peptides are primed for apoptosis and they depend on the expression of anti-apoptotic proteins for their survival[220, 221]. Since the anti-apoptotic protein is in primed cells largely occupied by activator BH3-only proteins, adding sensitizer peptides will induce MOMP by competitively binding the anti-apoptotic protein and displacing the activator BH3-only protein[219]. The fact that each anti-apoptotic BCL-2 family member has a selective affinity for the different sensitizer BH3-only proteins makes it possible to determine to which anti-apoptotic BCL-2 family member a cell is addicted. BCL-2 has affinity for BAD (BCL2 associated agonist of cell death) but not for HRK (harakiri) and NOXA, while MCL-1 does not bind BAD and HRK but does bind NOXA. Furthermore, BCL2A1 (BCL2 related protein A1) binds none of the sensitizers except for PUMA while BCL-X_L has a high affinity for HRK. Therefore, depending on the pattern of peptides that are capable to induce MOMP, one can deduce the addiction to a particular anti-apoptotic protein[219].

Over the past years, the technique has evolved and improved. In the beginning, mitochondria had to be isolated to perform the technique[219]. Now, methods that permeabilize the plasma membrane without permeabilizing the mitochondrial membranes are used to allow peptide diffusion into the cell. In addition, instead of measuring the release of apoptogenic factors via antibody staining, ELISA or Western blot, the collapse of the transmembrane mitochondrial potential can be used as a measure for MOMP. The change in the potential can be visualized with potentiometric dyes allowing MOMP to be detected with flow cytometry or plate-based assays[222]. The newest method, intracellular BH3 profiling (iBH3), uses formaldehyde fixation after the exposure to BH3 peptides. By fixing the cells, variance due to the time sensitivity of potential measurements is removed, infectious particles in the sample are killed and samples can be analyzed on a later time point. Upon MOMP, cyt c escapes the mitochondria and also the permeabilized cell while intact mitochondria will stain positively for cyt c, a feature that can be detected with flow cytometry[223].

2.3. Chemotherapy and apoptosis

Cancer cells are often more sensitive to chemotherapeutic agents than normal cells. This can be explained by the fact that they are already closer to the "apoptotic threshold" and "primed for death". As mentioned above, cancer cells endure already death signaling triggered by all the intrinsic stresses they experience. Although anti-apoptotic proteins can sequester these pro-apoptotic factors and prevent cell death, their anti-apoptotic reserve is in the meantime decreased making them more sensitive to chemotherapy. Whether a cell is "primed for death" or not, can be measured using BH3 profiling[210, 219]. Most notably, the clinical response of cancer patients to chemotherapy correlates with the pretreatment proximity of the tumor cells to the apoptotic threshold. Mitochondria from patients with chemosensitive cancer are more "primed for death" than those from chemoresistant cancer and normal tissues[224].

Most conventional chemotherapeutic agents trigger the intrinsic pathway of apoptosis[225]. Nevertheless, it is important to realize that also the extrinsic pathway of apoptosis and even nonapoptotic modes of cell death such as autophagy and necrosis can be responsible for the cell death caused by cytotoxic agents[226]. The conventional chemotherapeutic agents used for the treatment of T-ALL induce DNA damage, microtubule damage or deprive cancer cells of important nutrients. These are all "intrinsic stresses" that can trigger the intrinsic apoptotic pathway[225].

Glucocorticoids directly regulate genes involved in apoptosis. They control gene transcription through activation of the glucocorticoid receptor, which then functions as a transcription factor. The resulting upregulation of *BCL2L11* (encoding BIM) and downregulation of *BCL2* can cause apoptosis. *BCL2L11* is also indirectly upregulated due to the downregulation of the miR17-92 cluster by glucocorticoids[26].

The fact that most chemotherapeutic agents execute their cytotoxic effect via the intrinsic pathway of apoptosis implicates that defects in apoptosis can produce multidrug resistance[225].

2.4. Pathways that contribute to the evasion of apoptosis in T-ALL

The PI3K/AKT/mTOR, IL7R/JAK/STAT and RAS/RAF/MEK/ERK pathway (Figure 11) are frequently hyperactivated in T-ALL. Canté-Barrett et al.[84] identified activating mutations in one of these pathways in 49% of their pediatric T-ALL patients. All three pathways lead to growth and prevention of apoptosis and they can interact and cross-regulate each other[227]. Activation of these pathways helps cancer cells to escape from apoptosis. Consequently, these pathways are interesting to target therapeutically. In addition, overexpression of RBP2 (retinoblastoma-binding protein 2) can upregulate *BCL2* in T-ALL[228].

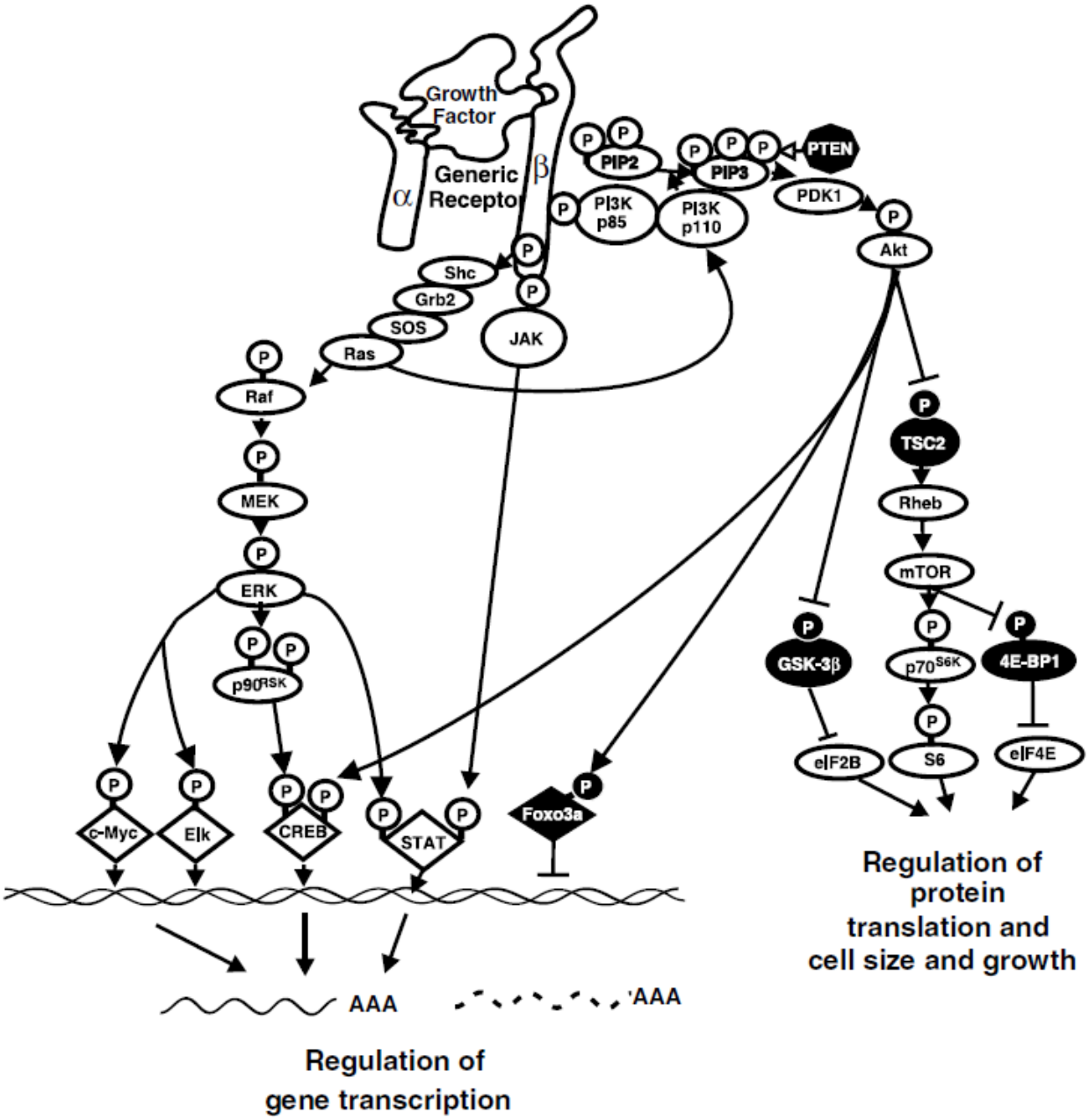

Figure 11. Overview of the PI3K/AKT/mTOR, RAS/RAF/MEK/ERK and JAK/STAT pathway. *The ligation of a growth factor or cytokine to its receptor activates the signaling pathways. Upon activation of RAS, RAF is recruited to the membrane and activated. RAF kinases phophorylate MEK which phophorylates and activates on its turn ERK1 and ERK2. ERK1 and ERK2 phosphorylate and activate a variety of substrates that regulate gene transcription. In addition, RAS can also activate the PI3K/AKT/mTOR pathway. PI3K consists of an 85-kDa regulatory subunit and a 110-kDa catalytic subunit. PI3K converts phosphatidylinositol 4,5-bisphosphate (PIP2) to phosphatidylinositol 3,4,5-trisphosphate (PIP3) which recruits PDK1 and AKT to the plasma membrane. PDK1 phophorylates and activates AKT. Activated AKT phosphorylates numerous proteins that play a role in the regulation of gene transcription or in the regulation of protein translation. mTOR is a key downstream protein that phosphorylates components of the protein synthesis machinery. An important negative regulator of the PI3K/AKT/mTOR pathway is the phosphatase PTEN. Another pathway activated after receptor ligation is the JAK/STAT pathway. Upon activation of cytokine receptors, receptor homodimers and heterodimers are formed which allows transphosphorylation of receptors and the activation of the associated JAKs (JAK1, JAK2, JAK3, TYK2) and STATs (STAT1, STAT2, STAT3, STAT4, STAT5a, STAT5b, STAT6). The phosphorylation of STATs by JAK proteins results in the formation of STAT dimers that move to the nucleus, bind DNA and activate transcription. Phosphorylation events that enhance the activity are shown by a black P in a white circle while phosphorylation events that inhibit activity are visualized by a white P in a black circle. Figure from Steelman et al.*[227]

PI3K/AKT/mTOR pathway

In response to many types of cellular stimuli, the kinase PI3K is activated and converts phosphatidylinositol 4,5-bisphosphate (PIP2) to phosphatidylinositol 3,4,5-trisphosphate (PIP3). PIP3 recruits the serine/threonine kinase AKT to the plasma membrane where it is activated (Figure 11). One of the important downstream target proteins of AKT is the serine/threonine kinase mTOR[229]. This pathway plays a key role in cell survival, apoptosis, drug resistance and many other processes[229] and is frequently hyperactivated in T-ALL[230]. Silva et al.[231] reported PI3K/AKT/mTOR pathway hyperactivation in 87.5% of primary T-ALL samples.

In addition to activating mutations in *PI3K* and *AKT* itself[232, 233], aberrations in phosphatase and tensin homolog (PTEN) lead to an overactivation of the pathway in T-ALL. The phosphatase PTEN is an important tumor suppressor that negatively regulates the PI3K/AKT/mTOR pathway by converting PIP3 to PIP2 (Figure 11). Deletions, mutations or posttranslational mechanisms that inactivate PTEN are frequently found in T-ALL patients[231-234]. Moreover, activating mutations in *NOTCH1*, occuring in more than 50% of T-ALLs[73], and *IL7R*[235, 236] also stimulate the PI3K/AKT/mTOR pathway. NOTCH1 downregulates PTEN via HES1 (hes family bHLH transcription factor 1)[237] while interleukin-7 (IL7)/IL7R is known to activate the PI3K/AKT/mTOR pathway in human thymocytes and T-ALL cells[238, 239].

Oncogenic PI3K/AKT/mTOR signaling can regulate BCL-2 family members. Examples of downstream effects include the direct phosphorylation of BAD (BCL-2 associated agonist of cell death) and BIM by AKT, resulting in inhibition or degradation of the respective pro-apoptotic factor. AKT can also phosphorylate GSK3B which suppresses its ability to phosphorylate MCL-1 and promote the degradation of MCL-1. Furthermore, AKT can repress the expression of *BCL2L11* (encoding BIM), *NOXA* and *PUMA* via phosphorylation of forkhead box O proteins (FOXO) and can upregulate *MCL1* and *BCL2* expression via the activation of cAMP response element-binding protein (CREB). In addition, AKT can activate the E3 ubiquitin-protein ligase MDM2, a negative regulator of p53[161, 227, 240]. PI3K, AKT and mTOR are druggable factors and some of the small molecule inhibitors against them are now evaluated in clinical trials[229]. Also in T-ALL, targeting the PI3K/AKT/mTOR pathway is investigated as a treatment strategy[241-244]. Interestingly, inhibitors working at different levels of the PI3K/AKT/mTOR pathway can show synergistic activities in the context of T-ALL[241]. Indeed, Hall et al.[245] demonstrated the use of the dual PI3K/mTOR inhibitor BEZ235 to enhance the antileukemic effects of glucocorticoids in T-ALL. BEZ235 in combination with dexamethasone was capable to increase BIM levels and induce apoptosis in T-ALL models. Furthermore, in another illustrative study, PI3K/AKT/mTOR signaling was found to be induced in nelarabine-resistant T-ALL cells upon treatment with nelarabine. The combination of pan-PI3K inhibition and nelarabine in resistant T-ALL cell lines resulted in the reduction of BCL-2 and BCL-X_L expression and in the concomitant increase of BAX and BAK expression. Notably, this combination synergistically induced apoptosis in nelarabine-resistant relapsed patient samples[246].

IL7R/JAK/STAT pathway

IL7 is a cytokine produced in the bone marrow and thymus that is required for normal human T cell development. However, the IL7R is also an oncogene since the aberrant activation of IL7R signaling contributes to the development of T-ALL. The two main downstream pathways activated by IL7/IL7R are the JAK/STAT5 and PI3K/AKT/mTOR pathway[247] (Figure 11).

Around 10% of T-ALL patients harbor somatic gain-of-function *IL7R* mutations that lead in most cases to constitutive signaling[235, 236]. Moreover, gain-of-function mutations in the downstream signaling molecules JAK1, JAK3 and STAT5 frequently occur and are mutually exclusive[69, 84, 248]. Especially in ETP-ALL, aberrant activation of the IL7R/JAK/STAT pathway is frequent[249] with about 20% of pediatric ETP-ALL cases harboring activating mutations in *IL7R* or in the downstream *JAK1* and *JAK3*[69]. Interestingly, IL7R/JAK/STAT promotes T-cell survival by inducing the expression of the anti-apoptotic factors BCL-2, MCL-1 and BCL-X_L[248, 250, 251]. Notably, NOTCH1 regulates IL7R and triggers this pathway also[252].

Upregulation of anti-apopotic BCL-2 family members via this pathway can be combat with JAK/STAT pathway inhibitors. In patient-derived murine xenograft models of ETP-ALL, the JAK1/2 inhibitor ruxolitinib displayed strong antileukemic effects[249].

Very recent work of Li et al.[253] described the association of mutations in IL7R signaling molecules (*IL7R*, *JAK1*, *JAK3*, *NF1* (neurofibromin 1), *NRAS*, *KRAS* and *AKT* genes) with steroid resistance and reduced survival in pediatric T-ALL patients. Overexpression of mutant IL7R, JAK1 or NRAS, as well as overexpression of wild-type NRAS or AKT in steroid-sensitive T-ALL cell lines, could indeed render the cells resistant to steroids by upregulating the anti-apoptotic MCL-1 and BCL-X_L and inactivating the pro-apoptotic BIM and its regulator GSK3B. By using small molecule inhibitors that target MEK/ERK or PI3K/AKT/mTOR signaling, the steroid response in most primary T-ALL samples could be increased[253, 254].

RAS/RAF/MEK/ERK pathway

After stimulation of the appropriate receptor by growth factors, cytokines or mitogens, RAS is activated and a kinase cascade is initiated with the RAF, MEK and ERK kinases (Figure 11), resulting in the promotion of cell survival and proliferation[216]. RAS is activated in 50% of T-ALL cases[255] and activating mutations in the pathway (*NRAS*, *KRAS*, *BRAF*, *NF1*, *FLT3* (fms related tyrosine kinase 3) and *PTPN11* (protein tyrosine phosphatase non-receptor type 11)) are recurring in T-ALL[69, 84].

Notably, the RAS/RAF/MEK/ERK pathway regulates the activity of several members of the BCL-2 family. Especially BIM is a key factor downstream of the pathway. Activated ERK1/2 phosphorylates the transcription factor FOXO3A leading to its proteasomal degradation and the prevention of FOXO3A-dependent expression of *BCL2L11* (encoding BIM). Additionally, the direct phosphorylation of BIM by ERK1/2 inhibits the interaction of BIM with BAX and pro-survival proteins and targets BIM for proteasomal degradation[216, 217]. The expression of the anti-apoptotic factors BCL-2, BCL-X_L and MCL-1 is also upregulated by the pathway and the MCL-1 protein is even stabilized through direct phosphorylation by ERK1/2[217].

Interestingly, drugs used in leukemia therapy, such as doxorubicin, can activate the RAS/RAF/MEK/ERK pathway. Treatment with doxorubicin results in the generation of reactive oxygen species (ROS) that can activate the pathway at multiple points. This activation can play a role in drug resistance[216].

Compounds targeting components of the pathway, such as RAF, MEK and ERK inhibitors are available and some are approved for the treatment of *BRAF*-mutant metastatic melanoma[256]. Moreover, the combination of MEK and PI3K-AKT inhibitors exerted synergistic effects on half of the primary T-ALL samples tested by Canté-Barrett et al.[84] and could therefore be a promising therapeutic option in T-ALL.

TYK2/STAT1/BCL2 pathway

A significant fraction of T-ALLs depends on tyrosine kinase 2 (TYK2) for survival. TYK2 is a member of the JAK kinase family and was shown to phosphorylate and activate STAT1 leading to the upregulation of *BCL2* expression. The TYK2/STAT1/BCL2 pathway can be activated by activating *TYK2* mutations, present in about 20% of T-ALL cell lines, or by IL10 signaling (Figure 12). The TYK2-dependent T-ALL cells can be pushed into apoptosis by using JAK kinase inhibitors that also exhibit activity against TYK2[257]. Another interesting therapeutic strategy is to disrupt TYK2 protein stability by pharmacological inhibition of heat shock protein 90 (HSP90) with NVP-AUY922 (AUY922), a small molecule inhibitor that is currently under investigation in clinical trials against several cancers. Treatment of T-ALL cells with AUY922 did not only result in the downregulation of BCL-2, also an upregulation of BIM and BAD was observed[258].

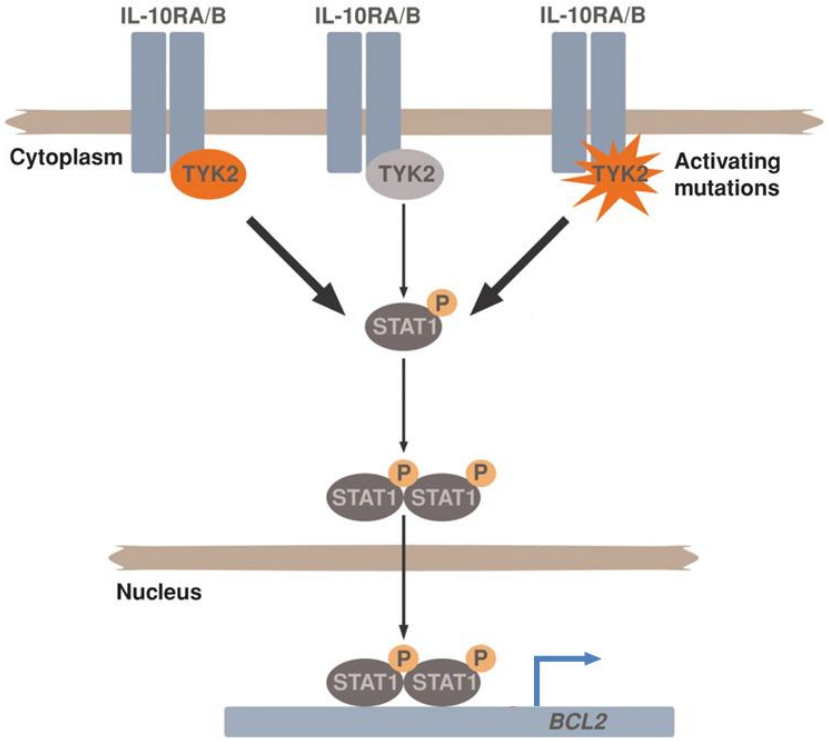

Figure 12. TYK2 signaling in T-ALL upregulates BCL2 expression. *Adapted from Fontan and Melnick[259].*

RBP2

An additional mechanism for the upregulation of *BCL2* in T-ALL was recently discovered. Wang et al.[228] investigated the role of the histone demethylase RBP2 in the context of adult ALL. RBP2, also known as lysine-specific demethylase 5A (KDM5A) or jumonji/ARID domain-containing protein 1A (JARID1A), is a member of the JARID protein family that demethylates tri- and di-methylated lysine 4 of histone H3. High RBP2 expression was found in both *de novo* and relapsed ALL. Notably, *BCL2* was upregulated by RBP2 and identified as a new direct target gene of RBP2[228].

3. Extrinsic pathway of apoptosis

The extrinsic pathway of apoptosis (Figure 13) is initiated by the binding of a ligand to a death receptor (DR). DRs all belong to the tumor necrosis factor (TNF) receptor superfamily and include type 1 TNF receptor (TNFR1), FAS, TNF-related apoptosis-inducing ligand receptor (TRAILR) 1 and 2, DR3 and DR6. These DRs have a cytoplasmic death domain that allows interaction with cytoplasmic adapter proteins. FAS and TRAILR recruit the FAS-associated protein with death domain (FADD) upon ligand binding. In the case of activated TNFR1, the mechanism is more complex. The adapter protein TNFR1-associated death domain protein (TRADD) is first bound which can ultimately also interact with FADD. Subsequently, procaspase-8 and the related procaspase-10 are recruited by FADD and a death-inducing signaling complex is formed resulting in activation of the initiator caspases (Figure 13)[260].

Caspase-8 does not only activate the executioner caspases but also cleaves the BH3-only protein BID which results in the formation of truncated BID (tBID) that can induce MOMP (Figure 13). In this way, the extrinsic and intrinsic pathway of apoptosis are linked. Moreover, MOMP induces the release of SMAC which antagonizes the XIAP-mediated inhibition of the executioner caspases. Some cells require this tBID-induced MOMP to undergo DR-induced apoptosis[260].

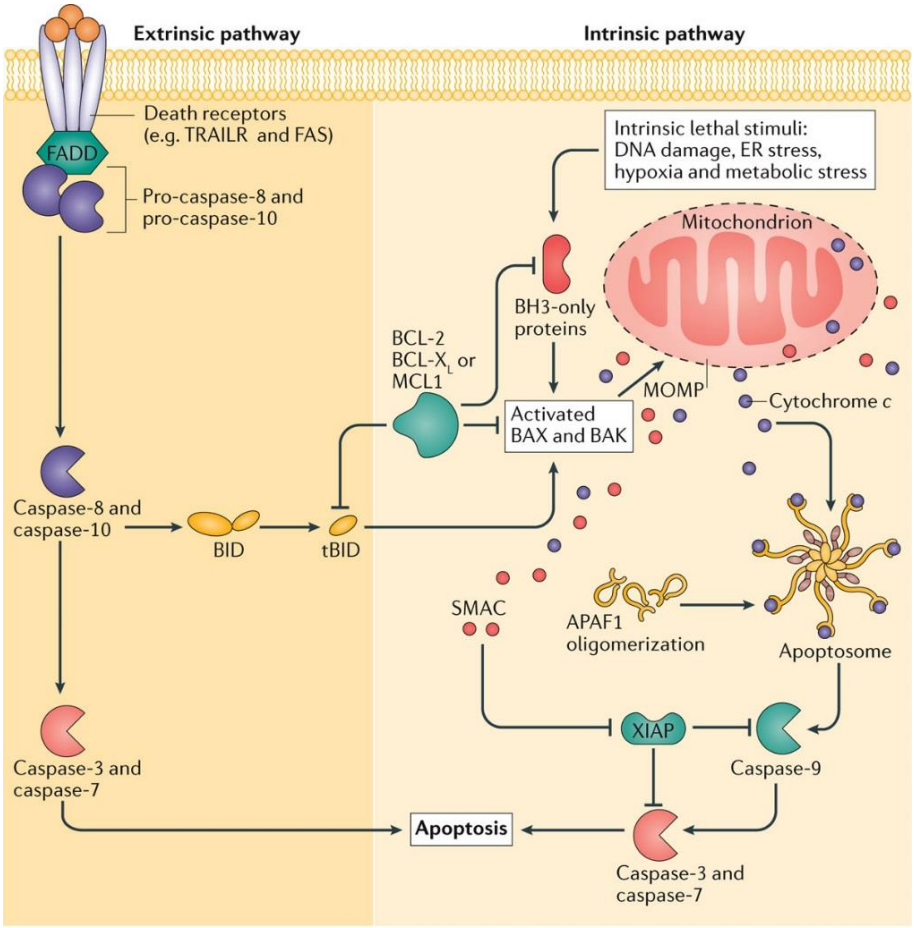

Figure 13. The extrinsic pathway of apoptosis is connected with the intrinsic pathway of apoptosis. *Upon the binding of a ligand to a death receptor, the extrinsic pathway of apoptosis is initiated. The caspase-8-mediated cleavage of BID can induce the intrinsic pathway of apoptosis*[261].

4. Strategies to target apoptosis pathways in cancer

4.1. Targeting the anti-apoptotic BCL-2 family

Instead of targeting the pathways that lead to the upregulation of anti-apoptotic BCL-2 family members, one could also target the anti-apoptotic proteins itself (Table 8).

Antisense oligonucleotides

A first strategy to target anti-apoptotic proteins is the use of antisense oligonucleotides (ASOs). ASOs are oligonucleotides that are complementary to a sequence of a specific mRNA and inhibit its expression by degrading the mRNA via an RNAse H-dependent mechanism or by sterically blocking the initiation of protein translation[262]. Oblimersen sodium (G3139, Genasense), an antisense phophorothioate DNA oligonucleotide targeting the first six codons of human *BCL2* mRNA, showed very promising preclinical results in several cancer types including lymphoma and melanoma[263]. In contrast, clinical trials in solid tumors and hematological malignancies with Oblimersen alone or in combination with conventional agents failed to demonstrate clear clinical benefit[210].

Table 8. Overview of molecules targeting anti-apoptotic BCL-2 family members. *Clinicaltrials.gov was consulted on 28th of December 2016. NHL: non-Hodgkin lymphoma, FL: follicular lymphoma, MM: multiple myeloma, DLBCL: diffuse large B-cell lymphoma, AML: acute myeloid leukemia.*

COMPOUND	TARGET	WORKING MECHANISM	CLINICAL TRIAL STAGE
OBLIMERSEN SODIUM (G3139, GENASENSE)	BCL-2	Antisense oligonucleotide	Phase I, II and III trials in several solid tumors and hematological malignancies have been unconvincing. Not approved by FDA.
AT101 (R(-)-GOSSYPOL)	BCL-2, BCL-X_L, MCL-1	BH3 mimetic	Phase I and II trials in solid and hematological malignancies
OBATOCLAX	BCL-2, BCL-X_L, BCL-W, BCL-B, BFL-1, MCL-1	BH3 mimetic	Phase I and II studies in solid and hematological malignancies
ABT-737	BCL-2, BCL-X_L, BCL-W	BH3 mimetic	Preclinical Poor physiochemical and pharmaceutical properties
ABT-263 (NAVITOCLAX)	BCL-2, BCL-X_L, BCL-W	BH3 mimetic	In phase I and II clinical studies as monotherapy or as part of combination therapies for lymphoid malignancies and solid tumors
ABT-199 (VENETOCLAX, GDC-0199	BCL-2	BH3 mimetic	In clinical studies as monotherapy or as part of combination therapies for NHL, FL, DLBCL, AML, MM FDA approved for CLL patients with 17p deletion and at least one prior therapy
S-055746	BCL-2	BH3 mimetic	Phase I studies in hematological malignancies
PNT-2258	BCL-2	DNAi	Phase I and II studies in solid and hematological malignancies
WEHI-539	BCL-X_L	BH3 mimetic	Preclinical
A-1155463	BCL-X_L	BH3 mimetic	Preclinical
S63845	MCL-1	BH3 mimetic	Preclinical

BH3 mimetics

Another strategy to target these pro-survival proteins is the development of small molecules that mimic the function of BH3-only proteins. These small molecules, called “BH3 mimetics”, bind to and inhibit the anti-apoptotic proteins to prevent the sequestration of pro-apoptotic factors[264]. Gossypol, a compound from cotton seed extracts, was found to inhibit BH3 binding to BCL-X_L in a screen on natural products using NMR-based binding assays and fluorescence polarization displacement assay[265]. Gossypol is a pan-BH3 mimetic with modest affinities to BCL-2, BCL-X_L and MCL-1. The R(-)-gossypol enantiomer (AT-101) has better pro-apoptotic and antitumor activities than the enantiomeric mixture. Nevertheless, AT-101 demonstrated only limited efficacy in clinical trials[266]. Another pan-BH3 mimetic, obatoclax (GX15-070), binds to all the pro-survival BCL-2 family members with modest affinity[267]. Although obatoclax was able to activate the intrinsic pathway of apoptosis in preclinical studies, induction of autophagy and necroptosis were also reported, suggesting the presence of additional targets outside the BCL-2 family[268-271]. Similar to Oblimersen and AT-101, obatoclax showed disappointing results in clinical trials[205, 210, 272].

Besides the molecules identified in screens, several BH3 mimetics were rationally designed to competitively inhibit the binding of pro-apoptotic proteins to the hydrophobic groove of a particular anti-apoptotic protein[210]. The first rationally designed BH3 mimetic was ABT-737, binding BCL-2, BCL-X_L and BCL-W with high affinity[273]. To improve its physiochemical and pharmaceutical properties, ABT-737 was optimized resulting in the orally bioavailable inhibitor ABT-263 that entered clinical trials[274]. An on-target dose-limiting toxicity of compounds targeting BCL-X_L is thrombocytopenia since BCL-X_L plays a critical role in platelet survival[275]. To circumvent this toxicity in cancers that depend on BCL-2, the highly selective BCL-2 inhibitor ABT-199 was developed[276]. Not all the cells that express BCL-2 will be sensitive to treatment by ABT-199. Several studies demonstrated the requirement for BCL-2 complexed to BIM in order to sensitize cells to BCL-2 inhibition by BH3 mimetics[276-278]. In cells where BCL-2 is unoccupied, binding of ABT-199 can reduce the anti-apoptotic reserve but will not likely cause MOMP as a single agent. The situation is different when BCL-2 is occupied by the pro-apoptotic factor BIM. Adding ABT-199 to these cells will displace BIM and induce MOMP (Figure 14)[210].

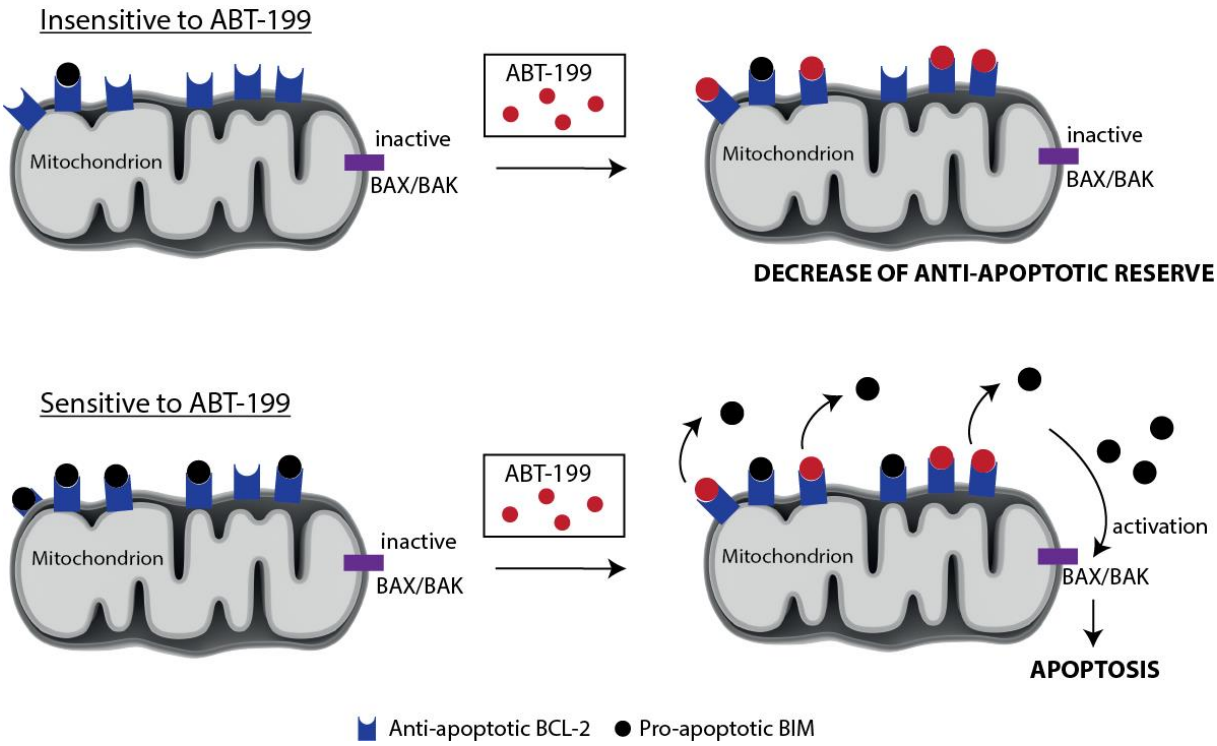

Figure 14. Schematic representation of the effect of ABT-199 in insensitive and sensitive cells. *(Top) In cells with largely unoccupied BCL-2, ABT-199 can bind to BCL-2 but can not release enough pro-apoptotic factors. Therefore, BAX/BAK remains inactive and there is no induction of apoptosis. (Bottom) In cells with a high occupation state of BCL-2, BIM will be released when ABT-199 competes for the BH3 binding site on BCL-2. Next, the released BIM can activate BAX/BAK and induce MOMP. This is true in case that there are no resistance mechanisms like high expression of other anti-apoptotic factors that can sequester the released BIM. Figure based on*[210]*.*

In the first small clinical trial with ABT-199, platelets were indeed spared but patients suffered from tumor lysis syndrome (TLS)[276]. TLS occurs when cancer cells lyse and release their contents into the bloodstream. This leads to hyperkalemia, hyperphosphatemia, hyperuricemia and hypocalcemia and can cause renal insufficiency, cardiac arrhythmias, seizures or even death due to multiorgan failure[279]. ABT-199 is highly effective and destroys cancer cells rapidly. To avoid TLS, stepwise increases in dose (ramp-up) were used in the subsequent clinical trials[280, 281]. A large part (79%) of patients with relapsed or refractory chronic lymphocytic leukemia (CLL) or small lymphocytic lymphoma (SLL) had a response to ABT-199 in a phase I dose escalation study. 20% of the patients even gained complete remission with a monotherapy of ABT-199[280]. ABT-199 received three separate Breakthrough Therapy Designations (BTDs) from the FDA which is exceptional. BTDs allow the FDA to accelerate the review of a drug for serious or life-threatening conditions. ABT-199 was granted a BTD for previously treated patients with CLL with 17p deletion, for patients with relapsed/refractory CLL in combination with rituximab and for the combination with hypomethylating agents for patients with first-line AML who can't receive high-dose chemotherapy. Since April 2016, ABT-199 is FDA-approved for the treatment of patients with CLL with 17p deletion and who have been treated with at least one prior therapy. Another BCL-2 specific inhibitor is S55746, which is currently evaluated in phase I clinical trials[264].

The development of small molecules that specifically target MCL-1 or BCL-X_L has been challenging. Lessene et al.[282] were the first to discover and develop a highly potent and selective BCL-X_L inhibitor, WEHI-539. Soon afterwards, the same group developed the more potent inhibitor A-1155463 with better physicochemical properties than WEHI-539. In addition, they could demonstrate *in vivo* activity and tumor growth inhibition in mice[283]. Very recently, the highly potent and MCL-1-specific inhibitor S63845 was designed and successfully tested in preclinical mouse models of diverse hematological malignancies. Interestingly, S63845 was tolerated in mice at efficacious doses suggesting that a suitable therapeutic window is achievable[284].

DNA interference

A new strategy to target the *BCL2* gene is DNA interference (DNAi). By using single-stranded unmodified sequences of DNA that are complementary to non-coding genomic DNA upstream of gene transcription start sites, gene expression can be modulated. Two possible working mechanisms have been described: binding of the DNA oligonucleotide to noncoding regions of the target gene prevents transcription or the oligonucleotide binds directly to transcription factors preventing the transcription[262].

PNT2258 is a 24-base DNA oligonucleotide sequence that is complementary to a region of the *BCL2* gene and encapsulated in protective amphoteric liposomes[285]. This DNAi therapeutic entered clinical trials.

4.2. SMAC mimetics

XIAP belongs together with the cellular inhibitor of apoptosis proteins (cIAP) and others to the family of inhibitor of apoptosis (IAP) proteins. As mentioned before, XIAP inhibits both the intrinsic and extrinsic pathway of apoptosis by binding and inhibiting caspase-3, -7 and -9. Other members of the IAP family also inhibit apoptosis but are not potent direct inhibitors of caspases. For example, cIAP1 and cIAP2 have a domain that acts as E3 ubiquitin ligase. The ubiquitination carried out by cIAP1 and cIAP2 promotes pro-survival NF-κB signaling pathways and blocks the assembly of pro-apoptotic protein signaling complexes[286, 287].

IAP proteins are overexpressed in various human cancers and are often associated with a poor prognosis. Therefore, a lot of interest exists in developing drugs that target these proteins[286, 287]. As SMAC is an endogenous antagonist of IAP proteins, SMAC mimetics are promising small molecule inhibitors. Several SMAC mimetics are currently evaluated in early clinical trials as monotherapy or as part of combination therapies in solid tumors and leukemias[287].

SMAC mimetics could also be used in the treatment of T-ALL. Hundsdoerfer et al.[288] detected a high expression of XIAP protein in childhood ALL compared to control bone marrow. Notably, increased expression of XIAP was associated with glucocorticoid resistance in T-ALL patients and *in vitro* treatment of ALL cells with a SMAC mimetic increased glucocorticoid-induced apoptosis[288]. Moreover, *ex vivo* drug response profiling of relapsed or refractory ALL cases identified a subset of patients with high sensitivity to the SMAC mimetic birinapant. Complete responses in the blood were even achieved with birinapant in patient-derived xenograft models. Intriguingly, birinapant activated simultaneously apoptosis and necroptosis in the sensitive high-risk ALL samples[289].

4.3. Recombinant TRAIL and TRAIL receptor agonists

TRAIL is the ligand of the death receptors TRAILR1 and TRAILR2 and can induce the extrinsic pathway of apoptosis. Interestingly, a variety of tumor cells are very sensitive to TRAIL-induced apoptosis as opposed to normal cells [290]. TRAIL is therefore a promising candidate for cancer therapeutics. Recombinant human TRAIL proteins and agonistic monoclonal antibodies specific for TRAILR1 and TRAILR2 have been developed and evaluated in many clinical trials for solid cancers. Although strong objective clinical responses have been reported, most patients showed no or only limited responses. In addition, multiple mechanisms of TRAIL resistance have been identified. It will be of crucial importance to find the right combination regimens and to select those patients that will most likely respond[208, 290, 291].

Resistance to *in vitro* treatment with human recombinant TRAIL was found in some human T-ALL cell lines and patient samples. The low expression of TRAILR1 and TRAILR2 in T-ALL can be responsible for this observed resistance[292]. Treatment with GSI resulted in increased TRAILR expression and an enhancement of TRAIL-induced apoptosis in the T-ALL cell line JURKAT[293].

References

1. Hanahan, D. and R.A. Weinberg, *Hallmarks of cancer: the next generation.* Cell, 2011. **144**(5): p. 646-74.
2. Doulatov, S., et al., *Hematopoiesis: a human perspective.* Cell Stem Cell, 2012. **10**(2): p. 120-36.
3. Petrie, H.T. and J.C. Zuniga-Pflucker, *Zoned out: functional mapping of stromal signaling microenvironments in the thymus.* Annu Rev Immunol, 2007. **25**: p. 649-79.
4. Vardiman, J.W., et al., *The 2008 revision of the World Health Organization (WHO) classification of myeloid neoplasms and acute leukemia: rationale and important changes.* Blood, 2009. **114**(5): p. 937-51.
5. Arber, D.A., et al., *The 2016 revision to the World Health Organization classification of myeloid neoplasms and acute leukemia.* Blood, 2016. **127**(20): p. 2391-405.
6. Hunger, S.P. and C.G. Mullighan, *Acute Lymphoblastic Leukemia in Children.* N Engl J Med, 2015. **373**(16): p. 1541-52.
7. Koch, U. and F. Radtke, *Mechanisms of T cell development and transformation.* Annu Rev Cell Dev Biol, 2011. **27**: p. 539-62.
8. Kaatsch, P., *Epidemiology of childhood cancer.* Cancer Treatment Reviews, 2010. **36**(4): p. 277-285.
9. Pui, C.-H., L.L. Robison, and A.T. Look, *Acute lymphoblastic leukaemia.* The Lancet, 2008. **371**(9617): p. 1030-1043.
10. Redaelli, A., et al., *A systematic literature review of the clinical and epidemiological burden of acute lymphoblastic leukaemia (ALL).* Eur J Cancer Care (Engl), 2005. **14**(1): p. 53-62.
11. Pui, C.-H., M.V. Relling, and J.R. Downing, *Acute Lymphoblastic Leukemia.* New England Journal of Medicine, 2004. **350**(15): p. 1535-1548.
12. Registry, B.C., *Cancer in Children and Adolescents*. 2013: Brussels.
13. Van Vlierberghe, P. and A. Ferrando, *The molecular basis of T cell acute lymphoblastic leukemia.* J Clin Invest, 2012. **122**(10): p. 3398-406.
14. Meijerink, J.P.P., *Genetic rearrangements in relation to immunophenotype and outcome in T-cell acute lymphoblastic leukaemia.* Best Practice & Research Clinical Haematology, 2010. **23**(3): p. 307-318.
15. Ferrando, A.A., et al., *Gene expression signatures define novel oncogenic pathways in T cell acute lymphoblastic leukemia.* Cancer Cell, 2002. **1**(1): p. 75-87.
16. Soulier, J., et al., *HOXA genes are included in genetic and biologic networks defining human acute T-cell leukemia (T-ALL).* Blood, 2005. **106**(1): p. 274-86.
17. Homminga, I., et al., *Integrated transcript and genome analyses reveal NKX2-1 and MEF2C as potential oncogenes in T cell acute lymphoblastic leukemia.* Cancer Cell, 2011. **19**(4): p. 484-97.
18. Taghon, T., E. Waegemans, and I. Van de Walle, *Notch signaling during human T cell development.* Curr Top Microbiol Immunol, 2012. **360**: p. 75-97.
19. Bene, M.C., et al., *Proposals for the immunological classification of acute leukemias. European Group for the Immunological Characterization of Leukemias (EGIL).* Leukemia, 1995. **9**(10): p. 1783-6.
20. Dworzak, M.N., et al., *AIEOP-BFM consensus guidelines 2016 for flow cytometric immunophenotyping of Pediatric acute lymphoblastic leukemia.* Cytometry B Clin Cytom, 2017.

21. Gutierrez, A., et al., *Absence of biallelic TCRgamma deletion predicts early treatment failure in pediatric T-cell acute lymphoblastic leukemia.* J Clin Oncol, 2010. **28**(24): p. 3816-23.
22. Zuurbier, L., et al., *Immature MEF2C-dysregulated T-cell leukemia patients have an early T-cell precursor acute lymphoblastic leukemia gene signature and typically have non-rearranged T-cell receptors.* Haematologica, 2014. **99**(1): p. 94-102.
23. Coustan-Smith, E., et al., *Early T-cell precursor leukaemia: a subtype of very high-risk acute lymphoblastic leukaemia.* Lancet Oncol, 2009. **10**(2): p. 147-56.
24. Pui, C.H., et al., *Pediatric acute lymphoblastic leukemia: where are we going and how do we get there?* Blood, 2012. **120**(6): p. 1165-1174.
25. Pui, C.H. and E. Thiel, *Central nervous system disease in hematologic malignancies: historical perspective and practical applications.* Semin Oncol, 2009. **36**(4 Suppl 2): p. S2-S16.
26. Pufall, M.A., *Glucocorticoids and Cancer.* Adv Exp Med Biol, 2015. **872**: p. 315-33.
27. Jordan, M.A., D. Thrower, and L. Wilson, *Mechanism of inhibition of cell proliferation by Vinca alkaloids.* Cancer Res, 1991. **51**(8): p. 2212-22.
28. Lopes, A.M., et al., *Therapeutic l-asparaginase: upstream, downstream and beyond.* Crit Rev Biotechnol, 2015: p. 1-18.
29. Beretta, G.L. and F. Zunino, *Molecular mechanisms of anthracycline activity.* Top Curr Chem, 2008. **283**: p. 1-19.
30. Madondo, M.T., M. Quinn, and M. Plebanski, *Low dose cyclophosphamide: Mechanisms of T cell modulation.* Cancer Treat Rev, 2016. **42**: p. 3-9.
31. Longo-Sorbello, G.S. and J.R. Bertino, *Current understanding of methotrexate pharmacology and efficacy in acute leukemias. Use of newer antifolates in clinical trials.* Haematologica, 2001. **86**(2): p. 121-7.
32. Galmarini, C.M., J.R. Mackey, and C. Dumontet, *Nucleoside analogues: mechanisms of drug resistance and reversal strategies.* Leukemia, 2001. **15**(6): p. 875-90.
33. Pui, C.H. and S. Jeha, *New therapeutic strategies for the treatment of acute lymphoblastic leukaemia.* Nat Rev Drug Discov, 2007. **6**(2): p. 149-65.
34. Litzow, M.R. and A.A. Ferrando, *How I treat T-cell acute lymphoblastic leukemia in adults.* Blood, 2015. **126**(7): p. 833-41.
35. Gokbuget, N., *How I treat older patients with ALL.* Blood, 2013. **122**(8): p. 1366-75.
36. Locatelli, F., et al., *How I treat relapsed childhood acute lymphoblastic leukemia.* Blood, 2012. **120**(14): p. 2807-16.
37. Oriol, A., et al., *Outcome after relapse of acute lymphoblastic leukemia in adult patients included in four consecutive risk-adapted trials by the PETHEMA Study Group.* Haematologica, 2010. **95**(4): p. 589-96.
38. Bhojwani, D. and C.H. Pui, *Relapsed childhood acute lymphoblastic leukaemia.* Lancet Oncol, 2013. **14**(6): p. e205-17.
39. Cohen, M.H., et al., *FDA drug approval summary: nelarabine (Arranon) for the treatment of T-cell lymphoblastic leukemia/lymphoma.* Oncologist, 2008. **13**(6): p. 709-14.
40. Silverman, L.B., *Balancing cure and long-term risks in acute lymphoblastic leukemia.* Hematology Am Soc Hematol Educ Program, 2014. **2014**(1): p. 190-7.
41. Lund, B., et al., *Risk factors for treatment related mortality in childhood acute lymphoblastic leukaemia.* Pediatr Blood Cancer, 2011. **56**(4): p. 551-9.
42. Oeffinger, K.C., et al., *Chronic health conditions in adult survivors of childhood cancer.* N Engl J Med, 2006. **355**(15): p. 1572-82.

43. Pui, C.H., et al., *A revised definition for cure of childhood acute lymphoblastic leukemia.* Leukemia, 2014. **28**(12): p. 2336-43.
44. Pui, C.H. and W.E. Evans, *A 50-year journey to cure childhood acute lymphoblastic leukemia.* Semin Hematol, 2013. **50**(3): p. 185-96.
45. Marks, D.I., et al., *T-cell acute lymphoblastic leukemia in adults: clinical features, immunophenotype, cytogenetics, and outcome from the large randomized prospective trial (UKALL XII/ECOG 2993).* Blood, 2009. **114**(25): p. 5136-45.
46. Bassan, R. and D. Hoelzer, *Modern therapy of acute lymphoblastic leukemia.* J Clin Oncol, 2011. **29**(5): p. 532-43.
47. Dinmohamed, A.G., et al., *Improved survival in adult patients with acute lymphoblastic leukemia in the Netherlands: a population-based study on treatment, trial participation and survival.* Leukemia, 2016. **30**(2): p. 310-7.
48. Pulte, D., et al., *Survival of adults with acute lymphoblastic leukemia in Germany and the United States.* PLoS One, 2014. **9**(1): p. e85554.
49. Rocha, J.M., et al., *Current Strategies for the Detection of Minimal Residual Disease in Childhood Acute Lymphoblastic Leukemia.* Mediterr J Hematol Infect Dis, 2016. **8**(1): p. e2016024.
50. Schrappe, M., et al., *Late MRD response determines relapse risk overall and in subsets of childhood T-cell ALL: results of the AIEOP-BFM-ALL 2000 study.* Blood, 2011. **118**(8): p. 2077-84.
51. Nguyen, K., et al., *Factors influencing survival after relapse from acute lymphoblastic leukemia: a Children's Oncology Group study.* Leukemia, 2008. **22**(12): p. 2142-50.
52. Gokbuget, N., et al., *Outcome of relapsed adult lymphoblastic leukemia depends on response to salvage chemotherapy, prognostic factors, and performance of stem cell transplantation.* Blood, 2012. **120**(10): p. 2032-41.
53. Inukai, T., et al., *Clinical significance of early T-cell precursor acute lymphoblastic leukaemia: results of the Tokyo Children's Cancer Study Group Study L99-15.* Br J Haematol, 2012. **156**(3): p. 358-65.
54. Neumann, M., et al., *Clinical and molecular characterization of early T-cell precursor leukemia: a high-risk subgroup in adult T-ALL with a high frequency of FLT3 mutations.* Blood Cancer J, 2012. **2**(1): p. e55.
55. Ma, M., et al., *Early T-cell precursor leukemia: a subtype of high risk childhood acute lymphoblastic leukemia.* Front Med, 2012. **6**(4): p. 416-20.
56. Jain, N., et al., *Early T-cell precursor acute lymphoblastic leukemia/lymphoma (ETP-ALL/LBL) in adolescents and adults: a high-risk subtype.* Blood, 2016. **127**(15): p. 1863-9.
57. Van Vlierberghe, P., et al., *Prognostic relevance of integrated genetic profiling in adult T-cell acute lymphoblastic leukemia.* Blood, 2013. **122**(1): p. 74-82.
58. Patrick, K., et al., *Outcome for children and young people with Early T-cell precursor acute lymphoblastic leukaemia treated on a contemporary protocol, UKALL 2003.* Br J Haematol, 2014. **166**(3): p. 421-4.
59. Goossens, S. and P. Van Vlierberghe, *Controlling pre-leukemic thymocyte self-renewal.* PLoS Genet, 2014. **10**(12): p. e1004881.
60. Tremblay, C.S. and D.J. Curtis, *The clonal evolution of leukemic stem cells in T-cell acute lymphoblastic leukemia.* Curr Opin Hematol, 2014. **21**(4): p. 320-5.
61. Shlush, L.I., et al., *Identification of pre-leukaemic haematopoietic stem cells in acute leukaemia.* Nature, 2014. **506**(7488): p. 328-33.

62. Gerby, B., et al., *SCL, LMO1 and Notch1 reprogram thymocytes into self-renewing cells.* PLoS Genet, 2014. **10**(12): p. e1004768.
63. McCormack, M.P., et al., *The Lmo2 oncogene initiates leukemia in mice by inducing thymocyte self-renewal.* Science, 2010. **327**(5967): p. 879-83.
64. McCormack, M.P., et al., *Requirement for Lyl1 in a model of Lmo2-driven early T-cell precursor ALL.* Blood, 2013. **122**(12): p. 2093-103.
65. Durinck, K., et al., *Novel biological insights in T-cell acute lymphoblastic leukemia.* Exp Hematol, 2015. **43**(8): p. 625-39.
66. Wolfe, A.L., et al., *RNA G-quadruplexes cause eIF4A-dependent oncogene translation in cancer.* Nature, 2014. **513**(7516): p. 65-70.
67. Schwarzer, A., et al., *Hyperactivation of mTORC1 and mTORC2 by multiple oncogenic events causes addiction to eIF4E-dependent mRNA translation in T-cell leukemia.* Oncogene, 2015. **34**(27): p. 3593-604.
68. De Keersmaecker, K., et al., *Exome sequencing identifies mutation in CNOT3 and ribosomal genes RPL5 and RPL10 in T-cell acute lymphoblastic leukemia.* Nat Genet, 2013. **45**(2): p. 186-90.
69. Zhang, J., et al., *The genetic basis of early T-cell precursor acute lymphoblastic leukaemia.* Nature, 2012. **481**(7380): p. 157-63.
70. Van Vlierberghe, P., et al., *ETV6 mutations in early immature human T cell leukemias.* J Exp Med, 2011. **208**(13): p. 2571-9.
71. Van Vlierberghe, P., et al., *PHF6 mutations in T-cell acute lymphoblastic leukemia.* Nat Genet, 2010. **42**(4): p. 338-42.
72. Sanchez-Martin, M. and A. Ferrando, *The NOTCH1-MYC highway toward T-cell acute lymphoblastic leukemia.* Blood, 2017. **129**(9): p. 1124-1133.
73. Weng, A.P., et al., *Activating mutations of NOTCH1 in human T cell acute lymphoblastic leukemia.* Science, 2004. **306**(5694): p. 269-71.
74. Deangelo, D.J., et al., *A phase I clinical trial of the notch inhibitor MK-0752 in patients with T-cell acute lymphoblastic leukemia/lymphoma (T-ALL) and other leukemias.* Journal of Clinical Oncology, 2006. **24**(18): p. 357s-357s.
75. Papayannidis, C., et al., *A Phase 1 study of the novel gamma-secretase inhibitor PF-03084014 in patients with T-cell acute lymphoblastic leukemia and T-cell lymphoblastic lymphoma.* Blood Cancer J, 2015. **5**: p. e350.
76. Herranz, D., et al., *Metabolic reprogramming induces resistance to anti-NOTCH1 therapies in T cell acute lymphoblastic leukemia.* Nat Med, 2015. **21**(10): p. 1182-9.
77. Chan, S.M., et al., *Notch signals positively regulate activity of the mTOR pathway in T-cell acute lymphoblastic leukemia.* Blood, 2007. **110**(1): p. 278-86.
78. Cullion, K., et al., *Targeting the Notch1 and mTOR pathways in a mouse T-ALL model.* Blood, 2009. **113**(24): p. 6172-81.
79. Real, P.J., et al., *Gamma-secretase inhibitors reverse glucocorticoid resistance in T cell acute lymphoblastic leukemia.* Nat Med, 2009. **15**(1): p. 50-8.
80. Aste-Amezaga, M., et al., *Characterization of Notch1 antibodies that inhibit signaling of both normal and mutated Notch1 receptors.* PLoS One, 2010. **5**(2): p. e9094.
81. Agnusdei, V., et al., *Therapeutic antibody targeting of Notch1 in T-acute lymphoblastic leukemia xenografts.* Leukemia, 2014. **28**(2): p. 278-88.
82. Moellering, R.E., et al., *Direct inhibition of the NOTCH transcription factor complex.* Nature, 2009. **462**(7270): p. 182-8.
83. Roti, G., et al., *Complementary genomic screens identify SERCA as a therapeutic target in NOTCH1 mutated cancer.* Cancer Cell, 2013. **23**(3): p. 390-405.

84. Cante-Barrett, K., et al., *MEK and PI3K-AKT inhibitors synergistically block activated IL7 receptor signaling in T-cell acute lymphoblastic leukemia.* Leukemia, 2016. **30**(9): p. 1832-43.
85. Gheldof, A., et al., *Evolutionary functional analysis and molecular regulation of the ZEB transcription factors.* Cell Mol Life Sci, 2012. **69**(15): p. 2527-41.
86. Sanchez-Tillo, E., et al., *Expanding roles of ZEB factors in tumorigenesis and tumor progression.* Am J Cancer Res, 2011. **1**(7): p. 897-912.
87. Conidi, A., V. van den Berghe, and D. Huylebroeck, *Aptamers and their potential to selectively target aspects of EGF, Wnt/beta-catenin and TGFbeta-smad family signaling.* Int J Mol Sci, 2013. **14**(4): p. 6690-719.
88. Lamouille, S., J. Xu, and R. Derynck, *Molecular mechanisms of epithelial-mesenchymal transition.* Nat Rev Mol Cell Biol, 2014. **15**(3): p. 178-96.
89. Qi, S., et al., *ZEB2 mediates multiple pathways regulating cell proliferation, migration, invasion, and apoptosis in glioma.* PLoS One, 2012. **7**(6): p. e38842.
90. Kahlert, C., et al., *Overexpression of ZEB2 at the invasion front of colorectal cancer is an independent prognostic marker and regulates tumor invasion in vitro.* Clin Cancer Res, 2011. **17**(24): p. 7654-63.
91. Fang, Y., et al., *Protein expression of ZEB2 in renal cell carcinoma and its prognostic significance in patient survival.* PLoS One, 2013. **8**(5): p. e62558.
92. Prislei, S., et al., *Role and prognostic significance of the epithelial-mesenchymal transition factor ZEB2 in ovarian cancer.* Oncotarget, 2015. **6**(22): p. 18966-79.
93. Caramel, J., et al., *A switch in the expression of embryonic EMT-inducers drives the development of malignant melanoma.* Cancer Cell, 2013. **24**(4): p. 466-80.
94. Goossens, S., et al., *The EMT regulator Zeb2/Sip1 is essential for murine embryonic hematopoietic stem/progenitor cell differentiation and mobilization.* Blood, 2011. **117**(21): p. 5620-30.
95. Li, J., et al., *The EMT transcription factor Zeb2 controls adult murine hematopoietic differentiation by regulating cytokine signaling.* Blood, 2016.
96. Goossens, S., et al., *ZEB2 drives immature T-cell lymphoblastic leukaemia development via enhanced tumour-initiating potential and IL-7 receptor signalling.* Nat Commun, 2015. **6**: p. 5794.
97. Bernard, O.A., et al., *A new recurrent and specific cryptic translocation, t(5;14)(q35;q32), is associated with expression of the Hox11L2 gene in T acute lymphoblastic leukemia.* Leukemia, 2001. **15**(10): p. 1495-504.
98. Nagel, S., et al., *The cardiac homeobox gene NKX2-5 is deregulated by juxtaposition with BCL11B in pediatric T-ALL cell lines via a novel t(5;14)(q35.1;q32.2).* Cancer Res, 2003. **63**(17): p. 5329-34.
99. Gutierrez, A., et al., *The BCL11B tumor suppressor is mutated across the major molecular subtypes of T-cell acute lymphoblastic leukemia.* Blood, 2011. **118**(15): p. 4169-73.
100. De Keersmaecker, K., et al., *The TLX1 oncogene drives aneuploidy in T cell transformation.* Nat Med, 2010. **16**(11): p. 1321-7.
101. Hacein-Bey-Abina, S., et al., *Insertional oncogenesis in 4 patients after retrovirus-mediated gene therapy of SCID-X1.* J Clin Invest, 2008. **118**(9): p. 3132-42.
102. Comijn, J., et al., *The two-handed E box binding zinc finger protein SIP1 downregulates E-cadherin and induces invasion.* Mol Cell, 2001. **7**(6): p. 1267-78.
103. Smith, S., et al., *LIM domain only-2 (LMO2) induces T-cell leukemia by two distinct pathways.* PLoS One, 2014. **9**(1): p. e85883.

104. Treanor, L.M., et al., *Interleukin-7 receptor mutants initiate early T cell precursor leukemia in murine thymocyte progenitors with multipotent potential.* J Exp Med, 2014. **211**(4): p. 701-13.
105. Degryse, S., et al., *JAK3 mutants transform hematopoietic cells through JAK1 activation, causing T-cell acute lymphoblastic leukemia in a mouse model.* Blood, 2014. **124**(20): p. 3092-100.
106. Li, H., et al., *The EMT regulator ZEB2 is a novel dependency of human and murine acute myeloid leukemia.* Blood, 2016.
107. Huether, R., et al., *The landscape of somatic mutations in epigenetic regulators across 1,000 paediatric cancer genomes.* Nat Commun, 2014. **5**: p. 3630.
108. Peirs, S., et al., *Epigenetics in T-cell acute lymphoblastic leukemia.* Immunol Rev, 2015. **263**(1): p. 50-67.
109. Grossmann, V., et al., *The molecular profile of adult T-cell acute lymphoblastic leukemia: Mutations in RUNX1 and DNMT3A are associated with poor prognosis in T-ALL.* Genes Chromosomes & Cancer, 2013. **52**(4): p. 410-422.
110. Simon, C., et al., *A key role for EZH2 and associated genes in mouse and human adult T-cell acute leukemia.* Genes Dev, 2012. **26**(7): p. 651-6.
111. Neumann, M., et al., *Whole-exome sequencing in adult ETP-ALL reveals a high rate of DNMT3A mutations.* Blood, 2013. **121**(23): p. 4749-52.
112. Aref, S., et al., *Clinicopathologic Effect of DNMT3A Mutation in Adult T-Cell Acute Lymphoblastic Leukemia.* Clin Lymphoma Myeloma Leuk, 2016. **16**(1): p. 43-8.
113. Ostler, K.R., et al., *Cancer cells express aberrant DNMT3B transcripts encoding truncated proteins.* Oncogene, 2007. **26**(38): p. 5553-63.
114. Kalender Atak, Z., et al., *High accuracy mutation detection in leukemia on a selected panel of cancer genes.* PLoS One, 2012. **7**(6): p. e38463.
115. Zhang, Y., et al., *Mutation analysis of isocitrate dehydrogenase in acute lymphoblastic leukemia.* Genet Test Mol Biomarkers, 2012. **16**(8): p. 991-5.
116. Ntziachristos, P., et al., *Genetic inactivation of the polycomb repressive complex 2 in T cell acute lymphoblastic leukemia.* Nat Med, 2012. **18**(2): p. 298-301.
117. Ntziachristos, P., et al., *Contrasting roles of histone 3 lysine 27 demethylases in acute lymphoblastic leukaemia.* Nature, 2014. **514**(7523): p. 513-7.
118. Moorman, A.V., S. Richards, and C.J. Harrison, *Involvement of the MLL gene in T-lineage acute lymphoblastic leukemia.* Blood, 2002. **100**(6): p. 2273-4.
119. Van Vlierberghe, P., et al., *The recurrent SET-NUP214 fusion as a new HOXA activation mechanism in pediatric T-cell acute lymphoblastic leukemia.* Blood, 2008. **111**(9): p. 4668-80.
120. Mullighan, C.G., et al., *CREBBP mutations in relapsed acute lymphoblastic leukaemia.* Nature, 2011. **471**(7337): p. 235-9.
121. Moreno, D.A., et al., *Differential expression of HDAC3, HDAC7 and HDAC9 is associated with prognosis and survival in childhood acute lymphoblastic leukaemia.* Br J Haematol, 2010. **150**(6): p. 665-73.
122. Gruhn, B., et al., *The expression of histone deacetylase 4 is associated with prednisone poor-response in childhood acute lymphoblastic leukemia.* Leuk Res, 2013. **37**(10): p. 1200-7.
123. Robertson, K.D., *DNA methylation and chromatin - unraveling the tangled web.* Oncogene, 2002. **21**(35): p. 5361-5379.
124. Baylin, S.B. and P.A. Jones, *A decade of exploring the cancer epigenome - biological and translational implications.* Nat Rev Cancer, 2011. **11**(10): p. 726-34.

125. Ribeiro, A.F., et al., *Mutant DNMT3A: a marker of poor prognosis in acute myeloid leukemia.* Blood, 2012. **119**(24): p. 5824-31.
126. Ley, T.J., et al., *DNMT3A mutations in acute myeloid leukemia.* N Engl J Med, 2010. **363**(25): p. 2424-33.
127. Kramer, A.C., et al., *Dnmt3a regulates T-cell development and suppresses T-ALL transformation.* Leukemia, 2017.
128. Shah, M.Y., et al., *DNMT3B7, a truncated DNMT3B isoform expressed in human tumors, disrupts embryonic development and accelerates lymphomagenesis.* Cancer Res, 2010. **70**(14): p. 5840-50.
129. Hackett, J.A., et al., *Germline DNA demethylation dynamics and imprint erasure through 5-hydroxymethylcytosine.* Science, 2013. **339**(6118): p. 448-52.
130. Guo, J.U., et al., *Hydroxylation of 5-methylcytosine by TET1 promotes active DNA demethylation in the adult brain.* Cell, 2011. **145**(3): p. 423-34.
131. Solary, E., et al., *The Ten-Eleven Translocation-2 (TET2) gene in hematopoiesis and hematopoietic diseases.* Leukemia, 2014. **28**(3): p. 485-96.
132. Andersson, A.K., et al., *IDH1 and IDH2 mutations in pediatric acute leukemia.* Leukemia, 2011. **25**(10): p. 1570-7.
133. Shahbazian, M.D. and M. Grunstein, *Functions of site-specific histone acetylation and deacetylation.* Annu Rev Biochem, 2007. **76**: p. 75-100.
134. Blobel, G.A., *CREB-binding protein and p300: molecular integrators of hematopoietic transcription.* Blood, 2000. **95**(3): p. 745-55.
135. Kung, A.L., et al., *Gene dose-dependent control of hematopoiesis and hematologic tumor suppression by CBP.* Genes Dev, 2000. **14**(3): p. 272-7.
136. Sonnemann, J., et al., *Increased activity of histone deacetylases in childhood acute lymphoblastic leukaemia and acute myeloid leukaemia: support for histone deacetylase inhibitors as antileukaemic agents.* Br J Haematol, 2012. **158**(5): p. 664-6.
137. Ferrando, A.A., et al., *Gene expression signatures in MLL-rearranged T-lineage and B-precursor acute leukemias: dominance of HOX dysregulation.* Blood, 2003. **102**(1): p. 262-8.
138. Speleman, F., et al., *A new recurrent inversion, inv(7)(p15q34), leads to transcriptional activation of HOXA10 and HOXA11 in a subset of T-cell acute lymphoblastic leukemias.* Leukemia, 2005. **19**(3): p. 358-66.
139. Dik, W.A., et al., *CALM-AF10+ T-ALL expression profiles are characterized by overexpression of HOXA and BMI1 oncogenes.* Leukemia, 2005. **19**(11): p. 1948-57.
140. Krivtsov, A.V., et al., *H3K79 methylation profiles define murine and human MLL-AF4 leukemias.* Cancer Cell, 2008. **14**(5): p. 355-68.
141. Chen, L., et al., *Abrogation of MLL-AF10 and CALM-AF10-mediated transformation through genetic inactivation or pharmacological inhibition of the H3K79 methyltransferase Dot1l.* Leukemia, 2013. **27**(4): p. 813-22.
142. Okada, Y., et al., *hDOT1L links histone methylation to leukemogenesis.* Cell, 2005. **121**(2): p. 167-78.
143. Nguyen, A.T., et al., *DOT1L, the H3K79 methyltransferase, is required for MLL-AF9-mediated leukemogenesis.* Blood, 2011. **117**(25): p. 6912-22.
144. Okada, Y., et al., *Leukaemic transformation by CALM-AF10 involves upregulation of Hoxa5 by hDOT1L.* Nat Cell Biol, 2006. **8**(9): p. 1017-24.
145. Wagner, E.J. and P.B. Carpenter, *Understanding the language of Lys36 methylation at histone H3.* Nat Rev Mol Cell Biol, 2012. **13**(2): p. 115-26.

146. Wallaert, A., et al., *T-ALL and thymocytes: a message of noncoding RNAs.* J Hematol Oncol, 2017. **10**(1): p. 66.
147. Tsapis, M., et al., *HDAC inhibitors induce apoptosis in glucocorticoid-resistant acute lymphatic leukemia cells despite a switch from the extrinsic to the intrinsic death pathway.* Int J Biochem Cell Biol, 2007. **39**(7-8): p. 1500-9.
148. Shao, N., et al., *Hyper-activation of WNT/beta-catenin signaling pathway mediates anti-tumor effects of histone deacetylase inhibitors in acute T lymphoblastic leukemia.* Leuk Lymphoma, 2012. **53**(9): p. 1769-78.
149. Batova, A., et al., *The histone deacetylase inhibitor AN-9 has selective toxicity to acute leukemia and drug-resistant primary leukemia and cancer cell lines.* Blood, 2002. **100**(9): p. 3319-24.
150. Lu, B.Y., et al., *Decitabine enhances chemosensitivity of early T-cell precursor-acute lymphoblastic leukemia cell lines and patient-derived samples.* Leuk Lymphoma, 2016. **57**(8): p. 1938-41.
151. Muller, S., P. Filippakopoulos, and S. Knapp, *Bromodomains as therapeutic targets.* Expert Rev Mol Med, 2011. **13**: p. e29.
152. Whyte, W.A., et al., *Master transcription factors and mediator establish super-enhancers at key cell identity genes.* Cell, 2013. **153**(2): p. 307-19.
153. Hnisz, D., et al., *Super-enhancers in the control of cell identity and disease.* Cell, 2013. **155**(4): p. 934-47.
154. Loven, J., et al., *Selective inhibition of tumor oncogenes by disruption of super-enhancers.* Cell, 2013. **153**(2): p. 320-34.
155. Wang, H., et al., *NOTCH1-RBPJ complexes drive target gene expression through dynamic interactions with superenhancers.* Proc Natl Acad Sci U S A, 2014. **111**(2): p. 705-10.
156. King, B., et al., *The ubiquitin ligase FBXW7 modulates leukemia-initiating cell activity by regulating MYC stability.* Cell, 2013. **153**(7): p. 1552-66.
157. Shi, J. and C.R. Vakoc, *The mechanisms behind the therapeutic activity of BET bromodomain inhibition.* Mol Cell, 2014. **54**(5): p. 728-36.
158. Filippakopoulos, P. and S. Knapp, *Targeting bromodomains: epigenetic readers of lysine acetylation.* Nat Rev Drug Discov, 2014. **13**(5): p. 337-56.
159. Roderick, J.E., et al., *c-Myc inhibition prevents leukemia initiation in mice and impairs the growth of relapsed and induction failure pediatric T-ALL cells.* Blood, 2014. **123**(7): p. 1040-50.
160. Loosveld, M., et al., *Therapeutic targeting of c-Myc in T-cell acute lymphoblastic leukemia, T-ALL.* Oncotarget, 2014. **5**(10): p. 3168-72.
161. Reynolds, C., et al., *Repression of BIM mediates survival signaling by MYC and AKT in high-risk T-cell acute lymphoblastic leukemia.* Leukemia, 2014.
162. Ott, C.J., et al., *BET bromodomain inhibition targets both c-Myc and IL7R in high-risk acute lymphoblastic leukemia.* Blood, 2012. **120**(14): p. 2843-52.
163. Zuber, J., et al., *An integrated approach to dissecting oncogene addiction implicates a Myb-coordinated self-renewal program as essential for leukemia maintenance.* Genes Dev, 2011. **25**(15): p. 1628-40.
164. Knoechel, B., et al., *An epigenetic mechanism of resistance to targeted therapy in T cell acute lymphoblastic leukemia.* Nat Genet, 2014. **46**(4): p. 364-70.
165. Tanaka, M., et al., *Design and characterization of bivalent BET inhibitors.* Nat Chem Biol, 2016. **12**(12): p. 1089-1096.

166. Winter, G.E., et al., *DRUG DEVELOPMENT. Phthalimide conjugation as a strategy for in vivo target protein degradation.* Science, 2015. **348**(6241): p. 1376-81.
167. Berthon, C., et al., *Bromodomain inhibitor OTX015 in patients with acute leukaemia: a dose-escalation, phase 1 study.* Lancet Haematol, 2016. **3**(4): p. e186-95.
168. Zhang, T., S. Cooper, and N. Brockdorff, *The interplay of histone modifications - writers that read.* EMBO Rep, 2015. **16**(11): p. 1467-81.
169. Rotili, D. and A. Mai, *Targeting Histone Demethylases: A New Avenue for the Fight against Cancer.* Genes Cancer, 2011. **2**(6): p. 663-79.
170. Amente, S., L. Lania, and B. Majello, *The histone LSD1 demethylase in stemness and cancer transcription programs.* Biochim Biophys Acta, 2013. **1829**(10): p. 981-6.
171. Greer, E.L. and Y. Shi, *Histone methylation: a dynamic mark in health, disease and inheritance.* Nat Rev Genet, 2012. **13**(5): p. 343-57.
172. Marabelli, C., B. Marrocco, and A. Mattevi, *The growing structural and functional complexity of the LSD1/KDM1A histone demethylase.* Curr Opin Struct Biol, 2016. **41**: p. 135-144.
173. Feng, J., et al., *Phosphorylation of LSD1 at Ser112 is crucial for its function in induction of EMT and metastasis in breast cancer.* Breast Cancer Res Treat, 2016. **159**(3): p. 443-56.
174. Zhou, A., et al., *Nuclear GSK3beta promotes tumorigenesis by phosphorylating KDM1A and inducing its deubiquitylation by USP22.* Nat Cell Biol, 2016. **18**(9): p. 954-66.
175. Peng, B., et al., *Modulation of LSD1 phosphorylation by CK2/WIP1 regulates RNF168-dependent 53BP1 recruitment in response to DNA damage.* Nucleic Acids Res, 2015. **43**(12): p. 5936-47.
176. Nalawansha, D.A. and M.K. Pflum, *LSD1 Substrate Binding and Gene Expression Are Affected by HDAC1-Mediated Deacetylation.* ACS Chem Biol, 2016.
177. Adamo, A., et al., *LSD1 regulates the balance between self-renewal and differentiation in human embryonic stem cells.* Nat Cell Biol, 2011. **13**(6): p. 652-9.
178. Whyte, W.A., et al., *Enhancer decommissioning by LSD1 during embryonic stem cell differentiation.* Nature, 2012. **482**(7384): p. 221-5.
179. McDonald, O.G., et al., *Genome-scale epigenetic reprogramming during epithelial-to-mesenchymal transition.* Nat Struct Mol Biol, 2011. **18**(8): p. 867-74.
180. Saleque, S., et al., *Epigenetic regulation of hematopoietic differentiation by Gfi-1 and Gfi-1b is mediated by the cofactors CoREST and LSD1.* Mol Cell, 2007. **27**(4): p. 562-72.
181. Hu, X., et al., *LSD1-mediated epigenetic modification is required for TAL1 function and hematopoiesis.* Proc Natl Acad Sci U S A, 2009. **106**(25): p. 10141-6.
182. Kerenyi, M.A., et al., *Histone demethylase Lsd1 represses hematopoietic stem and progenitor cell signatures during blood cell maturation.* Elife, 2013. **2**: p. e00633.
183. Hayami, S., et al., *Overexpression of LSD1 contributes to human carcinogenesis through chromatin regulation in various cancers.* Int J Cancer, 2011. **128**(3): p. 574-86.
184. Lv, T., et al., *Over-expression of LSD1 promotes proliferation, migration and invasion in non-small cell lung cancer.* PLoS One, 2012. **7**(4): p. e35065.
185. Kahl, P., et al., *Androgen receptor coactivators lysine-specific histone demethylase 1 and four and a half LIM domain protein 2 predict risk of prostate cancer recurrence.* Cancer Res, 2006. **66**(23): p. 11341-7.

186. Lim, S., et al., *Lysine-specific demethylase 1 (LSD1) is highly expressed in ER-negative breast cancers and a biomarker predicting aggressive biology.* Carcinogenesis, 2010. **31**(3): p. 512-20.
187. Ambrosio, S., et al., *LSD1 mediates MYCN control of epithelial-mesenchymal transition through silencing of metastatic suppressor NDRG1 gene.* Oncotarget, 2016.
188. Schulte, J.H., et al., *Lysine-specific demethylase 1 is strongly expressed in poorly differentiated neuroblastoma: implications for therapy.* Cancer Res, 2009. **69**(5): p. 2065-71.
189. Wang, Y., et al., *The histone demethylase LSD1 is a novel oncogene and therapeutic target in oral cancer.* Cancer Lett, 2016. **374**(1): p. 12-21.
190. Liu, Y., et al., *LSD1 binds to HPV16 E7 and promotes the epithelial-mesenchymal transition in cervical cancer by demethylating histones at the Vimentin promoter.* Oncotarget, 2016.
191. Niebel, D., et al., *Lysine-specific demethylase 1 (LSD1) in hematopoietic and lymphoid neoplasms.* Blood, 2014. **124**(1): p. 151-2.
192. Harris, W.J., et al., *The histone demethylase KDM1A sustains the oncogenic potential of MLL-AF9 leukemia stem cells.* Cancer Cell, 2012. **21**(4): p. 473-87.
193. Feng, Z., et al., *Pharmacological inhibition of LSD1 for the treatment of MLL-rearranged leukemia.* J Hematol Oncol, 2016. **9**: p. 24.
194. McGrath, J.P., et al., *Pharmacological Inhibition of the Histone Lysine Demethylase KDM1A Suppresses the Growth of Multiple Acute Myeloid Leukemia Subtypes.* Cancer Res, 2016. **76**(7): p. 1975-88.
195. Wada, T., et al., *Overexpression of the shortest isoform of histone demethylase LSD1 primes hematopoietic stem cells for malignant transformation.* Blood, 2015. **125**(24): p. 3731-3746.
196. Yatim, A., et al., *NOTCH1 nuclear interactome reveals key regulators of its transcriptional activity and oncogenic function.* Mol Cell, 2012. **48**(3): p. 445-58.
197. Li, Y., et al., *Dynamic interaction between TAL1 oncoprotein and LSD1 regulates TAL1 function in hematopoiesis and leukemogenesis.* Oncogene, 2012. **31**(48): p. 5007-18.
198. Zheng, Y.C., et al., *A Systematic Review of Histone Lysine-Specific Demethylase 1 and Its Inhibitors.* Med Res Rev, 2015. **35**(5): p. 1032-71.
199. Mould, D.P., et al., *Reversible inhibitors of LSD1 as therapeutic agents in acute myeloid leukemia: clinical significance and progress to date.* Med Res Rev, 2015. **35**(3): p. 586-618.
200. Schenk, T., et al., *Inhibition of the LSD1 (KDM1A) demethylase reactivates the all-trans-retinoic acid differentiation pathway in acute myeloid leukemia.* Nat Med, 2012. **18**(4): p. 605-11.
201. Vianello, P., et al., *Discovery of a Novel Inhibitor of Histone Lysine-Specific Demethylase 1A (KDM1A/LSD1) as Orally Active Antitumor Agent.* J Med Chem, 2016. **59**(4): p. 1501-17.
202. Mohammad, H.P., et al., *A DNA Hypomethylation Signature Predicts Antitumor Activity of LSD1 Inhibitors in SCLC.* Cancer Cell, 2015. **28**(1): p. 57-69.
203. Ishikawa, Y., et al., *A novel LSD1 inhibitor T-3775440 disrupts GFI1B-containing complex leading to transdifferentiation and impaired growth of AML cells.* Mol Cancer Ther, 2016.
204. Fuchs, Y. and H. Steller, *Programmed cell death in animal development and disease.* Cell, 2011. **147**(4): p. 742-58.

205. Hata, A.N., J.A. Engelman, and A.C. Faber, *The BCL2 Family: Key Mediators of the Apoptotic Response to Targeted Anticancer Therapeutics.* Cancer Discov, 2015. **5**(5): p. 475-87.
206. Wallach, D., et al., *Programmed necrosis in inflammation: Toward identification of the effector molecules.* Science, 2016. **352**(6281): p. aaf2154.
207. Tait, S.W. and D.R. Green, *Mitochondria and cell death: outer membrane permeabilization and beyond.* Nat Rev Mol Cell Biol, 2010. **11**(9): p. 621-32.
208. Baig, S., et al., *Potential of apoptotic pathway-targeted cancer therapeutic research: Where do we stand?* Cell Death Dis, 2016. **7**: p. e2058.
209. Juin, P., et al., *Decoding and unlocking the BCL-2 dependency of cancer cells.* Nat Rev Cancer, 2013. **13**(7): p. 455-65.
210. Davids, M.S. and A. Letai, *Targeting the B-cell lymphoma/leukemia 2 family in cancer.* J Clin Oncol, 2012. **30**(25): p. 3127-35.
211. Czabotar, P.E., et al., *Control of apoptosis by the BCL-2 protein family: implications for physiology and therapy.* Nat Rev Mol Cell Biol, 2014. **15**(1): p. 49-63.
212. Green, D.R. and G. Kroemer, *Cytoplasmic functions of the tumour suppressor p53.* Nature, 2009. **458**(7242): p. 1127-30.
213. Hemann, M.T. and S.W. Lowe, *The p53-Bcl-2 connection.* Cell Death Differ, 2006. **13**(8): p. 1256-9.
214. Speidel, D., *Transcription-independent p53 apoptosis: an alternative route to death.* Trends Cell Biol, 2010. **20**(1): p. 14-24.
215. Moll, U.M., et al., *Transcription-independent pro-apoptotic functions of p53.* Curr Opin Cell Biol, 2005. **17**(6): p. 631-6.
216. Steelman, L.S., et al., *Roles of the Ras/Raf/MEK/ERK pathway in leukemia therapy.* Leukemia, 2011. **25**(7): p. 1080-94.
217. Balmanno, K. and S.J. Cook, *Tumour cell survival signalling by the ERK1/2 pathway.* Cell Death Differ, 2009. **16**(3): p. 368-77.
218. Dai, H., et al., *Contribution of Bcl-2 phosphorylation to Bak binding and drug resistance.* Cancer Res, 2013. **73**(23): p. 6998-7008.
219. Certo, M., et al., *Mitochondria primed by death signals determine cellular addiction to antiapoptotic BCL-2 family members.* Cancer Cell, 2006. **9**(5): p. 351-65.
220. Deng, J., et al., *BH3 profiling identifies three distinct classes of apoptotic blocks to predict response to ABT-737 and conventional chemotherapeutic agents.* Cancer Cell, 2007. **12**(2): p. 171-85.
221. Bose, P., V. Gandhi, and M. Konopleva, *Pathways and mechanisms of venetoclax resistance.* Leuk Lymphoma, 2017: p. 1-17.
222. Ryan, J. and A. Letai, *BH3 profiling in whole cells by fluorimeter or FACS.* Methods, 2013. **61**(2): p. 156-64.
223. Ryan, J., et al., *iBH3: simple, fixable BH3 profiling to determine apoptotic priming in primary tissue by flow cytometry.* Biol Chem, 2016. **397**(7): p. 671-8.
224. Ni Chonghaile, T., et al., *Pretreatment mitochondrial priming correlates with clinical response to cytotoxic chemotherapy.* Science, 2011. **334**(6059): p. 1129-33.
225. Johnstone, R.W., A.A. Ruefli, and S.W. Lowe, *Apoptosis: a link between cancer genetics and chemotherapy.* Cell, 2002. **108**(2): p. 153-64.
226. Fulda, S. and K.M. Debatin, *Extrinsic versus intrinsic apoptosis pathways in anticancer chemotherapy.* Oncogene, 2006. **25**(34): p. 4798-811.
227. Steelman, L.S., et al., *Contributions of the Raf/MEK/ERK, PI3K/PTEN/Akt/mTOR and Jak/STAT pathways to leukemia.* Leukemia, 2008. **22**(4): p. 686-707.

228. Wang, X., et al., *RBP2 Promotes Adult Acute Lymphoblastic Leukemia by Upregulating BCL2.* PLoS One, 2016. **11**(3): p. e0152142.
229. Bertacchini, J., et al., *Targeting PI3K/AKT/mTOR network for treatment of leukemia.* Cell Mol Life Sci, 2015. **72**(12): p. 2337-47.
230. Zhao, W.L., *Targeted therapy in T-cell malignancies: dysregulation of the cellular signaling pathways.* Leukemia, 2010. **24**(1): p. 13-21.
231. Silva, A., et al., *PTEN posttranslational inactivation and hyperactivation of the PI3K/Akt pathway sustain primary T cell leukemia viability.* J Clin Invest, 2008. **118**(11): p. 3762-74.
232. Zuurbier, L., et al., *The significance of PTEN and AKT aberrations in pediatric T-cell acute lymphoblastic leukemia.* Haematologica, 2012. **97**(9): p. 1405-13.
233. Gutierrez, A., et al., *High frequency of PTEN, PI3K, and AKT abnormalities in T-cell acute lymphoblastic leukemia.* Blood, 2009. **114**(3): p. 647-50.
234. Mendes, R.D., et al., *PTEN microdeletions in T-cell acute lymphoblastic leukemia are caused by illegitimate RAG-mediated recombination events.* Blood, 2014. **124**(4): p. 567-78.
235. Zenatti, P.P., et al., *Oncogenic IL7R gain-of-function mutations in childhood T-cell acute lymphoblastic leukemia.* Nat Genet, 2011. **43**(10): p. 932-9.
236. Shochat, C., et al., *Gain-of-function mutations in interleukin-7 receptor-alpha (IL7R) in childhood acute lymphoblastic leukemias.* J Exp Med, 2011. **208**(5): p. 901-8.
237. Palomero, T., M. Dominguez, and A.A. Ferrando, *The role of the PTEN/AKT Pathway in NOTCH1-induced leukemia.* Cell Cycle, 2008. **7**(8): p. 965-70.
238. Barata, J.T., et al., *Activation of PI3K is indispensable for interleukin 7-mediated viability, proliferation, glucose use, and growth of T cell acute lymphoblastic leukemia cells.* J Exp Med, 2004. **200**(5): p. 659-69.
239. Johnson, S.E., et al., *IL-7 activates the phosphatidylinositol 3-kinase/AKT pathway in normal human thymocytes but not normal human B cell precursors.* J Immunol, 2008. **180**(12): p. 8109-17.
240. Manning, B.D. and L.C. Cantley, *AKT/PKB signaling: navigating downstream.* Cell, 2007. **129**(7): p. 1261-74.
241. Bressanin, D., et al., *Harnessing the PI3K/Akt/mTOR pathway in T-cell acute lymphoblastic leukemia: eliminating activity by targeting at different levels.* Oncotarget, 2012. **3**(8): p. 811-23.
242. Chiarini, F., et al., *Activity of the novel dual phosphatidylinositol 3-kinase/mammalian target of rapamycin inhibitor NVP-BEZ235 against T-cell acute lymphoblastic leukemia.* Cancer Res, 2010. **70**(20): p. 8097-107.
243. Lynch, J.T., et al., *Identification of differential PI3K pathway target dependencies in T-cell acute lymphoblastic leukemia through a large cancer cell panel screen.* Oncotarget, 2016. **7**(16): p. 22128-39.
244. Simioni, C., et al., *Cytotoxic activity of the novel Akt inhibitor, MK-2206, in T-cell acute lymphoblastic leukemia.* Leukemia, 2012. **26**(11): p. 2336-42.
245. Hall, C.P., C.P. Reynolds, and M.H. Kang, *Modulation of Glucocorticoid Resistance in Pediatric T-cell Acute Lymphoblastic Leukemia by Increasing BIM Expression with the PI3K/mTOR Inhibitor BEZ235.* Clin Cancer Res, 2016. **22**(3): p. 621-32.
246. Lonetti, A., et al., *Improving nelarabine efficacy in T cell acute lymphoblastic leukemia by targeting aberrant PI3K/AKT/mTOR signaling pathway.* J Hematol Oncol, 2016. **9**(1): p. 114.

247. Ribeiro, D., A. Melao, and J.T. Barata, *IL-7R-mediated signaling in T-cell acute lymphoblastic leukemia.* Adv Biol Regul, 2013. **53**(2): p. 211-22.
248. Kontro, M., et al., *Novel activating STAT5B mutations as putative drivers of T-cell acute lymphoblastic leukemia.* Leukemia, 2014. **28**(8): p. 1738-42.
249. Maude, S.L., et al., *Efficacy of JAK/STAT pathway inhibition in murine xenograft models of early T-cell precursor (ETP) acute lymphoblastic leukemia.* Blood, 2015. **125**(11): p. 1759-67.
250. Carrette, F. and C.D. Surh, *IL-7 signaling and CD127 receptor regulation in the control of T cell homeostasis.* Semin Immunol, 2012. **24**(3): p. 209-17.
251. Chetoui, N., et al., *Interleukin-7 promotes the survival of human CD4+ effector/memory T cells by up-regulating Bcl-2 proteins and activating the JAK/STAT signalling pathway.* Immunology, 2010. **130**(3): p. 418-26.
252. Gonzalez-Garcia, S., et al., *CSL-MAML-dependent Notch1 signaling controls T lineage-specific IL-7R{alpha} gene expression in early human thymopoiesis and leukemia.* J Exp Med, 2009. **206**(4): p. 779-91.
253. Li, Y., et al., *IL-7 Receptor Mutations and Steroid Resistance in Pediatric T cell Acute Lymphoblastic Leukemia: A Genome Sequencing Study.* PLoS Med, 2016. **13**(12): p. e1002200.
254. Goossens, S. and P. Van Vlierberghe, *Overcoming Steroid Resistance in T Cell Acute Lymphoblastic Leukemia.* PLoS Med, 2016. **13**(12): p. e1002208.
255. von Lintig, F.C., et al., *Ras activation in normal white blood cells and childhood acute lymphoblastic leukemia.* Clin Cancer Res, 2000. **6**(5): p. 1804-10.
256. Samatar, A.A. and P.I. Poulikakos, *Targeting RAS-ERK signalling in cancer: promises and challenges.* Nat Rev Drug Discov, 2014. **13**(12): p. 928-42.
257. Sanda, T., et al., *TYK2-STAT1-BCL2 pathway dependence in T-cell acute lymphoblastic leukemia.* Cancer Discov, 2013. **3**(5): p. 564-77.
258. Akahane, K., et al., *HSP90 inhibition leads to degradation of the TYK2 kinase and apoptotic cell death in T-cell acute lymphoblastic leukemia.* Leukemia, 2016. **30**(1): p. 219-28.
259. Fontan, L. and A. Melnick, *Discovering what makes STAT signaling TYK in T-ALL.* Cancer Discov, 2013. **3**(5): p. 494-6.
260. Walczak, H., *Death receptor-ligand systems in cancer, cell death, and inflammation.* Cold Spring Harb Perspect Biol, 2013. **5**(5): p. a008698.
261. Ichim, G. and S.W.G. Tait, *A fate worse than death: apoptosis as an oncogenic process.* Nature Reviews Cancer, 2016. **16**(8): p. 539-548.
262. Ebrahim, A.S., et al., *Hematologic malignancies: newer strategies to counter the BCL-2 protein.* J Cancer Res Clin Oncol, 2016. **142**(9): p. 2013-22.
263. Dias, N. and C.A. Stein, *Potential roles of antisense oligonucleotides in cancer therapy. The example of Bcl-2 antisense oligonucleotides.* Eur J Pharm Biopharm, 2002. **54**(3): p. 263-9.
264. Delbridge, A.R., et al., *Thirty years of BCL-2: translating cell death discoveries into novel cancer therapies.* Nat Rev Cancer, 2016. **16**(2): p. 99-109.
265. Kitada, S., et al., *Discovery, characterization, and structure-activity relationships studies of proapoptotic polyphenols targeting B-cell lymphocyte/leukemia-2 proteins.* J Med Chem, 2003. **46**(20): p. 4259-64.
266. Billard, C., *BH3 mimetics: status of the field and new developments.* Mol Cancer Ther, 2013. **12**(9): p. 1691-700.

267. Zhai, D., et al., *Comparison of chemical inhibitors of antiapoptotic Bcl-2-family proteins.* Cell Death Differ, 2006. **13**(8): p. 1419-21.
268. Konopleva, M., et al., *Mechanisms of antileukemic activity of the novel Bcl-2 homology domain-3 mimetic GX15-070 (obatoclax).* Cancer Res, 2008. **68**(9): p. 3413-20.
269. McCoy, F., et al., *Obatoclax induces Atg7-dependent autophagy independent of beclin-1 and BAX/BAK.* Cell Death Dis, 2010. **1**: p. e108.
270. Vogler, M., et al., *Different forms of cell death induced by putative BCL2 inhibitors.* Cell Death Differ, 2009. **16**(7): p. 1030-9.
271. Urtishak, K.A., et al., *Potent obatoclax cytotoxicity and activation of triple death mode killing across infant acute lymphoblastic leukemia.* Blood, 2013. **121**(14): p. 2689-703.
272. Vela, L. and I. Marzo, *Bcl-2 family of proteins as drug targets for cancer chemotherapy: the long way of BH3 mimetics from bench to bedside.* Curr Opin Pharmacol, 2015. **23**: p. 74-81.
273. Oltersdorf, T., et al., *An inhibitor of Bcl-2 family proteins induces regression of solid tumours.* Nature, 2005. **435**(7042): p. 677-81.
274. Tse, C., et al., *ABT-263: a potent and orally bioavailable Bcl-2 family inhibitor.* Cancer Res, 2008. **68**(9): p. 3421-8.
275. Zhang, H., et al., *Bcl-2 family proteins are essential for platelet survival.* Cell Death Differ, 2007. **14**(5): p. 943-51.
276. Souers, A.J., et al., *ABT-199, a potent and selective BCL-2 inhibitor, achieves antitumor activity while sparing platelets.* Nat Med, 2013. **19**(2): p. 202-8.
277. Del Gaizo Moore, V., et al., *Chronic lymphocytic leukemia requires BCL2 to sequester prodeath BIM, explaining sensitivity to BCL2 antagonist ABT-737.* J Clin Invest, 2007. **117**(1): p. 112-21.
278. Merino, D., et al., *Bcl-2, Bcl-x(L), and Bcl-w are not equivalent targets of ABT-737 and navitoclax (ABT-263) in lymphoid and leukemic cells.* Blood, 2012. **119**(24): p. 5807-16.
279. Howard, S.C., D.P. Jones, and C.H. Pui, *The tumor lysis syndrome.* N Engl J Med, 2011. **364**(19): p. 1844-54.
280. Roberts, A.W., et al., *Targeting BCL2 with Venetoclax in Relapsed Chronic Lymphocytic Leukemia.* N Engl J Med, 2016. **374**(4): p. 311-322.
281. *Venetoclax Yields Strong Responses in CLL.* Cancer Discov, 2016. **6**(2): p. 113-4.
282. Lessene, G., et al., *Structure-guided design of a selective BCL-X(L) inhibitor.* Nat Chem Biol, 2013. **9**(6): p. 390-7.
283. Tao, Z.F., et al., *Discovery of a Potent and Selective BCL-XL Inhibitor with in Vivo Activity.* ACS Med Chem Lett, 2014. **5**(10): p. 1088-93.
284. Kotschy, A., et al., *The MCL1 inhibitor S63845 is tolerable and effective in diverse cancer models.* Nature, 2016. **538**(7626): p. 477-482.
285. Rodrigueza, W.V., et al., *Development and antitumor activity of a BCL-2 targeted single-stranded DNA oligonucleotide.* Cancer Chemother Pharmacol, 2014. **74**(1): p. 151-66.
286. Fulda, S. and D. Vucic, *Targeting IAP proteins for therapeutic intervention in cancer.* Nat Rev Drug Discov, 2012. **11**(2): p. 109-24.
287. Fulda, S., *Promises and Challenges of Smac Mimetics as Cancer Therapeutics.* Clin Cancer Res, 2015. **21**(22): p. 5030-6.

288. Hundsdoerfer, P., et al., *XIAP expression is post-transcriptionally upregulated in childhood ALL and is associated with glucocorticoid response in T-cell ALL.* Pediatr Blood Cancer, 2010. **55**(2): p. 260-6.
289. McComb, S., et al., *Activation of concurrent apoptosis and necroptosis by SMAC mimetics for the treatment of refractory and relapsed ALL.* Sci Transl Med, 2016. **8**(339): p. 339ra70.
290. Amarante-Mendes, G.P. and T.S. Griffith, *Therapeutic applications of TRAIL receptor agonists in cancer and beyond.* Pharmacol Ther, 2015. **155**: p. 117-31.
291. Dimberg, L.Y., et al., *On the TRAIL to successful cancer therapy? Predicting and counteracting resistance against TRAIL-based therapeutics.* Oncogene, 2013. **32**(11): p. 1341-50.
292. Akahane, K., et al., *Resistance of T-cell acute lymphoblastic leukemia to tumor necrosis factor--related apoptosis-inducing ligand-mediated apoptosis.* Exp Hematol, 2010. **38**(10): p. 885-95.
293. Greene, L.M., S.M. Nathwani, and D.M. Zisterer, *Inhibition of gamma-secretase activity synergistically enhances tumour necrosis factor-related apoptosis-inducing ligand induced apoptosis in T-cell acute lymphoblastic leukemia cells via upregulation of death receptor 5.* Oncol Lett, 2016. **12**(4): p. 2900-2905.

CHAPTER 2
Research objectives

Research objectives

Although the overall survival rates of children diagnosed with ALL are nowadays reaching 85%, there is still a substantial part of children that does not respond to therapy or relapses and presents therefore with very dismal survival perspectives. For adults, the survival rates are lower and risk of relapse higher. Moreover, the current high-dose multi-agent chemotherapy treatment schedules are very intensive and are associated with acute and long-term side effects. Therefore, there is an urgent need for more effective and less toxic therapies for the treatment of ALL.

In the lab of Prof. Pieter Van Vlierberghe, we focus on T-cell acute lymphoblastic leukemia which accounts for 15% of childhood and 25% of adult ALL cases. By in-depth investigation of genetic and epigenetic alterations in T-ALL, a better understanding of the disease can be obtained. Unraveling the pathways and biological processes related to these alterations can lead to the identification of new druggable targets and eventually to the development of therapies that are less toxic and more effective than the current ones. The aim of this thesis was to gain novel molecular insights in the disease and to evaluate novel molecular therapies for the treatment of T-ALL. Moreover, the main focus was on early immature T-ALLs because this subgroup has been associated with a poor prognosis and is therefore in need of more effective treatment strategies. The objectives of this research were:

Objective 1: Evaluate BCL-2 inhibition as a novel therapy in T-ALL
The early immature T-ALL subgroup shows a high genetic diversity, making it difficult to find a common genetic alteration that can be targeted to treat patients with this disease. Therefore, we analysed gene expression profiles of T-ALL patients to discover genes that are differentially expressed in these early immature T-ALL patients compared to other subtypes. The finding that the anti-apoptotic factor *BCL2* was overexpressed in the early immature group of T-ALL urged us to test BCL-2 inhibition as a novel therapy in human T-ALL (**paper 1, Blood 2014**). For this purpose, the potent and selective BCL-2 inhibitor ABT-199 (Venetoclax) was used. The antileukemic effects of ABT-199 were evaluated in several T-ALL subtypes by using a panel of human T-ALL cell lines and primary patient samples. Furthermore, using a xenograft mouse model, its potential for the treatment of T-ALL could also be proven *in vivo*.

Objective 2: Identification of successful combination therapies with the BCL-2 inhibitor ABT-199 in T-ALL
After the encouraging results with ABT-199 as monotherapy in T-ALL, research on this topic was continued. Since monotherapy with a drug always raises the concern of resistance, synergistic combination therapies with ABT-199 were searched for. In a first step, combinations with conventional chemotherapeutic agents were tested to investigate whether adding BCL-2 inhibitors to the current treatment schedule could be useful (**paper 1, Blood 2014**). Second, a screen in primary patient samples was performed in which ABT-199 was combined with several clinically relevant drugs. The BET bromodomain inhibitor JQ1 was identified as the most promising combination with ABT-199. Subsequently, this combination was thoroughly investigated, both in T-ALL cell lines and primary patient samples as well as in xenograft models. Moreover, the working mechanism of JQ1 was studied and mechanistic insights in the synergism were obtained (**paper 2, Leukemia 2017**).

Objective 3: Identification of the interaction partners of the oncogenic transcription factor ZEB2 in T-ALL

Early immature T-ALLs express high levels of *ZEB2* compared to other T-ALL subtypes. Moreover, ZEB2 is an oncogenic driver of early immature T-ALL. ZEB2 has several domains that mediate protein-protein interactions and these interactions with other transcription factors or cofactors play an important role in determining its function. Therefore, identifying the interaction partners of ZEB2 in the context of T-ALL could help to clarify how ZEB2 contributes to the development of T-ALL. Furthermore, targeting interaction partners that are essential for ZEB2's oncogenic properties could potentially be used as a novel therapy to treat ZEB2-positive T-ALL. In our study, we identified the interaction partners of ZEB2 via protein complex pull-down experiments on nuclear extracts of Zeb2-overexpressing mouse T-ALL cell lines (**paper 3, Blood 2017**).

Objective 4: Evaluation of the pharmacological inhibition of the interaction partner KDM1A as a novel therapy in ZEB2-positive T-ALL

One of the newly identified interaction partners of ZEB2, was the lysine demethylase 1A (KDM1A). Also in the human T-ALL cell line LOUCY, a cell line characterized by high *ZEB2* levels and a transcriptional profile resembling early immature T-ALLs, this interaction was confirmed. Since KDM1A is a druggable target for which specific inhibitors are available and being tested in clinical trials, we decided to determine the efficacy of KDM1A inhibition in T-ALL. The sensitivity of ZEB2-positive and –negative cells to the KDM1A-specific inhibitor GSK2879552 was evaluated in mouse and human T-ALL cell lines. Finally, xenograft mouse models were used to study the *in vivo* effects of GSK2879552 in T-ALL (**paper 3, Blood 2017**).

CHAPTER 3
Results

PART I The BCL-2 inhibitor ABT-199 as monotherapy and part of combination therapies for the treatment of T-ALL

Paper 1: ABT-199 mediated inhibition of BCL-2 as a novel therapeutic strategy in T-cell acute lymphoblastic leukemia (published in Blood, 2014)

Paper 2: Targeting BET proteins improves the therapeutic efficacy of BCL-2 inhibition in T-cell acute lymphoblastic leukemia (published in Leukemia, 2017)

Paper 1

ABT-199 MEDIATED INHIBITION OF BCL-2 AS A NOVEL THERAPEUTIC STRATEGY IN T-CELL ACUTE LYMPHOBLASTIC LEUKEMIA

Sofie Peirs[1], Filip Matthijssens[1], Steven Goossens[2], Inge Van de Walle[3], Katia Ruggero[4], Charles E. de Bock[5], Sandrine Degryse[5], Kirsten Canté-Barrett[6], Delphine Briot[7], Emmanuelle Clappier[7], Tim Lammens[8], Barbara De Moerloose[8], Yves Benoit[8], Bruce Poppe[1], Jules Meijerink[6], Jan Cools[5], Jean Soulier[7], Terence H. Rabbitts[4], Tom Taghon[3], Frank Speleman[1] and Pieter Van Vlierberghe[1]

[1]Center for Medical Genetics, Ghent University, Ghent, Belgium

[2]VIB Inflammation Research Center, Ghent University, Ghent, Belgium

[3]Department of Clinical Chemistry, Microbiology and Immunology, Ghent University, Ghent, Belgium

[4]MRC Molecular Haematology Unit, Weatherall Institute of Molecular Medicine, University of Oxford, John Radcliffe Hospital, Oxford, United Kingdom

[5]Laboratory for the Molecular Biology of Leukemia, Center for Human Genetics, KU Leuven and Center for the Biology of Disease, VIB, Leuven, Belgium

[6]Department of Pediatric Oncology/Hematology, Erasmus Medical Center, Rotterdam, The Netherlands

[7]Genome Rearrangements and Cancer Laboratory, U462 INSERM, Laboratoire Central d'Hématologie and Institut Universitaire d'Hématologie, Hopital Saint-Louis, France

[8]Department of Pediatric Hematology-Oncology and Stem Cell Transplantation, Ghent University Hospital, Ghent, Belgium

Published in BLOOD, 11 December 2014; volume 124; number 25; page 3738-3747

Key Point

High levels of the anti-apoptotic factor BCL-2 can be therapeutically exploited by the BH3 mimetic ABT-199 in human T-ALL.

Abstract

T-cell acute lymphoblastic leukemia (T-ALL) is a high-risk subtype of ALL with gradually improved survival through introduction of intensified chemotherapy. However, therapy-resistant or refractory T-ALL remains a major clinical challenge. Here, we evaluated BCL-2 inhibition by the BH3 mimetic ABT-199 as a new therapeutic strategy in human T-ALL. The T-ALL cell line LOUCY, which shows a transcriptional program related to immature T-ALL, exhibited high *in vitro* and *in vivo* sensitivity for ABT-199 in correspondence with high levels of BCL-2. In addition, ABT-199 showed synergistic therapeutic effects with different chemotherapeutic agents including doxorubicin, L-asparaginase and dexamethasone. Furthermore, *in vitro* analysis of primary patient samples indicated that some immature, *TLX3*- or *HOXA*- positive primary T-ALLs are highly sensitive to BCL-2 inhibition, whereas *TAL1* driven tumors mostly showed poor ABT-199 responses. Because *BCL-2* shows high expression in early T-cell precursors and gradually decreases during normal T-cell differentiation, differences in ABT-199 sensitivity could partially be mediated by distinct stages of differentiation arrest between different molecular genetic subtypes of human T-ALL. In conclusion, our study highlights BCL-2 as an attractive molecular target in specific subtypes of human T-ALL that could be exploited by ABT-199.

Introduction

T-cell acute lymphoblastic leukemia (T-ALL) is an aggressive hematological cancer that occurs in children and adolescents. Despite significant insights in T-ALL biology, only limited therapeutic options are available for patients with primary resistant or relapsed disease**.** Current T-ALL treatment schedules consist of high-dose chemotherapy and are often associated with acute and chronic life-threatening and debilitating toxicities[1-3]. Consequently, there is an urgent clinical need for optimized treatment stratification and more effective antileukemic drugs for the treatment of human T-ALL[3].

Genetic studies have collectively shown that T-ALLs can be divided into subgroups that are characterized by unique gene expression signatures and relate to stages of T-cell differentiation at which the leukemic cells arrest. Each molecular subgroup has characteristic genetic abnormalities that cause aberrant activation of specific T-ALL transcription factor oncogenes, including *LYL1*/*MEF2C*, *HOXA*, *TLX1*, *TLX3* and *TAL1/LMO2* driven T-ALL[3-6]. Notably, the recently described early T-cell precursor (ETP)-acute lymphoblastic leukemia (ALL) patients[7] have leukemic cells that show an early block in T-cell differentiation and significantly overlap with *LYL1*-positive T-ALL[4] and *MEF2C*-dysregulated immature T-ALL[5,8]. These immature T-cell leukemias often express myeloid markers such as CD13 and CD33, and show a transcriptional program related to hematopoietic stem cells and myeloid progenitors[5]. Importantly, these tumors are associated with poor prognosis and reduced overall survival[7,9,10]. Preclinical mouse models of *LMO2*-dependent T-cell neoplasia are thought to recapitulate at least some features of early immature human T-ALL including a pre-leukemic T-cell differentiation arrest[11]. In general, T-ALLs can be classified in pro-T

($CD7^+$, $CD2^-$, $CD5^-$), pre-T ($CD7^+$, $CD2^+$, $CD5^{\pm}$), cortical-T ($CD1a^+$) and mature T-cell stages ($sCD3^+$, $CD1a^-$) according to the European Group for the Immunological Characterization of Leukaemias classification system[12].

In an effort to improve patient prognosis and survival, targeted therapeutics are beginning to emerge as powerful agents against hematological malignancies. One such example is the small molecule ABT-199, a highly potent, orally bioavailable B-cell lymphoma (BCL)-2 specific inhibitor[13]. The anti-tumor effects of ABT-199 have been reported in a growing number of tumor entities, including acute myeloid leukemia (AML)[14,15], chronic lymphocytic leukemia (CLL)[16], multiple myeloma[17], estrogen receptor-positive breast cancer[18] and lymphoma[19]. Currently, phase-I clinical trials of ABT-199 in CLL are ongoing and the first preliminary results show a high overall response rate. Notably, some patients included in this trial experienced tumor lysis syndrome as a result of the massive cell death induced by ABT-199[20].

Given these promising antitumor results for ABT-199, we sought to establish the extent and level of BCL-2 expression across different T-ALL molecular subgroups and evaluated the therapeutic potential of the BCL-2 inhibitor ABT-199 in the context of human T-ALL.

Methods

Patient samples, cell lines and mouse tumor cells

The cell lines were purchased from the DSMZ repository (Braunschweig, Germany) and cultured in RPMI 1640 medium supplemented with 10% or 20% fetal bovine serum (FBS), 100 U/ml penicillin, 100 µg/ml streptomycin, 100 µg/ml kanamycin sulfate and 2 mM L-glutamine at 37°C with 5% CO_2.

Bone marrow lymphoblast samples from 64 T-ALL patients (15 immature, 25 *TAL/LMO*, 17 *TLX1/TLX3* and 7 *HOXA*) were collected with informed consent according to the declaration of Helsinki from Saint-Louis Hospital, Paris, France, and the study was approved by the Institut Universitaire d'Hematologie Institutional Review Board. This primary T-ALL cohort was previously investigated[21] and the high-quality RNA samples from this cohort were used for gene expression profiling.

Primary T-ALL cells for *in vitro* ABT-199 treatment and xenograft studies were acquired by informed consent from the Department of Pediatric Hemato-Oncology at Ghent University Hospital. These primary T-ALL samples were assigned to a specific molecular genetic subclass based on qPCR of *SIL-TAL1* or *MLL* fusion transcripts, *TLX1*/*TLX3* expression analysis by quantitative polymerase chain reaction or fluorescence in situ hybridization analysis of the *LMO2* locus.

Leukemic T-cells obtained from splenic tissue derived from secondary transplanted tumors that originally developed in the *Lck-Lmo2* mouse model (K.R. & T.H.R., manuscript in preparation) were a kind gift of T.H.R.

Isolation of thymocyte subsets from human thymus tissue

Human thymocytes were extracted from thymus tissue from children undergoing cardiac surgery and were obtained and used according to the guidelines of the Medical Ethical Commission of the Ghent University Hospital, Beglium. The thymus was dissected into small

pieces and the released cell suspension was passed through a 40 µm cell strainer. Enrichment of viable mononuclear cells was done by a Lymphoprep density gradient.

CD34-positive cells were isolated by magnetic activated cell sorting (MACS) and purified by fluorescence-activated cell sorter (FACS)-mediated cell sorting. For the isolation of immature single positive cells ($CD4^+$ $CD8^-$ $CD3^-$), the cells were first labeled with an unlabeled anti-glycophorin-A monoclonal antibody, and subsequently with unlabeled anti-CD8 and anti-CD3 monoclonal antibodies for depletion of residual red blood cells and $CD8^+$ and $CD3^+$ cells. Magnetic anti-mouse immunoglobulin-coated Dynabeads were used to obtain a CD3, CD8 and red blood cell depleted thymocyte fraction by means of the DynaMag Magnet. This fraction could then be further purified into pre- and post-β-selection $CD4^+CD3^-CD8^-CD28^-$ and $CD4^+CD3^-CD8^-CD28^+$ subsets by staining the cells with anti-human CD4, CD3, CD34, CD8 and CD28 antibodies followed by FACS. Isolation of double-positive and single-positive thymocytes was performed by staining the cells with CD4, CD8 and CD3 antibodies followed by FACS analysis. T-cell receptor (TCR)$\gamma\delta^+$ cells were isolated via MACS by labeling the thymocytes with anti-TCRγδ Hapten antibodies and adding MACS Anti-Hapten MicroBeads fluorescein isothiocyanate. To separate immature and mature TCR$\gamma\delta^+$ cells, the MACS-enriched cells were stained with CD3 and CD1 monoclonal antibodies and sorted via FACS.

Gene expression profiling of primary T-ALL samples and T-cell subsets

Total RNA was isolated using the miRNeasy or RNeasy mini kit (Qiagen) and the RNA quality was evaluated on the Agilent 2100 bioanalyzer (Agilent Technologies, Santa Clara, CA). Whole human genome expression profiling was performed using the GeneChip Human Genome U133 2.0 Plus arrays (Affymetrix, Santa Clara, CA) according to standardized procedures at the IGBMC (www.igbmc.fr, Strasbourg, France). Normalization of microarray intensities was done using the variance stabilization and calibration (VSN) R package in R. Differential expression analysis was done using the Comparative Marker Selection module in GenePattern[22]. Microarray data have been deposited in the NCBI Gene Expression Omnibus (GEO) with accession number GSE62156. An independent and publically available[5] cohort of human T-ALL samples was used to validate the findings about *BCL-2* expression levels.

Treatment of cells with ABT-199 followed by viability or apoptosis assay

Cells from T-ALL cell lines (Supplementary Table 1) were plated at 100 000 cells per well in 96-well plates. The cells were incubated for 48 hours in 100 µl medium with 10% FBS to which 5 µl of the appropriate ABT-199 dilution or dimethylsulfoxide (DMSO) was added. The assays were performed with the Celltiter-Glo Luminescent Cell Viability Assay according to the manufacturer's instructions (Promega). To determine the half maximal inhibitory concentration (IC_{50}), 6 to 8 concentration points (twofold increase) were chosen for each cell line so that the IC_{50} point was approximately in the middle of the concentration range. The IC_{50} values were calculated using the CalcuSyn software (Biosoft, Cambridge, MA). The experiment was performed 2 or 3 times independently and in every experiment, each concentration was tested in duplicate for every cell line.

For the apoptosis assay, cells were plated at 10 000 cells per well in 96-well plates. The cells were incubated for 24 hours in 95 µl medium with 10% FBS to which 5 µl of the appropriate ABT-199 dilution or DMSO was added. The assay was performed with the Caspase-Glo 3/7 Assay according to the manufacturer's instructions (Promega). The experiment was performed 3 times and every concentration point was each time tested in duplicate for each cell line.

For the treatment of primary T-ALLs, enriched mononuclear cells or full bone marrow from primary leukemia samples were suspended in complete culture medium supplemented with 10% FBS. Cells were plated at 50 000 cells per well in 96-well plates to which 5 µl of the appropriate ABT-199 dilution (9 to 13 concentrations) or DMSO was added (total volume 100 µl). Cell viability was measured 16 hours after adding the compound and the IC_{50} values were calculated. Each concentration was tested in duplicate for every patient sample. The *Lck-Lmo2* mouse tumor T-cells were thawed and treated with ABT-199 in medium with 10% FBS for 16 hours. The IC_{50} values were determined as described above (50 000 cells per well). Two independent experiments were performed in which each concentration was tested in duplicate.

Quantitative real-time reverse transcription polymerase chain reactions (qRT-PCR)
Total RNA was isolated using the miRNeasy mini kit (Qiagen) and the RNAse-Free Dnase set (Qiagen). The iScript cDNA synthesis kit (Bio-Rad) was used to synthesize cDNA. The qRT-PCRs were performed using the SsoAdvanced SYBR Green Supermix (Bio-Rad) and were run on the LightCycler 480 (Roche, model LC480). Every sample was analyzed in duplicate and the gene expression was standardized against at least 3 reference genes. The primer sequences are listed in Supplementary Table 2.

Western blotting
Cells were lysed with radioimmunoprecipitation assay (RIPA) buffer and protein concentration was measured with the Pierce BCA protein assay kit. Denatured protein was loaded on a 10% polyacrylamide gel and the sodium dodecyl sulfate-polyacrylamide gel electrophoresis was run followed by western blotting on a nitrocellulose membrane. The used primary antibodies were: Bcl-2 antibody (C-2) (sc-7382; Santa Cruz Biotechnology; dilution 1:1000), BCL-X_L antibody (#2762; Cell Signaling Technology; dilution 1:1000) and anti-β-actin antibody (Clone AC-75; A2228; Sigma-Aldrich; dilution 1:2000). The protein bands were densitometric analyzed using ImageJ software (National Institutes of Health).

In vivo treatment of xenografts with ABT-199
Luciferase-positive LOUCY cells were generated by infecting the LOUCY cell line with PWPI-LUC lentiviruses. Nonconcentrated virus was produced in HEK293TN cells using JetPEI polyplus reagent with pMD2.G (envelope plasmid), psPAX2 (packaging plasmid) and pWPI-LUC (target plasmid) in 0.1/0.9/1 ratios. Transduced cells expressing enhanced green fluorescent protein were selected 72 hours after infection by cell sorting on a S3 cell sorter (Bio-Rad).

Nonobese diabetic/severe combined immunodeficient γ (NSG) mice were injected at 6 weeks of age in the tail vein with 150 µl phosphate-buffered saline containing 5 $x10^6$ luciferase-labeled LOUCY cells. At regular time points, the bioluminescence was measured using the IVIS Lumina II imaging system (PerkinElmer). At 6 weeks, the cells were engrafted and the mice were randomly divided into 2 groups (with an equal number of males and females in both groups), and the treatment was started on day 0. Mice were treated with 100 mg ABT-199/kg body weight or with vehicle via oral gavage for four 4 consecutive days. ABT-199 was formulated in 60% phosal 50 propylene glycol, 30% polyethylene glycol 400 and 10% ethanol. At days 0, 2 and 4 the bioluminescene was measured. Before imaging, the mice were injected intraperitoneally with 200 µl of a 15 mg/ml firefly D-luciferin potassium salt solution and anesthetized by inhalation of 5% isoflurane. The mice were imaged 10 minutes after luciferin injection. The total bioluminescence signal in each mouse was calculated via the region of interest tool (total counts) in the Living Image software (PerkinElmer).

A xenograft of primary human T-ALL cells from patient 3 was established in NSG mice by retro-orbital injection[21]. Upon establishment of disease, human leukemic cells were isolated from the spleen and retransplanted into secondary recipients. Next, tertiary xenograft injections were performed in a cohort of 10 NSG mice and leukemia engraftment was monitored by human CD45 staining (CD45-FITC antibody; Miltenyi Biotec) in peripheral blood using FACS analysis with the S3 cell sorter (Bio-Rad). Upon detection of human $CD45^+$ leukemic blasts in peripheral blood, mice were randomized in 2 groups and treated with vehicle or 100 mg ABT-199/kg body weight for 7 consecutive days. After treatment, animals were sacrificed and the percentage human CD45 (hCD45)-positive leukemic blasts in bone marrow were determined by FACS as described above.

The ethical committee on animal welfare at Ghent University Hospital approved all animal experiments.

Combination treatment of cells with ABT-199 and chemotherapeutic agents

T-ALL cell lines were plated at 20 000 cells per well in 96-well plates, and twofold dilution series of ABT-199 and the chemotherapeutic were made around the IC_{50} point for every cell line. For the combination therapy, 5 µl of each compound dilution was added at a constant concentration ratio and every concentration point was tested in duplicate within 1 experiment. The final concentration of solvent was equal for all the concentrations of a particular compound. Cell viability was assessed 48 hours after adding the compounds by CellTiter-Glo Assay and Calcusyn was used to calculate the combination index (CI). The chemotherapeutics used were: doxorubicin hydrochloride (D1515, solvent dimethylsulfoxide; Sigma-Aldrich), L-asparaginase (Erwinase, PL 01511/0272, solvent NaCl 0.9%) and dexamethasone (Aacidexam; NV Organon; solvent water).

Statistical analysis

GraphPad Prism 5.04 (La Jolla, CA) was used for statistical analyses.

Results

BCL-2 expression in genetic subtypes of human T-ALL and normal T-cells

To evaluate BCL-2 as a potential therapeutic target in human T-ALL, we analyzed *BCL-2* expression levels in T-ALL patients and sorted subsets of normal human thymocytes. Here, we performed microarray gene expression profiling on a panel of 64 primary T-ALL samples and used these gene expression signatures to define different molecular-genetic subtypes of human T-ALL as previously described[6]. Notably, this analysis revealed that high expression of anti-apoptotic *BCL-2* is a hallmark of immature subtypes of T-ALL (Figure 1A). Moreover, *BCL-2* levels were variable in *TLX1*, *TLX3* and *HOXA* driven T-ALLs and predominantly low in *TAL1* rearranged T-cell leukemias (Figure 1A). Importantly, these findings were validated and confirmed in an independent cohort of 117 genetically well-characterized human T-ALL samples for which gene expression signatures are publically available[5] (Figure 1B). In this validation series, the average *BCL-2* expression in the *HOXA* subgroup was similar to the one in the immature T-ALL subgroup.

As normal T-cell development serves as the conceptual framework for the understanding of T-ALL biology[23], we hypothesized that high *BCL-2* expression in immature T-ALL is a reflection of the spatiotemporal regulation of *BCL-2* during normal T-cell development. Indeed, *BCL-2* expression was high in $CD34^+$ T-cell progenitors and gradually decreased

during differentiation with the lowest values in $CD4^+CD8^+$ double-positive T-cells (Supplementary Figure 1A). Interestingly, *BCL-2L1* (the gene encoding BCL-X_L) expression showed an inverse trend (Supplementary Figure 1A). Furthermore, BCL-2 and BCL-X_L expression in $CD34^+$ T-cell progenitors as compared to sorted $CD4^+$/$CD8^+$ and TCRγδ$^+$ T-cell fractions was confirmed at the protein level (Supplementary Figure 1B).

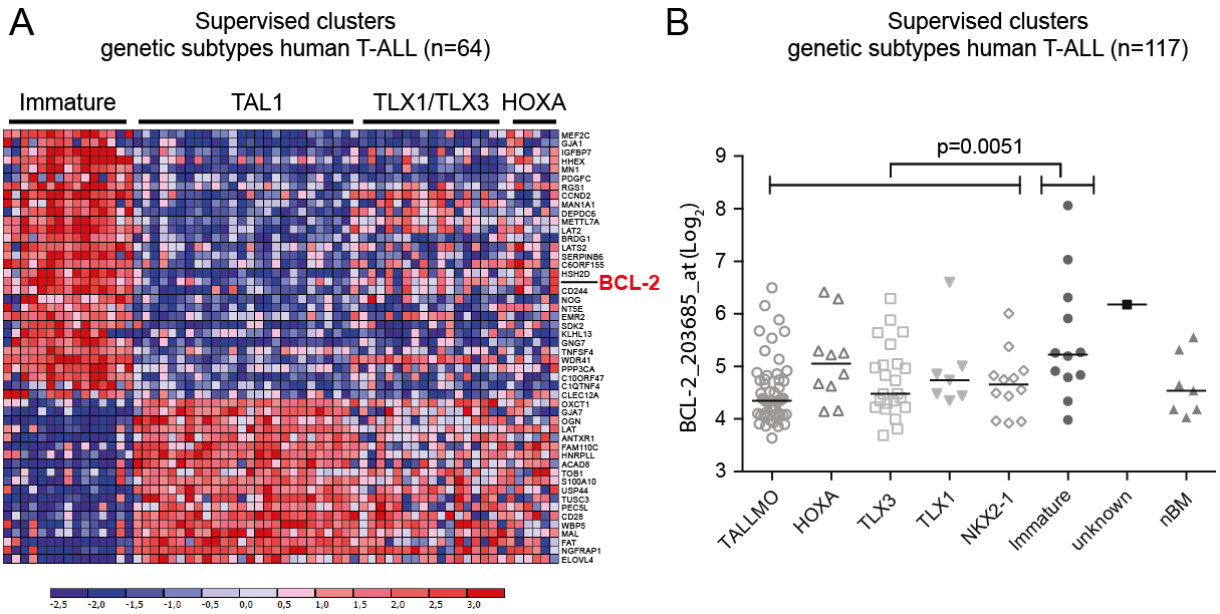

Figure 1. BCL-2 expression in malignant human T-cells. *(A) Differential gene expression profiling of primary immature T-ALLs vs T-ALLs from other subgroups (log_2[fold change]>2; P<.05). A heat map of the top 50 differentially expressed genes is shown. Genes in the heat map are shown in rows and each individual leukemia sample is shown in 1 column. Expression levels are visualized as color-coded differential expression from the mean in standard deviation units with red indicating higher levels and blue lower levels of expression. This primary T-ALL cohort has previously been investigated[21] and hierarchical clustering was used to define molecular-genetic subtypes of human T-ALL, as previously described[6]. (B) BCL-2 expression levels (probe 203685_at) in an independent cohort of 117 human T-ALL samples. Molecular-genetic subtypes of human T-ALL have been defined as previously described[5]. nBM: normal bone marrow. P = 0.0051.*

ABT-199 sensitivity in human T-ALL cell lines

Next, we determined IC_{50} values for ABT-199 in a panel of 11 human T-ALL cell lines. Mature T-ALL cell lines, including ALL-SIL, CUTLL1, TALL-1, KOPTK1, DND-41, PF-382, KARPAS-45, PEER, JURKAT and CCRF-CEM, showed modest responses towards ABT-199 treatment with IC_{50} values ranging from 0.2 to 10 µM (Figure 2A). Most notably and in line with a previous report[24], the T-ALL cell line LOUCY, which shows a transcriptional program related to early immature T-ALLs[25], was highly sensitive toward ABT-199 treatment (IC_{50} = 13.9nM). As expected, induction of apoptosis upon treatment of LOUCY with 20 nM ABT-199 for 24 hours was associated with increased caspase activity (Figure 2B). This induction at low ABT-199 concentration was significantly higher (P = 0.0088; 2-sided t test) in LOUCY cells as compared with ALL-SIL, the second most ABT-199 sensitive T-ALL cell line (Figure 2B). Moreover, we observed a negative correlation between ABT-199 IC_{50} values and *BCL-2* mRNA (Spearman ρ = -0.855; P = 0.0015) and BCL-2 protein (Spearman ρ = -0.7; P = 0.0204) levels in human T-ALL cell lines (Figure 2C-F).

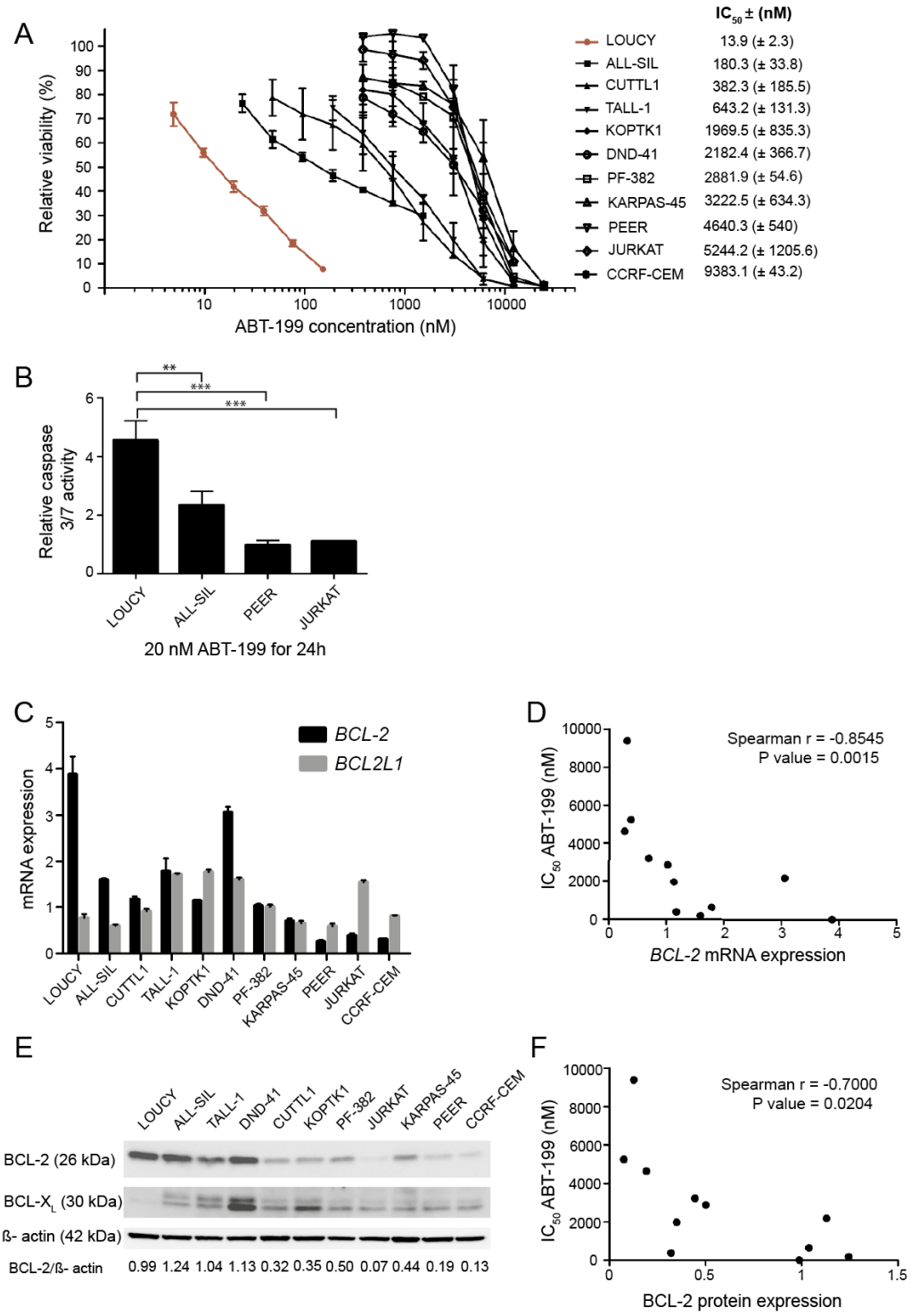

***Figure 2*. ABT-199 response in human T-ALL cell lines.** *(A) The effect of 48 hours ABT-199 treatment on the viability of human T-ALL cell lines relative to cells treated with dimethylsulfoxide (100%). The results represent the average and standard deviation for at least 2 independent experiments. SD, standard deviation. (B) Caspase 3/7 activity was measured 24 hours after adding ABT-199 and was plotted relative to the DMSO control. The average and standard deviation of 3 independent experiments is shown. The caspase activity after treatment with 20 nM of ABT-199 was significantly higher in LOUCY than ALL-SIL (P=0.0088; 2-sided t test), PEER (P=0.0008; 2-sided t test) or JURKAT (P=0.0119; 2-sided t test with Welch's correction). (C) BCL-2 and BCL-2L1 expression measured with quantitative real-time polymerase chain reactions in a panel of T-ALL cell lines. The graph shows the calibrated normalized relative quantities values and corresponding standard error as calculated with qbasePLUS. The gene expression was standardized against HMBS, TBP and UBC. (D) Correlation between the IC_{50} values for ABT-199 and BCL-2 mRNA expression in human T-ALL cell lines. (E) Western blot of BCL-2 and BCL-XL in T-ALL cell lines with β-actin as the loading control. (F) Correlation between the IC_{50} values for ABT-199 and BCL-2 protein levels in human T-ALL cell lines.*

To test the efficacy of ABT-199 *in vivo*, we performed xenograft experiments using luciferase positive LOUCY cells in immune-deficient NSG mice (Figure 3). Treatment of established xenografted tumors with 100 mg ABT-199/kg for 4 days resulted in a significant reduction of leukemic burden (P = 0.0048; 2-sided t test), suggesting that BCL-2 inhibition can selectively restrain leukemic cell growth of the T-ALL cell line LOUCY *in vivo*.

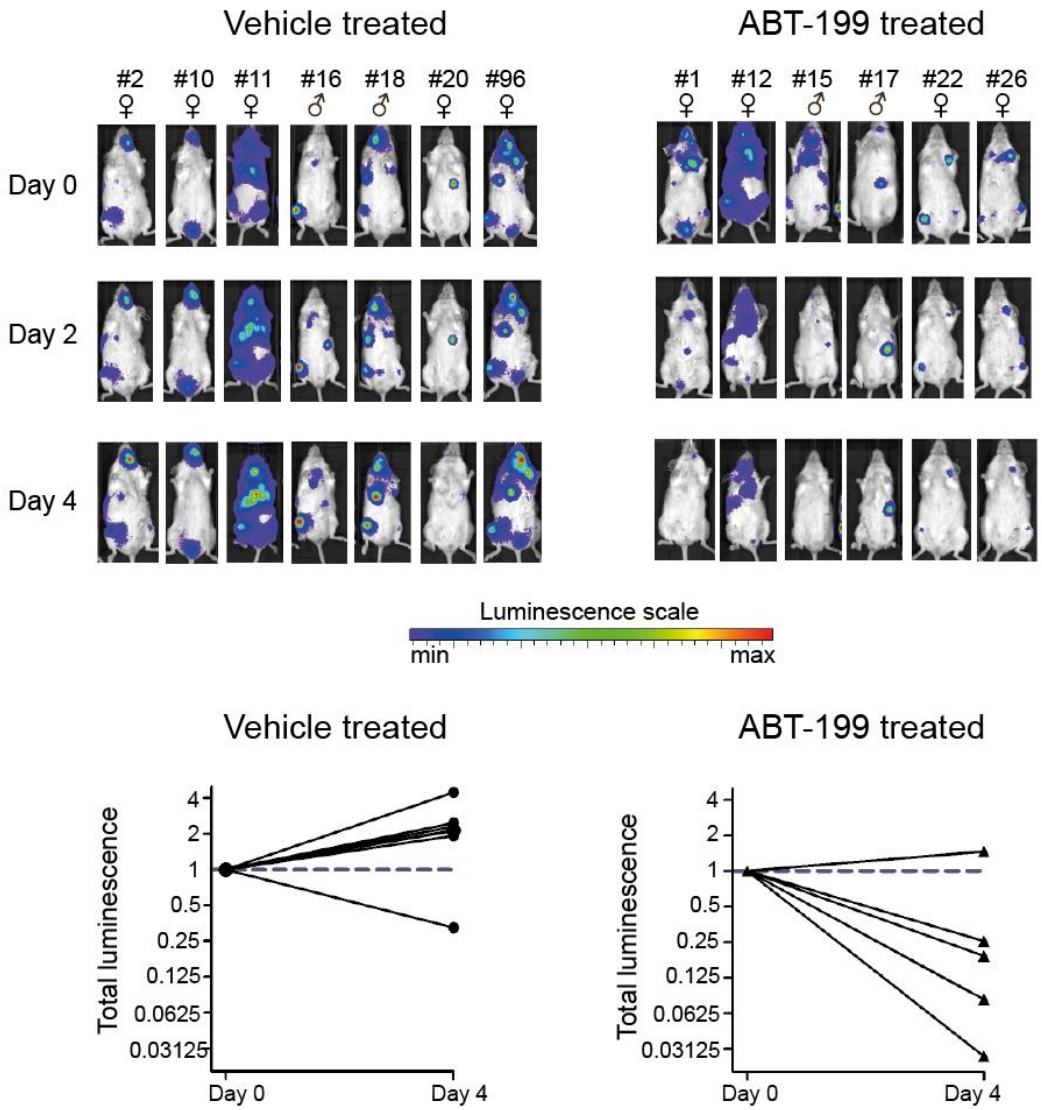

Figure 3. ABT-199 sensitivity in a mouse xenograft model of the T-ALL cell line LOUCY*. Thirteen mice xenografted with luciferase positive LOUCY cells were vehicle treated or ABT-199 treated (100 mg/kg body weight) for 4 days. The bioluminescence was measured before the start of the treatment (day 0) and after 2 and 4 days of treatment. Each column with pictures represents 1 individual mouse. The total bioluminescence signal after 4 days of treatment is plotted relative to the start value at day 0 for each mouse.*

Mouse model of immature T-ALL responds to ABT-199

To further study the association between ABT-199 sensitivity and tumor immune phenotype in T-ALL, we used the *Lck-Lmo2* transgenic mouse model. Overexpression of the *Lmo2* oncogene in the thymi of these *Lck-Lmo2* mice results in the development of murine T-cell tumors with an average latency of 10 months (K.R. and T.H.R., manuscript in preparation), comparable to the *CD2-Lmo2* transgenic strain[11,26]. Interestingly, the resulting *Lck-Lmo2*

driven murine tumors show considerable immunophenotypic tumor heterogeneity, providing an opportunity to study the potential connection between tumor immunophenotype and ABT-199 response in a homogeneous genetic background.

For this, we determined ABT-199 IC_{50} values in leukemic blasts obtained from 2 immunophenotypically different *Lck-Lmo2* murine tumors that sustained their phenotype during transplantation. One *Lck-Lmo2* tumor (#39365) showed an immature phenotype with about 90% CD4/CD8 double-negative blasts, whereas the second tumor (#39354) presented with a more mature phenotype consisting of about 30% CD4/CD8 double-positive and 40% CD4 single-positive leukemic blasts. Interestingly, we identified a 100-fold difference in ABT-199 IC_{50} value between the immature (#39365; IC_{50} = 2.2 nM) (Figure 4A) and mature murine T-cell tumor (#39354; IC_{50} = 214 nM) (Figure 4A), and this differential ABT-199 response was associated with enhanced levels of BCL-2 in the immature murine T-cell tumor (Figure 4B).

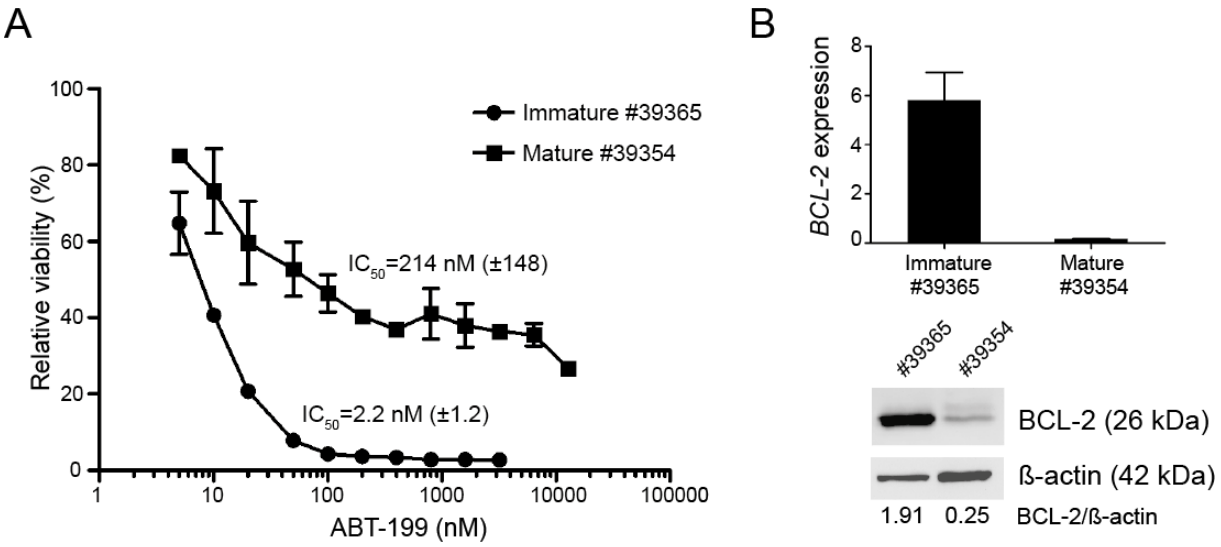

Figure 4. BCL-2 expression and ABT-199 sensitivity in the Lck-Lmo2 transgenic mouse model. *(A) ABT-199 response of tumor cells obtained from Lck-Lmo2 transgenic mice. T-cell tumor #39365 consists of approximately 90% double-negative T-cells (approximately 40% double-negative 1, 60% double-negative 2), whereas tumor #39354 consists of about 30% double-positive and 40% $CD4^+$ single-positive T-cells. The viability (average and standard deviation of 2 independent experiments) is shown relative to the cells incubated with dimethylsulfoxide (100%). Based on these data, the IC_{50} values were calculated. (B) BCL-2 expression in the Lck-LMO2 mouse tumors. The top panel shows the mRNA expression (quantitative real-time polymerase chain reactions, calibrated normalized relative quantities values and corresponding standard errors) and the bottom panel shows the protein expression with β-actin as loading control. The messenger RNA gene expression was standardized against Hmbs, Tbp and Ubc.*

ABT-199 response in primary T-ALL samples

To define ABT-199 sensitivity in primary patient material, we subsequently selected a panel of 17 pediatric primary T-ALL samples that represent major immunophenotypic maturation stages and molecular genetic subtypes of T-ALL (Figure 5A; Supplementary Figure 2). Leukemic samples belonging to the early stages of maturation based on the EGIL criteria[12] were predominantly sensitive to ABT-199 treatment with all $CD4^-$ $CD8^-$ double negative T-ALL samples showing an IC_{50} lower than 300 nM. In contrast, mature T-ALL patient samples showed modest ABT-199 responses with most *SIL-TAL1*-positive T-ALLs showing an IC_{50} > 800 nM. Although only few *HOXA* and *TLX3* rearranged T-ALLs were included in this patient

series, some *TLX3*- or *HOXA*- positive leukemias were also highly sensitive to BCL-2 inhibition (Figure 5A; Supplementary Figure 2).

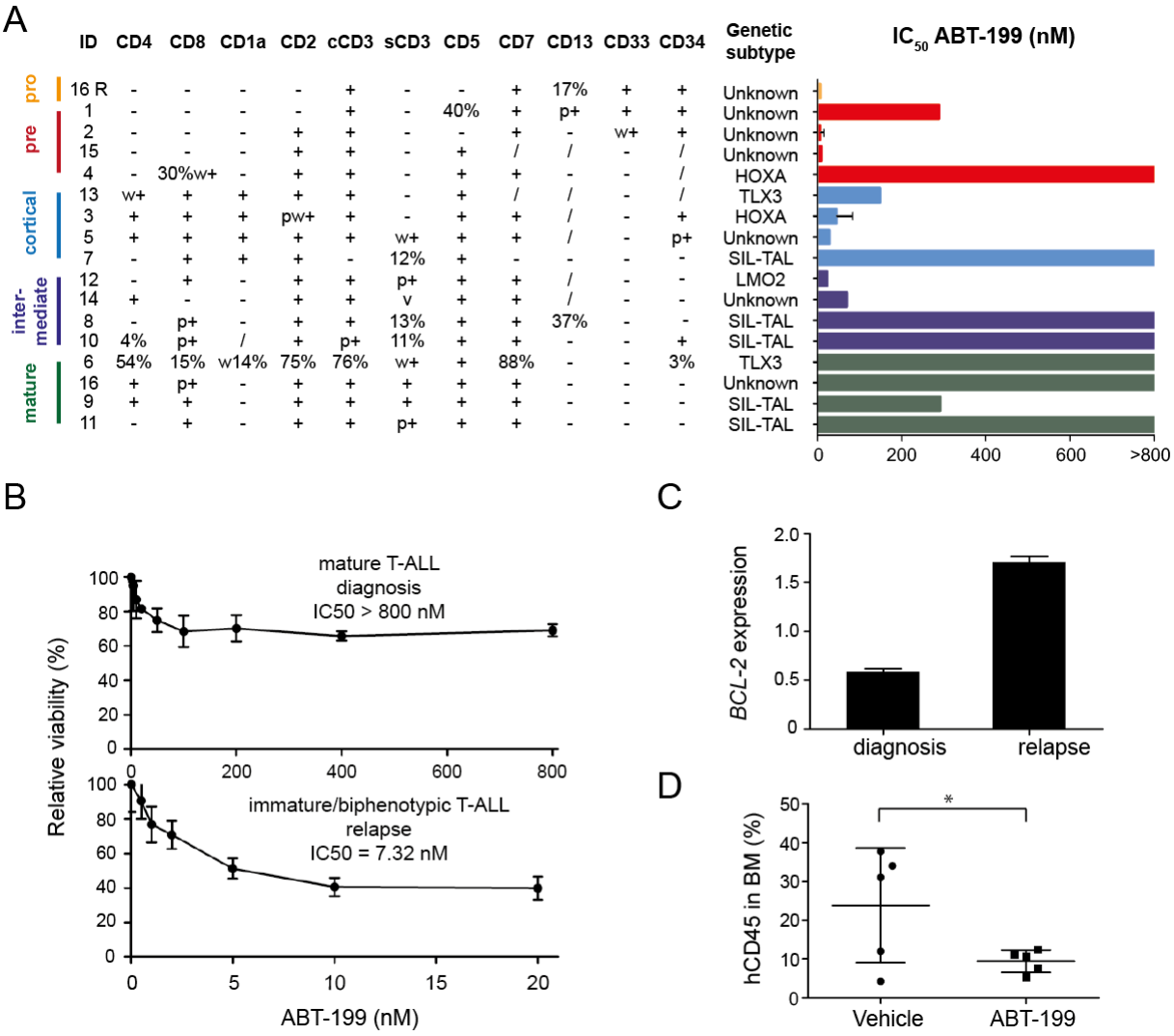

Figure 5. ABT-199 sensitivity in primary human T-ALL patient samples. *(A) ABT-199 IC_{50} values for a panel of primary T-ALL samples. Patient samples are classified based on their immunophenotype in pro-, pre-, cortical, intermediate between cortical and mature and mature T-ALL with markers scored on the blast gate. Molecular classification is based on fluorescence in situ hybridization and/or expression analysis. (B) Cell viability of diagnostic and relapse material from T-ALL patient 16 after 16 hours of ABT-199 treatment using different concentrations relative to cells incubated with dimethylsulfoxide (100%). (C) BCL-2 expression (quantitative real-time polymerase chain reactions, calibrated normalized relative quantities values and corresponding standard errors) analysis of diagnostic and relapse material obtained from T-ALL patient 16. The expression was standardized against B2M, HPRT1, RPL13A and TBP. (D) Percentage of human CD45 in the bone marrow of NSG mice injected with a patient-derived xenograft from T-ALL #3 (MLL rearranged, HOXA-positive) after 7 days of treatment with vehicle or ABT-199. /, not known; BM, bone marrow; cCD3, cytoplasmic CD3; p+, partial positive; R, relapse; s, surface; v, variable; w, weak. *P = 0.0498.*

Interestingly, the putative relation between tumor immunophenotype and ABT-199 sensitivity was further strengthened by a unique T-ALL sample that presented with a mature T-ALL at diagnosis, but suffered from an immature/biphenotypic T-ALL at relapse 11 months after initial diagnosis (Supplementary Figure 3). Notably, the leukemic clone with an immature/biphenotypic immunophenotype that eventually gave rise to the relapse was

already detected at day 15 and day 35 after induction therapy. Notably, *in vitro* analysis of these paired samples obtained at diagnosis and relapse revealed marked differences in ABT-199 sensitivity. The immature leukemic cells at relapse were highly sensitive to ABT-199 treatment (IC_{50} = 7.32 nM), whereas the mature leukemic cell population at diagnosis barely responded to ABT-199 (IC_{50} > 800 nM) (Figure 5B). Interestingly, the marked difference in ABT-199 sensitivity was accompanied by a notable difference in *BCL-2* expression between the diagnostic and relapse sample (Figure 5C).

Finally, we established a patient-derived xenograft (PDX) in NSG mice from the *HOXA*-positive (*MLL* rearranged) T-ALL patient sample #3 that showed ABT-199 sensitivity *in vitro* (Figure 5A; Supplementary Figure 2). ABT-199 treatment of this PDX for 7 consecutive days resulted in a significant lower percentage of human CD45-positive cells in the bone marrow (P = 0.0498; one-sided t test with Welch's correction) as compared to the vehicle-treated mice (Figure 5D).

Combination of ABT-199 and chemotherapeutics

To evaluate potential synergism between ABT-199 and conventional chemotherapeutic agents, T-ALL cell lines were treated with combinations of ABT-199 and doxorubicin, L-asparaginase (Erwinase) or dexamethasone (Aacidexam). LOUCY and ALL-SIL displayed higher synergism with doxorubicin and L-asparaginase as compared to the ABT-199-insensitive JURKAT cell line (Figure 6A-B; Supplementary Table 3). In addition, the combination of ABT-199 with dexamethasone was strongly synergistic in LOUCY cells (Figure 6C; Supplementary Table 3) and could not be evaluated in JURKAT and ALL-SIL because of the high dexamethasone IC_{50} values in these cell lines.

Discussion

T-ALL is a genetically heterogeneous disease with cure rates in modern protocols reaching >80% in children and about 50% in adults[27]. The standard antileukemic therapy consists of intensive multiagent chemotherapy and is associated with considerable toxicities and long-term side effects. Therefore, novel molecularly driven therapeutic approaches should be developed to improve clinical care for T-ALL patients in the near future.

Evasion of apoptosis is a hallmark of human cancer[28] and is often mediated by overexpression of prosurvival BCL-2 family proteins, and can act as a major determinant of chemotherapy resistance[29]. Hence, the search for compounds that could target prosurvival BCL-2 family members has been actively explored[30]. ABT-737[31] and its orally bioavailable derivative ABT-263[32] (navitoclax) are BH3 mimetics that inhibit the anti-apoptotic proteins BCL-2, BCL-X_L and BCL-W. Initial clinical trials using navitoclax have shown promising antitumoral effects particularly in CLL[33]. Unfortunately, navitoclax treatment was associated with dose-limiting thrombocytopenia, given the critical role of BCL-X_L in platelet survival[32,34]. As a consequence, ABT-199[13] was developed as a highly specific inhibitor that only targeted BCL-2 and therefore spared platelets.

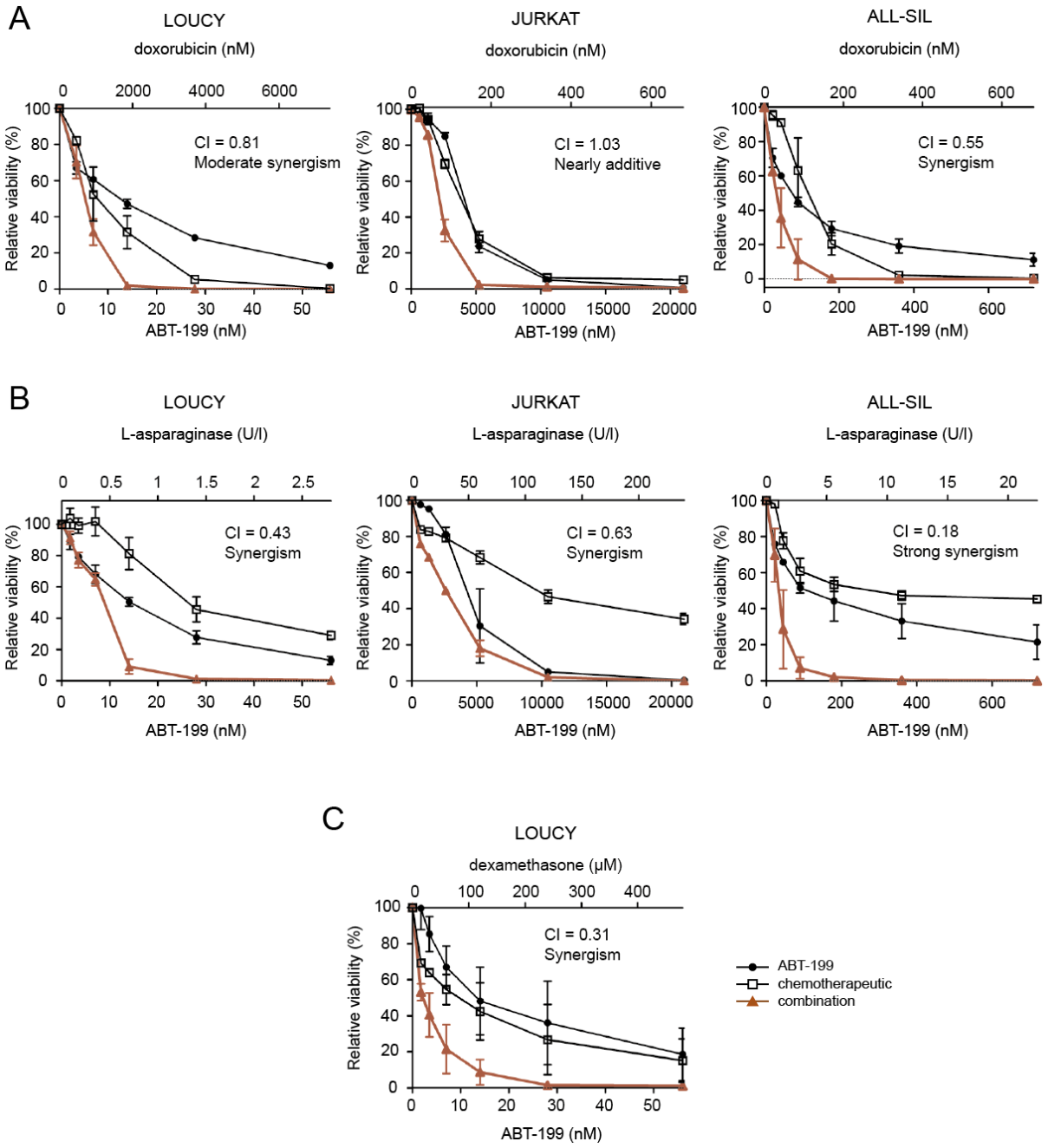

Figure 6. ABT-199 in combination with chemotherapeutic agents in human T-ALL cell lines. *The effect of monotherapy or combination therapy on the viability of T-ALL cell lines is visualized. Cell viability is expressed relative to cells treated with dimethylsulfoxide and the average and standard deviation of 2 independent experiments is plotted for each combination. Combination of ABT-199 with doxorubicin (A) or L-asparaginase (B) in the T-ALL cell lines LOUCY, JURKAT and ALL-SIL. (C) Combination of ABT-199 and dexamethasone is only shown for the LOUCY cell line. The combination index (CI) shown represents the average of the CIs at the ED50, ED75 and ED90 effect levels for each experiment. 0.9<CI<1.1: nearly additive; 0.85<CI<0.9: slight synergism; 0.7<CI<0.85: moderate synergism; 0.3<CI<0.7: synergism; 0.1<CI<0.3: strong synergism; CI<0.1: very strong synergism.*

To evaluate BCL-2 as a molecular target for therapy in human T-ALL, we analyzed the pattern of *BCL-2* expression across 181 primary T-ALL samples and documented high *BCL-2* expression in immature T-ALLs. Notably, these results are in line with a study by Ferrando et al.[4] that reported high *BCL-2* expression in so-called *LYL1* positive T-ALLs, a molecular subtype of human T-ALL that closely resembles immature T-ALL[5] and partially overlaps with

the more recently identified subclass of poor prognostic ETP-ALL. In addition, we observed intermediate *BCL-2* expression in *TLX1*, *TLX3* or *HOXA* driven T-ALLs, whereas mature T-ALLs, which are often characterized by *TAL1* or *LMO2* oncogene activation, displayed low levels of *BCL-2*.

In the past, transcriptional profiling studies have established a genetic classification of human T-ALL[4-7]. Collectively, these analyses showed that gene expression signatures of molecular genetic T-ALL subgroups are closely related to those of normal thymocytes at distinct stages of T-cell development[4]. Given this, we analyzed *BCL-2* expression in 11 subsets of human thymocytes that collectively reflect the chronological steps in human T-cell differentiation. Early T-cell precursors that enter the thymus from the bone marrow showed high *BCL-2* levels and this expression pattern was maintained until the $CD28^-$ immature single positive (ISP) stage. At this point, $CD28^-CD4^+$ ISP thymic precursors will undergo the process of β-selection, which coincides with loss of *BCL-2* expression as the cells move into the αβ lineage. Hence, we observed the lowest levels of *BCL-2* in $CD3^-CD4^+CD8^+$ T-cells. In contrast, *BCL-2L1* showed an opposite pattern of expression with high *BCL-2L1* levels in $CD4^+CD8^+$ T-cells, suggesting an anti-apoptotic switch from *BCL-2* to *BCL-2L1* during human T-cell maturation. Finally, $CD28^-CD4^+$ ISP cells that rearrange their TCRδ and TCRγ loci into functional TCRδ and TCRγ chains will develop into the γδ lineage, and these were shown to retain most of their BCL-2 expression. Altogether, *BCL-2* expression analysis in 2 genetically well-defined primary T-ALL patient cohorts and sorted subsets of T-cells confirmed the tight association between normal and malignant T-cell development and provided a rationale for targeting BCL-2 in immature subtypes of human T-ALL.

In vitro analysis of human T-ALL cell lines showed marked differences between cell lines that reflect different molecular genetic T-ALL subtypes and unraveled a significant association between ABT-199 sensitivity and *BCL-2* expression levels. Most notably, the T-ALL cell line LOUCY showed the highest *BCL-2* expression and was highly sensitive to BCL-2 inhibition by ABT-199 both *in vitro*[24] and *in vivo* using xenografts of human LOUCY cells. Although the gene expression profile of the T-ALL cell line LOUCY closely resembles the gene signature observed in lymphoblasts from primary immature human T-ALLs[25], this cell line shows characteristic activation of *HOXA* expression due to the presence of the *SET-NUP214 (nucleoporin 214)* fusion oncogene[35], which has been associated with corticosteroid and chemotherapy resistance[36]. In addition, the LOUCY cell line is $TCR\gamma\delta^+$-positive, suggesting that it combines immature transcriptional features with a mature TCRγδ immunophenotype. Therefore, its high BCL-2 expression mimics normal T-cell development where *BCL-2* levels remain high in T-cells that differentiate along the γδ lineage. All together, these data suggest that *BCL-2* levels could predict ABT-199 sensitivity in human T-ALL and suggest that BCL-2 inhibition might be particularly relevant as a novel therapeutic strategy in immature and *HOXA*-positive T-ALL.

To obtain further evidence for the close association between tumor immune phenotype, BCL-2 expression and ABT-199 sensitivity, we used the *Lck-Lmo2* transgenic mouse model (K.R. and T.H.R., manuscript in preparation). The *Lck-Lmo2* transgenic shows similar characteristics as the *CD2-Lmo2* mouse model[11,26], in which *Lmo2* promotes self-renewal of preleukemic thymocytes and sets the stage for the accumulation of additional genetic mutations required for leukemic transformation[37]. In this model, *BCL-2* expression was associated with the differentiation arrest of the tumor cells and defined the ABT-199

response of these murine tumors. Therefore, the tumor susceptibility towards BCL-2 inhibition is initially dictated by the tumor cell of origin and is conserved in mice.

In a next step, ABT-199 was able to affect the viability of primary T-ALL samples *in vitro*. Especially $CD4^-$ $CD8^-$ samples and samples belonging to the pro-T, pre-T and cortical T immunophenotypic maturation stages were responsive to ABT-199 treatment, whereas mature subtypes that differentiate along the αβ lineage were largely insensitive. Intriguingly, a T-ALL patient that was characterized by an immunophenotypic switch between diagnosis and relapse further exemplified the association between ABT-199 sensitivity and tumor immunophenotype. Notably, immature therapy-resistant leukemia cells at relapse were highly sensitive to ABT-199 *in vitro*, suggesting that BCL-2 inhibition could also serve as a promising therapeutic strategy for refractory T-cell leukemias. In addition, and as previously shown[38], *in vitro* sensitivity of an *MLL* rearranged T-ALL patient corresponded with reduced tumor burden upon ABT-199 treatment *in vivo* using a PDX with material from that *HOXA*-positive T-ALL. Based on these observations, we hypothesize that immunophenotypic features and *BCL-2* expression levels largely determine ABT-199 sensitivity in human T-ALL. Importantly, our study confirms the recent work from Ni Chonghaile et al.[39], which was mainly focused on the potential use of ABT-199 for the treatment of human ETP-ALL. However, our study suggests that genetic subtypes of human T-ALL that might benefit from ABT-199 treatment might extend beyond ETP-ALL and could also include *TLX1*, *TLX3* or *HOXA*-positive T-ALLs as well as mature $TCR\gamma\delta^+$-positive leukemias.

Most conventional chemotherapeutic agents execute their action via the mitochondrial pathway of apoptosis by activation of pro-apoptotic or inactivation of anti-apoptotic BCL-2 family proteins. Whether malignant cells are sensitive to a chemotherapeutic agent may depend on their pretreatment priming (ie. the proximity of a malignant cell to an apoptotic threshold)[40]. Given this, the combination of ABT-199 and chemotherapeutic agents could increase the chemosensitivity of malignant cells by reduction of their anti-apoptotic reserve[40]. Moreover, the combination of ABT-199 with chemotherapeutic agents or other targeted therapies could avoid the emergence of therapy resistance and result in reduced cytotoxic side effects due to lower chemotherapy dosage. In myeloid and ALL cell lines, ABT-737 was shown to increase sensitivity towards chemotherapeutic agents[40,41]. In addition, a strong synergism between ABT-199 and cytarabine has been previously reported in the T-ALL cell line LOUCY[24]. These findings were further extended in our study, in which we showed synergistic effects between ABT-199, doxorubicin, L-asparaginase and dexamethasone mainly in T-ALL cell lines with low ABT-199 IC_{50} values.

Altogether, our study defines BCL-2 as an attractive molecular target in human T-ALL and provides a rationale for including T-ALL patients in clinical trials for the BH3-mimetic ABT-199 in combination with conventional chemotherapeutics.

Acknowledgements

The authors thank Béatrice Lintermans and Lindy Reunes for excellent technical assistance, the *in vivo* small animal imaging laboratory (Innovative Flemish in vivo Imaging technology, [INFINITY]) at Ghent University Hospital, and Wim Schuermans for interpretation of immunophenotypic patient data.

This work was supported by the Research Foundation Flanders (FWO) research projects G.0202.09, G.0869.10N (F.S.), G065614, 3GA00113N and G.0C47.13N (P.V.V.); G0B2913N and 3G002711 (T.T.), PhD grant (S.P.), postdoctoral grants (T.T., P.V.V., S.G. and I.V.d.W.) and a senior clinical investigator grant (B.P.); the Belgian Foundation against Cancer (F.S. and S.G.) and grant 2010-187 (T.L.); the Flemish Liga against Cancer (VLK) Postdoc grant (F.M.); Ghent University (Concerted Research Action grant 12051203) (F.S.); the Cancer Plan from the Federal Public Service of Health (F.S.,Y.B.), the Children Cancer Fund Ghent (F.S.,Y.B.); the Belgian Program of Interuniversity Poles of Attraction (365O9110) (F.S.); additional funding by the Cancéropole Ile-De-France, the Cartes d'Identité des Tumeurs program from the Ligue Contre le Cancer, European Research Council Consolidator Grant 311660, the Saint-Louis Institute program (ANR-10-IBHU-0002 to J.S); and grants from Leukaemia & Lymphoma Research, Medical Research Council and the Wellcome Trust (Lmo2 mouse model work to T.H.R.).

Authorship

Contribution: S.P. analyzed experiments; S.P., F.M., S.G., I.V.d.W., C.E.d.B. and S.D. performed experiments; D.B., E.C. and J.S provided RNA of primary T-ALL patient samples for gene expression analysis; T.L., B.D.M. and Y.B. provided primary T-ALL patient samples; K.R. and T.H.R. shared cells of the Lck-LMO2 mouse model; J.C., B.P., F.S. and P.V.V. designed experiments, directed research and analyzed data; S.P., J.C., B.P., F.S. and P.V.V. wrote the paper; and all authors read and edited the manuscript.

Conflict-of-interest disclosure

The authors declare no competing financial interests.

References

1. Barrett AJ, Horowitz MM, Pollock BH, et al. Bone marrow transplants from HLA-identical siblings as compared with chemotherapy for children with acute lymphoblastic leukemia in a second remission. *N Engl J Med.* 1994;331(19):1253-1258.
2. Goldberg JM, Silverman LB, Levy DE, et al. Childhood T-cell acute lymphoblastic leukemia: the Dana-Farber Cancer Institute acute lymphoblastic leukemia consortium experience. *J Clin Oncol.* 2003;21(19):3616-3622.
3. Van Vlierberghe P, Ferrando A. The molecular basis of T cell acute lymphoblastic leukemia. *J Clin Invest.* 2012;122(10):3398-3406.
4. Ferrando AA, Neuberg DS, Staunton J, et al. Gene expression signatures define novel oncogenic pathways in T cell acute lymphoblastic leukemia. *Cancer Cell.* 2002;1(1):75-87.
5. Homminga I, Pieters R, Langerak AW, et al. Integrated transcript and genome analyses reveal NKX2-1 and MEF2C as potential oncogenes in T cell acute lymphoblastic leukemia. *Cancer Cell.* 2011;19(4):484-497.
6. Soulier J, Clappier E, Cayuela JM, et al. HOXA genes are included in genetic and biologic networks defining human acute T-cell leukemia (T-ALL). *Blood.* 2005;106(1):274-286.
7. Coustan-Smith E, Mullighan CG, Onciu M, et al. Early T-cell precursor leukaemia: a subtype of very high-risk acute lymphoblastic leukaemia. *Lancet Oncol.* 2009;10(2):147-156.
8. Zuurbier L, Gutierrez A, Mullighan CG, et al. Immature MEF2C-dysregulated T-cell leukemia patients have an early T-cell precursor acute lymphoblastic leukemia gene signature and typically have non-rearranged T-cell receptors. *Haematologica.* 2014;99(1):94-102.
9. Inukai T, Kiyokawa N, Campana D, et al. Clinical significance of early T-cell precursor acute lymphoblastic leukaemia: results of the Tokyo Children's Cancer Study Group Study L99-15. *Br J Haematol.* 2012;156(3):358-365.
10. Van Vlierberghe P, Ambesi-Impiombato A, De Keersmaecker K, et al. Prognostic relevance of integrated genetic profiling in adult T-cell acute lymphoblastic leukemia. *Blood.* 2013;122(1):74-82.
11. Larson RC, Osada H, Larson TA, Lavenir I, Rabbitts TH. The oncogenic LIM protein Rbtn2 causes thymic developmental aberrations that precede malignancy in transgenic mice. *Oncogene.* 1995;11(5):853-862.
12. Bene MC, Castoldi G, Knapp W, et al. Proposals for the immunological classification of acute leukemias. European Group for the Immunological Characterization of Leukemias (EGIL). *Leukemia.* 1995;9(10):1783-1786.
13. Souers AJ, Leverson JD, Boghaert ER, et al. ABT-199, a potent and selective BCL-2 inhibitor, achieves antitumor activity while sparing platelets. *Nat Med.* 2013;19(2):202-208.
14. Niu X, Wang G, Wang Y, et al. Acute myeloid leukemia cells harboring MLL fusion genes or with the acute promyelocytic leukemia phenotype are sensitive to the Bcl-2-selective inhibitor ABT-199. *Leukemia.* 2014.
15. Pan R, Hogdal LJ, Benito JM, et al. Selective BCL-2 inhibition by ABT-199 causes on-target cell death in acute myeloid leukemia. *Cancer Discov.* 2014;4(3):362-375.

16. Vogler M, Dinsdale D, Dyer MJ, Cohen GM. ABT-199 selectively inhibits BCL2 but not BCL2L1 and efficiently induces apoptosis of chronic lymphocytic leukaemic cells but not platelets. *Br J Haematol.* 2013;163(1):139-142.
17. Touzeau C, Dousset C, Le Gouill S, et al. The Bcl-2 specific BH3 mimetic ABT-199: a promising targeted therapy for t(11;14) multiple myeloma. *Leukemia.* 2014;28(1):210-212.
18. Vaillant F, Merino D, Lee L, et al. Targeting BCL-2 with the BH3 mimetic ABT-199 in estrogen receptor-positive breast cancer. *Cancer Cell.* 2013;24(1):120-129.
19. Vandenberg CJ, Cory S. ABT-199, a new Bcl-2-specific BH3 mimetic, has in vivo efficacy against aggressive Myc-driven mouse lymphomas without provoking thrombocytopenia. *Blood.* 2013;121(12):2285-2288.
20. BCL-2 Inhibitor Yields High Response in CLL and SLL. *Cancer Discov.* 2014;4(2):OF5.
21. Clappier E, Gerby B, Sigaux F, et al. Clonal selection in xenografted human T cell acute lymphoblastic leukemia recapitulates gain of malignancy at relapse. *J Exp Med.* 2011;208(4):653-661.
22. Reich M, Liefeld T, Gould J, Lerner J, Tamayo P, Mesirov JP. GenePattern 2.0. *Nat Genet.* 2006;38(5):500-501.
23. Taghon T, Waegemans E, Van de Walle I. Notch signaling during human T cell development. *Curr Top Microbiol Immunol.* 2012;360:75-97.
24. Anderson NM, Harrold I, Mansour MR, et al. BCL2-specific inhibitor ABT-199 synergizes strongly with cytarabine against the early immature LOUCY cell line but not more-differentiated T-ALL cell lines. *Leukemia.* 2013.
25. Van Vlierberghe P, Ambesi-Impiombato A, Perez-Garcia A, et al. ETV6 mutations in early immature human T cell leukemias. *J Exp Med.* 2011;208(13):2571-2579.
26. Larson RC, Fisch P, Larson TA, et al. T cell tumours of disparate phenotype in mice transgenic for Rbtn-2. *Oncogene.* 1994;9(12):3675-3681.
27. Pui CH, Robison LL, Look AT. Acute lymphoblastic leukaemia. *Lancet.* 2008;371(9617):1030-1043.
28. Hanahan D, Weinberg RA. The hallmarks of cancer. *Cell.* 2000;100(1):57-70.
29. Adams JM, Cory S. The Bcl-2 apoptotic switch in cancer development and therapy. *Oncogene.* 2007;26(9):1324-1337.
30. Juin P, Geneste O, Gautier F, Depil S, Campone M. Decoding and unlocking the BCL-2 dependency of cancer cells. *Nat Rev Cancer.* 2013;13(7):455-465.
31. Oltersdorf T, Elmore SW, Shoemaker AR, et al. An inhibitor of Bcl-2 family proteins induces regression of solid tumours. *Nature.* 2005;435(7042):677-681.
32. Tse C, Shoemaker AR, Adickes J, et al. ABT-263: a potent and orally bioavailable Bcl-2 family inhibitor. *Cancer Res.* 2008;68(9):3421-3428.
33. Roberts AW, Seymour JF, Brown JR, et al. Substantial susceptibility of chronic lymphocytic leukemia to BCL2 inhibition: results of a phase I study of navitoclax in patients with relapsed or refractory disease. *J Clin Oncol.* 2012;30(5):488-496.
34. Zhang H, Nimmer PM, Tahir SK, et al. Bcl-2 family proteins are essential for platelet survival. *Cell Death Differ.* 2007;14(5):943-951.
35. Van Vlierberghe P, van Grotel M, Tchinda J, et al. The recurrent SET-NUP214 fusion as a new HOXA activation mechanism in pediatric T-cell acute lymphoblastic leukemia. *Blood.* 2008;111(9):4668-4680.

36. Ben Abdelali R, Roggy A, Leguay T, et al. SET-NUP214 is a recurrent gammadelta lineage-specific fusion transcript associated with corticosteroid/chemotherapy resistance in adult T-ALL. *Blood.* 2014;123(12):1860-1863.
37. McCormack MP, Young LF, Vasudevan S, et al. The Lmo2 oncogene initiates leukemia in mice by inducing thymocyte self-renewal. *Science.* 2010;327(5967):879-883.
38. Suryani S, Carol H, Chonghaile TN, et al. Cell and Molecular Determinants of In Vivo Efficacy of the BH3 Mimetic ABT-263 against Pediatric Acute Lymphoblastic Leukemia Xenografts. *Clin Cancer Res.* 2014.
39. Chonghaile TN, Roderick JE, Glenfield C, et al. Maturation Stage of T-cell Acute Lymphoblastic Leukemia Determines BCL-2 versus BCL-XL Dependence and Sensitivity to ABT-199. *Cancer Discov.* 2014.
40. Ni Chonghaile T, Sarosiek KA, Vo TT, et al. Pretreatment mitochondrial priming correlates with clinical response to cytotoxic chemotherapy. *Science.* 2011;334(6059):1129-1133.
41. Kang MH, Kang YH, Szymanska B, et al. Activity of vincristine, L-ASP, and dexamethasone against acute lymphoblastic leukemia is enhanced by the BH3-mimetic ABT-737 in vitro and in vivo. *Blood.* 2007;110(6):2057-2066.

Supplementary Figures

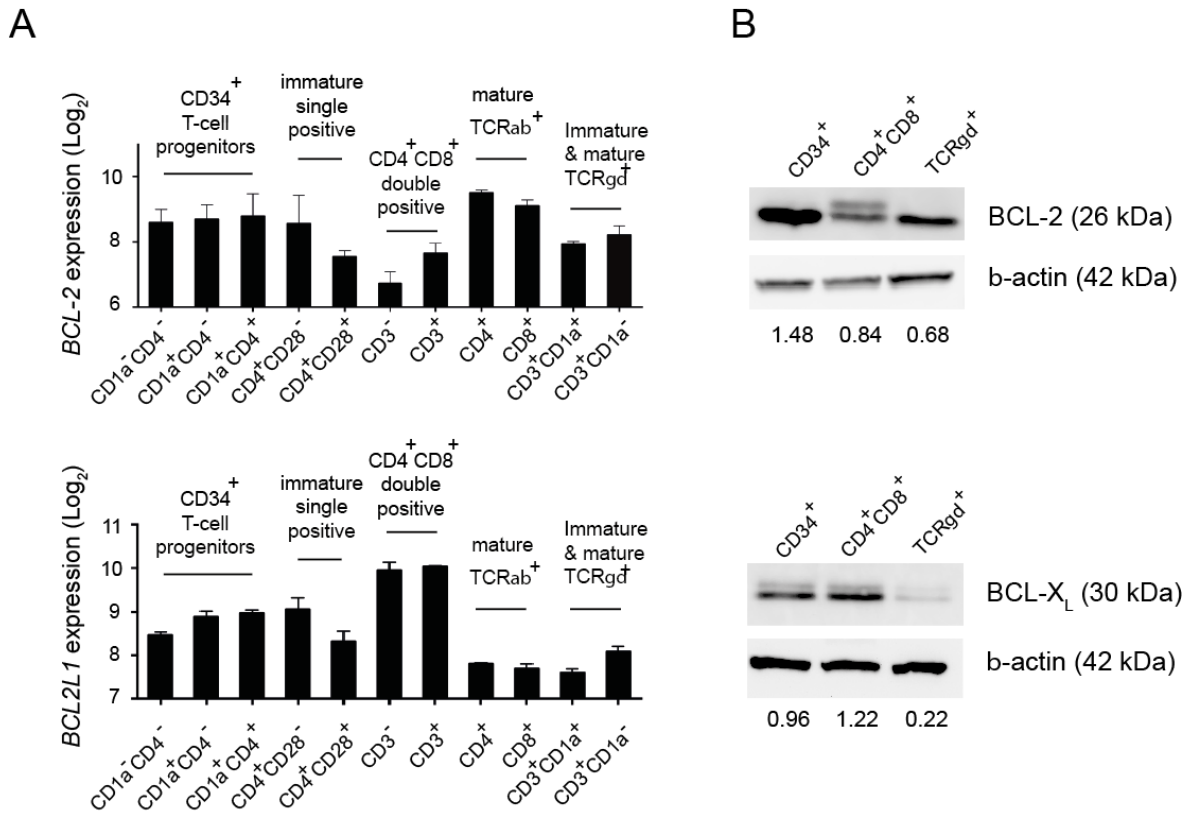

Supplementary Figure 1. BCL-2 expression in normal human T-cells. *(A) BCL-2 (probe 203685_at) and BCL-2L1 expression (probe X212312_at) in sorted subsets of human thymocytes. Average expression and standard deviation of two donors is shown. (B) Western blot analysis of BCL-2 and BCL-XL (encoded by BCL-2L1) in CD34+, CD4+ CD8+ double-positive and TCRγδ+ thymocytes. β-actin was used as loading control. For the CD4+ CD8+ double-positive cells only the lower band on the BCL-2 blot was quantified.*

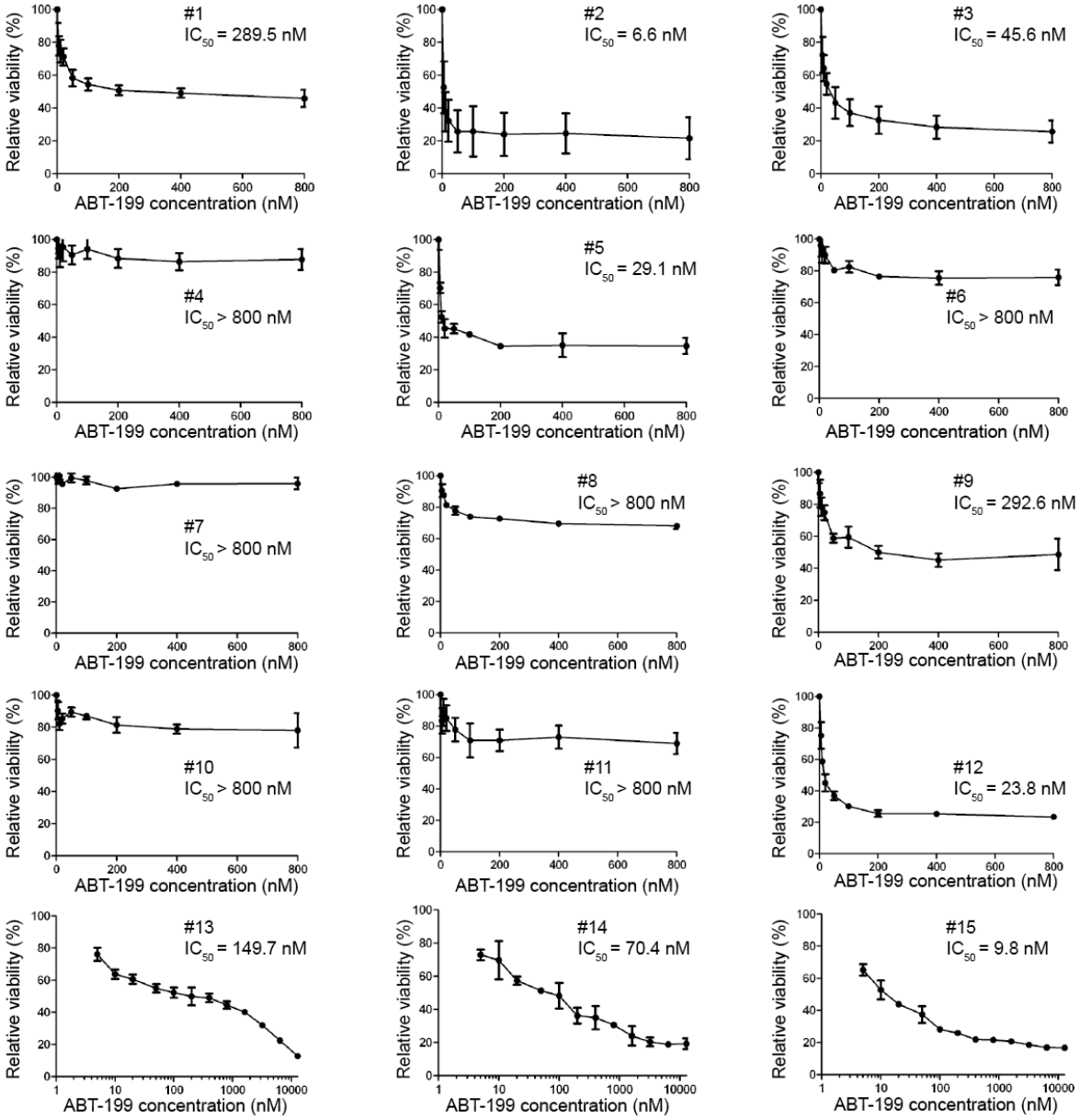

Supplementary Figure 2. In vitro ABT-199 sensitivity in primary human T-ALL samples. *The viability of 15 primary T-ALL samples after 16h treatment with different concentrations of ABT-199 is shown relative to cells incubated with DMSO (100%). The results represent the average and standard deviation of one experiment in which every concentration was tested in duplicate for every sample. The IC_{50} value for every primary sample is mentioned. Sample#2 was analyzed in three independent experiments, sample #3 and #8 in two independent experiments. For these samples the average and standard deviation of the independent experiments is shown.*

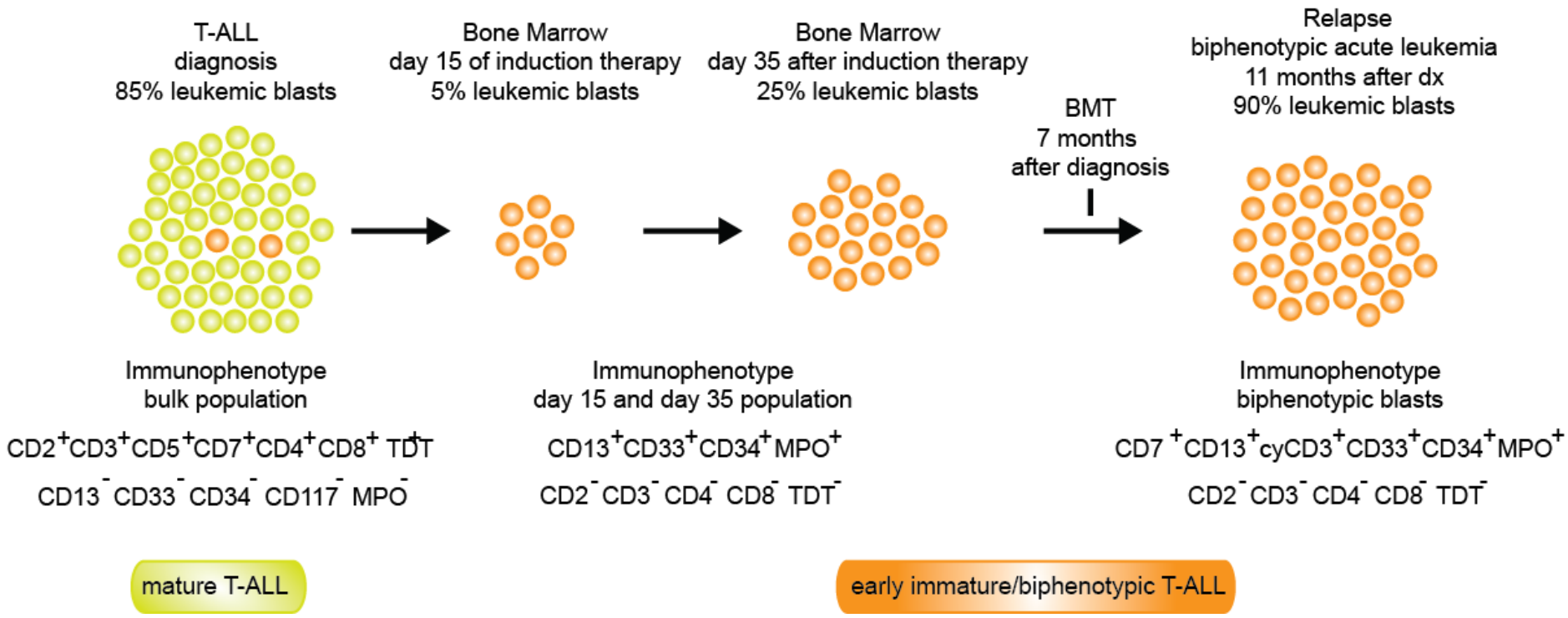

Supplementary Figure 3. Clinical course of a primary T-ALL patient. *Primary T-ALL patient #16 was diagnosed with leukemic T-cells with a characteristic mature immunophenotype. At day 15 and day 35 post induction therapy, resistant leukemic cells with an immature/biphenotypic immunophenotype persisted. At 7 months, the patient received a bone marrow transplantation (BMT). Eleven months after initial diagnosis, the patient relapsed with a leukemic burden that consisted of the presumably therapy-resistant clone that showed the immature/biphenotypic immunophenotype.*

.

Supplementary Tables

Supplementary Table 1. Characteristics of human T-ALL cell lines.

Cell line	Karyotype	TCR	Immunology	Fusion transcript/molecular subgroup
LOUCY[1]	hypodiploid karyotype with 16% polyploidy 45<2n>X, -X, del(1)(p3?2p3?4), del(5)(q14-15q34-35), t(16;20)(p1?1;q1?3) - sideline with del(6)(q23) - 1p32, 1p34 and 6q- recurrent in T-ALL	αβ- γδ+	CD2- CD3+ CD4- CD5+ CD6+ CD7+ CD8- CD13- CD19- CD34-	SET-NUP214 fusion/ expression of *MEF2C*
ALL-SIL[1]	hypertetraploid karyotype - 90-95<4n>XX/XXYY, +6, +8, +8, t(1;13)(p32;q32)x2, del(6)(q25)x2, del(9)(?p23p24)x2, t(10;14)(q24;q11.2)x2, add(17)(p11)x2 - sideline with idem, -20, -20 - carries t(10;14) effecting TLX1-TRD@ (HOX11-TCRD) juxtaposition	αβ- γδ-	cyCD3+ CD3- CD4+ CD5+ CD6+ CD7+ CD8+ CD13- CD19- CD34-	NUP214-ABL1 fusion/ *TLX1* expression
PEER[1]	pseudodiploid karyotype with 7% polyploidy - 46(42-47)<2n>XX, der(4)?dup ins(4;4)(?p11;?q21q25), del(5)(q22q31), del(6)(q13q22), del(9)(p11p22), del(9)(q22)	αβ- γδ+	CD2- CD3+ CD4+ CD5+ CD6+ CD7+ CD8+ CD13- CD19- CD34-	NUP214-ABL1 fusion/ expression of *NKX2-5* and *MEF2C*
JURKAT[1]	flat-moded hypotetraploid karyotype with 7.8% polyploidy - 87(78-91)<4n>XX, -Y, -Y, -5, -16, -17, -22, add(2)(p21)/del(2)(p23)x2 - sideline with additional der(5)t(5;10)(q11;p15), del(9)(p11)	αβ+ γδ-	CD2+ CD3+ CD4+ CD5+ CD6+ CD7+ CD8- CD13- CD19-	High *TAL1* expression
KARPAS-45[1]	hypotetraploid karyotype with 8% polyploidy - 87(84-88)<4n>XX/XXY, -Y, -3, +6, -14, -18, +mar, t(X;11)(q13;q23), der(X)t(X;11)(q13;q23), t(1;5)(q21;q12.2)x2, del(4)(q22), der(X)t(X;11)(q13;q23)t(11;14)(p13;q11) - sideline with	αβ- γδ-	CD2+ CD3- CD4+ CD5+ CD6(+) CD7+ CD8+ CD13- CD19- CD34-	MLL-AFX fusion

	del(16)(q22)			
TALL-1[1]	flat-moded hypertetraploid karyotype - 90-102<4n>XXY/XXYY, -3, -9, -12, +13, +14, +14, -15, +20, +20, +21, +21, +2-4mar, der(X;1)(p10;p10)/add(1)(q11), add(1)(p11), add(5)(p1?5), del(2)(p22p24), del(12)(q24.1), dup(21)(q11qter)x3-4	αβ+ γδ-	CD2+ CD3+ CD4+ CD5+ CD6+ CD7+ CD8+ CD13- CD19- CD34-	
DND-41[1]	flat-moded near-tetraploid karyotype with 12% polyploidy - 92(86-98)<4n>XXYY, -9, -15, +20, +mar	αβ- γδ-	CD2+ CD3+ CD6- CD7+ CD8- CD13- CD19- CD34-	*CDKN2B* and *CDKN2A* deletions and *TP53* mutation *TLX3* expression
PF-382[1]	near-diploid karyotype with 9% near-tetraploid and 15% polyploid sidelines - 45/46(43-47)<2n>X/XX, -10, +14 - sideline with +add(?15)(p11), add(1)(p32)	αβ- γδ-	CD2+ CD3- CD4+ CD5+ CD6+ CD7+ CD8+ CD13- CD19- CD34+	
CUTTL1[2]	hyperdiploid karyotype [50, XY, t(7;9),+16,+18,+20,+21] with a characteristic t(7;9)(q34;q34) translocation	αβ+γδ-	CD1a(10%) CD2+ CD3+ CD4+ CD5+ CD7+ CD8+ CD34-	*TCRB-NOTCH1* fusion: aberrant NOTCH1 signaling
CCRF-CEM[1]	near-tetraploid karyotype with extensive subclonal variation - 90(88-101)<4n>XX, -X, -X, +20, +20, t(8;9)(p11;p24)x2, der(9)del(9)(p21-22)del(9)(q11q13-21)x2 - sideline with +5, +21, add(13)(q3?3), del(16)(q12)	αβ+γδ-	CD2- CD3+ CD4+ CD5+ CD6+ CD7+ CD8- CD13- CD14- CD15+ CD19- CD33- CD34- HLA-DR-	expression of *NKX2-5*

[1]Information taken from the website of DSMZ

[2]Palomero et al. CUTLL1, a novel human T-cell lymphoma cell line with t(7;9) rearrangement, aberrant NOTCH1 activation and high sensitivity to gamma-secretase inhibitors. *Leukemia*. 2006;20(7): 1279-87 .

Supplementary Table 2. Primer sequences used for qRT-PCR.

Gene	Forward primer	Reverse primer
Human and mouse BCL2	5'-CATGTGTGTGGAGAGCGTCAA-3'	5'-GCCGGTTCAGGTACTCAGTCA-3'
Human BCL2L1	5'-TTTGTGGCCTCAGAATTGAT-3'	5'-TTGCATCTTTATCCCAAGCA-3'
Reference genes		
Human HMBS	5'-GGCAATGCGGCTGCAA-3'	5'-GGGTACCCACGCGAATCAC-3'
Human TBP	5'-CACGAACCACGGCACTGATT-3'	5'-TTTTCTTGCTGCCAGTCTGGAC-3'
Human B2M	5'-GCTGTCTCCATGTTTGATGTATCT-3'	5'-TCTCTGCTCCCCACCTCTAAGT-3'
Human RPL13A	5'-CCTGGAGGAGAAGAGGAAAGAGA-3'	5'-TTGAGGACCTCTGTGTATTTGTCAA-3'
Human HPRT1	5'-TGACACTGGCAAAACAATGCA-3'	5'-GGTCCTTTTCACCAGCAAGCT-3'
Human UBC	5'-ATTTGGGTCGCGGTTCTTG-3'	5'-TGCCTTGACATTCTCGATGGT-3'
Mouse Tbp	5'-CCCCACAACTCTTCCATTCT-3'	5'-GCAGGAGTGATAGGGGTCAT-3'
Mouse Ubc	5'-GCAGATCTTTGTGAAGACCC-3'	5'-GAAGGTACGTCTGTCTTCCT-3'
Mouse Hmbs	5'-GAATTCAGTGCCATCGTCCT-3'	5'-AATGCAGCGAAGCAGAGTTT-3'

Supplementary Table 3. Combination index (CI) for combination of ABT-199 with doxorubicine, L-asparaginase or dexamethasone in T-ALL cell lines.

Combination ABT-199 and doxorubicin

LOUCY	CI values at ED50	ED75	ED90
Experiment 1	1.11574	0.77131	0.58237
Experiment 1	1.10649	0.73571	0.55409
range ABT-199		3.475 - 55.6 nM	
range doxorubicin		462.1 - 7393.6 nM	

JURKAT	CI values at ED50	ED75	ED90
Experiment 1	1.00621	1.00595	1.00982
Experiment 2	1.10958	1.04412	0.98304
range ABT-199		655.5 – 20976 nM	
range doxorubicin		21.25 – 680 nM	

ALL-SIL	CI values at ED50	ED75	ED90
Experiment 1	0.95642	0.57942	0.4021
Experiment 1	0.58748	0.40951	0.34317
range ABT-199		22.5 – 720 nM	
range doxorubicin		21.25 – 680 nM	

Combination ABT-199 and L-asparaginase

LOUCY	CI values at ED50	ED75	ED90
Experiment 1	0.69755	0.41294	0.25066
Experiment 1	0.55506	0.39018	0.28453
range ABT-199		1.75 – 56 nM	
range L-asparaginase		0.0875 – 2.8 U/l	

JURKAT	CI values at ED50	ED75	ED90
Experiment 1	0.66792	0.57169	0.55323
Experiment 2	0.65231	0.63455	0.68977
range ABT-199		655.5 – 20976 nM	
L-asparaginase		7.5 – 240 U/l	

ALL-SIL	CI values at ED50	ED75	ED90
Experiment 1	0.3086	0.14291	0.0673
Experiment 1	0.37071	0.12689	0.05161
range ABT-199		22.5 -720 nM	
range L-asparaginase		0.7 – 22.4 U/l	

Combination ABT-199 and doxorubicin

LOUCY	CI values at ED50	ED75	ED90
Experiment 1	0.4284	0.1511	0.06867
Experiment 1	0.49285	0.40344	0.33497
range ABT-199		1.75 – 56nM	
range dexamethasone		15 - 480 µM	

Paper 2

TARGETING BET PROTEINS IMPROVES THE THERAPEUTIC EFFICACY OF BCL-2 INHIBITION IN T-CELL ACUTE LYMPHOBLASTIC LEUKEMIA

Sofie Peirs[1,2,*], Viktoras Frismantas[3,*], Filip Matthijssens[1,2], Wouter Van Loocke[1,2], Tim Pieters[1,2,4,5], Niels Vandamme[2,4,5], Béatrice Lintermans[1,2], Maria Pamela Dobay[6], Geert Berx[2,4,5], Bruce Poppe[1,2], Steven Goossens[1,2,4,5], Beat C Bornhauser[3], Jean-Pierre Bourquin[3,**] and Pieter Van Vlierberghe[1,2,**]

[1]Center for Medical Genetics, Ghent University, Ghent, Belgium
[2]Cancer Research Institute Ghent (CRIG), Ghent, Belgium
[3]Department of Pediatric Oncology, Children's Research Centre, University Children's Hospital Zurich, Zurich, Switzerland
[4]Molecular and Cellular Oncology Lab, VIB Inflammation Research Center, Ghent University, Ghent, Belgium
[5]Department of Biomedical Molecular Biology, Ghent University, Ghent, Belgium
[6]Swiss Institute of Bioinformatics (SIB), Lausanne, Switzerland

*SP and VF contributed equally to this work
**JPB and PVV contributed equally to this work

Published in LEUKEMIA, 11 January 2017; Epub ahead of print

Abstract

Inhibition of anti-apoptotic BCL-2 (B-cell lymphoma 2) has recently emerged as a promising new therapeutic strategy for the treatment of a variety of human cancers, including leukemia. Here, we used T-cell acute lymphoblastic leukemia (T-ALL) as a model system to identify novel synergistic drug combinations with the BH3 mimetic venetoclax (ABT-199). *In vitro* drug screening in primary leukemia specimens that were derived from patients with high risk of relapse or relapse and cell lines revealed synergistic activity between venetoclax and the BET (bromodomain and extraterminal) bromodomain inhibitor JQ1. Notably, this drug synergism was confirmed *in vivo* using T-ALL cell line and patient-derived xenograft models. Moreover, the therapeutic benefit of this drug combination might, at least in part, be mediated by an acute induction of the pro-apoptotic factor *BCL2L11* and concomitant reduction of BCL-2 upon BET bromodomain inhibition, ultimately resulting in an enhanced binding of BIM (encoded by *BCL2L11*) to BCL-2. Altogether, our work provides a rationale to develop a new type of targeted combination therapy for selected subgroups of high-risk leukemia patients.

Introduction

T-cell acute lymphoblastic leukemia (T-ALL) arises from the malignant transformation of T-cell progenitors and accounts for about 15% of childhood and 25% of adult ALL cases[1]. The cure rate for childhood T-ALL has steadily increased over the past decades, with current survival rates reaching ~ 85%[2,3]. Although these numbers are high, the clinical perspective for children who fail induction therapy or suffer from relapsed disease remains extremely poor, with only a 7–23% subset of relapsed T-ALL patients surviving beyond 3 to 5 years after the initial diagnosis[4]. Compared with childhood leukemia, the clinical picture for adult T-ALL is even worse, with high relapse rates and long-term disease-free survival of ~ 40%[5–7]. Altogether, these figures suggest that better and less toxic treatment strategies are urgently required to further improve the clinical management of childhood and adult T-ALL patients.

Recently, we and other research groups reported promising therapeutic activity for venetoclax (ABT-199), a highly specific inhibitor of the anti-apoptotic protein BCL-2 (B-cell lymphoma 2), in immature subtypes of human T-ALL[8–10]. Nevertheless, venetoclax sensitivity is variable between different T-ALL patient samples and the emergence of resistance to venetoclax[11–13] as well as the occurrence of dose-limiting toxicities[14] provides a rationale for the evaluation of venetoclax as part of a combination therapy. Indeed, previous studies have shown that venetoclax can synergize with conventional chemotherapeutic agents in human T-ALL, including doxorubicin, L-asparaginase, dexamethasone and cytarabine[8,9]. Venetoclax has recently also been approved by the FDA (Food and Drug Administration) for the treatment of chronic lymphocytic leukemia. Indeed, clinical trials demonstrated progress-free survival in more than two-thirds of relapsed chronic lymphocytic leukemia patients[14], including poor prognostic chronic lymphocytic leukemia patients who carry a 17p deletion[15]. Nevertheless, complete remission remained uncommon[14], further reinforcing the need for the evaluation of combined therapeutic strategies.

Bromodomains of the bromodomain and extraterminal (BET) protein family recognize ε-N-acetylation of lysine residues on histone tails. BRD4 is an important BET protein that recruits the positive transcription elongation factor complex (P-TEFb) to acetylated chromatin[16]. The

transcriptional coactivators BRD4 and Mediator co-occupy enhancers and promoters of active genes and are enriched at large stretches of enhancer sequences, often termed super-enhancers[17–19]. Notably, these enhancers regulate the expression of critical oncogenes in a variety of human cancers, providing a rationale for the use of BET bromodomain inhibitors, such as JQ1, as powerful anticancer agents[17–19]. In addition, in T-ALL, BET bromodomain inhibitors have shown therapeutic efficacy in a number of *in vitro* and *in vivo* model systems and were shown to inhibit the expression of the T-ALL oncogene *MYC*[20–22]. Furthermore, super-enhancers have been identified in a panel of T-ALL cell lines near putative oncogenes, including *MYB*, *TAL1*, *CDK6* and *NOTCH1*[18].

In this study, we identified synergistic drug combinations with the BH3 mimetic venetoclax in the context of human T-ALL. Most notably, we show that combined targeting of BCL-2 and BET bromodomain proteins synergistically affects leukemic tumor growth in T-ALLs that were resistant to conventional chemotherapeutic agents.

Materials and methods

Primary patient samples

Primary human ALL cells were recovered from cryopreserved bone marrow aspirates of patients enrolled in the ALL-BFM 2000, 2009 and ALL-REZ-BFM 2002 study. Informed consent was given in accordance with the Declaration of Helsinki and the ethics commission of the Kanton Zurich (approval number 2014-0383). Samples were classified as standard risk, medium risk, high risk, very high risk or relapse samples according to the clinical criteria used in ALL-BFM 2000[23].

Drug-screening platform

The *in vitro* drug response of T-ALL primary patient samples was assessed in co-culture with hTERT-immortalized primary bone marrow mesenchymal stromal cells as described previously.[23] Details are provided in the Supplementary Data.

Cell lines

Cell lines were purchased from the DSMZ repository (Braunschweig, Germany), except for CUTLL1 (gift from Professor Adolfo Ferrando, Columbia University, New York, NY, USA) and KOPTK1 (gift from Professor Hans-Guido Wendel, Memorial Sloan Kettering Cancer Center, New York, NY, USA). Cells were cultured in RPMI-1640 medium (52400-025; Life Technologies, Carlsbad, CA, USA) supplemented with 10 or 20% fetal bovine serum, 100 U/ml penicillin, 100 µg/ml streptomycin (15140-148; Life Technologies), 100 µg/ml kanamycin sulfate (15160-047; Life Technologies) and 2 mM L-glutamine (25030024; Life Technologies) at 37 °C with 5% CO2.

In vitro evaluation of synergism between venetoclax and JQ1 in human T-ALL cell lines and primary samples

The 48h treatment of the cell lines with venetoclax (2253-1; BioVision, Milpitas, CA, USA) and/or (+)-JQ1 (27401; BPS Bioscience, San Diego, CA, USA) and viability measurements via the CellTiter Glo Viability assay (Promega, Madison, WI, USA) were done as described in Peirs et al.[8] CalcuSyn software (Biosoft, Cambridge, UK) was used to calculate the combination index (CI) with the Chou–Talalay method. The reported CI is the average of the values obtained at the effective dose (ED) points ED_{50}, ED_{75} and ED_{90}. Primary patient

samples co-titration experiments were performed for selected drugs. T-ALL cell plates were prepared and handled in the same manner as for drug combination screening described above. Selected drugs in combination with venetoclax were dispensed using Tecan D300 digital dispenser (Tecan Group, Männedorf, Switzerland) in a concentration matrix. The concentration range tested for venetoclax and JQ1 were determined for each patient based on initial drug response screening. CI was calculated using Chou–Talalay method as implemented in R package (https://github.com/xtmgah/DDCV).

Western blot

Western blot analysis was performed as previously described[8]. The primary antibodies used were Bcl-2 antibody (C-2) (1:500, sc-7382; Santa Cruz Biotechnology, Dallas, TX, USA), PARP-1 antibody (F-2) (1:1000, sc-8007; Santa Cruz Biotechnology), BIM antibody (1:1000, AB17003; EMD Millipore, Darmstadt, Germany), β-actin antibody (1:10 000, Clone AC-75, A2228; Sigma-Aldrich, St Louis, MO, USA) and α-tubulin antibody (1:10 000, T5168; Sigma-Aldrich). The detection of the blots was done with ChemiDoc-It Imaging System (UVP, Upland, CA, USA). Densitometric analysis of the protein bands was performed using ImageJ (NIH, Bethesda, MD, USA). Images have been cropped for presentation.

Annexin V/propidium iodide (PI) staining

FITC Annexin V Apoptosis Detection Kit I (556547; BD Biosciences, San Jose, CA, USA) was used and samples were measured on the S3 cell sorter (Bio-Rad, Hercules, CA, USA).

Mice experiments

Female nonobese diabetic/severe combined immunodeficient γ (NSG) mice were injected in the tail vein with 150 µl phosphate-buffered saline containing 5×10^6 luciferase-positive LOUCY cells[8], 5×10^6 ALL-SIL cells or 1×10^6 cells from a secondary xenograft of patient T-VHR-26. Engraftment of the cells was followed by bioluminescence imaging as previously described[8] or by measuring the percentage of leukemic cells in the blood. Once there was clear engraftment (day 0), mice were randomly divided into four groups (control, venetoclax, JQ1 and combination) and treatment was started. Mice received daily 50 mg venetoclax per kg body weight via oral gavage and/or 50 mg JQ1 per kg body weight via intraperitoneal injection. Venetoclax (Axon Medchem, Groningen, The Netherlands) was formulated in 60% phosal 50 propylene glycol, 30% polyethylene glycol 400 and 10% ethanol. (+)-JQ1 (MedChem Express, South Brunswick Township, NJ, USA) was formulated in 10% dimethyl sulfoxide and 90% of a 10% 2-hydroxypropyl-β-cyclodextrin solution. At the end of the treatment period, blood was taken and mice were killed. The percentage of leukemic cells was analyzed by staining the cells with phycoerythrin-labeled antibody for human CD45 (hCD45; 130-098-141; Miltenyi Biotec, Bergisch Gladbach, Germany), performing red blood cell lysis and measuring the percentage on a LSRII flow cytometer using FACSDiva software (BD Bioscience). The ethical committees on animal welfare at Ghent University Hospital and University Children's Hospital Zurich approved all animal experiments.

Gene expression profiling and GSEA

LOUCY cells were treated with dimethyl sulfoxide or (+)-JQ1. Three biological replicates of this treatment were performed and RNA was isolated using the miRNeasy mini kit (Qiagen, Venlo, The Netherlands) with on-column DNase digestion. RNA quality was evaluated by the Experion RNA StdSens analysis kit (Bio-Rad). RNA was amplified and labeled using the Low Input Quick Amp Labeling Kit, One Color (5190-2305; Agilent Technologies, Santa Clara, CA, USA) and hybridized with the Gene Expression Hybridization Kit (5188-5242; Agilent

Technologies) to the SurePrint G3 Human Gene Expression Microarray G4851A (design ID 028004, Agilent Technologies). Normalization of microarray intensities was done using the variance stabilization and calibration (VSN, Bioconductor release 3.30.0) package in R software (version 3.0.2)[24]. Only probes with a signal 10% higher than the negative control probes were considered for analysis. Differential expression analysis was performed using the limma package (Bioconductor release 3.18.13) with P-value adjustment using the Benjamini and Hochberg method. The design matrix took into account the pairing information of the data. Enrichment analysis was performed with the Molecular Signatures database (MSigDB) c2 gene sets collection using the GSEA (Gene Set Enrichment Analysis) desktop application (version 2.2.0, Broad Institute, Cambridge, MA, USA)) run with the default parameters and with gene set permutations. The data have been deposited in NCBI Gene Expression Omnibus (GEO)[25] and are accessible through GEO Series accession number GSE81918.

qRT-PCR

The miRNeasy mini kit (Qiagen) and the RNase-Free DNase set (Qiagen) were used to isolate RNA. For determination of mRNA levels, complementary DNA (cDNA) synthesis was performed with the iScript Advanced cDNA synthesis kit (Bio-Rad). The SsoAdvanced Universal SYBR Green Supermix (Bio-Rad) was used for the PCR reactions. Every sample was analyzed in duplicate and the gene expression was normalized against three housekeeping genes. For quantification of mature microRNAs, the miScript II RT kit (Qiagen) and target-specific miScript Primer Assays (Qiagen) together with the miScript SYBR Green PCR Kit were used. All real-time quantitative PCR reactions were run on the LightCycler 480 (Roche, Vilvoorde, Belgium) and qBasePLUS software (Biogazelle, Zwijnaarde, Belgium) was used for analysis. Primer sequences and miScript Primer Assays are listed Supplementary Table 5.

Co-immunoprecipitation

Protein lysates were incubated with 2 µg of antibody. After 4 h of rotation at 4 °C, 20 µl of Protein A UltraLink Resin (53139; Thermo Scientific, Waltham, MA, USA) was added for overnight incubation at 4 °C. Beads were washed 3 times with RIPA buffer and immunoprecipitates were eluted by heating the beads at 95 °C in 2 × SDS loading buffer (62 mM Tris-HCl (pH 6.8), 4% SDS, 20% glycerol, 0.01% BFB (bromophenol blue) and 2.5% β-mercaptoethanol) for 10 min. A part of the original lysates were similarly denaturated by heating at 95 °C for 10 min after adding 5 × SDS loading buffer (155 mM Tris-HCl (pH 6.8), 5% SDS, 32% glycerol, 0.025% BFB and 2.5% β-mercaptoethanol).

Modulation of BIM expression

The pENTR223-BCL2L11 (LMBP ORF81079-A09) plasmid was available from the BCCM/LMBP Plasmid Collection[26] and was used to clone *BCL2L11* in the pInducer21 plasmid[27]. The MISSION lentiviral shBCL2L11 TRCN0000001051 (Sigma-Aldrich) vector (BCCM/LMBP Collection[26]), in which the puromycin resistance cassette was replaced by eGFP (enhanced green fluorescent protein), was used to perform BIM knockdown. As nontargeting small hairpin RNA control, MISSION pLKO.1-puro Non-Mammalian small hairpin RNA Control Plasmid (SHC002), in which puro was also replaced by eGFP, was used. Virus production was performed in HEK293TN cells using JetPEI polyplus with pMD2.G (envelope plasmid), psPAX2 (packaging plasmid) and target plasmid in 0.1:0.9:1 ratios. Transduced KARPAS-45 cells expressing GFP (green fluorescent protein) were

selected by cell sorting. *BCL2L11* expression was induced by adding doxycyclin (1 µg/ml) and sensitivity to venetoclax was evaluated by adding venetoclax together with or without doxycycline for 48 h to the cells. To evaluate the effect of BIM knockdown, cells were treated with venetoclax, JQ1 or the combination for 48 h. Viability was evaluated with CellTiter Glo as described above.

Statistics

GraphPad Prism 5.04 (La Jolla, CA, USA) was used for statistical analyses.

Results

Identification of synergistic drug combinations with venetoclax in primary human T-ALL

Previous studies have shown promising antitumor activity for venetoclax in the context of human T-ALL[8–10]. However, drug responses have been variable across patients both *in vitro* and in xenografts, suggesting the need for predictive biomarkers and further investigation toward synergistic drug combinations with venetoclax. Given this, we took advantage of a drug-profiling platform[28,29] (Figure 1a) to test 21 clinically relevant compounds (Supplementary Table 1) for their ability to synergize with venetoclax in six primary human T-ALLs, including five diagnostic and one relapse specimen. Notably, the selected patient samples represented different molecular genetic subtypes of human T-ALL and displayed a variety of tumor immunophenotypes. In addition, they displayed variable levels of BCL-2 and BIM protein expression (Supplementary Figure 1a) and most of these high-risk T-ALL patient samples experienced significant levels of minimal residual disease upon first-line therapy (Supplementary Table 2).

First, we generated venetoclax response curves for each T-ALL sample and selected a sublethal dose of venetoclax for screening purposes (Figure 1a). Two T-ALL samples were sensitive at concentrations below 100 nM, whereas the remaining cases were more resistant to venetoclax (Supplementary Figure 1b). This variability in venetoclax sensitivity amongst T-ALL patient samples corresponded to large differences in the area under the curve, a parameter that captures both IC_{50} (half-maximal inhibitory concentration) and E_{max} (maximal efficacy) as relevant end points of drug activity (Figure 1b). Next, we generated dose response curves (1 nM, 10 nM, 100 nM, 1 µM and 10 µM) for the 21 compounds in the presence or absence of a sublethal dose of venetoclax (Figure 1a). The results of this initial screening are visualized by scatterplots of area under the curve values, in which decreased area under the curve upon addition of venetoclax is indicative of increased antileukemic activity (Figure 1b and Supplementary Figure 2). In line with previous studies, the combination of venetoclax with conventional chemotherapeutic agents including vincristine, dexamethasone and etoposide increased therapeutic efficacy in some of the T-ALL cases analyzed (Figure 1b). The strongest effects, however, were observed for the combination of venetoclax with JQ1 that resulted in reduced leukemic tumor growth in 5 out of 6 primary T-ALL patient samples (Figure 1b). As a confirmation, we validated responsive (Figure 1c) as well as nonresponsive (Supplementary Figure 3) drug interactions identified in this initial screen. Altogether, this screening effort identified clinically relevant drugs that could increase the therapeutic efficacy of venetoclax in the context of T-ALL.

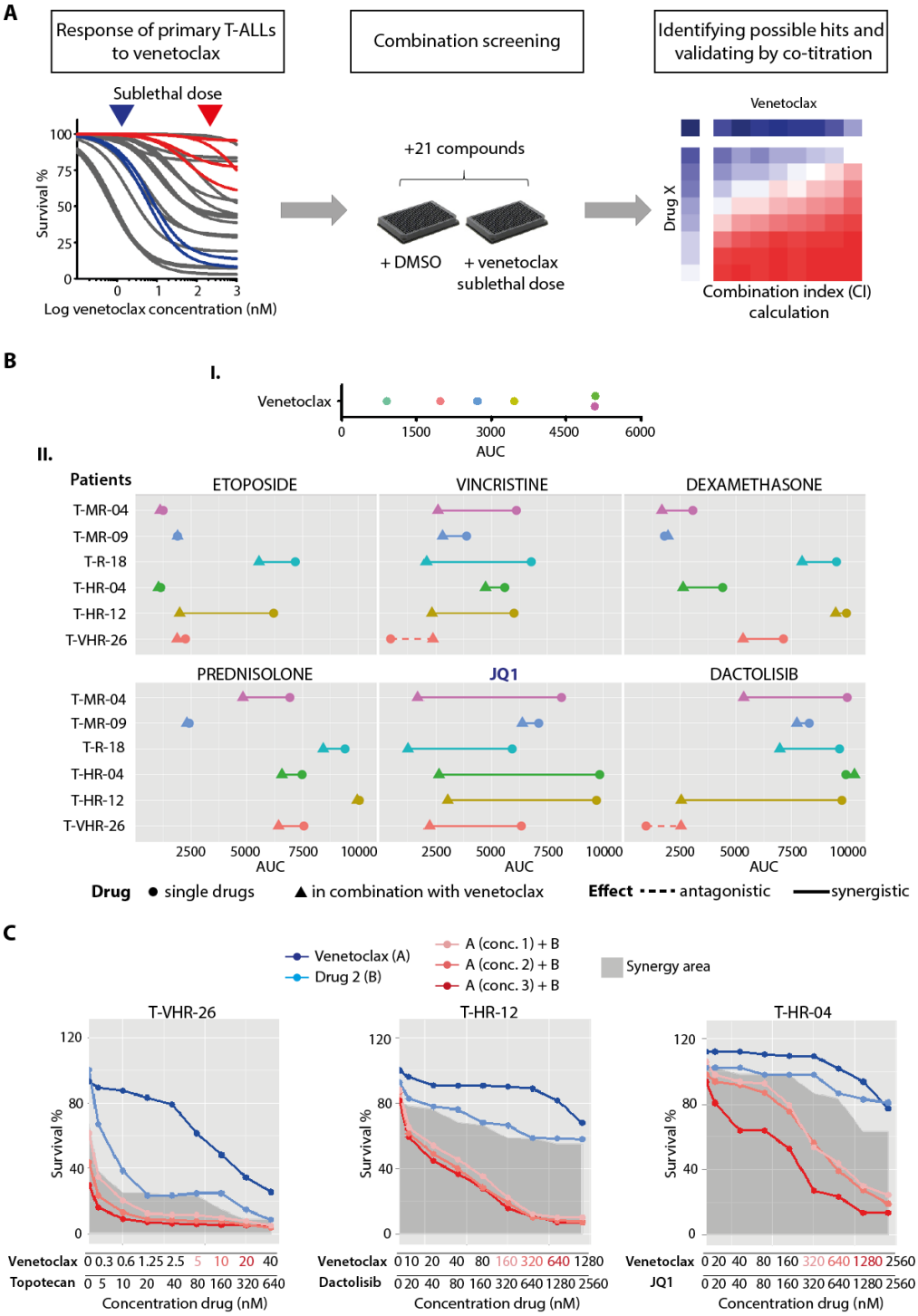

Figure 1. Drug-screening platform to identify novel synergistic combinations of venetoclax and other drugs. *(a) In a panel of primary T-ALL samples the effect of venetoclax treatment on cell viability was measured by flow cytometry using 7-aminoactinomycin D (7-AAD) 72 h after venetoclax treatment. Six representative samples (blue curves: sensitive to venetoclax; red curves: more resistant to venetoclax) were selected. For each sample, an optimal sublethal dose of venetoclax was calculated based on area under the curve (AUC) calculations of venetoclax as single agent. A single venetoclax dose was combined with selected clinically relevant compounds and the response change was compared with the control plate. Promising single compound combinations were validated in co-titration experiments. (bi) Scatterplots representing response of T-ALL samples (N=6) to venetoclax alone, shown as AUC. (bii) Responses of T-ALL patient samples to combination of a sublethal venetoclax dose and indicated chemotherapeutic agents. AUC values of dose response curves from individual drug treatments (circles) or combined with venetoclax (triangles) are shown. (c) Representative examples of co-titration assays for compounds found to synergize with venetoclax in preselected T-ALL samples from initial combination screening: topoisomerase I inhibitor topotecan (left), dual PI3K and mTOR inhibitor dactolosib (middle) and BRD4 inhibitor JQ1 (right).*

Combined targeting of BCL-2 and BET bromodomain proteins in human T-ALL

Given that our initial screen pointed toward increased efficacy of venetoclax upon BET bromodomain inhibition in a significant proportion of T-ALLs, we subsequently analyzed the synergistic potential of this drug combination in more detail by performing co-titration experiments with individually optimized concentration ranges in primary leukemias and a panel of human T-ALL cell lines.

First, we determined the CIs for the six primary T-ALLs that were also used for the initial screening and identified synergistic activities (CI<1) between venetoclax and JQ1 in five out of six cases analyzed (Figure 2a). Notably, similar results were obtained using OTX015 (MK-8628), another BET bromodomain inhibitor currently being tested in clinical trials for various tumor entities[30,31] (Supplementary Figure 4).

Next, we determined dose response curves in a panel of 13 human T-ALL cell lines with different BCL-2 levels and varying sensitivities toward venetoclax (Figure 2b and Supplementary Figure 5). Notably, T-ALL cell lines displayed variable levels of synergism with the lowest CI values (strongest synergism) detected for tumor lines with high BCL-2 expression (Figure 2b). Indeed, the CI showed a negative correlation with BCL-2 protein levels in T-ALL cell lines (Figure 2c). Moreover, synergistic activity of this drug combination corresponded to increased cell death induction in T-ALL cell lines with low CI values (Supplementary Figure 6).

Evaluation of the venetoclax and JQ1 combination therapy in xenograft models

To evaluate the therapeutic potential of combined BCL-2 and BET bromodomain inhibition in human T-ALL, we subsequently performed *in vivo* drug treatment experiments using xenograft models. At 4 weeks after injection of luciferase-positive LOUCY cells[8] in immunodeficient mice, successful engraftment was confirmed by bioluminescence imaging and daily drug treatment was initiated (days 1–13). Leukemia still progressed under JQ1 monotherapy (n = 5), although to a lesser extent as compared with vehicle-treated control mice (n = 8; Figure 3a and Supplementary Figure 7). Mice treated for 13 days with venetoclax alone (n=5) initially showed disease regression, but this therapeutic response was not durable (Figure 3a and Supplementary Figure 7). In contrast, combination of venetoclax with JQ1 (n = 5) resulted in durable disease regression (Figures 3a and b). In line with these results, analysis of the percentage of human leukemic cells in peripheral blood and bone marrow as well as examination of the spleen size confirmed the superior therapeutic effect of this combination treatment (Figure 3c and d and Supplementary Figure 8). Of note, mice receiving JQ1 alone or in combination with venetoclax displayed significant weight loss (Supplementary Figure 8), a putative side effect of BET bromodomain inhibition.
The synergistic effect of combined BCL-2 and BET bromodomain inhibition was also confirmed in the *TLX1*-positive T-ALL cell line ALL-SIL (Supplementary Figure 9). The genetic characteristics of LOUCY and ALL-SIL are summarized in Supplementary Table 3.

Finally, we performed a similar *in vivo* drug treatment experiment using a primary patient-derived xenograft. For this, leukemic cells from the very high risk T-ALL patient (T-VHR-26) were engrafted and treated with a similar drug regimen as mentioned above. Notably, this experiment confirmed the superior therapeutic effect of combined BCL-2 and BET bromodomain inhibition for the treatment of this high risk T-ALL patient sample (Figure 4 and

Supplementary Figure 10). Of note, in this experiment, no significant weight loss was observed in any of the treatment groups (Supplementary Figure 10c).

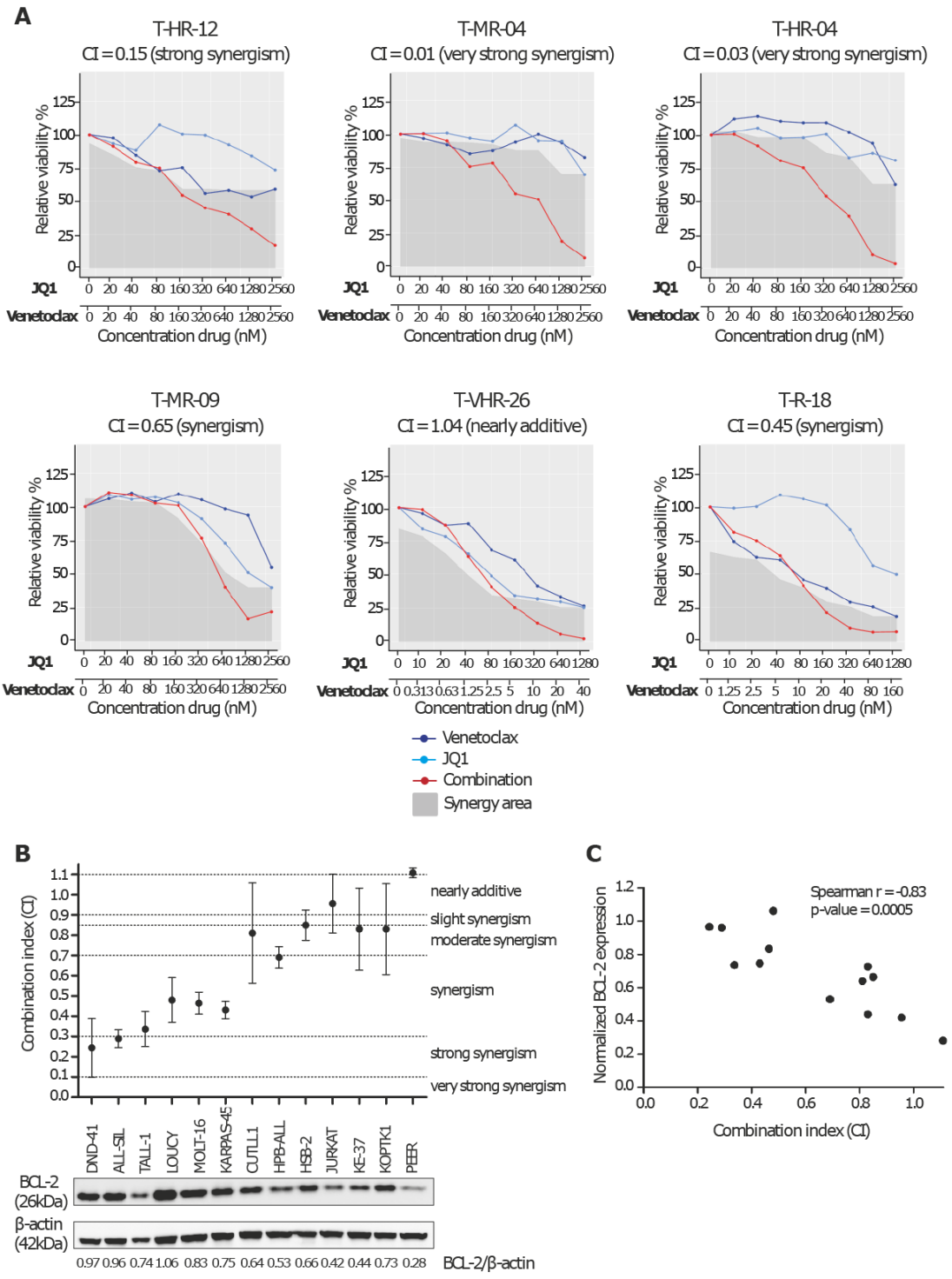

Figure 2. In vitro synergism between venetoclax and JQ1 in primary patient samples and T-ALL cell lines. *(a) Dose response curves are given for co-titration assays in primary T-ALL samples treated for 72h with increasing concentrations of both venetoclax and the BRD4 inhibitor JQ1. CIs indicate synergism for five of the six cases, and additive activity for the remaining sample. (b) Overview of CIs between venetoclax and JQ1 in a panel of human T-ALL cell lines treated for 48h with indication of the degree of synergism. Mean and s.d. of at least three independent experiments per cell line are represented. Western blot (bottom panel) indicates the BCL-2 protein levels in this cell line panel with β-actin as loading control. (c) Scatterplot demonstrating the correlation between BCL-2 protein level and CI in the T-ALL cell lines.*

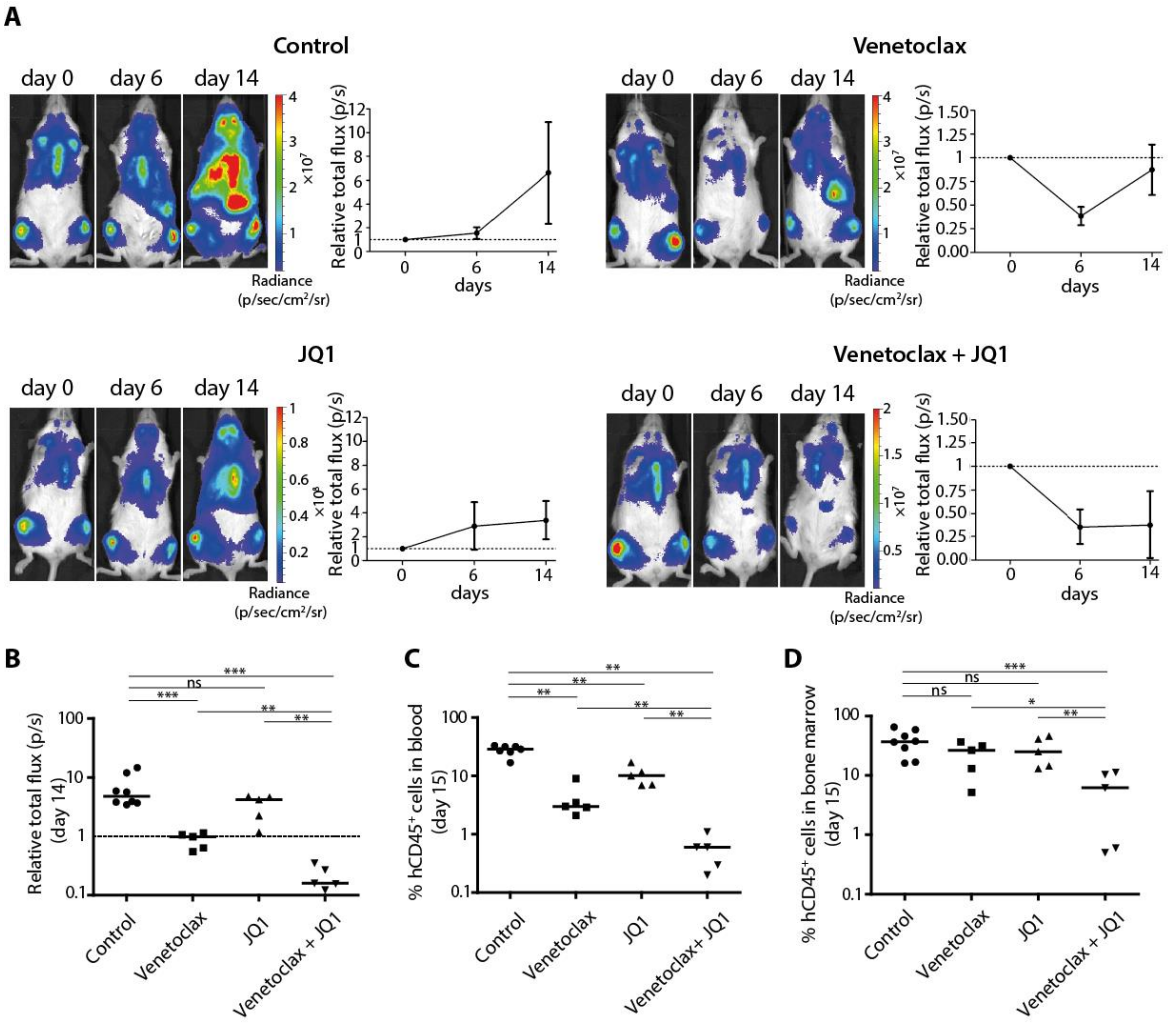

Figure 3. Combination treatment of mice xenografted with luciferase-positive human LOUCY cells. *(a) Leukemic burden was followed during the experiment on the basis of the luminescence of the leukemia cells. For each treatment group, one mouse is represented from day 0 (that is, the day before the treatment started) till day 14 (that is, the end of the experiment). The graph shows the average and s.d. of the total flux of luminescence for all the mice in the group relative to the signal on day 0. (b) Total flux of each mouse within a treatment group on day 14 relative to day 0. (c) Percentage of hCD45+ leukemic cells in the peripheral blood for each mouse. All viable cells after red blood cell lysis were selected based on the forward and side scatter parameters. One sample from the control group could not be analyzed correctly. (d) Percentage of hCD45+ leukemic cells in the bone marrow for each mouse. All the viable cells after red blood cell lysis were selected based on the forward and side scatter parameters. The one-tailed Mann–Whitney test was used to compare the treatment groups statistically. NS, not significant, *P<0.05, **P<0.01, ***P<0.001. Horizontal lines on the graph indicate the median for each group.*

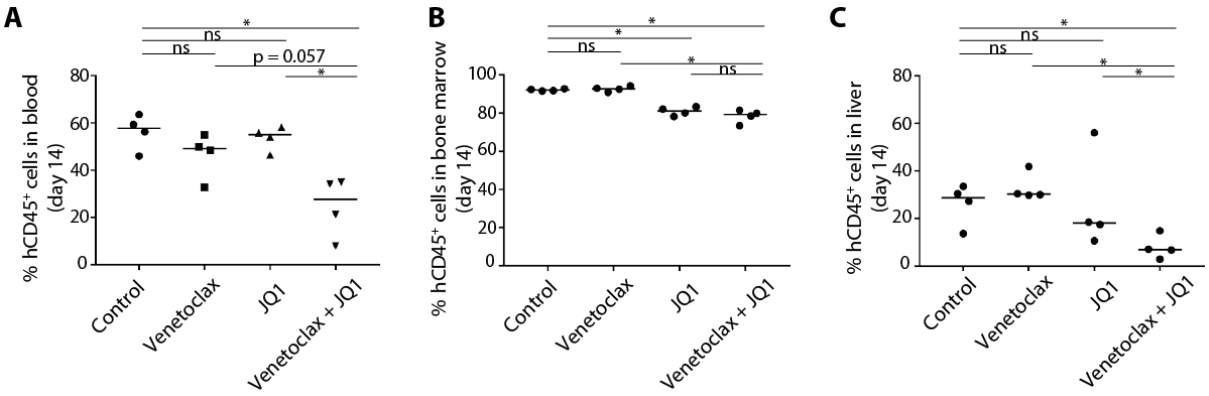

Figure 4. Combination treatment of patient (T-VHR-26)-derived xenograft. *(a) Percentage of hCD45+ leukemic cells in the peripheral blood for each mouse after 14 days of treatment. (b) Percentage of hCD45+ leukemic cells in the bone marrow for each mouse after 14 days of treatment. (c) Percentage of hCD45+ leukemic cells in the liver for each mouse after 14 days of treatment. The one-tailed Mann–Whitney test was used to compare the treatment groups statistically. NS, not significant, *P<0.05. Horizontal lines on the graph indicate the median for each group.*

Mechanistic insights into the synergistic activities of venetoclax and JQ1 in human T-ALL

To understand how BET bromodomain inhibition might synergize with the BCL-2 inhibitor venetoclax, we subsequently analyzed the transcriptional consequences of JQ1 treatment in the T-ALL cell line LOUCY by microarray analysis. Short-term exposure to a low dose of JQ1 (4 h, 250 nM) provided insights into the genes whose expression was immediately affected by BET bromodomain inhibition (Figure 5a, left). In contrast, sustained exposure at a higher concentration (48 h, 1 µM) revealed broader transcriptional effects with more than half of the expressed probe sets showing significant up- or downregulation (adjusted P-value<0.05; Figure 5a, right). Significantly downregulated genes upon shortterm drug treatment included stem-cell associated genes and putative oncogenes such as *BAALC*, *WT1*, *MN1* (*meningioma 1*), *MEF2C*, *LMO1* and *LMO2*, whereas other oncogenic factors, including *BCL2*, *IGFBP7* (*insulin like growth factor binding protein 7*), *ZEB2*, *GFI1B*, *MYB* and *LYL1*, only changed significantly after 48 h.

In line with previous reports[17–19], these JQ1-responsive genes were regulated by strong and active enhancer elements characterized by broad binding of the H3K27ac histone mark in LOUCY cells[32] (Figure 5b). Indeed, genes associated with the 500 highest ranked enhancer regions in LOUCY were significantly enriched in genes downregulated after JQ1 treatment (Figure 5c). Moreover, enrichment analysis using gene sets from the MSigDB revealed that genes upregulated after JQ1 in LOUCY cells significantly overlapped with genes activated upon histone deacetylase (HDAC) inhibition (Figure 5d). In line with this notion, the LINCS (Library of Integrated Cellular Signatures) revealed a strong connection between the JQ1-induced expression signature in LOUCY and gene signatures induced by HDAC inhibitors (Supplementary Table 4).

Given that binding of the pro-apoptotic BIM (encoded by *BCL2L11*) to the BH3 domain of BCL-2 is an important mediator of venetoclax activity[33–36], we subsequently focused on the transcriptional effects of JQ1 on the expression of both factors. Notably, in LOUCY cells, *BCL2L11* expression was induced after short-term JQ1 exposure (Figure 5a, left), whereas

downregulation of *BCL2* expression was only detected at later time points (Figure 5a, right). In addition, the expression of the miR17-92 cluster, a known negative regulator of BIM[37], was not affected after 4 h of JQ1 treatment but was clearly downregulated after 48 h (Supplementary Figure 11a). Upregulation of pro-apoptotic *BCL2L11* and concomitant downregulation of anti-apoptotic *BCL2* could be confirmed in all T-ALL cell lines that displayed strong synergy (CI<0.5) for the ABT199/JQ1 drug combination. As a result, BET bromodomain inhibition triggered an increased BIM to BCL-2 ratio (Figure 6a and Supplementary Figure 11b), providing a putative explanation for the improved therapeutic efficacy of venetoclax upon JQ1 treatment. Indeed, co-immunoprecipitation experiments demonstrated an increased BIM to BCL-2 binding (Figure 6b) upon JQ1 treatment. Finally, doxycycline-inducible overexpression of BIM in the KARPAS-45 cell line mimicked the effect of JQ1 and resulted in an increased sensitivity toward venetoclax (Figure 6c), whereas knockdown of BIM lowered the sensitivity to ABT-199, JQ1 and combination treatment (Figure 6d).

Discussion

Venetoclax is a promising new molecular therapy that is currently being evaluated in clinical trials for different hematological malignancies[14,15,38]. However, the limited number of complete remissions[14] and the emergence of resistance with venetoclax as single agent prompts for a systematic evaluation of combinations with rationally designed small molecules to assess its true therapeutic potential. Indeed, synergistic cytotoxic effects have been described for the combination of venetoclax with Bruton tyrosine kinase (BTK)[39–41], galectin[42], aurora kinase A[43], cyclin-dependent kinase[44,45] and PI3K/AKT/mTOR (phosphatidylinositol-3-kinase/AKT/mammalian target of rapamycin) inhibition[13,46].

Given the promising single-agent activity of venetoclax in human T-ALL subsets[8–10], we systematically evaluated clinically relevant drugs in order to identify synergistic combinations with venetoclax. The strongest and most consistent effect was detected for the combination with the bromodomain inhibitors JQ1 and OTX015, both targeting critical mechanisms that are deregulated in cancer cells. This effect could be validated *in vivo* using leukemia xenograft models. Notably, this concept has recently been suggested as an experimental therapy for double-hit lymphoma, triple-hit lymphoma and mantle cell lymphoma in which both *MYC* and *BCL2* are deregulated[47–49]. Interestingly, our preclinical data indicate that relevant activity can be obtained with this combination of agents irrespective of their activity as single agent that may possibly broaden the cohort of eligible cancer types (or subsets) for clinical translation. However, the challenge will be to identify useful biomarkers to better define patients who may benefit from such experimental combinations. Interestingly, an increase of BCL-2 protein levels in human T-ALL cell lines correlated with synergism between venetoclax and JQ1. Nevertheless, the value of additional methodologies such as BH3-profiling[50] should also be taken into consideration in future studies of this therapeutic rationale.

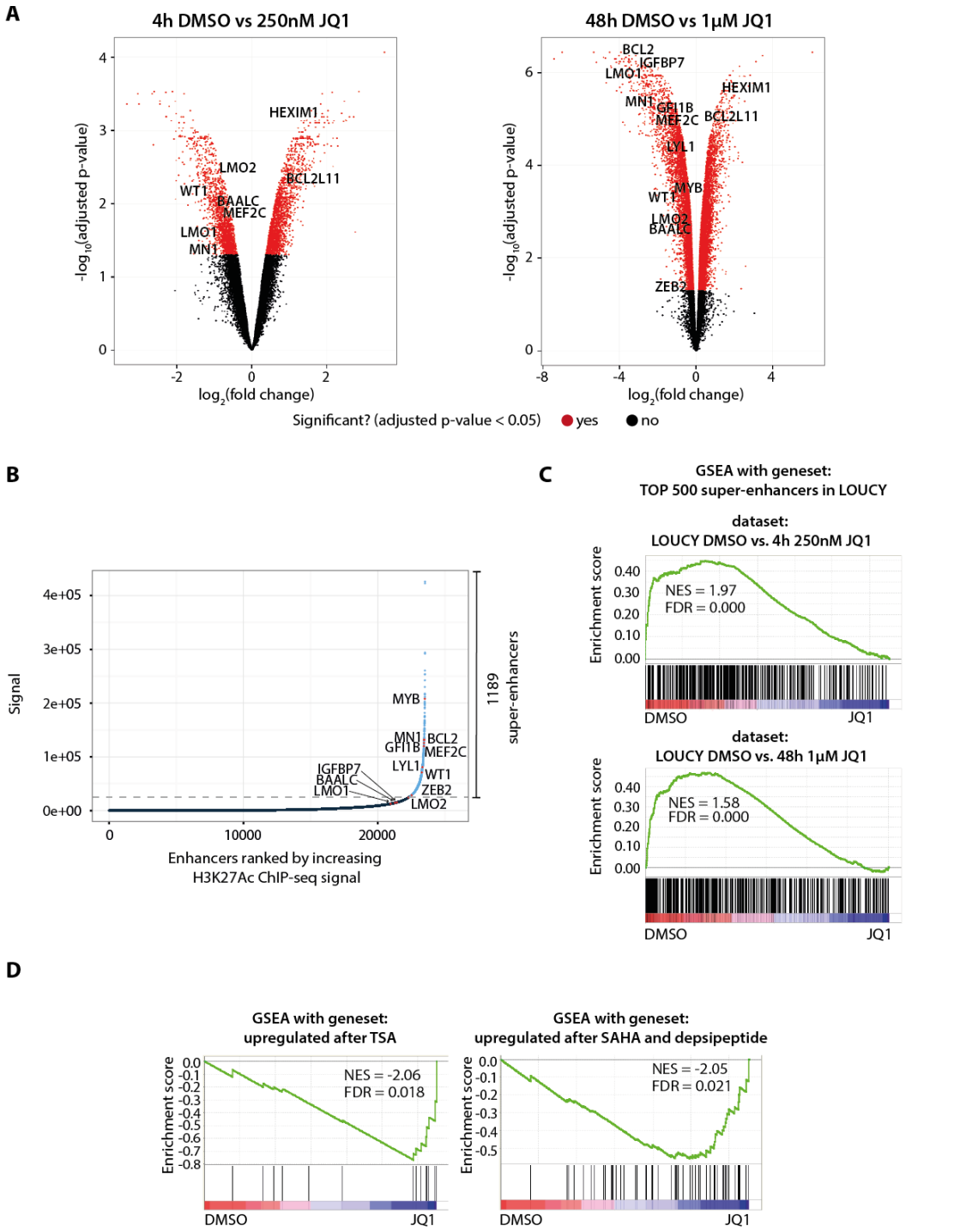

Figure 5. Transcriptional effects of JQ1 on LOUCY. *(a) Volcano plots displaying the differentially expressed genes in LOUCY after 4 h of treatment with 250 nM JQ1 (left) and 48 h of treatment with 1 µM JQ1 (right). In case multiple probes for one gene were present on the array, the differentially expressed probe with largest fold change was plotted. (b) Hockey-stick plot showing the ranked H3K27Ac-seq signal of all enhancers in LOUCY. Super-enhancers are indicated with blue dots. The red dots are examples of enhancers associated with interesting downregulated genes upon JQ1 treatment. (c) GSEA showing a significant enrichment of the genes associated with the top 500 superenhancers in LOUCY among the downregulated genes after treatment with 250 nM JQ1 for 4 h (top) or 1 µM JQ1 for 48 h (bottom). The nearest transcriptionally active gene (TSS) to each super-enhancer was determined via Peak Analyzer (OriginLab, Northampton, MA, USA). This list of super-enhancerassociated genes was then used as a gene set for GSEA. (d) GSEA showing a significant enrichment of gene sets containing upregulated genes after HDAC inhibition among the upregulated genes after treatment of LOUCY with 250 nM JQ1 for 4 h. (d, left) DALESSIO_TSA_RESPONSE, that is, top genes upregulated in HEK293 cells in response to trichostatin A (TSA). (d, right) PEART_HDAC_PROLIFERATION_CLUSTER_UP, that is, cell proliferation genes upregulated by HDAC inhibitors SAHA and depsipeptide.*

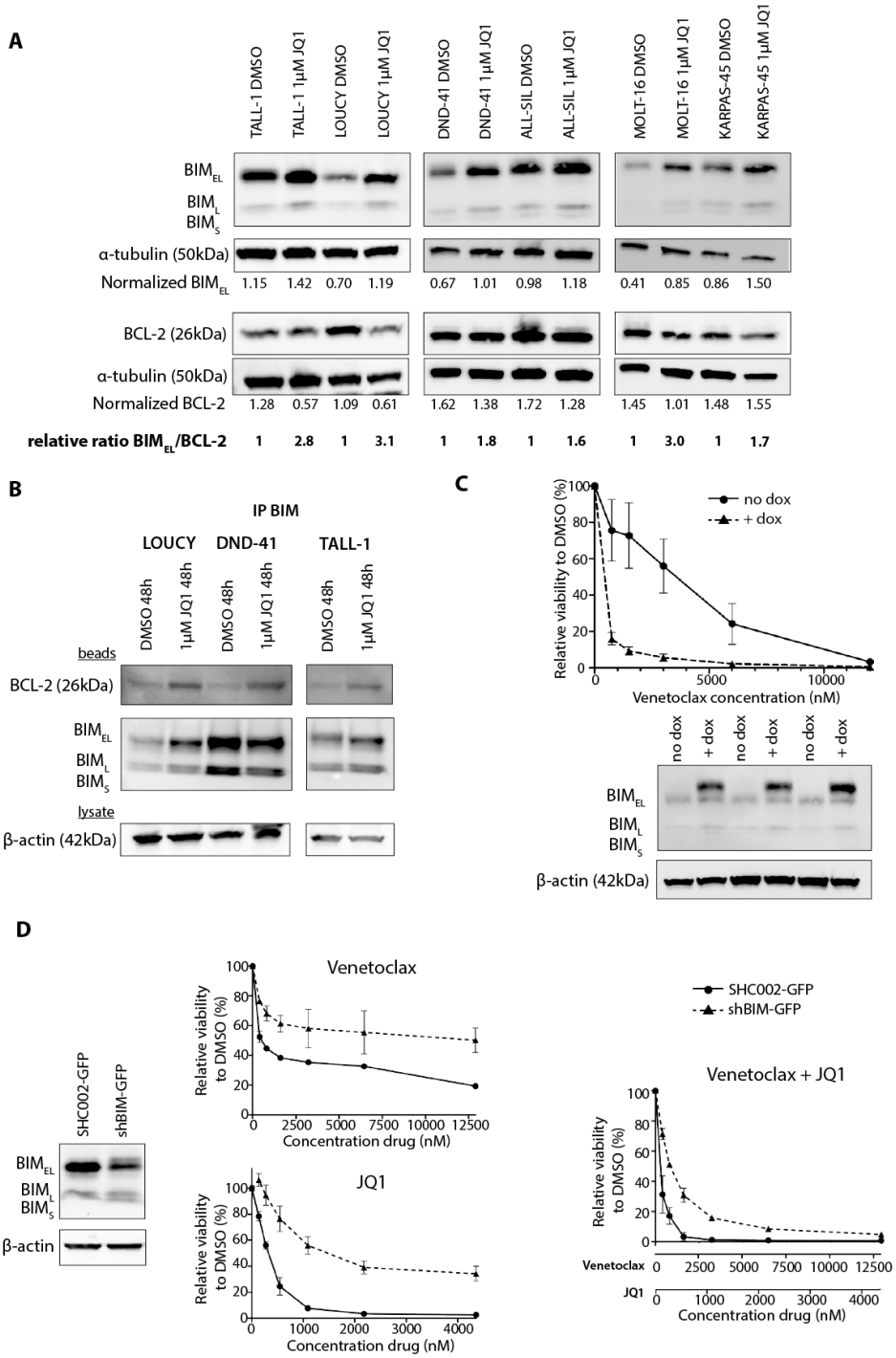

Figure 6. Molecular insights into the mechanism of synergism. *(a) Western blot showing the increase of the BIM/BCL-2 protein ratio in synergistic T-ALL cell lines upon treatment with 1 µM JQ1 for 48 h. Only the upper band of BIM was quantified. (b) Immunoprecipitation with anti-BIM antibody illustrates the increased binding of BIM to BCL-2 after JQ1 treatment. (c) Induction of BIM expression in KARPAS-45 pInducer21-BCL2L11 cells increases the sensitivity to venetoclax. The average and s.d. from three independent experiments is plotted. Western blot shows BIM induction for three independent replicates. The doublet seen for BIM_{EL} (largest isoform) may represent phosphorylation. (d) Knockdown of BIM in KARPAS-45 affects sensitivity to venetoclax, JQ1 and combination treatment. The average and s.d. from two independent experiments is plotted. Western blot shows knockdown of BIM in the cells.*

The importance of BRD4 in processes that lead to abnormal activation of cancer driving genetic programs is increasingly being understood[17–19]. The proof of concept in T-ALL was provided by studies of BET bromodomain inhibitors with a focus on *MYC* inhibition[20–22]. Given the central importance of super-enhancer deregulation in cancer[18,19], a similar principle may apply to many different transcriptional programs in leukemia cells. However, the broad transcriptional effects of these inhibitors on T-ALL cells remain largely unexplored. Gene expression profiling of LOUCY cells treated with JQ1 confirmed that BET bromodomain inhibition results in reduced expression of super-enhancer-associated oncogenes as previously described by Lovén et al.[17]. Similar effects have also previously been reported for the T-ALL cell line ALL-SIL[51]. Although there is some overlap between superenhancers in different T-ALL cell lines[18,51], each cell line seems to have a pretty unique spectrum of super-enhancer sequences. However, we also observed acute gene activation within 4 h of JQ1 treatment. In the gene signature that was activated upon JQ1 treatment in LOUCY cells, HDAC inhibitor-associated gene sets were enriched. This is in accordance with Bhadury et al.[52] who describe a large overlap between genes induced by BET and HDAC inhibitors.

BCL2L11 (encoding BIM) is one of the genes that showed such an acute induction of gene expression upon JQ1 treatment in the context of T-ALL. BIM is an activator BH3-only pro-apoptotic protein that can directly interact with BAX and/or BAK to induce apoptosis. BCL-2 can prevent apoptosis by sequestering pro-apoptotic proteins such as BIM[53]. Studies demonstrated the requirement for BCL-2 complexed to the pro-apoptotic activator BIM in order to sensitize lymphoid cells to BCL-2 inhibition by venetoclax or ABT-737[33–36]. In our study, BET bromodomain inhibition increased BIM to BCL-2 binding, and could provide a putative explanation for the observed synergism between venetoclax and JQ1/OTX015 in the context of human T-ALL. Importantly, upregulation of pro-apoptotic BIM upon JQ1 treatment has also been described in a variety of other tumor entities[47,54–56], suggesting that the synergistic activity between these molecules might not be restricted to human T-ALL. Xu et al.[57] attributed the upregulation of *BCL2L11* in response to JQ1 to the downregulation of the miR17-92 cluster. We also observed a downregulation of the miR17-92 cluster but not yet after 4 h of JQ1 treatment, a time point with already significant upregulation of *BCL2L11* in LOUCY. Therefore, this mechanism does not explain the acute upregulation of *BCL2L11* but this could definitely contribute to sustain the upregulation of *BCL2L11*.

In summary, our study provides a rationale to select patients with treatment-resistant T-ALL for an innovative combination treatment based on mechanisms that are not exploited by conventional chemotherapy regimens. Interference with the balance between pro- and anti-apoptotic proteins in BCL2-dependent T-ALL using the combination BET bromodomain inhibition and the BCL-2 inhibitor venetoclax should be considered in future clinical trials for this indication.

Conflict of interest

The authors declare no conflict of interest.

Acknowledgments

We thank the following funding agencies: Fund for Scientific Research Flanders ('FWO Vlaanderen' research projects GA00113N, 3G065614, G.0C47.13N and 31500615W to PVV; research projects G.0529.12N and G.0817.13N to GB; doctoral grant to SP; postdoctoral grant to SG; BP is a senior clinical investigator), Children Cancer Fund Ghent, Belgian Foundation Against Cancer (Grants 365W3415W and B/13590) and the Belgian Stand Up To Cancer Foundation (Research Grant 365Y9115W; doctoral grant to SP; postdoctoral grants to TP and FM), agency for Innovation by Science and Technology ('IWT', SB Grant 111528 to NV), Geconcerteerde Onderzoeksacties Ghent University (GOA-01GB1013W to GB), Cancer League of the Canton of Zurich, Empiris Foundation, Kinderkrebsforschung Schweiz, Sassella Foundation, Stiftung für Krebsbekämpfung, Swiss National Science Foundation (310030-133108), Fondation Panacée and the clinical research focus program 'Human Hemato-Lymphatic Diseases' of the University of Zurich. We also thank Lindy Reunes for excellent technical assistance and the Innovative Flemish in vivo imaging technology (INFINITY) laboratory at Ghent University Hospital. Finally, the computational resources (Stevin Supercomputer Infrastructure) and services used in this work were provided by the VSC (Flemish Supercomputer Center), funded by Ghent University, the Hercules Foundation and the Flemish Government–Department EWI.

References

1. Pui C-H, Relling MV, Downing JR. Acute Lymphoblastic Leukemia. N Engl J Med. 2004;350(15):1535-48.
2. Pui CH, Pei D, Campana D, Cheng C, Sandlund JT, Bowman WP, et al. A revised definition for cure of childhood acute lymphoblastic leukemia. Leukemia. 2014;28(12):2336-43.
3. Pui CH, Mullighan CG, Evans WE, Relling MV. Pediatric acute lymphoblastic leukemia: where are we going and how do we get there? Blood. 2012;120(6):1165-74.
4. Bhojwani D, Pui CH. Relapsed childhood acute lymphoblastic leukaemia. Lancet Oncol. 2013;14(6):e205-17.
5. Bassan R, Hoelzer D. Modern therapy of acute lymphoblastic leukemia. J Clin Oncol. 2011;29(5):532-43.
6. Oriol A, Vives S, Hernandez-Rivas JM, Tormo M, Heras I, Rivas C, et al. Outcome after relapse of acute lymphoblastic leukemia in adult patients included in four consecutive risk-adapted trials by the PETHEMA Study Group. Haematologica. 2010;95(4):589-96.
7. Faderl S, O'Brien S, Pui CH, Stock W, Wetzler M, Hoelzer D, et al. Adult acute lymphoblastic leukemia: concepts and strategies. Cancer. 2010;116(5):1165-76.
8. Peirs S, Matthijssens F, Goossens S, Van de Walle I, Ruggero K, de Bock CE, et al. ABT-199 mediated inhibition of BCL-2 as a novel therapeutic strategy in T-cell acute lymphoblastic leukemia. Blood. 2014;124(25):3738-47.
9. Anderson NM, Harrold I, Mansour MR, Sanda T, McKeown M, Nagykary N, et al. BCL2-specific inhibitor ABT-199 synergizes strongly with cytarabine against the early immature LOUCY cell line but not more-differentiated T-ALL cell lines. Leukemia. 2014;28(5):1145-8.

10. Chonghaile TN, Roderick JE, Glenfield C, Ryan J, Sallan SE, Silverman LB, et al. Maturation Stage of T-cell Acute Lymphoblastic Leukemia Determines BCL-2 versus BCL-XL Dependence and Sensitivity to ABT-199. Cancer discovery. 2014.
11. Fresquet V, Rieger M, Carolis C, Garcia-Barchino MJ, Martinez-Climent JA. Acquired mutations in BCL2 family proteins conferring resistance to the BH3 mimetic ABT-199 in lymphoma. Blood. 2014;123(26):4111-9.
12. Tahir SK, Smith ML, Hessler P, Roberts-Rapp L, Leverson JD, Lam LT. Abstract B30: Mechanisms of resistance to ABT-199 in leukemia and lymphoma cell lines. Clin Cancer Res. 2015;21(4 Supplement):B30.
13. Choudhary GS, Al-Harbi S, Mazumder S, Hill BT, Smith MR, Bodo J, et al. MCL-1 and BCL-xL-dependent resistance to the BCL-2 inhibitor ABT-199 can be overcome by preventing PI3K/AKT/mTOR activation in lymphoid malignancies. Cell death & disease. 2015;6:e1593.
14. Roberts AW, Davids MS, Pagel JM, Kahl BS, Puvvada SD, Gerecitano JF, et al. Targeting BCL2 with Venetoclax in Relapsed Chronic Lymphocytic Leukemia. N Engl J Med. 2016;374(4):311-22.
15. Stilgenbauer S, Eichhorst B, Schetelig J, Coutre S, Seymour JF, Munir T, et al. Venetoclax in relapsed or refractory chronic lymphocytic leukaemia with 17p deletion: a multicentre, open-label, phase 2 study. The Lancet Oncology. 2016.
16. Filippakopoulos P, Qi J, Picaud S, Shen Y, Smith WB, Fedorov O, et al. Selective inhibition of BET bromodomains. Nature. 2010;468(7327):1067-73.
17. Loven J, Hoke HA, Lin CY, Lau A, Orlando DA, Vakoc CR, et al. Selective inhibition of tumor oncogenes by disruption of super-enhancers. Cell. 2013;153(2):320-34.
18. Hnisz D, Abraham BJ, Lee TI, Lau A, Saint-Andre V, Sigova AA, et al. Super-enhancers in the control of cell identity and disease. Cell. 2013;155(4):934-47.
19. Filippakopoulos P, Knapp S. Targeting bromodomains: epigenetic readers of lysine acetylation. Nat Rev Drug Discov. 2014;13(5):337-56.
20. Loosveld M, Castellano R, Gon S, Goubard A, Crouzet T, Pouyet L, et al. Therapeutic targeting of c-Myc in T-cell acute lymphoblastic leukemia, T-ALL. Oncotarget. 2014;5(10):3168-72.
21. Roderick JE, Tesell J, Shultz LD, Brehm MA, Greiner DL, Harris MH, et al. c-Myc inhibition prevents leukemia initiation in mice and impairs the growth of relapsed and induction failure pediatric T-ALL cells. Blood. 2014;123(7):1040-50.
22. King B, Trimarchi T, Reavie L, Xu L, Mullenders J, Ntziachristos P, et al. The ubiquitin ligase FBXW7 modulates leukemia-initiating cell activity by regulating MYC stability. Cell. 2013;153(7):1552-66.
23. Bonapace L, Bornhauser BC, Schmitz M, Cario G, Ziegler U, Niggli FK, et al. Induction of autophagy-dependent necroptosis is required for childhood acute lymphoblastic leukemia cells to overcome glucocorticoid resistance. J Clin Invest. 2010;120(4):1310-23.
24. R Development Core Team. R: A language and environment for statistical computing. R Foundation for Statistical Computing, Vianna, Austria, 2008. ISBN 3-900051-07-0. Available at: http://www.R-project.org.http://wwproject.org.
25. Edgar R, Domrachev M, Lash AE. Gene Expression Omnibus: NCBI gene expression and hybridization array data repository. Nucleic Acids Res. 2002;30(1):207-10.
26. Yang X, Boehm JS, Yang X, Salehi-Ashtiani K, Hao T, Shen Y, et al. A public genome-scale lentiviral expression library of human ORFs. Nat Methods. 2011;8(8):659-61.

27. Meerbrey KL, Hu G, Kessler JD, Roarty K, Li MZ, Fang JE, et al. The pINDUCER lentiviral toolkit for inducible RNA interference in vitro and in vivo. Proc Natl Acad Sci U S A. 2011;108(9):3665-70.
28. Fischer U, Forster M, Rinaldi A, Risch T, Sungalee S, Warnatz HJ, et al. Genomics and drug profiling of fatal TCF3-HLF-positive acute lymphoblastic leukemia identifies recurrent mutation patterns and therapeutic options. Nat Genet. 2015;47(9):1020-9.
29. Frismantas V., Dobay MP, Rinaldi A, Tchinda J, Dunn SH et al. Ex vivo drug response profiling detects recurrent sensitivity patterns in drug resistant ALL. Blood 2017.
30. Berthon C, Raffoux E, Thomas X, Vey N, Gomez-Roca C, Yee K, et al. Bromodomain inhibitor OTX015 in patients with acute leukaemia: a dose-escalation, phase 1 study. Lancet Haematol. 2016;3(4):e186-95.
31. Amorim S, Stathis A, Gleeson M, Iyengar S, Magarotto V, Leleu X, et al. Bromodomain inhibitor OTX015 in patients with lymphoma or multiple myeloma: a dose-escalation, open-label, pharmacokinetic, phase 1 study. Lancet Haematol. 2016;3(4):e196-204.
32. Wallaert A, Durinck K, Van Loocke W, Van de Walle I, Matthijssens F, Volders PJ, et al. Long noncoding RNA signatures define oncogenic subtypes in T-cell acute lymphoblastic leukemia. Leukemia. 2016.
33. Souers AJ, Leverson JD, Boghaert ER, Ackler SL, Catron ND, Chen J, et al. ABT-199, a potent and selective BCL-2 inhibitor, achieves antitumor activity while sparing platelets. Nat Med. 2013;19(2):202-8.
34. Del Gaizo Moore V, Brown JR, Certo M, Love TM, Novina CD, Letai A. Chronic lymphocytic leukemia requires BCL2 to sequester prodeath BIM, explaining sensitivity to BCL2 antagonist ABT-737. J Clin Invest. 2007;117(1):112-21.
35. Merino D, Khaw SL, Glaser SP, Anderson DJ, Belmont LD, Wong C, et al. Bcl-2, Bcl-x(L), and Bcl-w are not equivalent targets of ABT-737 and navitoclax (ABT-263) in lymphoid and leukemic cells. Blood. 2012;119(24):5807-16.
36. Khaw SL, Merino D, Anderson MA, Glaser SP, Bouillet P, Roberts AW, et al. Both leukaemic and normal peripheral B lymphoid cells are highly sensitive to the selective pharmacological inhibition of prosurvival Bcl-2 with ABT-199. Leukemia. 2014;28(6):1207-15.
37. Mogilyansky E, Rigoutsos I. The miR-17/92 cluster: a comprehensive update on its genomics, genetics, functions and increasingly important and numerous roles in health and disease. Cell Death Differ. 2013;20(12):1603-14.
38. Cang S, Iragavarapu C, Savooji J, Song Y, Liu D. ABT-199 (venetoclax) and BCL-2 inhibitors in clinical development. J Hematol Oncol. 2015;8:129.
39. Cervantes-Gomez F, Lamothe B, Woyach JA, Wierda WG, Keating MJ, Balakrishnan K, et al. Pharmacological and Protein Profiling Suggests Venetoclax (ABT-199) as Optimal Partner with Ibrutinib in Chronic Lymphocytic Leukemia. Clin Cancer Res. 2015;21(16):3705-15.
40. Chiron D, Dousset C, Brosseau C, Touzeau C, Maiga S, Moreau P, et al. Biological rational for sequential targeting of Bruton tyrosine kinase and Bcl-2 to overcome CD40-induced ABT-199 resistance in mantle cell lymphoma. Oncotarget. 2015;6(11):8750-9.
41. Zhao X, Bodo J, Sun D, Durkin L, Lin J, Smith MR, et al. Combination of ibrutinib with ABT-199: synergistic effects on proliferation inhibition and apoptosis in mantle cell lymphoma cells through perturbation of BTK, AKT and BCL2 pathways. Br J Haematol. 2015;168(5):765-8.

42. Ruvolo PP, Ruvolo VR, Benton CB, AlRawi A, Burks JK, Schober W, et al. Combination of galectin inhibitor GCS-100 and BH3 mimetics eliminates both p53 wild type and p53 null AML cells. Biochim Biophys Acta. 2016;1863(4):562-71.
43. Ham J, Costa C, Sano R, Lochmann TL, Sennott EM, Patel NU, et al. Exploitation of the Apoptosis-Primed State of MYCN-Amplified Neuroblastoma to Develop a Potent and Specific Targeted Therapy Combination. Cancer Cell. 2016;29(2):159-72.
44. Phillips DC, Xiao Y, Lam LT, Litvinovich E, Roberts-Rapp L, Souers AJ, et al. Loss in MCL-1 function sensitizes non-Hodgkin's lymphoma cell lines to the BCL-2-selective inhibitor venetoclax (ABT-199). Blood Cancer J. 2015;5:e368.
45. Choudhary GS, Tat TT, Misra S, Hill BT, Smith MR, Almasan A, et al. Cyclin E/Cdk2-dependent phosphorylation of Mcl-1 determines its stability and cellular sensitivity to BH3 mimetics. Oncotarget. 2015;6(19):16912-25.
46. Lee JS, Tang SS, Ortiz V, Vo TT, Fruman DA. MCL-1-independent mechanisms of synergy between dual PI3K/mTOR and BCL-2 inhibition in diffuse large B cell lymphoma. Oncotarget. 2015;6(34):35202-17.
47. Sun B, Shah B, Fiskus W, Qi J, Rajapakshe K, Coarfa C, et al. Synergistic activity of BET protein antagonist-based combinations in mantle cell lymphoma cells sensitive or resistant to ibrutinib. Blood. 2015;126(13):1565-74.
48. Cinar M, Rosenfelt F, Rokhsar S, Lopategui J, Pillai R, Cervania M, et al. Concurrent inhibition of MYC and BCL2 is a potentially effective treatment strategy for double hit and triple hit B-cell lymphomas. Leuk Res. 2015;39(7):730-8.
49. Johnson-Farley N, Veliz J, Bhagavathi S, Bertino JR. ABT-199, a BH3 mimetic that specifically targets Bcl-2, enhances the antitumor activity of chemotherapy, bortezomib and JQ1 in "double hit" lymphoma cells. Leuk Lymphoma. 2015;56(7):2146-52.
50. Certo M, Del Gaizo Moore V, Nishino M, Wei G, Korsmeyer S, Armstrong SA, et al. Mitochondria primed by death signals determine cellular addiction to anti-apoptotic BCL-2 family members. Cancer Cell. 2006;9(5):351-65.
51. Durinck K, Van Loocke W, Van der Meulen J, Van de Walle I, Ongenaert M, Rondou P, et al. Characterization of the genome-wide TLX1 binding profile in T-cell acute lymphoblastic leukemia. Leukemia. 2015;29(12):2317-27.
52. Bhadury J, Nilsson LM, Muralidharan SV, Green LC, Li Z, Gesner EM, et al. BET and HDAC inhibitors induce similar genes and biological effects and synergize to kill in Myc-induced murine lymphoma. Proc Natl Acad Sci U S A. 2014;111(26):E2721-30.
53. Hata AN, Engelman JA, Faber AC. The BCL2 Family: Key Mediators of the Apoptotic Response to Targeted Anticancer Therapeutics. Cancer discovery. 2015;5(5):475-87.
54. Tinsley S, Meja K, Shepherd C, Khwaja A. Synergistic induction of cell death in haematological malignancies by combined phosphoinositide-3-kinase and BET bromodomain inhibition. Br J Haematol. 2015;170(2):275-8.
55. Patel AJ, Liao CP, Chen Z, Liu C, Wang Y, Le LQ. BET bromodomain inhibition triggers apoptosis of NF1-associated malignant peripheral nerve sheath tumors through Bim induction. Cell reports. 2014;6(1):81-92.
56. Li GQ, Guo WZ, Zhang Y, Seng JJ, Zhang HP, Ma XX, et al. Suppression of BRD4 inhibits human hepatocellular carcinoma by repressing MYC and enhancing BIM expression. Oncotarget. 2016;7(3):2462-74.
57. Xu Z, Sharp PP, Yao Y, Segal D, Ang CH, Khaw SL, et al. BET inhibition represses miR17-92 to drive BIM-initiated apoptosis of normal and transformed hematopoietic cells. Leukemia. 2016;30(7):1531-41.

Supplementary Figures

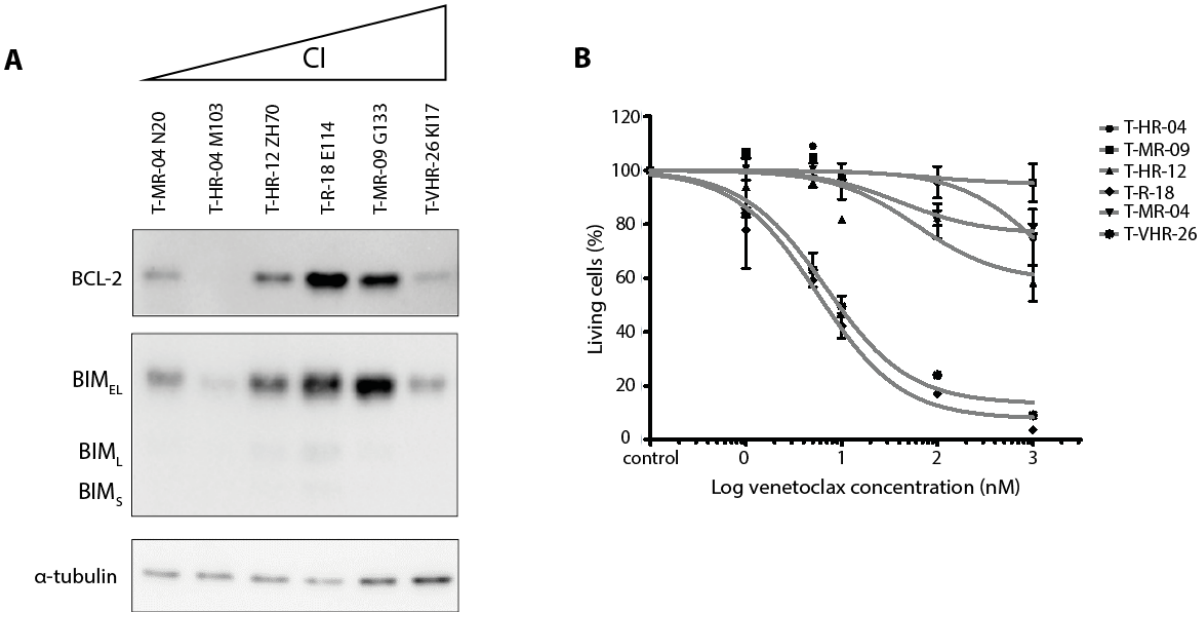

Supplementary Figure 1. BCL-2 and BIM protein levels and venetoclax dose response curves for the 6 primary T-ALL patient samples. *(A) Western blot with BCL-2 and BIM levels in panel of T-ALL patients. Protein samples were obtained from primary, secondary or tertiary mice xenografts. (B) In vitro response of six T-ALL samples to the BCL-2 inhibitor venetoclax in co-culture with mesenchymal stromal cells (MSC) and used for combination screening. Cell viability was measured by flow cytometry using 7-AAD after 72h of treatment and normalized to DMSO-treated controls. Sensitive and resistant cases were defined by a mixture model fit of the distribution of IC_{50} (log[nM]) measured after 72h.*

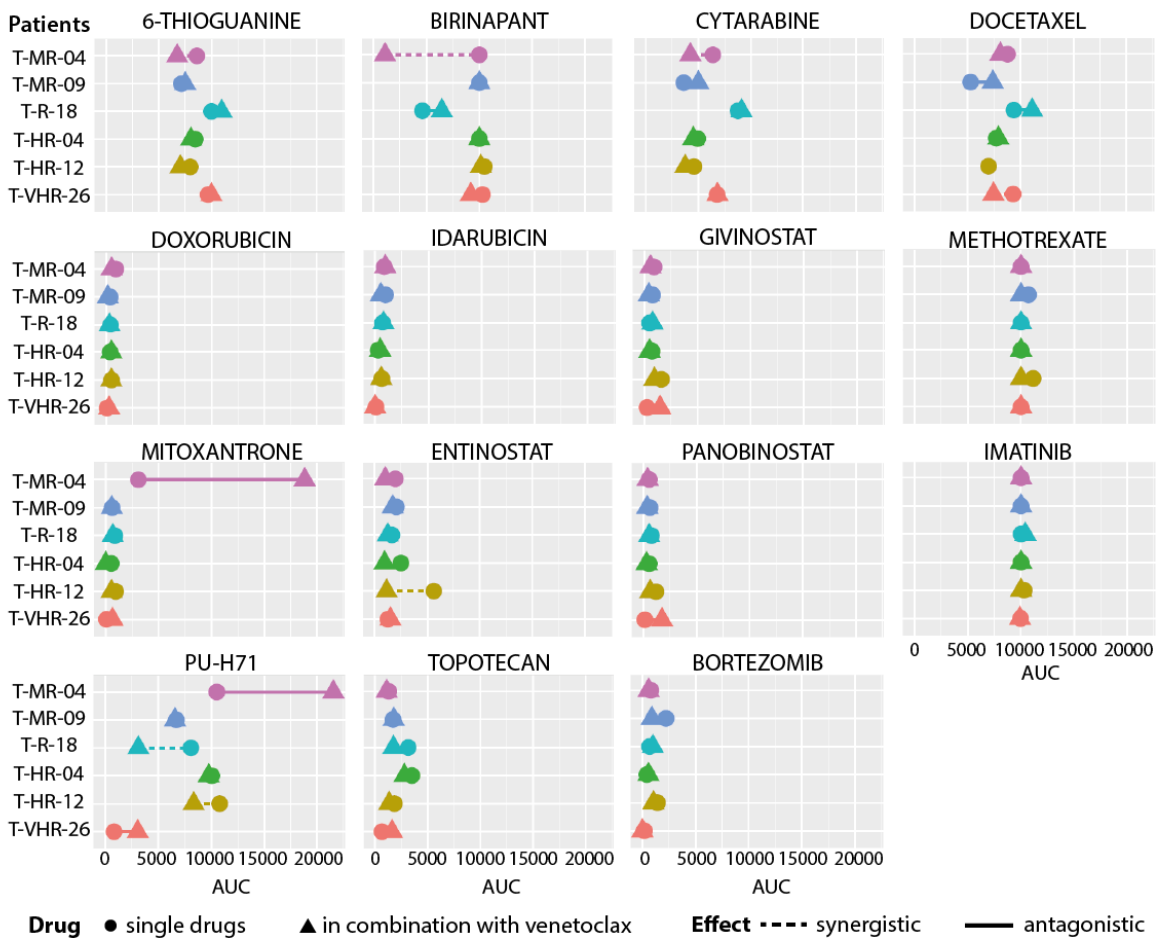

Supplementary Figure 2. Effect of adding venetoclax on area under the curve (AUC) for 21 compounds in 6 primary T-ALL patient samples. *Plot showing the AUC for 21 compounds in 6 primary T-ALL samples without and with the addition of a sub-lethal dose of venetoclax. Indicated are the AUC values for dose response curves with (triangles) or without (circles) venetoclax.*

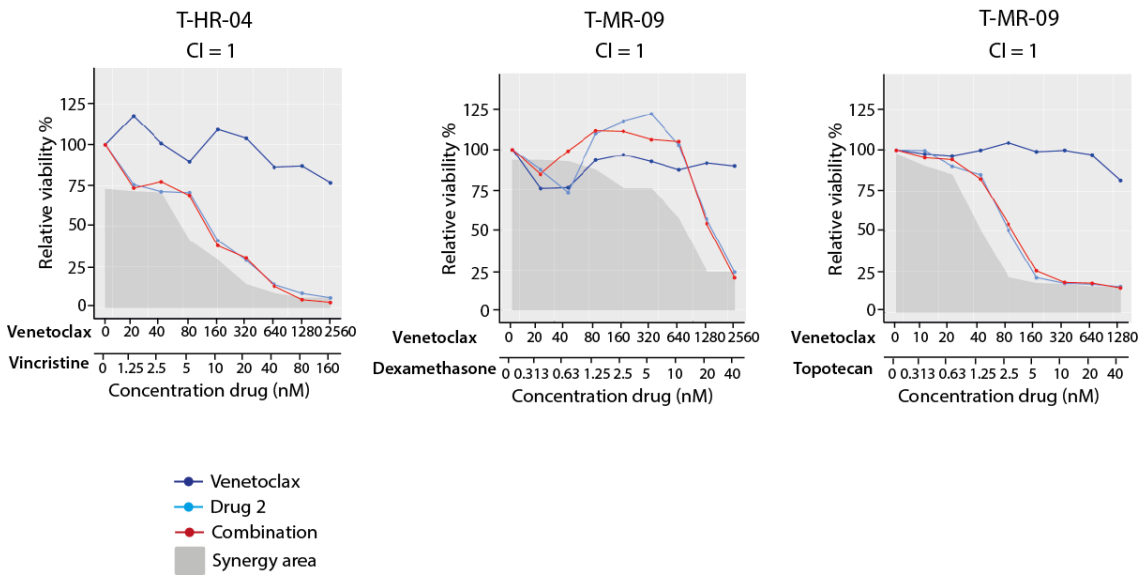

Supplementary Figure 3. Validation of some of the non-responsive drug interactions identified in the initial screen. *Representative examples of co-titration assays for compounds detected to not synergize with venetoclax in preselected T-ALL samples from initial combination screening.*

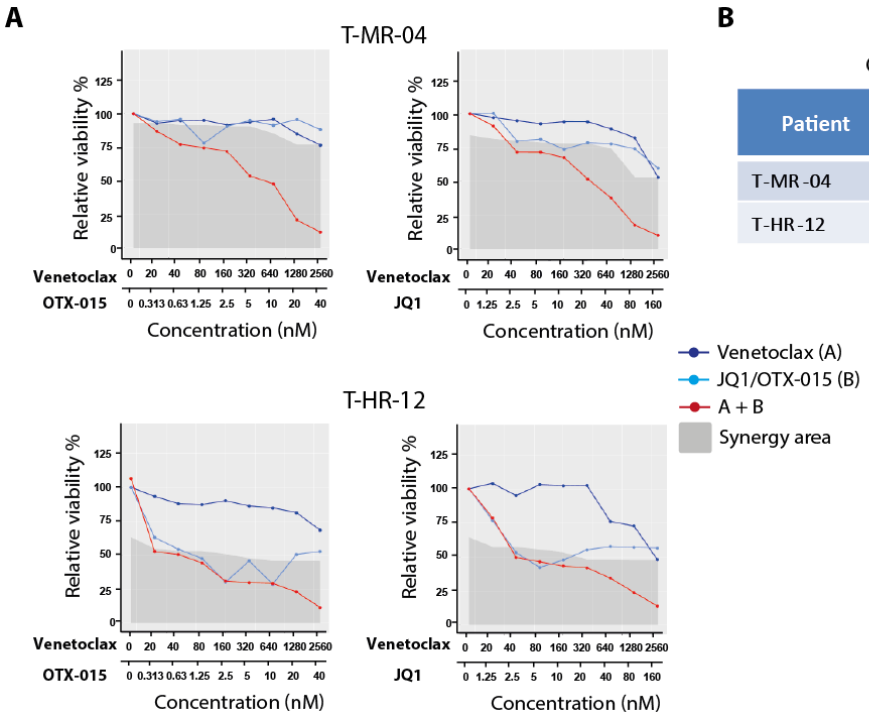

B

Combination index (CI)

Patient	Venetoclax / OTX-015	Venetoclax / JQ1
T-MR-04	<0.01	0.06
T-HR-12	0.13	0.13

Supplementary Figure 4. Synergistic activity of venetoclax with BRD4 inhibitors OTX-015 and JQ1. *(A) Titration assay of venetoclax with OTX-015 or JQ1 for 2 primary T-ALL samples. (B) Combination index determined by Chou-Talalay method.*

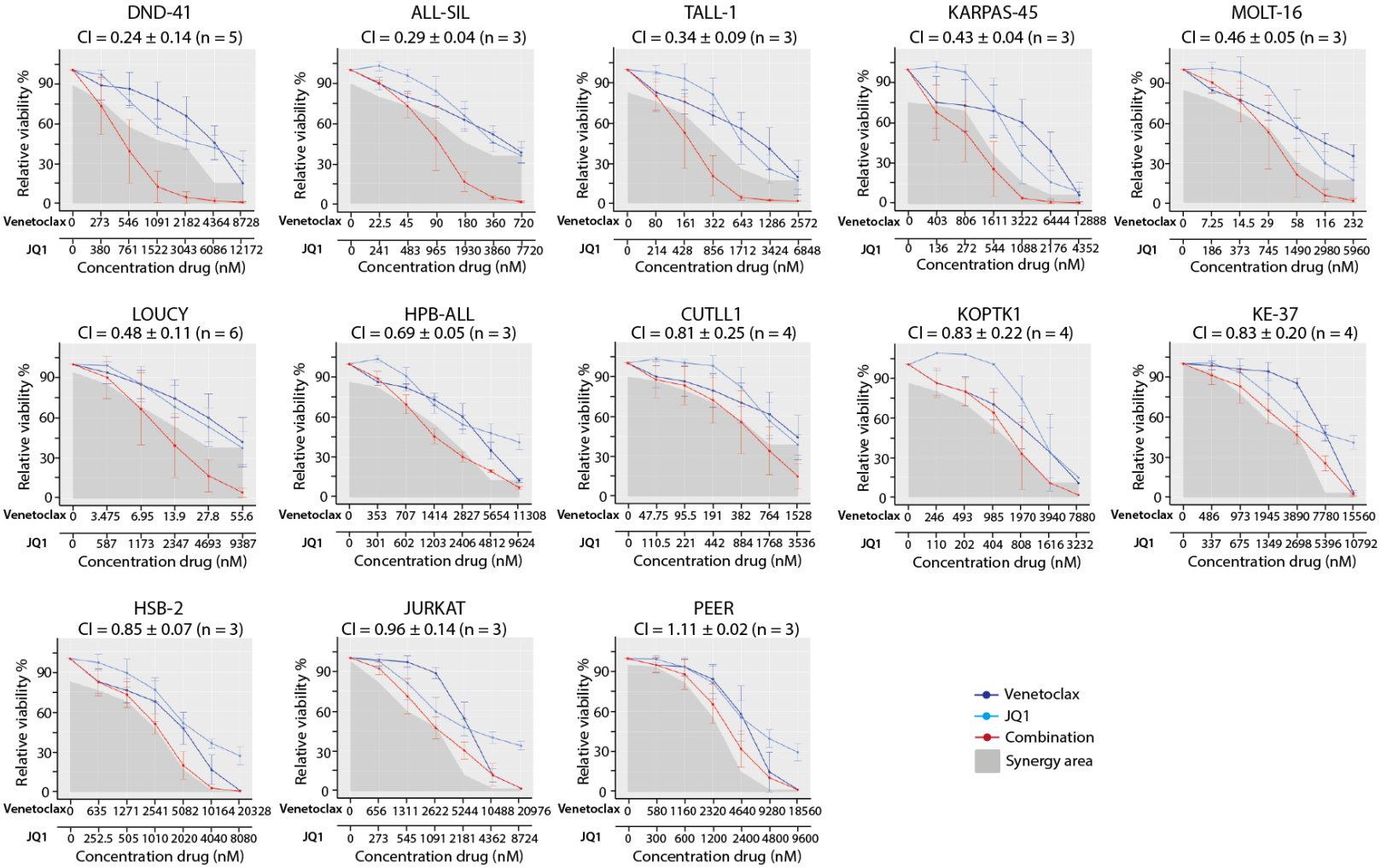

Supplementary Figure 5. Cell viability curves and combination indexes (CI) for T-ALL cell lines treated with venetoclax and/or JQ1. *The effect of venetoclax and JQ1 monotherapy and combination therapy on the viability of T-ALL cell lines is visualized. Cell viability is expressed relative to cells treated with dimethylsulfoxide (DMSO) and the average and standard deviation of at least 3 independent experiments is plotted for each cell line.*

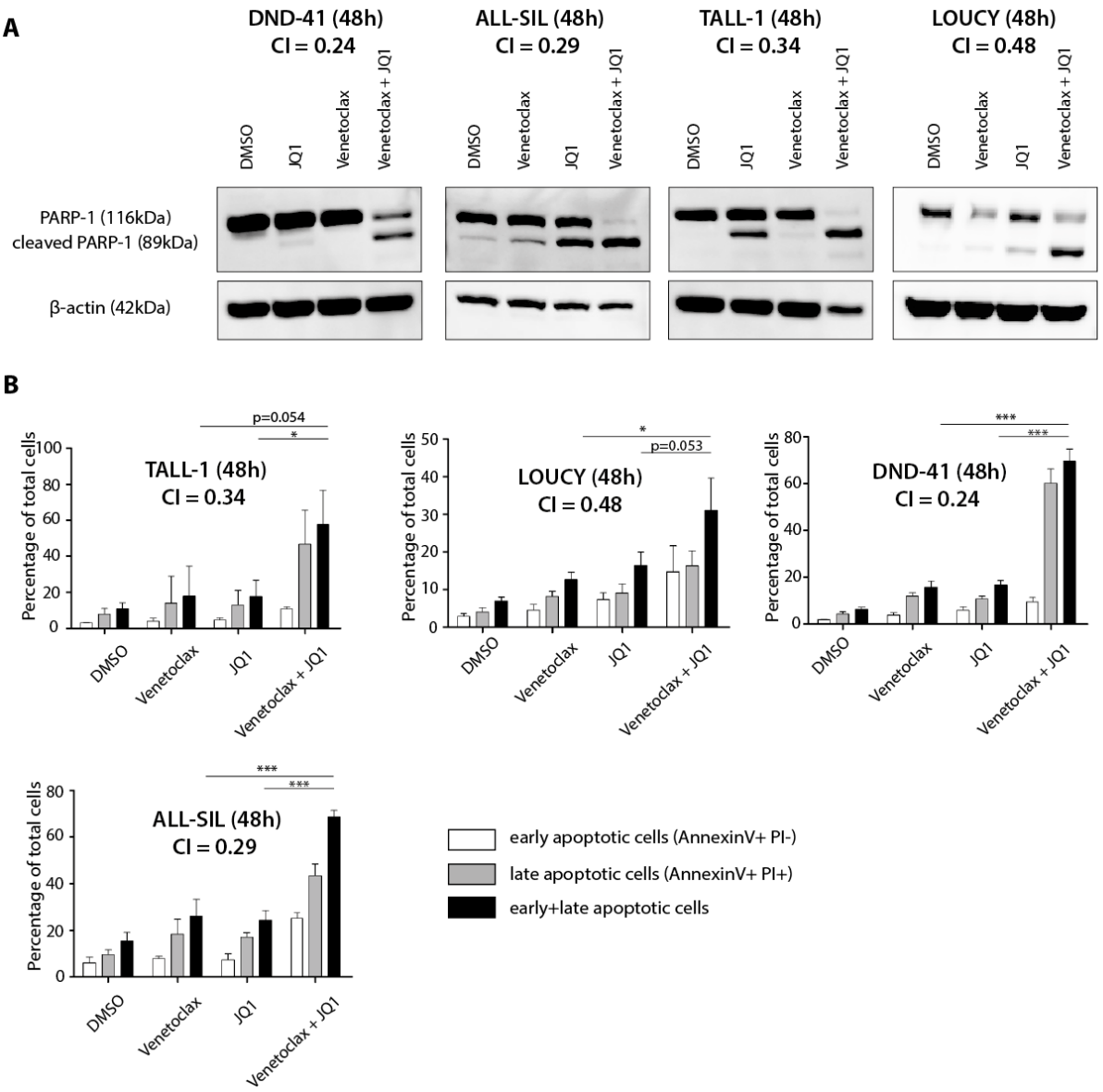

Supplementary Figure 6 Induction of cell death in human T-ALL cell lines. *(A) Induction of cell death represented by Western blot of PARP-1. Treatment with venetoclax, JQ1 and especially with the combination of both induced the cleavage of PARP-1. Half of the IC_{50} dose was used to treat the cell lines for 48h. (B) Percentage of cells in early apoptosis and late apoptosis based on Annexin V/PI staining after 48h treatment with the half of their IC_{50} dose. Average and standard deviation for 3 independent experiments is shown. Two-tailed t tests were used to compare the total apoptotic cells between the monotherapies and combination therapy. * P<0.05, ** P<0.01, *** P<0.001.*

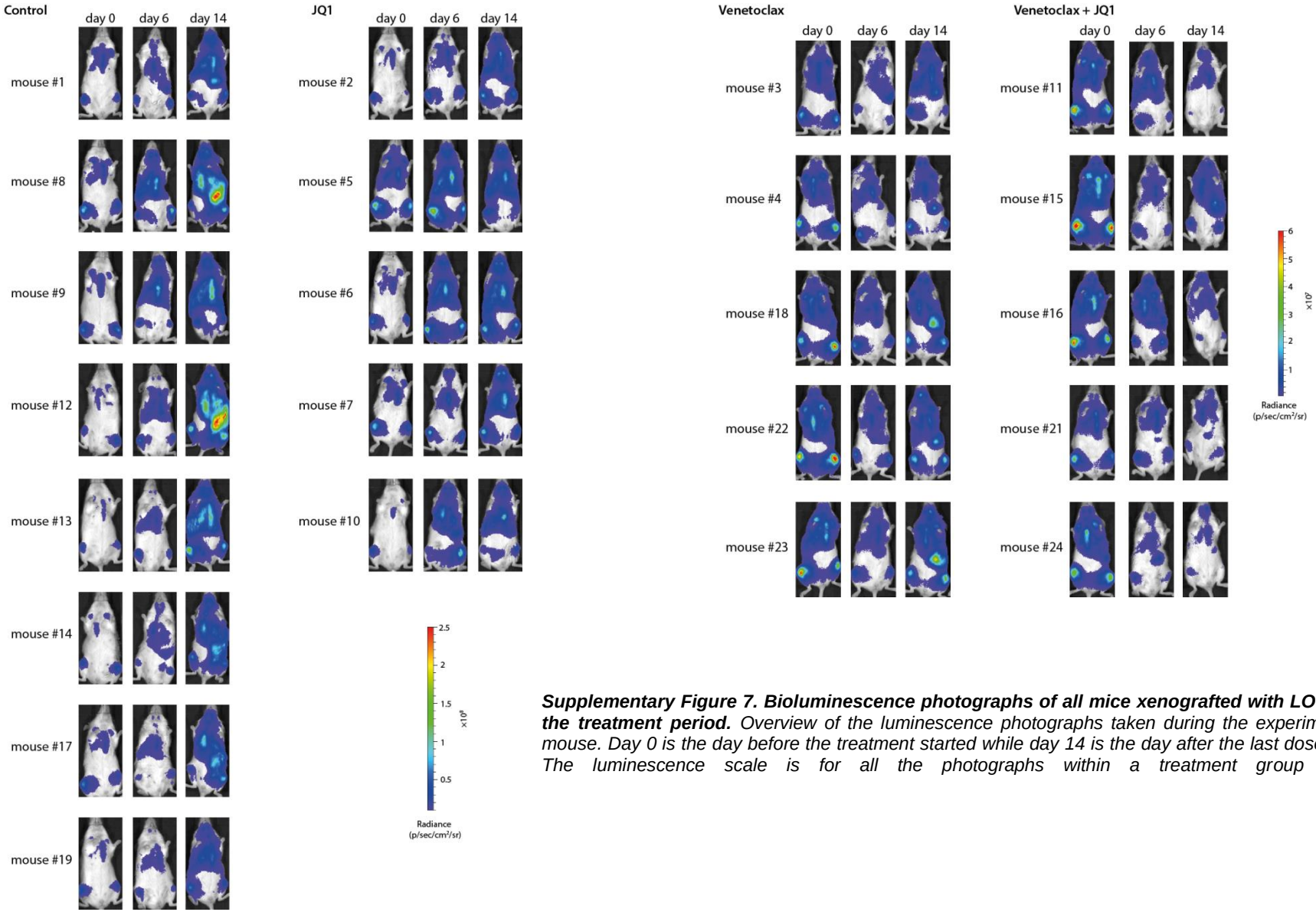

Supplementary Figure 7. Bioluminescence photographs of all mice xenografted with LOUCY during the treatment period. *Overview of the luminescence photographs taken during the experiment of each mouse. Day 0 is the day before the treatment started while day 14 is the day after the last dose was given. The luminescence scale is for all the photographs within a treatment group the same.*

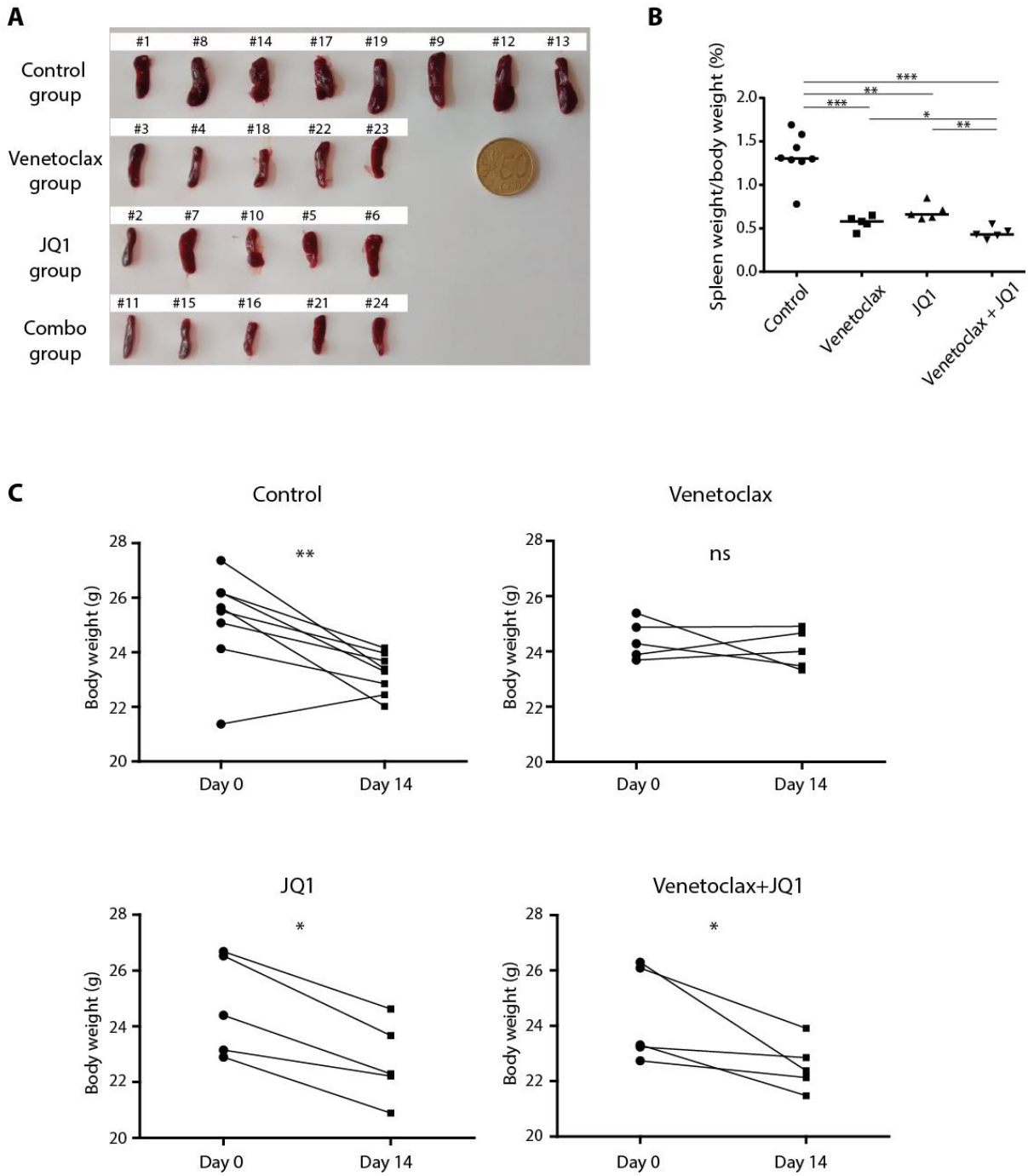

Supplementary Figure 8. Spleen size and evolution of body weight in treated mice xenografted with LOUCY. *(A) Spleens of all the mice after 13 days of treatment. (B) Spleen-to-body weight percentage at the end of the experiment for each mouse in a particular treatment group. The one-tailed Mann-Whitney test was used to compare the treatment groups statistically. ns not significant, * P<0.05, ** P<0.01, *** P<0.001. Horizontal lines on the graph indicate the median for each group. (C) The weight of each mouse on the day before the treatment started (day 0) and at the end of the experiment (day 14) is plotted. One-tailed Wilcoxon signed rank test was used to compare the weight loss within a group. ns not significant, * P<0.05, ** P<0.01, *** P<0.001.*

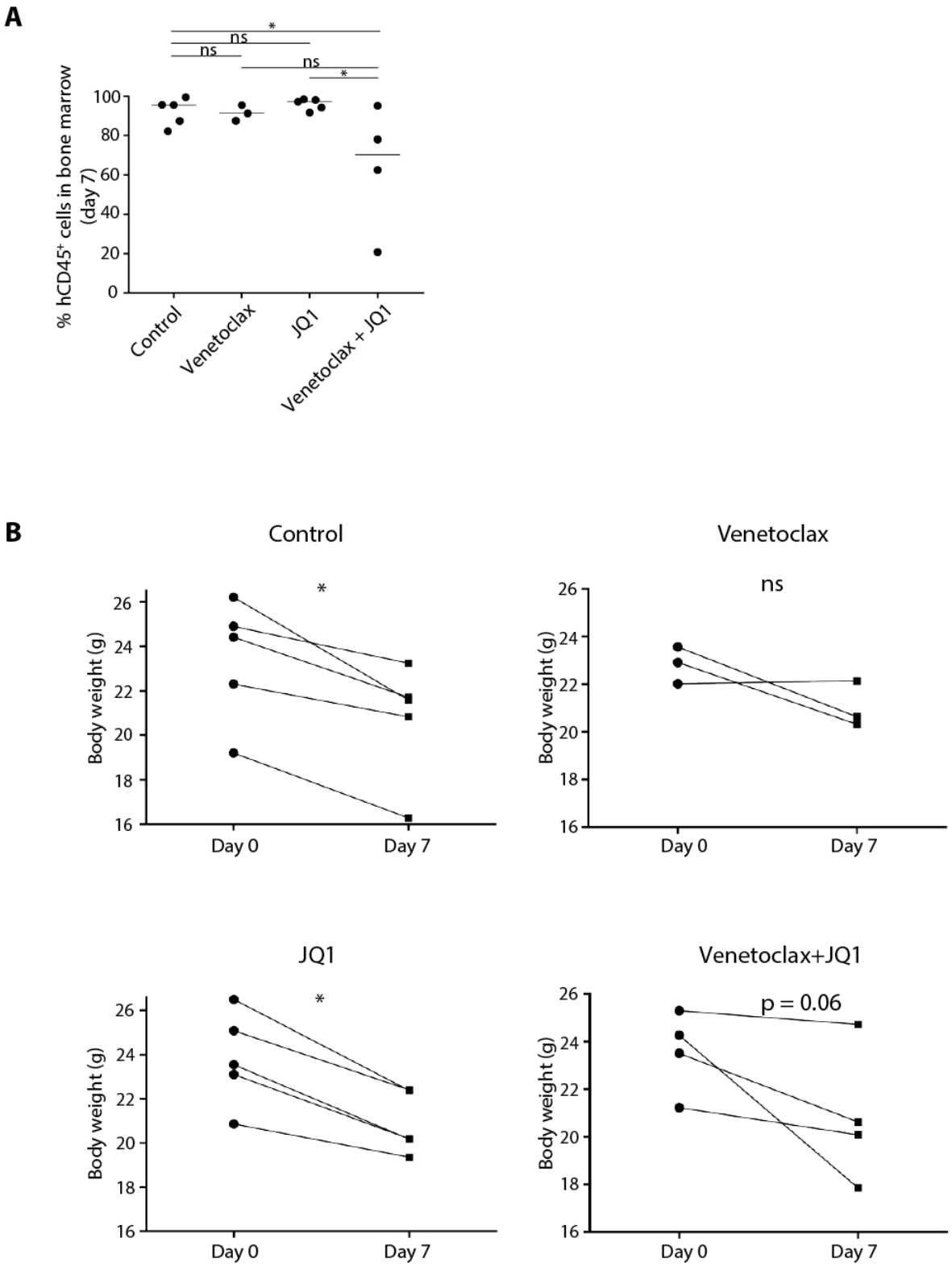

Supplementary Figure 9. Treatment of mice xenografted with ALL-SIL. *(A) Percentage hCD45+ leukemic cells in bone marrow for each mouse after 7 days of treatment. The one-tailed Mann-Whitney test was used to compare the treatment groups statistically. ns not significant, * P<0.05, ** P<0.01, *** P<0.001. Horizontal lines on the graph indicate the median for each group. (B) The weight of each mouse on the day the treatment started (day 0) and at the end of the experiment, after 7 days of treatment (day 7), is plotted. One-tailed Wilcoxon signed rank test was used to compare the weight loss within a group. ns not significant, * P<0.05, ** P<0.01, *** P<0.001.*

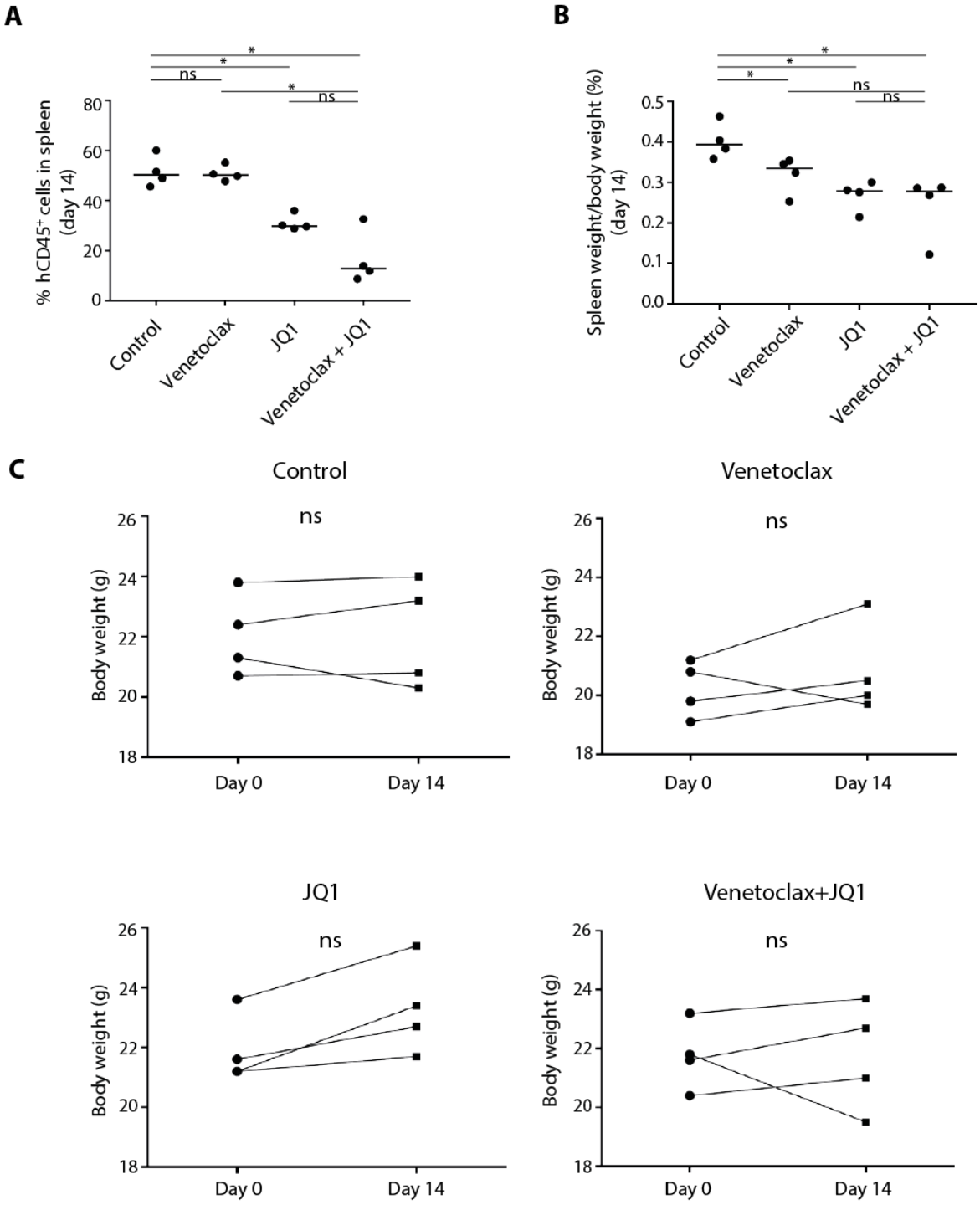

Supplementary Figure 10 Leukemic burden in spleen and evolution of body weight in treated patient-derived (T-VHR-26) xenografts. *(A) Percentage hCD45+ leukemic cells in the spleen for each mouse after 14 days of treatment. Spleens were not a lot enlarged in the control mice. Spleen weights were for all mice less than 100mg. The one-tailed Mann-Whitney test was used to compare the treatment groups statistically. ns not significant, * P<0.05, ** P<0.01, *** P<0.001. Horizontal lines on the graph indicate the median for each group. (B) Spleen-to-body weight percentage for each mouse after 14 days of treatment. Spleens were not a lot enlarged in the control mice. Spleen weights were for all mice less than 100mg. The one-tailed Mann-Whitney test was used to compare the treatment groups statistically. ns not significant, * P<0.05, ** P<0.01, *** P<0.001. Horizontal lines on the graph indicate the median for each group. (C) The weight of each mouse on the day the treatment started (day 0) and at the end of the experiment, after 14 days of treatment (day 14), is plotted. One-tailed Wilcoxon signed rank test was used to compare the weight loss within a group. ns not significant, * P<0.05, ** P<0.01, *** P<0.001.*

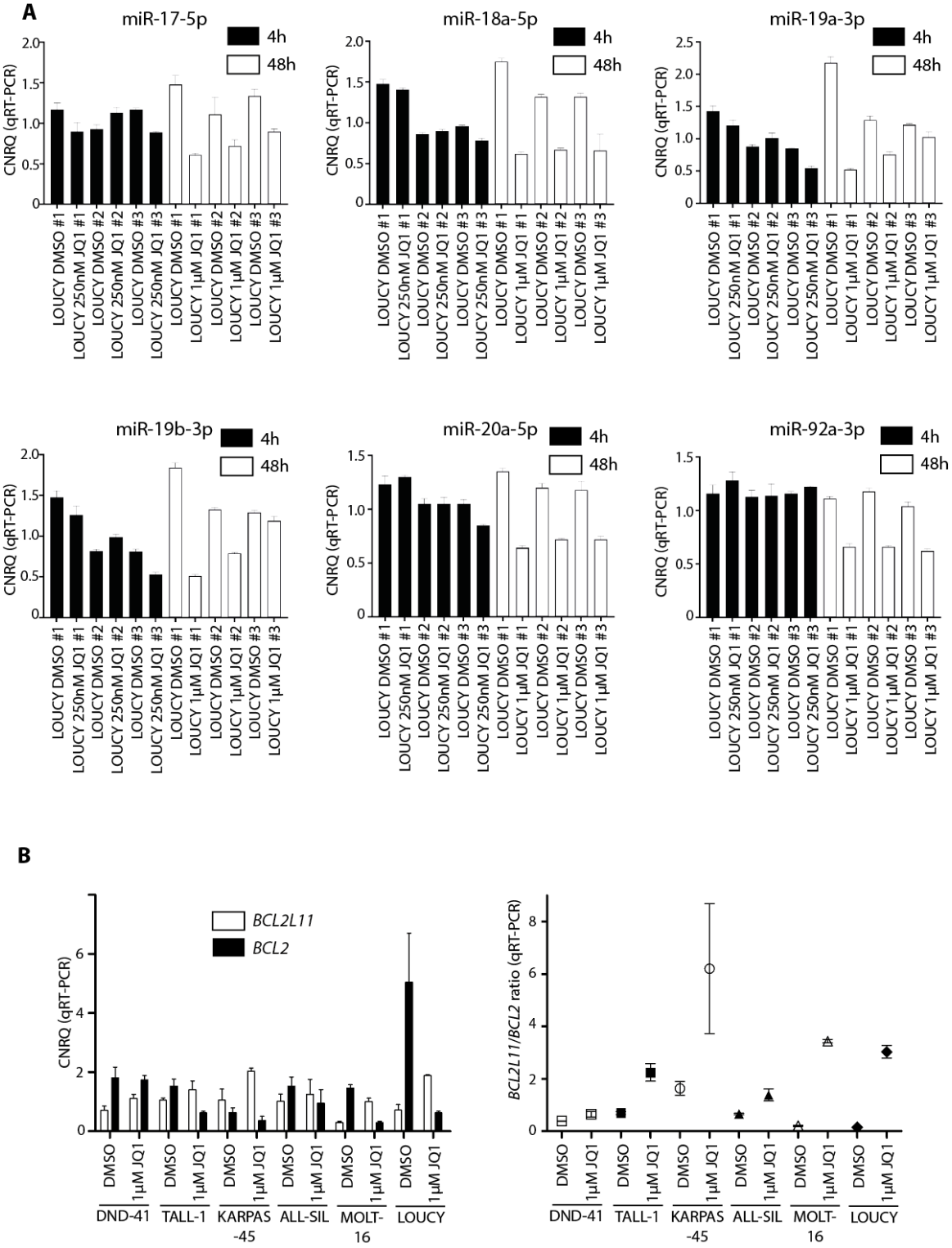

Supplementary Figure 11 Effect of JQ1 on miR17-92 cluster and knockdown of BIM. *(A) Quantification of the miR17-92 cluster in LOUCY treated with DMSO or JQ1. These samples were the same as the one used for the microarray-based expression profiles. 3 independent replicates of each treatment were performed. Calibrated normalized relative quantities (CNRQ) and their standard error are plotted. (B) The BCL2L11 (coding for BIM)/BCL2 mRNA ratio increases in synergistic T-ALL cell lines upon treatment with 1µM JQ1 for 48h. The average and standard deviation of the ratio of calibrated normalized relative quantities (CNRQ) from three independent experiments is plotted. The two-tailed t test was used to compare the DMSO and JQ1 treatment. * P<0.05, ** P<0.01, *** P<0.001.*

Supplementary Tables

Supplementary Table 1. Overview of compounds used in drug-screening.

Compound	Drug class	Clinical stage	Availability for ALL/clinical trial number
Thioguanine	Antimetabolites	Clinical	Standard ALL drug
Cytarabine		Clinical	Standard ALL drug
Methotrexate		Clinical	Standard ALL drug
Docetaxel	Antimitotics	Clinical	Pediatric ALL, phase II, NCT00021242
Vincristine		Clinical	Standard ALL drug
JQ-1	BRD4 inhibitor	No	
Dexamethasone	Glucocorticoids	Clinical	Standard ALL drug
Prednisolone		Clinical	Standard ALL drug
Givinostat	HDAC inhibitors	Phase II	CLL, NCT00792831
Entinostat		Phase I-II	Adult ALL, NCT00462605
Panobinostat		Phase I-II	Pediatric ALL, phase I, NCT01321346
PU-H71	HSP90 inhibitor	Phase I	Lymphoma, NCT01393509
Dactolisib	Kinase inhibitor (PI3K//mTOR)	Phase I-II	Terminated, NCT01756118
Imatinib	Kinase inhibitors (PDGFR, c-Kik, BCR-ABL1)	Clinical	
Bortezomib	Proteasome inhibitor	Clinical	Pediatric ALL, phase III, NCT02112916
Doxorubicin	Topoisomerase inhibitors and anthracyclines	Clinical	Standard ALL drug
Etoposide		Clinical	Pediatric ALL, Phase I, NCT00991133
Idarubicin		Clinical	Pediatric ALL, Phase IV, NCT01990807
Mitoxantrone		Clinical	Pediatric ALL, Phase III, NCT02101853
Topotecan		Clinical	Pediatric ALL, Phase II, NCT00003735
Birinapant	SMAC mimetic	Phase I-II	AML and ALL, phase I-II, NCT01486784

Supplementary Table 2. Characteristics of primary T-ALL patient samples. *No matched diagnosis sample was available for the relapsed sample.*

		Genomic aberrations										Molecular-genetic subtypes								
Patient ID/ Risk group	**Patient at:**	**SIL-TAL deletion**	**LEF deletion**	**CASP8AP2 deletion**	**MLLT3 deletion**	**MTAP deletion**	**CDKN2A deletion**	**CDKN2B deletion**	**PTEN deletion**	**MYB amplification**	**NUP214-ABL1 fusion**	**SIL-TAL1**	**HOX11**	**HOX11L**	**HOXA9**	**Age**	**Sex**	**Immuno-phenotype**	**Prednisolone response**	**Outcome**	**Cell viability after thawing %**
T-MR-09	Diagnosis					1	2	2	1				Y			8.0	male	8	P	R	90
T-MR-04	Diagnosis	1		1			2					Y				14.3	male	8	G	CCR	90
T-HR-04	Diagnosis	1		1			2					Y				15.0	male	7	P	CCR	90
T-VHR-26	Diagnosis					1	1	1								3.8	female	9	P	R	90
T-R-18	Relapse														Y	6.7	male	9			80
T-HR-12	Diagnosis				1	1	2	2								8.4	male	9	P	CCR	90

SR – standard risk;
MR – medium risk;
HR – high risk;
VHR – very high risk;
R – relapse;

1 – heterozygous;
2 – homozygous deletion,
Y – yes.

7 – Pre-T-ALL;
8 – Cortical T-ALL;
9 – Mature T-ALL.

G – good;
P – poor.

CCR – complete responder;
R – relapsed

Supplementary Table 3. Characteristics of T-ALL cell lines used for xenograft experiments.

		Genomic aberrations											Molecular-genetic subtypes						
Cell line	**Patient at:**	**SIL-TAL deletion**	**LEF deletion**	**CASP8AP2 deletion**	**MLLT3 deletion**	**MTAP deletion**	**CDKN2A deletion**	**CDKN2B deletion**	**PTEN deletion**	**MYB amplification**	**NUP214-ABL1 fusion**	**SET-NUP214 fusion (results in HOXA activation)**	**SIL-TAL1**	**HOX11**	**HOX11L**	**HOXA9**	**Age**	**Sex**	**Immuno-phenotype**
LOUCY	Diagnosis (no remission achieved)					1	1		1			Y					38	female	*
ALL-SIL	Relapse					2	2			Y	Y			Y			17	male	8

1 – heterozygous;
2 – homozygous deletion,
Y – yes.

7 – Pre-T-ALL;
8 – Cortical T-ALL;
9 – Mature T-ALL.

* is considered to be a model for immature T-ALL because it has a transcriptional program highly related to early immature T-ALLs (Van Vlierberghe et al., J Exp Med 2011). However, immunophenotypically this cell line has sCD3 and TCRγδ expression.

Supplementary Table 4. Top 30 compound connections (LINCS). *The Library of Integrated Cellular Signatures (LINCS), accessed via the website lincscloud.org, was used to search for the most connected compounds with our JQ1-induced signature in LOUCY. Using the up- and downregulated genes after 4h of JQ1 treatment (adjusted p-value<0.01), 10 known HDAC inhibitors were found in the top 30 of compound connections. The compound connections are ranked according to the score_best4, i.e. the mean connectivity score across the four cell lines in which the perturbagen connected most strongly to the query.*

Rank	Name of perturbagen	Type of perturbagen	Score_best4
1	TG-101348	JAK2 inhibitor	99.925
2	XMD-1150	Unknown?	99.802
3	BRD-K52163391	Unknown?	99.708
4	THM-I-94	Unknown?	99.63
5	BI-2536	Plk1 inhibitor	99.606
6	ISOX	Unknown?	99.243
7	XMD-885	Unknown?	98.986
8	BRD-A11087911	Unknown?	98.895
9	BRD-K10361096	Unknown?	98.64
10	JWE-035	Unknown?	98.512
11	trichostatin-a	**HDACi**	98.478
12	HC-toxin	**HDACi**	98.46
13	XMD-1185H	Unknown?	98.373
14	scriptaid	**HDACi**	98.018
15	XMD-892	ERK5/BMK1 inhibitor	98.015
16	BRD-K75081836	Unknown?	97.98
17	XMD-16144	Unknown?	97.846
18	Vorinostat	**HDACi**	97.845
19	KM-00927	Unknown?	97.831
20	KU-0060648	inhibitor of DNA-PK and PI3Kα, PI3Kβ, PI3Kδ	97.83
21	trichostatin-a	**HDACi**	97.82
22	panobinostat	**HDACi**	97.796
23	LY-303511	blocks voltage-gated potassium channels, inhibits IL-1β-stimulated NF-κB activation and inhibits the BET bromodomain proteins BRD2, BRD3 and BRD4	97.482
24	Belinostat	**HDACi**	96.987
25	BRD-K23412959	Unknown?	96.546
26	Dacinostat	**HDACi**	96.176
27	NCH-51	**HDACi**	96.15
28	Apicidin	**HDACi**	96.019
29	Piperlongumine	Unknown?	95.941
30	BRD-K88622704	Unknown?	95.531

Supplementary Table 5. Primer sequences and miScript Primer Assays. *Sequences of all the primers used for the qRT-PCR reactions and miScript Primer Assays to quantifiy mature miRNAs.*

Gene	**Forward primer**	**Reverse primer**
BCL2	5'-CATGTGTGTGGAGAGCGTCAA-3'	5'-GCCGGTTCAGGTACTCAGTCA-3'
BCL2L11 (BIM)	5'-TGGCAAAGCAACCTTCTGATG-3'	5'-GCAGGCTGCAATTGTCTACCT-3'
Reference genes		
HMBS	5'-GGCAATGCGGCTGCAA-3'	5'-GGGTACCCACGCGAATCAC-3'
RPL13A	5'-CCTGGAGGAGAAGAGGAAAGAGA-3'	5'-TTGAGGACCTCTGTGTATTTGTCAA-3'
YWHAZ	5'- ACTTTTGGTACATTGTGGCTTCAA -3'	5'- CCGCCAGGACAAACCAGTAT -3'
miRNA	**miScript Primer Assay (Qiagen)**	
miR-17-5p	MS00029274	
miR-18a-5p	MS00031514	
miR-19a-3p	MS00003192	
miR-19b-3p	MS00031584	
miR-20a-5p	MS00003199	
miR-92a-3p	MS00006594	
Assays used for normalization		
miR-16-5p	MS00031493	
miR-26a-5p	MS00029239	
miR-26b-5p	MS00003234	

Supplementary Materials and Methods

Drug-screening platform

MSC (2,500 cells/well) were plated in 384-well plates (Greiner, REF781090) in 30µL serum-free medium (AIM-V®, Life Technologies). After 24h incubation at 37°C, 5% CO2, $2.5x10^4$ viable leukemia cells were suspended in 27.5µL medium and incubated for an additional 24h. All compounds used in the screening (Supplementary Table 1) had been diluted in DMSO to reach a 10mM concentration and stored at -80°C. Serial dilutions were performed from a starting dose of $1x10^5$ nM diluted 10x over four additional points using an epMotion 5070 robot (Eppendorf). Compounds were tested in duplicate. For combination screening two plates had been prepared: one as control (DMSO) and second with selected sub-lethal venetoclax dose in all wells. After 72h of incubation with compounds, live cell numbers were evaluated using CyQUANT® live cell staining (Life Technologies). 20µL staining mix (AIM-V medium, CyQUANT (1:300), Repressor (1:20)) was added into each well and incubated for 1h at 37°C, 5 % CO2. Automated imaging was performed using the ImageXpressMicro microscope (Molecular Devices) equipped with a CoolLSNap HQ camera (Photometrics) and a 10x Plan Fluor objective with 0.3 NA (Nikon). Nine images were taken per well (MetaXpress), covering 50% of the well surface. Images were processed using the CellProfiler software (Broad Institute). Cells were classified and counted using the Advanced Cell Classifier software (1, 2). This software uses the random forest classification method to identify T-ALL cells from MSCs. More information on the two imaging processing programs used can be found on http://acc.ethz.ch/.

1. Horvath P, Wild T, Kutay U, Csucs G. Machine learning improves the precision and robustness of high-content screens: using nonlinear multiparametric methods to analyze screening results. J Biomol Screen. 2011;16(9):1059-67.
2. Misselwitz B, Strittmatter G, Periaswamy B, Schlumberger MC, Rout S, Horvath P, et al. Enhanced CellClassifier: a multi-class classification tool for microscopy images. BMC Bioinformatics. 2010;11:30.

PART II Pharmacological inhibition of LSD1/KDM1A for the treatment of T-ALL

Paper 3: Oncogenic ZEB2 activation drives sensitivity towards KDM1A inhibition in T-cell acute lymphoblastic leukemia (published in Blood, 2017)

Paper 3

ONCOGENIC ZEB2 ACTIVATION DRIVES SENSITIVITY TOWARDS KDM1A INHIBITION IN T-CELL ACUTE LYMPHOBLASTIC LEUKEMIA

Steven Goossens[1,2,3,4,5,*], Sofie Peirs[4,5,*], Wouter Van Loocke[4,5], Jueqiong Wang[1], Mina Takawy[1,6], Filip Matthijssens[4,5], Stefan E. Sonderegger[7], Katharina Haigh[1], Thao Nguyen[1], Niels Vandamme[2,3,4], Magdaline Costa[1], Catherine Carmichael[1] , Filip Van Nieuwerburgh[8], Dieter Deforce[8], Oded Kleifeld[9], David J. Curtis[7], Geert Berx[2,3,4], Pieter Van Vlierberghe[4,5,**] and Jody J. Haigh[1,**]

[1]Mammalian Functional Genetics Group, Australian Centre for Blood Diseases, Monash University, Melbourne, Australia
[2]Molecular and Cellular Oncology Lab, VIB Inflammation Research Center, Ghent, Belgium
[3]Department for Biomedical Molecular Biology, Ghent University, Ghent, Belgium
[4]Cancer Research Institute Ghent (CRIG), Ghent, Belgium
[5]Centre for Medical Genetics, Ghent University and University Hospital, Ghent, Belgium
[6]Biochemistry and Physiology Laboratory, Department of Biological applications, Radioisotopes applications Division, Nuclear Research Centre, Egyptian Atomic Energy Authority, Abu-Zabal, Egypt
[7]Stem Cell Research Group, Australian Centre for Blood Diseases, Monash University, Melbourne, Australia
[8]Laboratory of Pharmaceutical Biotechnology, Ghent University, 9000, Ghent, Belgium
[9]Monash Biomedical Proteomics Facility, Monash University, Melbourne, Australia

*SG and SP contributed equally to this work
**PVV and JH contributed equally to this work

Published in BLOOD, 23 February 2017; volume 129; number 8; page 981-990.

Key Points

- ZEB2, a novel driver of immature T-cell acute lymphoblastic leukemia (T-ALL), interacts with the Lysine-specific demethylase KDM1A
- KDM1A function is critical for leukemic survival of T-ALL cells with high *ZEB2* levels

Abstract

Elevated expression of the Zinc finger E-box binding homeobox transcription factor-2 (*ZEB2*) is correlated with poor prognosis and patient outcome in a variety of human cancer subtypes. Using a conditional gain-of-function mouse model, we recently demonstrated that ZEB2 is an oncogenic driver of immature T-cell acute lymphoblastic leukemia (T-ALL), a heterogenic subgroup of human leukemia characterized by a high incidence of remission failure or hematological relapse after conventional chemotherapy. Here, we identified the Lysine-specific demethylase KDM1A as a novel interaction partner of ZEB2 and demonstrated that mouse and human T-ALLs with increased *ZEB2* levels critically depend on KDM1A activity for survival. Therefore, targeting the ZEB2 protein complex through direct disruption of the ZEB2-KDM1A interaction or pharmacological inhibition of the KDM1A demethylase activity itself, could serve as a novel therapeutic strategy for this aggressive subtype of human leukemia, and possibly other ZEB2-driven malignancies.

Introduction

ZEB2 is a member of the Zinc finger E-box binding homeobox transcription factor family that mediates epithelial to mesenchymal transition (EMT) events during development and disease[1]. Induced expression of ZEB2 in epithelial cancer cell lines results in the repression of a wide range of genes responsible for cellular adhesion, allowing these cells to become motile and upon xenotransplantation disseminate into the surrounding tissue and metastasize[2]. Moreover, increased expression of EMT transcription factors (EMT-TFs), such as ZEB2, is associated with the acquisition of cancer stem cell (CSC) properties that have the potential to self-renew and form secondary tumors upon transplantation[3-5]. Currently, little is known about how EMT-TFs regulate CSC properties at the molecular level. It has been proposed that targeting EMT-TFs is a promising novel therapeutic strategy that not only prevents EMT-mediated spreading of tumor cells but also targets radio/chemoresistent cancer stem cells[6].

Using a conditional loss of function approach, we have demonstrated that ZEB2 is an essential transcription factor during embryonic and adult hematopoiesis[7, 8]. In contrast, conditional *Zeb2* overexpression leads to the spontaneous formation of an immature early thymic progenitor subtype of T-cell acute lymphoblastic leukemia (ETP-ALL)[5]. ETP-ALL is a refractory and aggressive form of leukaemia, characterized by the co-expression of early T-cell and myeloid progenitor cell gene expression profiles[9]. *Zeb2*-overexpressing primary T-ALL cells show significant overlap with the expression profile of human ETP-ALL, and exhibit a marked increase of hematopoietic stem cell markers and leukemia-initiation potential[5].

ZEB2 is a large multidomain homeobox transcription factor that recognizes bipartite E-box motifs through its amino- and carboxyterminal Zinc finger domains[10]. The domains outside

the Zn-finger clusters have been shown to be essential for the recruitment of various tissue-specific co-activators/repressors, which ultimately regulates ZEB2's tissue-specific activity[11]. Therefore, identification and targeting of novel interaction partners that are essential for ZEB2's oncogenic properties in the context of T-ALL, represents a feasible option for the development of novel therapeutics to treat aggressive leukemia.

Recent studies have shown the importance of epigenetic changes during cancer initiation/progression. Clonal evolution studies have suggested the existence of pre-leukemic epigenetic changes within hematopoietic progenitors that allows clonal expansion and accumulation of genetic lesions that eventually results in overt leukemia[12-14]. KDM1A is a flavin-containing amino oxidase that specifically catalyzes the demethylation of mono- and di-methylated lysines on histone 3 (H3K4 and H3K9, typically associated with gene repression and activation respectively). KDM1A regulates the balance between self-renewal and differentiation of pluripotent stem cells[15] and its expression is upregulated in various cancers. Pharmacological inhibition of KDM1A has emerged as a promising novel therapy to treat and kill cancer stem cells and novel potent inhibitors are being tested in clinical trials[16, 17]. Within the hematopoietic system, conditional loss of KDM1A results in a pancytopenia with impaired HSC self-renewal and differentiation potential[18]. Inversely, KDM1A gain-of-function results in enhanced self-renewal and skewing towards the T-cell lineage, eventually leading to the development of T-cell lymphoblastic leukemia[19]. Although KDM1A inhibition has been identified as a promising novel epigenetic therapy for various subtypes of human cancers including acute myeloid leukemia (AML), the molecular mechanisms that drive susceptibility to KDM1A inhibition and/or biomarkers that could predict KDM1A sensitivity remain to be further explored.

Here, we identify KDM1A as a novel interaction partner for ZEB2 in T-ALL and demonstrate that increased ZEB2 expression can drive sensitivity towards KDM1A inhibition.

Methods

Pull-downs, Mass Spectrometry

Mouse T-ALL cells were washed once with phosphate-buffered saline and nuclear extracts were prepared as described previously[20] and in supplements. Anti-FLAG M2 agarose beads (Sigma) were used to pull down FLAG-ZEB2 containing protein complexes overnight at 4°C, rotating. Beads were washed five times and eluted four times with 0.6 mg/ml FLAG tripeptide (Sigma) for 15 min at room temperature. Fractions were loaded onto a 10% Mini-Protean TGX precast gel (BioRad) and silver stained (Thermo Fisher Scientific). Elutions containing the majority of FLAG-ZEB2 were loaded onto a 10% SDS-PAA gel (Thermo Scientific) and separated by a short SDS-PAGE gel run. Entire lanes were excised and subjected to in-gel tryptic digestion and liquid chromatography tandem mass spectrometry (LC-MS/MS) analysis as previously described[21]. Raw data were processed and searched by MaxQuant software (version 1.5.2.8)[22]. Database searching was done against mouse protein sequences downloaded from Uniprot (03/2015 release) using MaxQaunt default settings. Significance of specific protein–protein interactions was performed using Perseus analysis software[23].

Co-immunoprecipitations

For FLAG-ZEB2 pull-downs, anti-FLAG M2 agarose beads (Sigma) were used as above. For

KDM1A pull-downs, the rabbit polyclonal anti-KDM1A (LSD1) antibody (Abcam) was used in combination with the Rabbit TrueBlot IP-set (Rockland). Western blot analysis was performed according to standard protocols and primary antibodies are listed in Supplementary information.

Chromatin immunoprecipitation (ChIP)

ChIPs were performed using the SimpleChIP Enzymatic Chromatin IP kit with magnetic beads (Cell Signaling Technology) using H3K4me2-specific mouse monoclonal Antibody (MABI 0303, Active Motif). The enriched DNA was quantified by qPCR with SimpleChIP Human *CD11b* Promoter Primers (#14271, Cell Signaling Technology).

Cell culture

T-ALL cell lines were grown as previously described[5] and in supplements. For the generation of KARPAS-45 cells overexpressing ZEB2, virus production was performed in HEK293TN cells using JetPEI polyplus with pMD2.G (envelope plasmid), psPAX2 (packaging plasmid) and pSIN-TRE-GW-3xHA hZEB2 (target plasmid) in 0.1/0.9/1 ratios. Transduced KARPAS-45 cells were selected by puromycin (1µg/ml). 48h before the start of the KDM1A inhibitor experiment, doxycyclin (1µg/ml) administration was started. GSK2879552 (ActiveBiochem) was dissolved in DMSO at a concentration of 10 mg/ml and diluted further in medium as indicated. Further cell culture details are listed in supplements.

SiRNA knockdown

For siRNA-mediated knockdown experiments, LOUCY was electroporated with 400nM of ZEB2-specific siRNAs (siZEB2-01: ON-TARGETplus Human ZEB2 siRNA J-006914-07, Dharmacon; siZEB2-02: Silencer Select Pre-designed Human ZEB2 siRNA s19034, ThermoFisher Scientific) or 400nM of scrambled siRNAs (ON-TARGETplus Non-targeting pool D-001810-10-05, Dharmacon). Also electroporation without adding siRNAs was performed as control. For the electroporation, an exponential decay pulse (300V, 1000mF; Genepulser MxCell, Bio-Rad) was used. After 72h and 120h, RNA was isolated and evaluated by qRT–PCR.

Cell viability assays

Cell viability was determined by combination of CellTiter Glo Luminiscent viability assay (Promega) and flow cytometric analysis on LSRII or Fortessa (BD Biosciences) and FACSDiva or FlowJo software (BD Biosciences). For viability, we used combination of AnnexinV/DAPI stain or the fixable viability Dye eFluor450 (eBioscience).

qRT-PCR was performed according to standard protocols and used primer sets are listed in supplements.

Allo/Xenotransplantations

T-ALL cell lines were intravenously injected in NOD scid gamma (NSG) mice. For the recipients transplanted with the mouse T-ALL cell lines, 1 X 10^6 cells were transplanted into 8-10 week-old male recipients via tail-vein injection and the KDM1A inhibitor treatment was started the day after cell injection with 1.5mg GSK2879552/kg body weight (or vehicle only) via oral gavage and was continued for 3 weeks. Mice were monitored for illness and leukemia development.

For the NSG mice injected with LOUCY or PEER cells, KDM1A inhibitor treatment was started when the first signs of engraftment were detected (hCD45+ cells in periphery). Mice

were treated (1.5 mg GSK2879552/kg body weight or vehicle via oral gavage) for 17 (PEER) or 18 (LOUCY) consecutive days. Mice were weighed daily and monitored. The percentage of leukemic cells in the blood was analyzed by staining the cells with an PE-labeled antibody (Miltenyi Biotec) for human CD45 (hCD45), red blood cell lysis and measuring the percentage with S3e cell sorter (Bio-Rad).

RNA sequencing and Bioinformatics

RNA was prepared using either the RNeasy mini Plus kit (Qiagen) or the miRNeasy mini kit (Qiagen). Library preparation was performed using the Illumina TruSeq RNA sample Prep Kit. Enriched cDNA libraries were sequenced using an Illumina NextSeq 500 sequencer instrument. Reads were aligned to GRCm38 and GRCh38 using STAR2.4.2a. Genes were quantified on Ensembl38_v81 and Gencode v23 respectively**.** Pathway analysis was performed by KEGG using standard settings. Finally, pre-ranked GSEA was performed with the c2 MSigDB gene sets collection using the GSEA desktop application (Broad Institute, version v2.2.0). Further details are provided in supplements.

Results

ZEB2 interacts with KDM1A

We derived 4 T-ALL cell lines from murine thymomas from our *Zeb2* overexpression mouse model that had been intercrossed onto a conditional p53-null tumor-prone background[5]: two p53 null primary T-ALL cell lines with *Zeb2* overexpression (further annotated as *P53/R26-Zeb2*$^{tg/tg}$) and two p53 null control cell lines without *Zeb2* overexpression (further annotated as *P53/R26*$^{+/+}$). In the *P53/R26-Zeb2*$^{tg/tg}$ tumor cell lines, the ZEB2 transgene contains an aminoterminal 3xFLAG/Strep-tag, providing a useful *in vitro* model system to isolate ZEB2-containing protein complexes and identify ZEB2 interaction partners in the context of T-ALL. We performed protein complex pull-down experiments on nuclear extracts of *P53/R26-Zeb2*$^{tg/tg}$ and *P53/R26*$^{+/+}$ T-ALL cell lines using anti-FLAG beads (Figure 1A), followed by mass spectrometry. Importantly, known ZEB2 interaction partners, such as CTBP1[24] and multiple subunits of the NuRD chromatin remodelling complex (i.e. CHD4/Mi-2β, MTA2 and HDAC1)[25], were co-purified in the FLAG-ZEB2 expressing tumor lines, confirming the validity of our approach (Table 1). We also identified novel putative ZEB2 interaction partners including the hematopoietic transcription factor RUNX1, MYB binding protein 1A (MYBBP1A), multiple proteins involved in pre-mRNA processing and RNA biogenesis (Hnrnph1, Snrpb/n, Snrpd2, Snrnp70, Ddx21), NUMA1 (nuclear mitotic apparatus protein 1) as well as the Lysine-specific demethylase-1 KDM1A (Table 1). Here, we focused on the ZEB2-KDM1A interaction for several reasons: 1) there is a significant overlap between the phenotypes observed after KDM1A and ZEB2 gain/loss *in vitro* (i.e. EMT phenotype switching[10, 26], regulation of the balance between self renewal and differentiation in embryonic stem cells[15, 27], as well as regulating proliferation and differentiation of acute myeloid leukemia cells[28, 29]) and *in vivo* (i.e. pancytopenia with loss of HSC differentiation potential upon loss of function[7, 18] and spontaneous T-ALL formation upon gain of function[5, 19], association with EMT and solid tumor metastasis[10, 26]) ; 2) KDM1A has previously been identified as being part of both the NuRD[26] and CTBP1 co-repressor complexes[30], known interactors of ZEB2 and also identified here, and 3) the existence of potent KDM1A inhibitors[16, 17, 31] that are presently being used in Phase I clinical trials .

We confirmed this ZEB2-KDM1A interaction using bidirectional co-immunoprecipitation experiments, with FLAG/ZEB2- and KDM1A-specific antibodies (Figure 1B-C). Finally, to prove that this interaction was not an overexpression artifact in our mouse T-ALL cell lines, we further confirmed this interaction in nuclear extracts from LOUCY cells (Figure 1D), a human T-ALL cell line with an immature expression profile and high *ZEB2* expression[5].

Table 1. Mass spectrometric analysis of peptides identified after pull down of FLAG-ZEB2 containing protein complexes in P53/R26-Zeb2$^{tg/tg}$ versus control P53/R26$^{+/+}$ mouse T-ALL cell lines.

Protein Name	Gene name	peptides P53/R26$^{+/+}$ control #1	peptides P53/R26$^{+/+}$ control #2	peptides P53/Zeb2$^{tg/tg}$ TG/TG #1	peptides P53/Zeb2$^{tg/tg}$ TG/TG #2
Gelsolin	Gsn	0	0	21	6
F-actin-capping protein subunit beta	Capzb	0	0	22	2
Zinc finger E-box-binding homeobox 2	Zeb2	0	0	13	4
Major vault protein	Mvp	0	0	10	3
Nuclear mitotic apparatus protein 1	Numa1	0	0	9	4
Actin-related protein 2/3 complex subunit 4	Arpc4	0	0	9	3
Heterogeneous nuclear ribonucleoprotein H	Hnrnph1	0	0	8	3
Small nuclear ribonucleoprotein-associated protein B/N	Snrpb;Snrpn	0	0	9	1
Histone deacetylase 1	Hdac1	0	0	7	3
Metastasis-associated protein MTA2	Mta2	0	0	7	2
Small nuclear ribonucleoprotein Sm D2	Snrpd2	0	0	8	1
Actin-related protein 3	Actr3	0	0	8	1
Myb-binding protein 1A	Mybbp1a	0	0	5	2
RuvB-like 1	Ruvbl1	0	0	5	2
Chromodomain-helicase-DNA-binding protein 4/5	Chd4;Chd5	0	0	6	1
U1 small nuclear ribonucleoprotein 70 kDa	Snrnp70	0	0	5	1
Runt-related transcription factor 1	Runx1	0	0	5	1
Tropomyosin alpha-3 chain	Tpm3	0	0	4	2
Lysine-specific histone demethylase 1A	Kdm1a	0	0	4	1
C-terminal-binding protein 1	Ctbp1	0	0	3	3
Spectrin beta chain, non-erythrocytic 1	Sptbn1	0	0	4	2
Nucleolar RNA helicase 2	Ddx21	0	0	3	2
Unconventional myosin-Ic	Myo1c	0	0	4	1

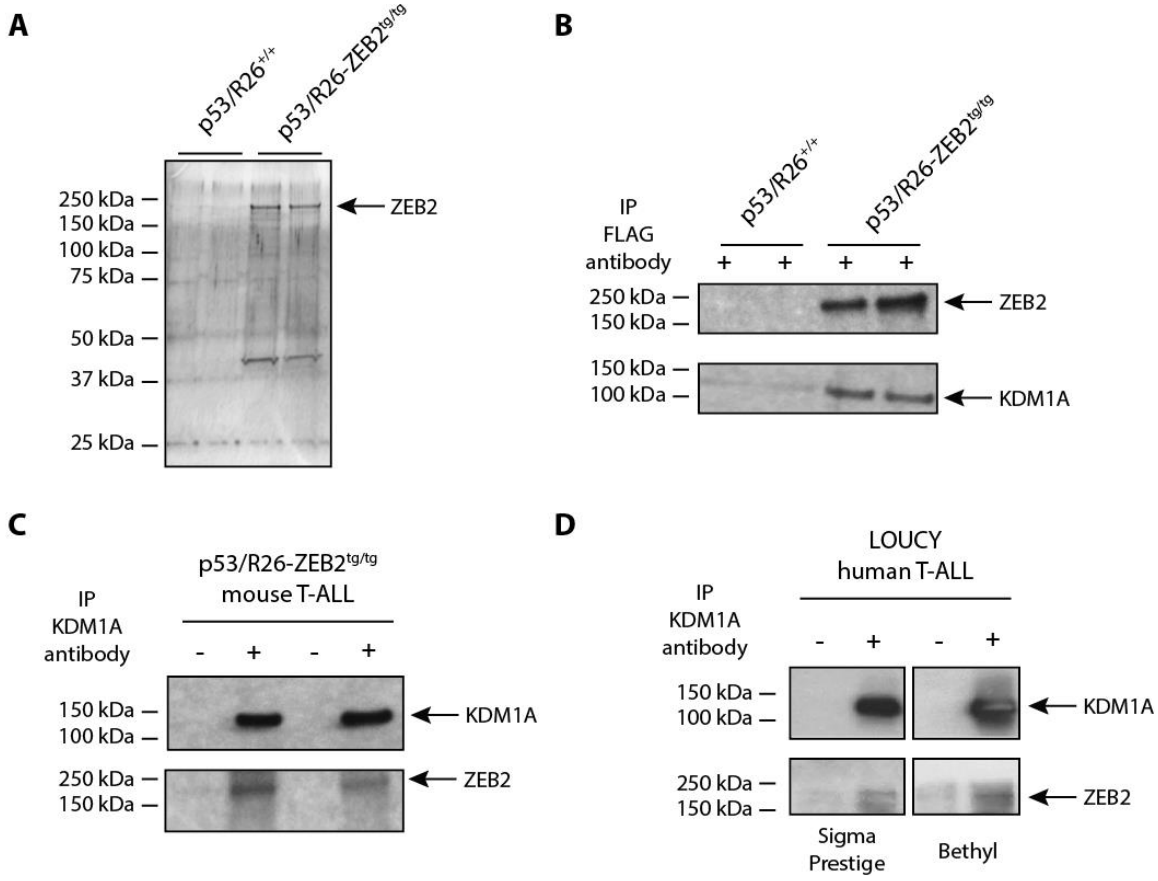

Figure 1. ZEB2 interacts with KDM1A in T-ALL cell lines. *(A) Silverstain of SDS-Page after pull downs of FLAG-ZEB2 protein complex (B) Co-immunoprecipitation of KDM1A after pull down of FLAG-ZEB2 protein complex in mouse T-ALL cell lines (C) Co-immunoprecipitation of ZEB2 after pull down of KDM1A protein complex in mouse T-ALL cell lines (D) Co-immunoprecipitation of ZEB2 after pull down of KDM1A protein complex in the human T-ALL cell line LOUCY, using 2 antibodies that recognize human ZEB2.*

Mouse T-ALL cell lines with high ZEB2 levels are sensitive to KDM1A inhibitors

To validate the functional relevance of this ZEB2-KDM1A interaction, we tested the effects of KDM1A inhibition on the mouse T-ALL cell lines with and without *Zeb2* overexpression. Strikingly, both *Zeb2*-overexpressing *P53/R26-Zeb2*$^{tg/tg}$ cell lines showed high sensitivity towards KDM1A inhibition (Figure 2A, Supplementary Figure 1). More specifically, T-ALL cells with enhanced *Zeb2* levels were sensitive to treatment with the commercially available KDM1A inhibitor GSK2879552 with an average IC_{50} at day 4 of 10.39nM (Figure 2A, Supplementary Figure 1). In contrast, no effects were observed for the control *P53/R26*$^{+/+}$ mouse T-ALL cell lines using these inhibitors (Figure 2A, Supplementary Figure 1). Both *P53/R26*$^{+/+}$ and *P53/R26-Zeb2*$^{tg/tg}$ expressed similar protein levels of KDM1A, illustrating that altered levels are not determining their sensitivity towards pharmacological KDM1A inhibition (Supplementary Figure 2A).

To obtain molecular insights into the pathways involved in ZEB2-driven KDM1A inhibitor sensitivity, we subsequently performed RNA-sequencing on two *P53/R26*$^{+/+}$ and two *P53/R26-Zeb2*$^{tg/tg}$ cell lines. As previously described[5], this analysis revealed that the *P53/R26*$^{+/+}$ and *P53/R26-Zeb2*$^{tg/tg}$ tumor lines displayed a very distinct gene expression signature under baseline (DMSO) conditions, with 6675 significantly differentially expressed

genes (adj. p-value<0.05; Supplementary Figure 3; Supplementary Table 1). KEGG pathway analysis revealed increased expression of AML related transcripts, decreased expression of NOTCH pathway genes involved in T-cell differentiation combined with activation of *JAK-STAT*/*MAPK* (mitogen-activated protein kinase 1) signalling in ZEB2-derived tumor lines (Supplementary Table 2). These differential gene patterns are in line with our previous observations that *Zeb2* driven thymomas reflect an immature T-ALL subtype with increased stem cell markers and activated IL7R/JAK-STAT signaling[5]. Given the pro-survival effects of activated IL7R/JAK-STAT signalling in the context of *Zeb2*-driven T-cell leukemogenesis, we wondered whether exogenous IL7 could partially rescue the apoptotic phenotype observed in these cells. Indeed, analysis of *Zeb2* transgenic cells in IL7-supplemented culture conditions revealed that IL7 inclusion could decrease the sensitivity to KDM1A inhibition in the *P53/R26-Zeb2*$^{tg/tg}$ cell lines (Figure 2B).

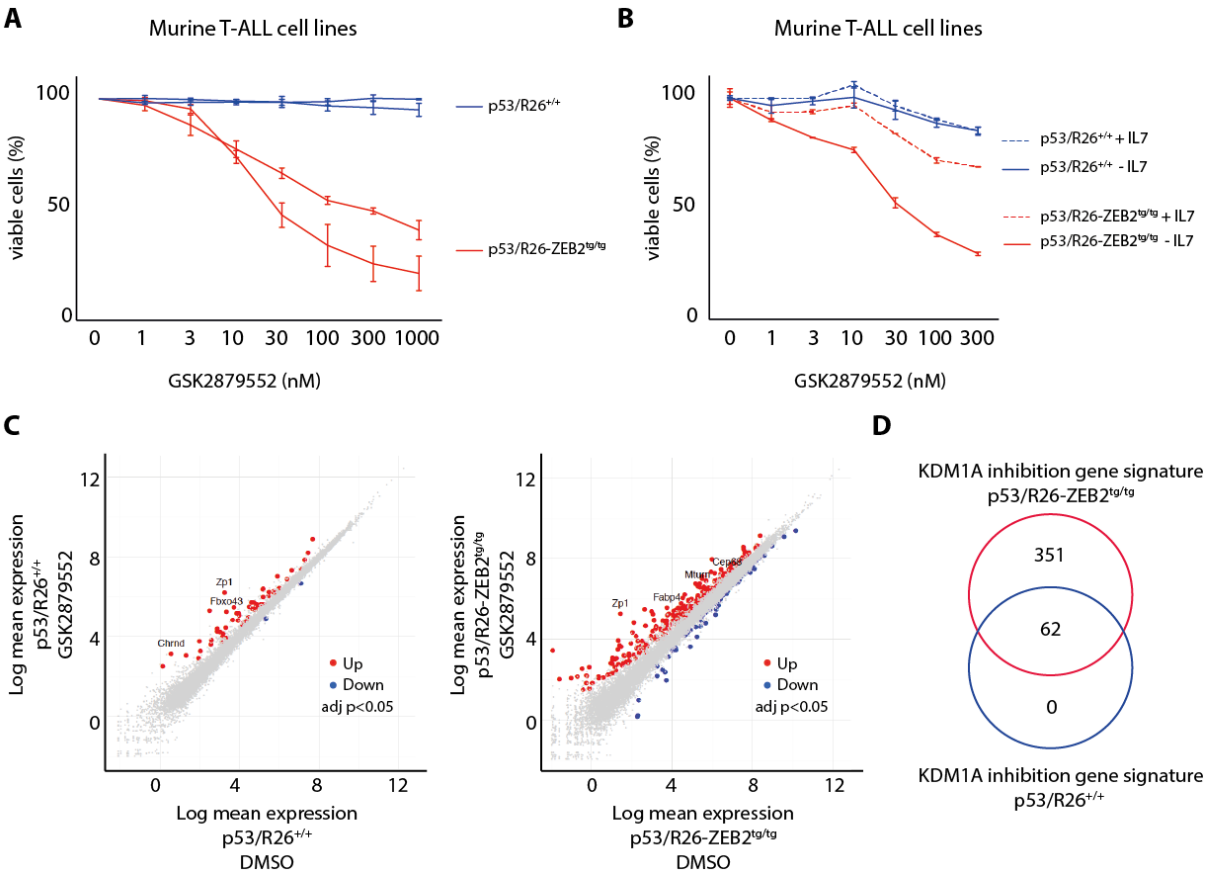

Figure 2. Mouse T-ALL cell lines with high ZEB2 levels are sensitive to KDM1A inhibition. *(A) Percentage of viable cells (CellTiter-Glo Luminescent Cell Viability Assay) in P53/R26-Zeb2*$^{tg/tg}$ *Zeb2 overexpressing mouse T-ALL cell lines compared to control P53/R26*$^{+/+}$ *cell lines treated with different concentrations of the KDM1A inhibitor GSK2879552 for 4 days. The average of three independent experiments and standard deviation is plotted. (B) Effects of exogenous IL7 on the sensitivity of P53/R26-Zeb2*$^{tg/tg}$ *Zeb2 overexpressing mouse T-ALL cell lines to KDM1A inhibition (CellTiter-Glo Luminescent Cell Viability Assay). Average of technical triplicates are plotted. Similar effects are observed with the second independent mouse T-ALL cell lines (C) Differential gene expression after KDM1A inhibition (24h, 100nM GSK2879552) in P53/R26*$^{+/+}$ *and P53/R26-Zeb2*$^{tg/tg}$ *mouse T-ALL cell lines (adjusted P-value < 0.05, triplicates). (D) Overlap between the KDM1A responsive gene signatures in P53/R26*$^{+/+}$ *and P53/R26-Zeb2*$^{tg/tg}$ *mouse T-ALL cell lines.*

Next, we analysed the transcriptional response upon short-term KDM1A inhibition (100nM GSK2879552 for 24h) in the absence of exogenous IL7 in both murine tumor entities.

Notably, and in line with the drug response phenotypes, KDM1A inhibition in control *P53/R26*$^{+/+}$ cell lines only caused limited effects on overall transcription with 62 differentially expressed genes (adj. p-value<0.05; Figure 2C). In contrast, gene transcription was more severely affected by KDM1A perturbations in the *P53/R26-Zeb2*$^{tg/tg}$ lines with significant changes in the expression of 413 transcripts (315 up- and 98 down-regulated; adj. p-value<0.05; Figure 2C; Supplementary Table 3). Notably, all 62 genes that showed differential expression upon KDM1A inhibition in *P53/R26*$^{+/+}$ cell lines, were also altered in the *P53/R26-Zeb2*$^{tg/tg}$ tumor lines (Figure 2D). All together, these results demonstrate that *Zeb2* overexpression modulates murine T-ALL responsiveness to KDM1A inhibitors.

Human T-ALL cell lines with high ZEB2 levels are sensitive to KDM1A inhibitors

To study the human relevance of our findings, we subsequently evaluated the putative correlation between *ZEB2* expression levels and KDM1A inhibitor sensitivity in a panel of human T-ALL cell lines. Interestingly, human T-ALL cell lines characterized by high (LOUCY) or moderate (PEER) *ZEB2* expression (Figure 3A) were sensitive towards KDM1A inhibition with average IC_{50} values at day 12 of 112.91nM (LOUCY) and 43.83nM (PEER) for GSK2879552 (Figure 3B). In addition, a time-course experiment in LOUCY cells revealed that the first overt effects on leukemic cell survival appear around 5-7 days of KDM1A inhibition treatment (Supplementary Figure 4). Moreover, this KDM1A inhibitor sensitivity was found to be similar to what has been described for acute myeloid leukemia (AML) cell lines[31] (Supplementary Figure 5). In contrast, the survival or proliferation of *ZEB2*-negative T-ALL cell lines, such as JURKAT, TALL-1 and ALL-SIL, was not affected by KDM1A inhibition (Figure 3B). Nevertheless, and in line with recent work[31], screening of additional T-ALL cell lines revealed that two other *ZEB2*-negative T-ALL cell lines, RPMI-8402 and HSB-2, were also highly sensitive to KDM1A inhibition, suggesting that alternative molecular mechanisms, independent of ZEB2, can also drive sensitivity towards KDM1A inhibition in the context of human T-ALL. Similarly, as seen in the mouse cell lines, no correlation was observed in the human T-ALL cell lines between KDM1A protein expression and KDM1A inhibitor sensitivity (Supplementary Figure 2B).

Although previous studies have suggested that KDM1A prevents differentiation and apoptosis in the context of *MLL* rearranged leukemia[28], we only observed minimal anti-leukemic effects upon GSK2879552 treatment in the *MLL-AFX* positive T-ALL cell line KARPAS-45 (Figure 3B). Given that this *MLL* rearranged T-ALL cell line is characterized by low levels of *ZEB2* (Figure 3A), we subsequently generated KARPAS-45 cells with doxycycline-inducible expression of ZEB2, to formally prove that ZEB2 can truly modulate KDM1A inhibitor sensitivity in the context of human T-ALL. Notably, doxycycline induced ZEB2 overexpression significantly increased KDM1A inhibitor sensitivity in this *in vitro* model system, as exemplified by decreased cell viability 12 days after the initiation of KDM1A inhibition (Figure 3C).

Next, we analysed the transcriptional response of KDM1A inhibition in human T-ALL cell lines. For this, RNA sequencing was performed on biological triplicates of the *ZEB2*-positive LOUCY and PEER cells, and the *ZEB2*-negatives RPMI-8402 and HSB-2 treated for 48 hours with 100nM GSK2879552 *versus* their corresponding DMSO treatment controls. Gene expression was affected by KDM1A inhibition in all sensitive T-ALL cell lines, but the effect was most pronounced in *ZEB2*-high LOUCY cells (Supplementary Figure 6A).

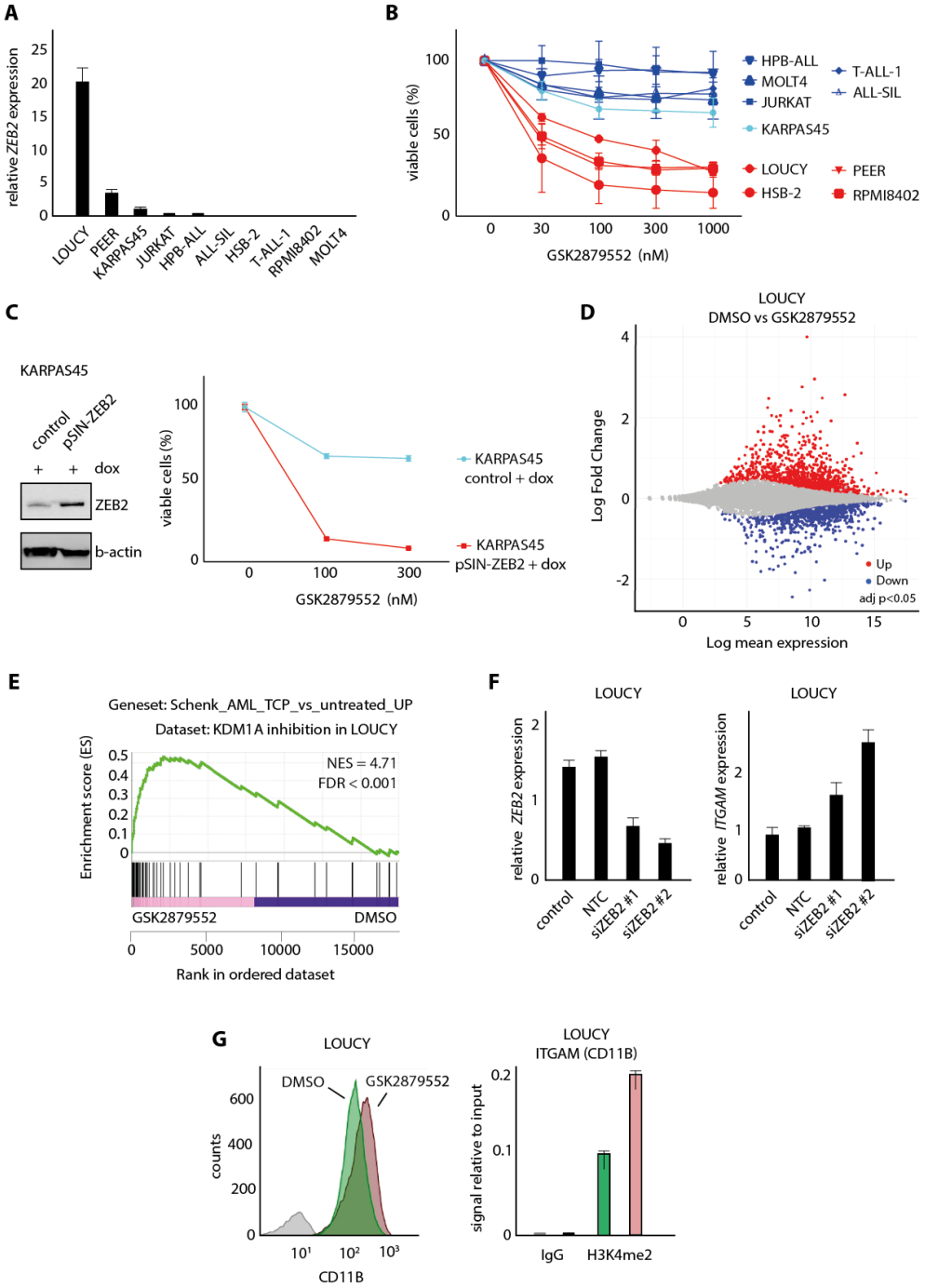

Figure 3. Human T-ALL cell lines with high ZEB2 levels are sensitive to KDM1A inhibition. *(A) Relative mRNA expression in a panel of human T-ALL cell lines analysed by qPCR (B) Cell viability (CellTiter-Glo Luminescent Cell Viability Assay) of human T-ALL cell lines with variable expression of ZEB2 mRNA after 12 days administration of the KDM1A inhibitor GSK2879552. The average and standard deviation of two independent experiments is plotted (C) Cell viability (CellTiter-Glo Luminescent Cell Viability Assay) of KARPAS-45 with dox-inducible overexpression of ZEB2 versus parental line after 12 days of GSK2879552 administration. Left, Western blot demonstrating level of dox-inducible ZEB2 overexpression; Right, % of cell viability. (D) Differential gene expression after KDM1A inhibition (48h, 100nM GSK2879552) in LOUCY (adjusted P-value < 0.05, triplicates) (E) Pre-ranked Gene Set Enrichment Analysis (GSEA) using probe set of genes upregulated upon KDM1A inhibition by TCP in human AML cell lines[33]. (F) ZEB2 and ITGAM mRNA expression levels upon siRNA-mediated ZEB2 knockdown in LOUCY cells (72h after electroporation). (G) Analysis of CD11B protein expression by flow cytometry after KDM1A inhibition (100nM GSK2879552, 72h) correlated with increased H3K4me2 levels at ITGAM promoter analysed by ChIP.*

Indeed, GSK2879552 treatment in LOUCY cells resulted in significant changes of 2800 transcripts (1382 up- and 1418 down-regulated; adj. p-value<0.05, Figure 3D), whereas PEER, RPMI-8402 and HSB-2 only displayed significant transcriptional changes in 333, 769 and 622 genes, respectively (Supplementary Table 4). In terms of overlap, only 41 genes were commonly differentially regulated in all 4 T-ALL cell lines (39 genes up and 2 genes down; Supplementary Figure 6B). Of note, cross-species comparison between LOUCY and *P53/R26-Zeb2*$^{tg/tg}$ murine tumor lines revealed a common KDM1A inhibitor response signature, which consisted of 87 genes (72 up and 15 down; Supplementary Figure 7).

Interestingly, pre-ranked Gene Set Enrichment Analysis (GSEA) revealed a significant overlap between the transcriptional response after KDM1A inhibition in the human LOUCY T-ALL cell line and the transcriptional response previously reported in the context of human AML[32] (Figure 3E). For example, common responsive genes that are re-expressed upon KDM1A inhibition in both AML and LOUCY included *GFI1*, vimentin (*VIM*) and integrin subunit alpha M (*ITGAM*; *enc*oding CD11B). Interestingly, recent work also demonstrated that loss of ZEB2 causes a similar re-induction of ITGAM expression in both mouse and human AML cell lines[29]. Most notably, siRNA-mediated *ZEB2* knockdown experiments in the T-ALL cell line LOUCY also resulted in increased *ITGAM* expression (Figure 3F). In line with this notion, we showed that CD11b induction upon KDM1A inhibition in LOUCY cells is associated with increased binding of the H3K4me2 mark at the *ITGAM* promoter region, as evaluated by chromatin immunoprecipitation (ChIP) (Figure 3G).

In vivo activity of KDM1A inhibition on high Zeb2 expressing murine and human T-ALL

Given that promising *in vivo* responses have been reported for small cell lung cancer using the commercially available KDM1A inhibitor GSK2879552[17], we subsequently explored the *in vivo* potential of GSK2879552 to prevent or delay secondary leukemia formation of ZEB2-overexpressing murine T-ALL cell lines. For this, *Zeb2*-overexpressing T-ALL cell lines were xenografted in immune deficient NOD scid gamma (NSG) mice and treated for 3 weeks with GSK2879552 (1.5 mg/kg bodyweight) or with vehicle (DMSO). Notably, although all mice eventually developed leukemia, KDM1A inhibition triggered a significant delay in tumor latency (Figure 4A).

To further evaluate the therapeutic relevance of KDM1A inhibition in the context of human T-ALL, we subsequently performed *in vivo* drug treatment experiments using T-ALL cell line xenografts. LOUCY (*ZEB2* high) and PEER (*ZEB2* moderate) were injected in the tail vein of NSG mice and treatment of established tumors (1.5 mg GSK2879552/kg bodyweight or vehicle) was initiated when the percentage of hCD45$^+$ cells in peripheral blood reached 2% (3 weeks (PEER) and 4 weeks (LOUCY) after injection). Notably, KDM1A inhibition resulted in a decrease in the percentage of circulating hCD45$^+$ for both cell lines, suggesting that GSK2879552 can trigger an *in vivo* effect on tumor burden and leukemia development (Figure 4B and Figure 4D). However, no changes in spleen weight (Figure 4C and Figure 4E) were observed and all animals showed signs of progressive disease, suggesting that KDM1A inhibition in human T-ALL might be particularly useful as part of a combination therapy.

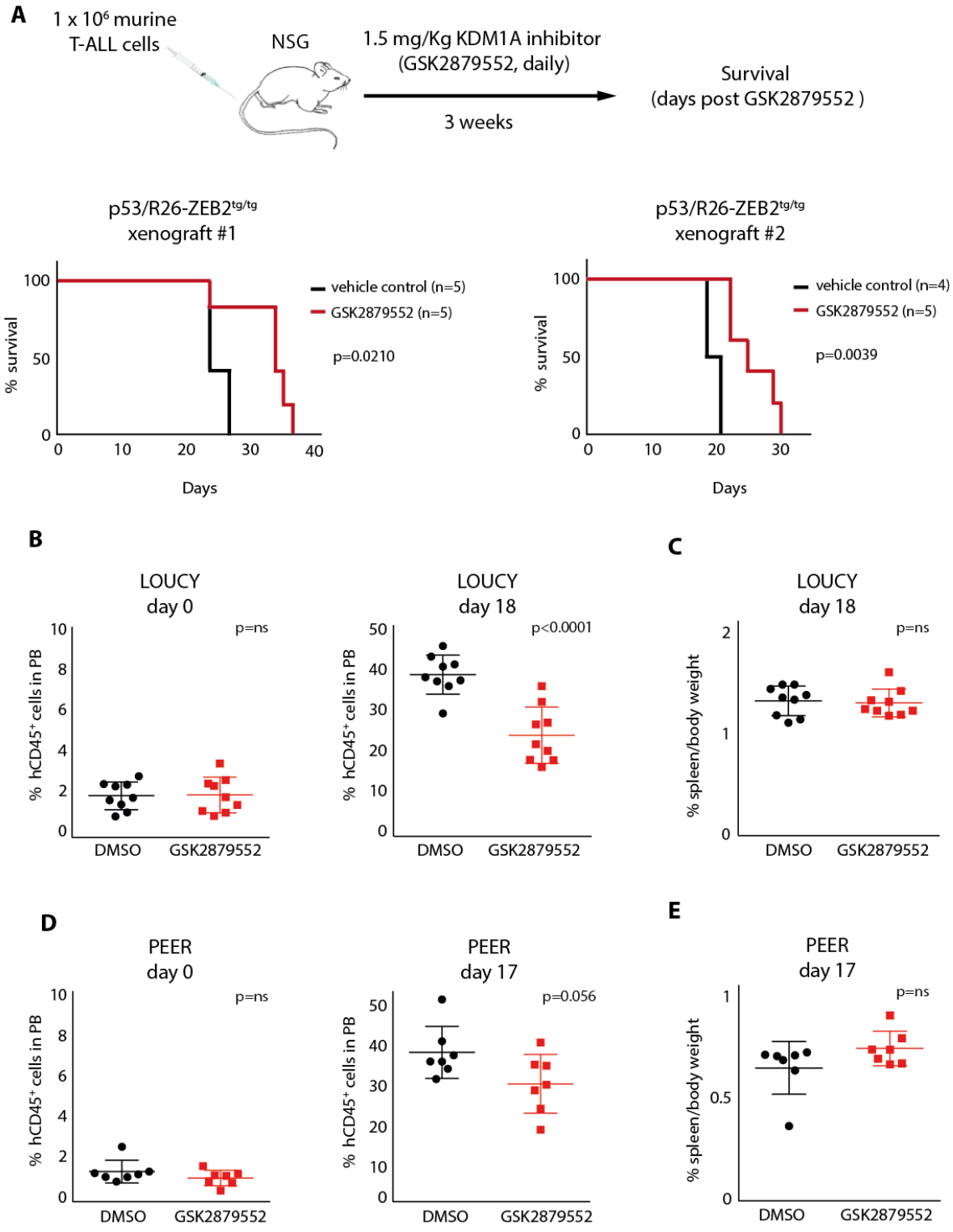

Figure 4. In vivo activity of KDM1A inhibitors on high Zeb2 expressing murine and human T-ALL. *(A) Kaplan-Meier survival curves of NSG mice injected with two P53/R26-Zeb2$^{tg/tg}$ murine tumor lines with and without 3 weeks of GSK2879552 administration (1.5 mg/kg bodyweight). (B) Percentage of hCD45+ T-ALL cells in peripheral blood of NSG mice xenotransplanted with LOUCY human T-ALL cells, before and after 18 days of GSK2879552 administration (1.5 mg/kg bodyweight) versus DMSO. (C) Percent spleen weight after 18 days of KDM1A inhibition (1.5 mg GSK2879552/kg bodyweight) versus DMSO. (D) Percentage of hCD45+ T-ALL cells in peripheral blood of NSG mice xenotransplanted with PEER human T-ALL cells, before and after 17 days of GSK2879552 administration (1.5 mg/kg bodyweight) versus DMSO (E) Percent spleen weight after 17 days of KDM1A inhibitor administration (1.5 mg/kg bodyweight) versus DMSO.*

Discussion

Relapsed T-ALL is a major clinical challenge. Therefore, current research efforts are focused on the development of more effective and less toxic anti-leukemic drugs, which will likely require an improved understanding of the molecular biology of chemotherapy-resistant residual tumor cells that eventually drive disease recurrence[33, 34]. In particular, immature T-ALL patients, which have a unique gene expression signature enriched for transcripts found in hematopoietic stem cells[35], have been associated with a poor response to current chemotherapy and significantly higher incidence of induction failure and hematological relapse[9].

We recently demonstrated that *ZEB2* is up-regulated in a subset of human T-ALLs and that *Zeb2* activation in the mouse results in the spontaneous formation of immature T-cell lymphoblastic leukemia with increased cancer stem cell properties and enhanced IL7 receptor expression[5]. Therefore, determining ZEB2 interaction partners involved in this oncogenic driver role may open up novel therapeutic strategies to specifically target aggressive forms of leukemia.

Here, we identified a number of novel putative ZEB2 interaction partners, including recurrently mutated proteins in T-ALL, such as the essential hematopoietic transcription factor RUNX1[35], the RNA processing protein HNRNPH1[36] and NUMA1, a protein involved in regulation of mitotic spindle organization and asymmetric/symmetric cell divisions[37]. More research is needed to confirm these novel ZEB2 interactions and to determine whether they are involved in the ZEB2-mediated T-ALL formation. The identification of known ZEB2 interaction partners in this study, such as CtBP1[38] and the NuRD chromatin remodeling complex[25, 39], confirms the validity of this approach and highlights their potential importance in T-ALL.

In this report, we identified and confirmed the interaction of ZEB2 with the Lysine-specific histone demethylase KDM1A in T-ALL cells. Whether this interaction is direct or part of a larger complex remains to be determined. Nevertheless, given that KDM1A has no DNA binding capacity, it depends on the interaction with transcription factors and transcriptional complexes to perform its function as a locus-specific epigenetic modifier. In that context, KDM1A has previously been identified in the CTBP1[30] and NuRD co-repressor[26] complexes, suggesting that these transcriptional complexes could also be functionally relevant in the context of T-cell transformation.

Similar as for ZEB2, KDM1A has been found to be involved in regulating cellular differentiation/self-renewal properties and EMT[26, 40]. Also other EMT-TF have been shown to interact with KDM1A and recruit it as a molecular hook to their target promoters[41], suggesting the presence of common regulatory mechanisms. Targeting either these interactions or the activity of KDM1A itself may therefore provide therapeutic avenues to prevent EMT and/or target chemo/radio-resistant cancer stem cells.

Here, we demonstrated that mouse and human T-ALL cell lines with high *Zeb2* mRNA expression levels are sensitive to KDM1A inhibition. Exactly how ZEB2 is capable of modulating KDM1A activity in the context of T-ALL remains to be determined. In AML cell lines, it was observed that KDM1A inhibition results in terminal differentiation by reactivation

of the all-trans-retinoic acid pathway, leading to a severe decline in proliferative capacity. Indeed, Li H. et al.[29] recently demonstrated that high ZEB2 levels are essential for AML progression and loss of ZEB2 in mouse and human AML cells results in myeloid differentiation, similar to what has been observed for KDM1A inhibition. Also in AML cells, a ZEB2-KDM1A interaction could be demonstrated via co-immunoprecipitation experiments, thereby confirming this interaction in a separate leukemic setting. Interestingly, we also observed that KDM1A inhibition results in upregulation of the myeloid differentiation marker CD11B in the human T-ALL cell line LOUCY, suggesting overlapping molecular mechanism downstream of KDM1A inhibition in both leukemic settings. Nevertheless, our study also revealed that *ZEB2*-negative human T-ALL cell lines also showed strong KDM1A inhibitor sensitivity, suggesting that other mechanisms or oncogenic drivers/transcriptional factors, such as GFI1, might be able to bind and alter KDM1A activity and drive KDM1A inhibitor sensitivity in a ZEB2-independent manner[41, 42].

In this study, we have used a commercially available KDM1A inhibitor, GSK2879552, which was previously successfully used to analyze the *in vivo* effects of KDM1A inhibition on human small cell lung cancer xenografts. Here, in the context of T-ALL, we only observed a partial reduction of the leukemic burden *in vivo*. Therefore, T-ALL cell lines might need higher dosing or combinations with other chemotherapeutic agents (e.g. ATRA or HDAC inhibitors), as reported for other tumor entities[43-45]. The differences observed between the therapeutic efficacy of KDM1A inhibition *in vitro* and *in vivo*, suggests that paracrine factors might regulate compensatory pathways that prevent cell death upon KDM1A inhibition *in vivo*. Here, we demonstrate that exogenous IL7 can decrease the sensitivity to KDM1A inhibition in *Zeb2* transgenic T-ALL cells. In line with this finding, human LOUCY T-ALL cells showed a similar up regulation of *IL7R* expression following KDM1A inhibition. Therefore, combination therapies inhibiting both KDM1A and the IL7R/JAK-STAT signalling pathway, e.g. using the JAK inhibitor Ruxolitinib, or inhibitors of the downstream effector BCL2, like ABT-199, may *in vivo* be more effective as compared to KDM1A monotherapy.

It remains to be determined whether or not the KDM1A interaction is also important for the phenotypes observed upon ZEB2 loss in adult hematopoietic stem cells. These include multilineage differentiation blocks with skewing to the granulocyte lineage, and a myeloproliferative disorder-like phenotype with perturbed cytokine receptor signaling pathways[8]. Similarly, it is not yet known whether this interaction is essential for other recently demonstrated roles of ZEB2 in cytotoxic T-cell differentiation[46, 47], NK terminal maturation[48], dendritic cell differentiation[49], as well as in other non-hematopoietic cell lineages such as melanocytes[50], neurons and oligodendroglial cell fate and migration where Zeb2 has been previously demonstrated to play important roles[51-53].

To conclude, we have identified a novel ZEB2-KDM1A interaction in the context of T-ALL, which is essential for the survival of *ZEB2* overexpressing cells. Also in human T-ALL cell lines we see increased KDM1A inhibitor sensitivity upon enforced ZEB2 expression, suggesting a putative novel therapeutic tool for the treatment of ZEB2-driven tumors.

Acknowledgments

We thank Raymond Poot and Danny Huylebroeck for their advice on protein complex pull down experiment and Trevor Wilson for his help with RNAseq. The authors would also like to thank Béatrice Lintermans and Lindy Reunes for excellent technical assistance. This work was supported by the Fund for Scientific Research – Flanders (FWO-V; G056813N to JJH, KaN 1500416N to SG, GA00113N, 3G065614, G0C4713N and 31500615W to PVV, G052912N and G081713N to GB), the Belgian Federation for the Study Against Cancer (BFAC, grant 365W3415W to PVV, B/13590 to GB), Belgian Stand Up To Cancer Foundation (grant 365Y9115W to PVV), Worldwide Cancer Research (grant 16-1157 to PVV, SG and JJH), the Swiss Bridge Award (to PVV and SG) and the Australian NH&MRC grants 1047995, 1104441 (JJH) and was part of the DevRepair (P7/07) IAP-VII network (SG, JJH). SG is postdoctoral fellow and SP is a PhD student supported by the FWO-V. NV and SP are PhD students funded by the Belgian Stand Up To Cancer Foundation (grant 365Z1215W and Emmanuel van der Schueren grant). The computational resources (Stevin Supercomputer Infrastructure) and services used in this work were provided by the VSC (Flemish Supercomputer Center), funded by Ghent University, the Hercules Foundation and the Flemish Government department EWI.

Authorship Contributions

S.G., S.P., P.V.V. and J.J.H. designed the studies. S.G., S.P., K.H., T.N., S.S., M.C., C.C., J.W., M.T., F.M. performed the experiments. S.G., S.P., W.V.L, O.K., P.V.V. and J.J.H. analyzed the data. D.D. and F.V.N performed RNA sequencing. N.V., O.K., D.C, G.B., P.V.V. and J.J.H., contributed reagents/materials/analysis tools. S.G., P.V.V and J.J.H. wrote the manuscript with help from the other authors.

Conflicts of Interest disclosures

The authors declare no competing financial interests.

References

1. Gheldof, A., et al., *Evolutionary functional analysis and molecular regulation of the ZEB transcription factors.* Cell Mol Life Sci, 2012. **69**(15): p. 2527-41.
2. De Craene, B. and G. Berx, *Regulatory networks defining EMT during cancer initiation and progression.* Nature Reviews Cancer, 2013. **13**(2): p. 97-110.
3. Mani, S.A., et al., *The epithelial-mesenchymal transition generates cells with properties of stem cells.* Cell, 2008. **133**(4): p. 704-715.
4. Brabletz, S. and T. Brabletz, *The ZEB/miR-200 feedback loop--a motor of cellular plasticity in development and cancer?* EMBO Rep, 2010. **11**(9): p. 670-7.
5. Goossens, S., et al., *ZEB2 drives immature T-cell lymphoblastic leukaemia development via enhanced tumour-initiating potential and IL-7 receptor signalling.* Nat Commun, 2015. **6**: p. 5794.

6. Marcucci, F., G. Stassi, and R. De Maria, *Epithelial-mesenchymal transition: a new target in anticancer drug discovery.* Nat Rev Drug Discov, 2016. **15**(5): p. 311-25.
7. Goossens, S., et al., *The EMT regulator Zeb2/Sip1 is essential for murine embryonic hematopoietic stem/progenitor cell differentiation and mobilization.* Blood, 2011. **117**(21): p. 5620-30.
8. Li, J., et al., *The EMT transcription factor Zeb2 controls adult murine hematopoietic differentiation by regulating cytokine signaling.* Blood, 2016.
9. Coustan-Smith, E., et al., *Early T-cell precursor leukaemia: a subtype of very high-risk acute lymphoblastic leukaemia.* Lancet Oncology, 2009. **10**(2): p. 147-156.
10. Comijn, J., et al., *The two-handed E box binding zinc finger protein SIP1 downregulates E-cadherin and induces invasion.* Molecular Cell, 2001. **7**(6): p. 1267-1278.
11. Postigo, A.A. and D.C. Dean, *Independent repressor domains in ZEB regulate muscle and T-cell differentiation.* Molecular and Cellular Biology, 1999. **19**(12): p. 7961-7971.
12. Mayle, A., et al., *Dnmt3a loss predisposes murine hematopoietic stem cells to malignant transformation.* Blood, 2015. **125**(4): p. 629-638.
13. Rasmussen, K.D., et al., *Loss of TET2 in hematopoietic cells leads to DNA hypermethylation of active enhancers and induction of leukemogenesis.* Genes & Development, 2015. **29**(9): p. 910-922.
14. Corces-Zimmerman, M.R., et al., *Preleukemic mutations in human acute myeloid leukemia affect epigenetic regulators and persist in remission.* Proceedings of the National Academy of Sciences of the United States of America, 2014. **111**(7): p. 2548-2553.
15. Adamo, A., et al., *LSD1 regulates the balance between self-renewal and differentiation in human embryonic stem cells.* Nature Cell Biology, 2011. **13**(6): p. 652-U265.
16. Wang, J., et al., *Novel Histone Demethylase LSD1 Inhibitors Selectively Target Cancer Cells with Pluripotent Stem Cell Properties.* Cancer Research, 2011. **71**(23): p. 7238-7249.
17. Mohammad, H.P., et al., *A DNA Hypomethylation Signature Predicts Antitumor Activity of LSD1 inhibitors in SCLC.* Cancer Cell, 2015. **28**(1): p. 57-69.
18. Kerenyi, M.A., et al., *Histone demethylase Lsd1 represses hematopoietic stem and progenitor cell signatures during blood cell maturation.* Elife, 2013. **2**.
19. Wada, T., et al., *Overexpression of the shortest isoform of histone demethylase LSD1 primes hematopoietic stem cells for malignant transformation.* Blood, 2015. **125**(24): p. 3731-3746.
20. Dignam, J.D., R.M. Lebovitz, and R.G. Roeder, *Accurate Transcription Initiation by Rna Polymerase-Ii in a Soluble Extract from Isolated Mammalian Nuclei.* Nucleic Acids Research, 1983. **11**(5): p. 1475-1489.
21. Alonso, H., et al., *Structural and mechanistic insight into alkane hydroxylation by Pseudomonas putida AlkB.* Biochemical Journal, 2014. **460**: p. 283-293.
22. Cox, J. and M. Mann, *MaxQuant enables high peptide identification rates, individualized p.p.b.-range mass accuracies and proteome-wide protein quantification.* Nature Biotechnology, 2008. **26**(12): p. 1367-1372.
23. Hubner, N.C. and M. Mann, *Extracting gene function from protein-protein interactions using Quantitative BAC InteraCtomics (QUBIC).* Methods, 2011. **53**(4): p. 453-459.

24. Grooteclaes, M.L. and S.M. Frisch, *Evidence for a function of CtBP in epithelial gene regulation and anoikis.* Oncogene, 2000. **19**(33): p. 3823-3828.
25. Verstappen, G., et al., *Atypical Mowat-Wilson patient confirms the importance of the novel association between ZFHX1B/SIP1 and NuRD corepressor complex.* Human Molecular Genetics, 2008. **17**(8): p. 1175-1183.
26. Wang, Y., et al., *LSD1 Is a Subunit of the NuRD Complex and Targets the Metastasis Programs in Breast Cancer.* Cell, 2009. **138**(4): p. 660-672.
27. Stryjewska, A., et al., *Zeb2 Regulates Cell Fate at the Exit from Epiblast State in Mouse Embryonic Stem Cells.* Stem Cells, 2016.
28. Harris, W.J., et al., *The histone demethylase KDM1A sustains the oncogenic potential of MLL-AF9 leukemia stem cells.* Cancer Cell, 2012. **21**(4): p. 473-87.
29. Li, H., et al., *The EMT regulator ZEB2 is a novel dependency of human and murine acute myeloid leukemia.* Blood, 2016.
30. Wang, J.X., et al., *Opposing LSD1 complexes function in developmental gene activation and repression programmes.* Nature, 2007. **446**(7138): p. 882-887.
31. McGrath, J.P., et al., *Pharmacological Inhibition of the Histone Lysine Demethylase KDM1A Suppresses the Growth of Multiple Acute Myeloid Leukemia Subtypes.* Cancer Research, 2016. **76**(7): p. 1975-1988.
32. Schenk, T., et al., *Inhibition of the LSD1 (KDM1A) demethylase reactivates the all-trans-retinoic acid differentiation pathway in acute myeloid leukemia.* Nat Med, 2012. **18**(4): p. 605-11.
33. Van Vlierberghe, P. and A. Ferrando, *The molecular basis of T cell acute lymphoblastic leukemia.* J Clin Invest, 2012. **122**(10): p. 3398-406.
34. Durinck, K., et al., *Novel biological insights in T-cell acute lymphoblastic leukemia.* Exp Hematol, 2015. **43**(8): p. 625-39.
35. Zhang, J.H., et al., *The genetic basis of early T-cell precursor acute lymphoblastic leukaemia.* Nature, 2012. **481**(7380): p. 157-163.
36. Brandimarte, L., et al., *New MLLT10 gene recombinations in pediatric T-acute lymphoblastic leukemia.* Blood, 2013. **121**(25): p. 5064-5067.
37. Williams, S.E., et al., *Asymmetric cell divisions promote Notch-dependent epidermal differentiation.* Nature, 2011. **470**(7334): p. 353-358.
38. van Grunsven, L.A., et al., *Interaction between Smad-interacting protein-1 and the corepressor C-terminal binding protein is dispensable for transcriptional repression of E-cadherin.* J Biol Chem, 2003. **278**(28): p. 26135-45.
39. Si, W.Z., et al., *Dysfunction of the Reciprocal Feedback Loop between GATA3-and ZEB2-Nucleated Repression Programs Contributes to Breast Cancer Metastasis.* Cancer Cell, 2015. **27**(6): p. 822-836.
40. Lin, T., et al., *Requirement of the histone demethylase LSD1 in Snail-mediated transcriptional repression during epithelial-mesenchymal transition.* Oncogene, 2010. **29**(35): p. 4896-4904.
41. Lin, Y.W., et al., *The SNAG domain of Snail1 functions as a molecular hook for recruiting lysine-specific demethylase 1.* Embo Journal, 2010. **29**(11): p. 1803-1816.
42. Saleque, S., et al., *Epigenetic regulation of hematopoietic differentiation by Gfi-1 and Gfi-1b is mediated by the cofactors CoREST and LSD1.* Molecular Cell, 2007. **27**(4): p. 562-572.
43. Ramirez, L., M. Singh, and J. Chandra, *HDAC and LSD1 Inhibitors Synergize to Induce Cell Death in Acute Leukemia Cells.* Blood, 2011. **118**(21): p. 620-620.

44. Singh, M.M., et al., *Inhibition of LSD1 sensitizes glioblastoma cells to histone deacetylase inhibitors.* Neuro-Oncology, 2011. **13**(8): p. 894-903.
45. Fiskus, W., et al., *Highly effective combination of LSD1 (KDM1A) antagonist and pan-histone deacetylase inhibitor against human AML cells.* Leukemia, 2014. **28**(11): p. 2155-64.
46. Omilusik, K.D., et al., *Transcriptional repressor ZEB2 promotes terminal differentiation of CD8(+) effector and memory T cell populations during infection.* Journal of Experimental Medicine, 2015. **212**(12): p. 2027-2039.
47. Dominguez, C.X., et al., *The transcription factors ZEB2 and T-bet cooperate to program cytotoxic T cell terminal differentiation in response to LCMV viral infection.* Journal of Experimental Medicine, 2015. **212**(12): p. 2041-2056.
48. van Helden, M.J., et al., *Terminal NK cell maturation is controlled by concerted actions of T-bet and Zeb2 and is essential for melanoma rejection.* Journal of Experimental Medicine, 2015. **212**(12): p. 2015-2025.
49. Scott, C.L., et al., *The transcription factor Zeb2 regulates development of conventional and plasmacytoid DCs by repressing Id2.* J Exp Med, 2016. **213**(6): p. 897-911.
50. Denecker, G., et al., *Identification of a ZEB2-MITF-ZEB1 transcriptional network that controls melanogenesis and melanoma progression.* Cell Death and Differentiation, 2014. **21**(8): p. 1250-1261.
51. Seuntjens, E., et al., *Sip1 regulates sequential fate decisions by feedback signaling from postmitotic neurons to progenitors.* Nature Neuroscience, 2009. **12**(11): p. 1373-1380.
52. van den Berghe, V., et al., *Directed Migration of Cortical Interneurons Depends on the Cell-Autonomous Action of Sip1.* Neuron, 2013. **77**(1): p. 70-82.
53. Weng, Q.J., et al., *Dual-Mode Modulation of Smad Signaling by Smad-Interacting Protein Sip1 Is Required for Myelination in the Central Nervous System (vol 73, pg 713, 2012).* Neuron, 2012. **76**(2): p. 462-462.

Supplementary Figures

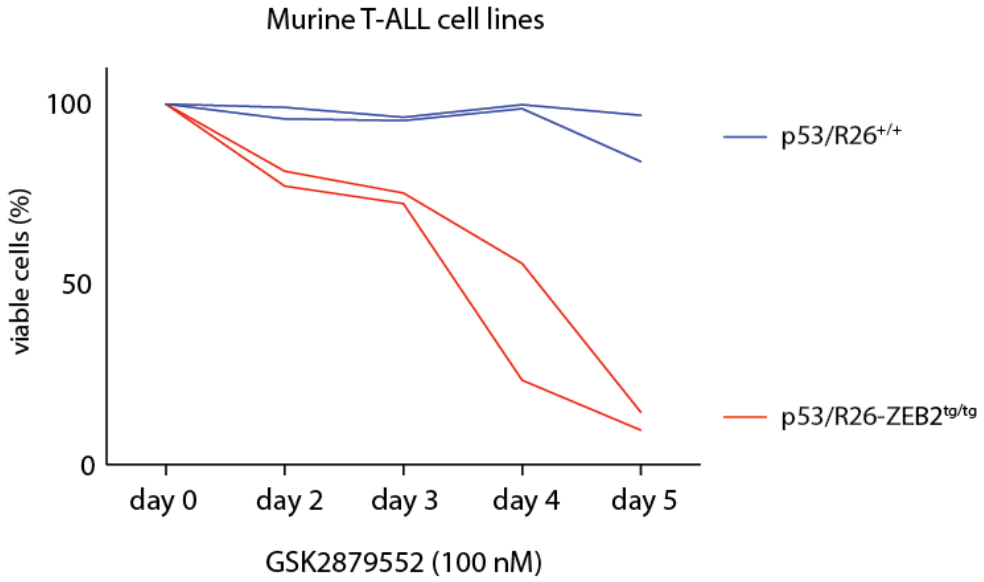

Supplementary Figure 1. *Sensitivity of two P53/R26-Zeb2$^{tg/tg}$ Zeb2 overexpressing mouse T-ALL cell lines compared to two control P53/R26$^{+/+}$ cell lines treated with 100nM GSK2879552 over a time period of 5 days. The CellTiter-Glo Luminescent Cell Viability Assay was used.*

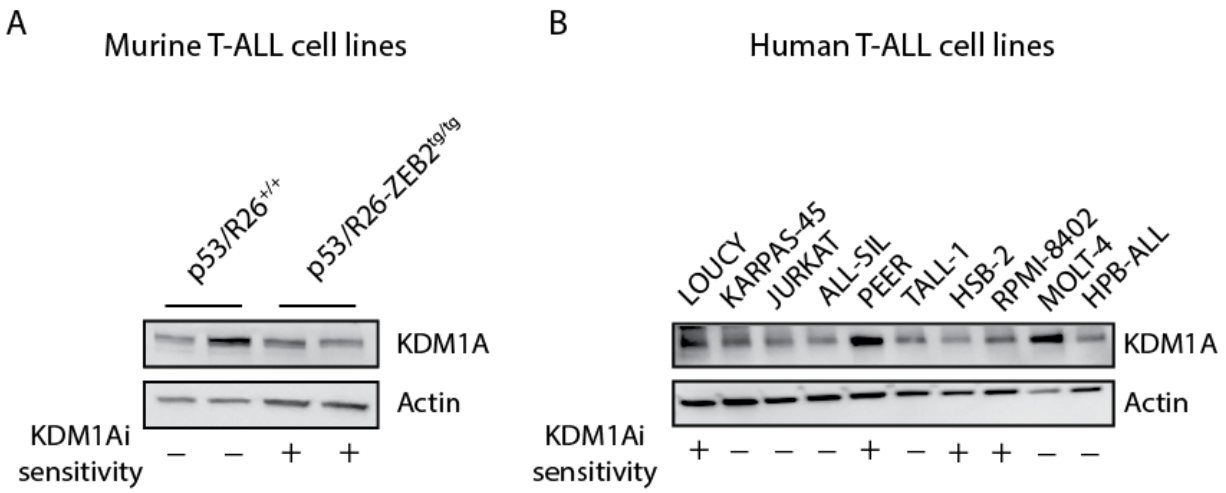

Supplementary Figure 2*. KDM1A protein levels in GSK2879552 sensitive and insensitive mouse and human T-ALL cell lines.*

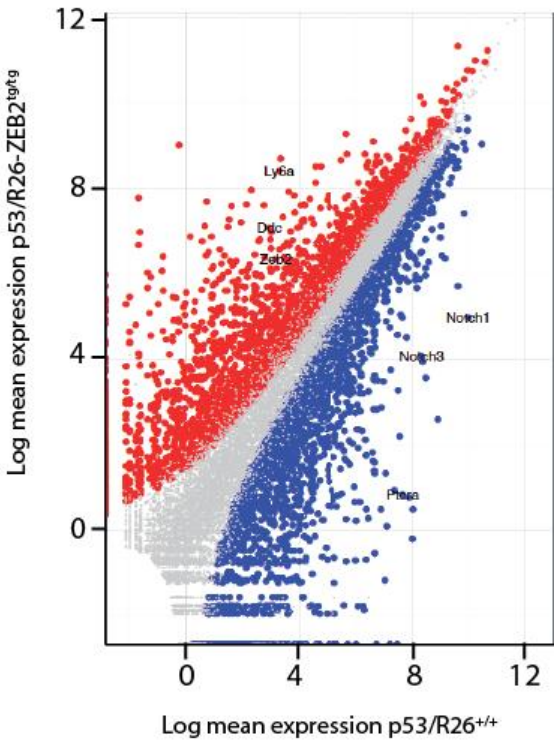

Supplementary Figure 3. *Differential gene expression pattern in P53/R26-Zeb2$^{tg/tg}$ versus control P53/R26$^{+/+}$ mouse T-ALL cell lines (adjusted P-value < 0.05, triplicates).*

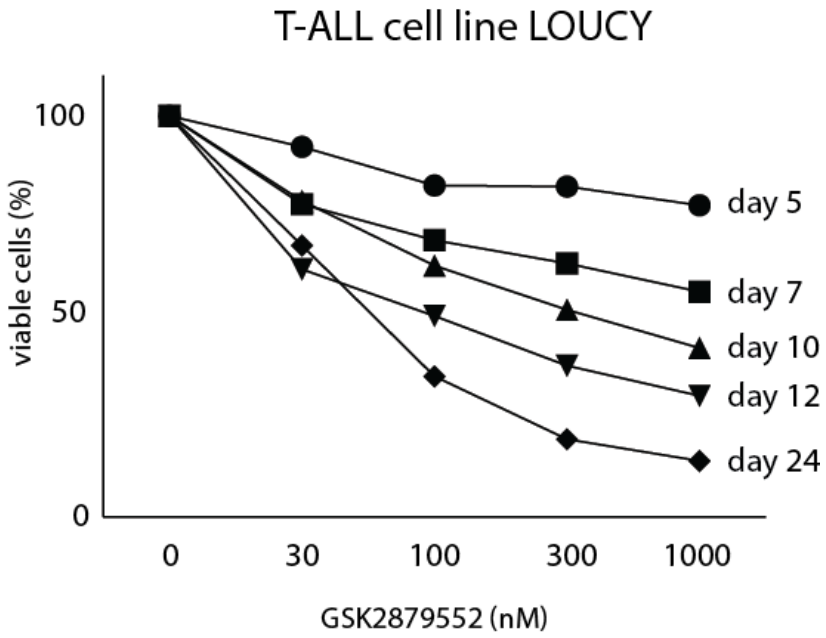

Supplementary Figure 4*. Sensitivity of human T-ALL cell line LOUCY treated with increasing concentrations of GSK2879552 over a time period of 24 days. The CellTiter-Glo Luminescent Cell Viability Assay was used.*

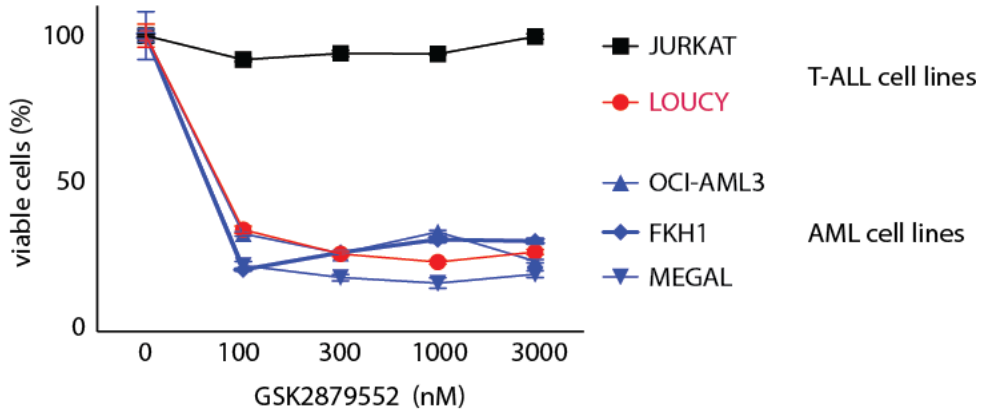

Supplementary Figure 5. *Sensitivity of human T-ALL cell line (LOUCY and JURKAT) compared to the human AML cell lines (MEGAL, FKH1 and OCI-AML3) treated with increasing concentrations of GSK2879552 for 12 days. The CellTiter-Glo Luminescent Cell Viability Assay was used.*

A

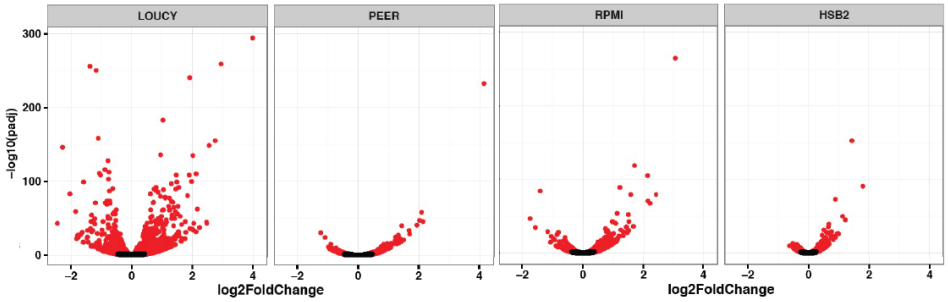

B

Common genes up after KDM1A inhibition human T-ALL cell lines		Common genes down after KDM1A inhibition human T-ALL cell lines
ADD3	LPAR6	GLUL
AIM1	NBPF9	PCDH9
ARHGEF11	NFKB1	
CALHM2	NKG7	
CAMSAP2	PI16	
CARD11	PIK3C2B	
CD44	PKM	
CEP112	PLEC	
CFH	RCBTB2	
CHRNA9	S1PR1	
CTNNA1	SAT2	
EMP3	SERPINB8	
GBP1	SH3BP5	
GLG1	SLC2A3	
GZMA	TIAM1	
ID3	TMEM243	
KCTD1	TMSB10	
KLF2	VIM	
	WFS1	
	YPEL1	

Supplementary Figure 6*. RNA sequencing results of human T-ALL cell lines (LOUCY, PEER, RPMI8402 and HSB2) after KDM1A inhibition (100nM, 48h). (A) Differential expression analysis represented by Volcano plots (B) List of common genes differentially expressed after KDM1A inhibition in all 4 human T-ALL cell lines.*

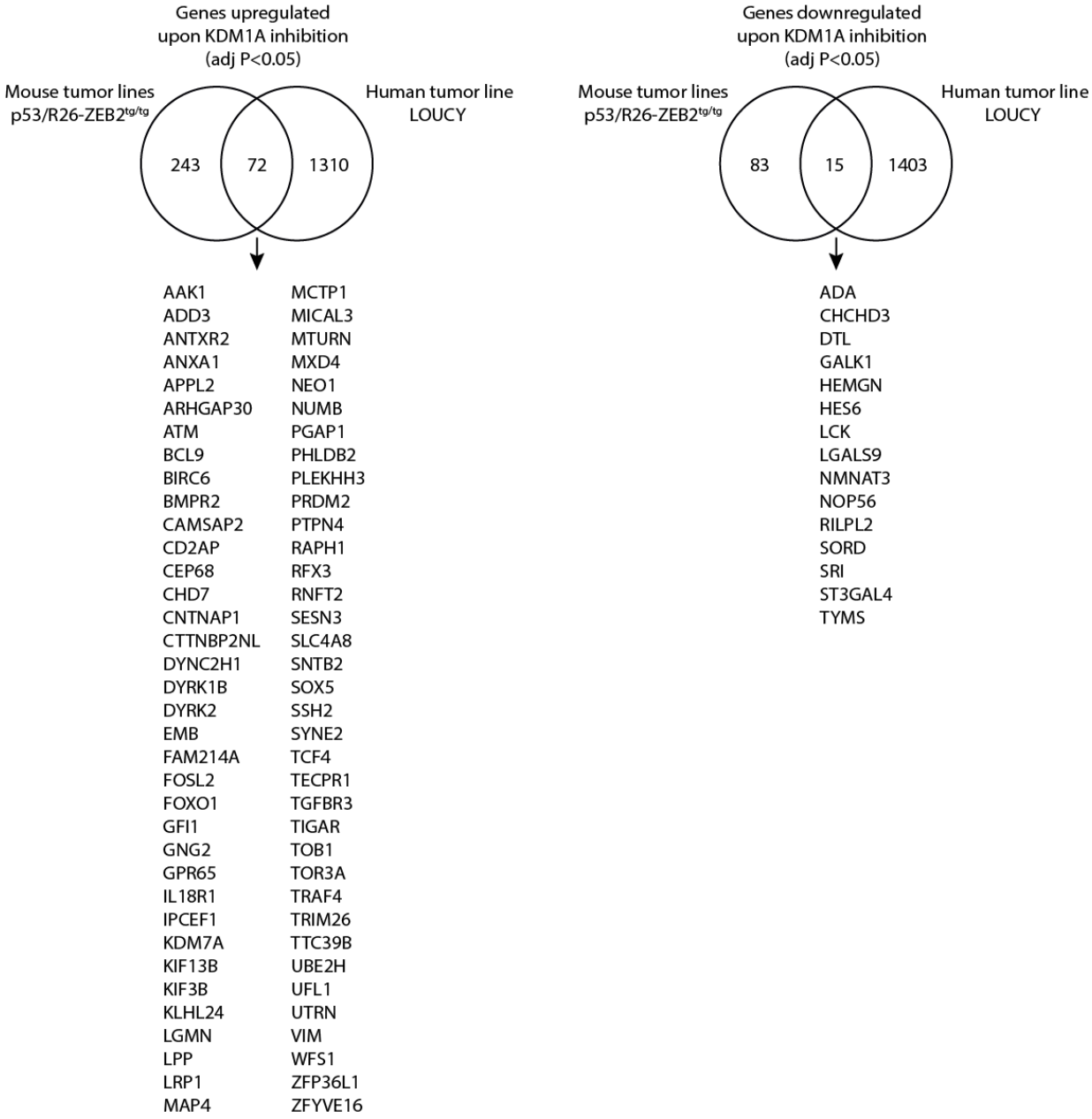

Supplementary Figure 7. *Venn diagram indicating overlap between genes affected in the human T-ALL cell lines LOUCY and mouse T-ALL cell lines upon short-term KDM1A inhibition. Left, upregulated gene signature. Right, downregulated gene signature.*

Supplementary Tables

The Supplementary Tables can be consulted on the Leukemia website in the online version of the paper.

***Supplementary Table 1**. Differential gene expression analysis between P53/R26$^{+/+}$ and P53/R26-ZEB2$^{tg/tg}$ tumor lines.*

***Supplementary Table 2.** KEGG pathway analyses based on genes up- and downregulated in P53/R26-ZEB2$^{tg/tg}$ tumor lines.*

***Supplementary Table 3**. Differential gene expression analysis based on RNA sequencing of P53/R26-ZEB2$^{tg/tg}$ tumor lines upon KDM1A inhibition*

***Supplementary Table 4**. Differential gene expression analysis based on RNA sequencing of the human T-ALL cell lines LOUCY, PEER, RPMI8402 and HSB2 upon KDM1A inhibition*

Supplementary Materials and Methods

Pull downs, Mass Spectrometry

1.5 X 10^8 mouse T-ALL cells were washed once with phosphate-buffered saline and nuclear extracts were prepared using a high salt lysis buffer and douncer and subsequently dialyzed for 2 times 2 hours at 4°C with 100 mM KCl using a Slide-A-Lyzer dialysis cassette (Thermo Scientific). Finally, nuclear extracts were transferred to non-stick Eppendorf tubes (Alpha Laboratories) and cleared by centrifugation for 15 min, 13000rpm, at 4°C. A total of 60 µl of anti-FLAG M2 agarose beads (Sigma), washed and equilibrated in buffer C-100 (20 mM HEPES, pH 7.6, 10% glycerol, 100 mM KCl, 1.5 mM $MgCl_2$, 0.2 mM EDTA, 1× complete EDTA-free protease inhibitor; Roche), was added to 1.5 ml of nuclear extract supplemented with 150U/ml Benzonase (Novagen) and incubated overnight at 4°C, rotating. Next day, beads were washed five times with 1 ml of C-100 buffer plus 0.02% NP-40 (C-100*) and eluted four times with C-100* containing 0.6 mg/ml FLAG tripeptide (Sigma) for 15 min at room temperature. Fractions were loaded onto a 10% Mini-Protean TGX precast gel (BioRad) and silver stained (Silverquest, Thermo Fisher Scientific). Western blot analysis confirmed that the most prominent band on silverstained gels is detected by anti-FLAG (Sigma) and anti-ZEB2 specific antibodies (Sigma). Elutions 1 and 2, containing the majority of FLAG-ZEB2 were loaded onto a 10% SDS-PAA gel (Thermo Scientific), the resulting proteins were separated by limited SDS-PAGE (5 minutes gel migration). For each sample the entire lane was excised and subjected to in-gel tryptic digestion and Liquid chromatography tandem mass spectrometry (LC-MS/MS) analysis as previously described[1]. Mass spectrometry raw data was processed and searched by MaxQuant software (version 1.5.2.8)[2]. Database searching was done against Mouse protein sequences downloaded from Uniprot (03/2015 release) using MaxQaunt default settings. Significance of specific protein–protein interactions was performed using Perseus analysis software as described in Hubner and Mann, 2011[3].

Co-immunoprecipitations and Western blotting

Nuclear extracts were prepared as above. For FLAG-ZEB2 pull downs, anti-FLAG M2

agarose beads were used. For KDM1A pull downs, the rabbit polyclonal anti-KDM1A/LSD1 antibody in combination with the Rabbit TrueBlot IP-set with beads (Rockland) was used according to manufacturer's instructions. After 5 times washing and elution from the beads by denaturation, proteins were loaded on a 10% SDS-PAA gel (Thermo Scientific), followed by blotting on a PVDF membrane (Millipore). Non-fat milk was used as blocking before immunodetection. Primary antibodies used for detection: rabbit polyclonal anti-KDM1A/LSD1 (1:1000; abcam), rabbit polyclonal anti-ZEB2 (1:1000, Sigma), rabbit polyclonal anti-SIP1 (1:1000, Bethyl Laboratories), mouse monoclonal anti-FLAG M2 (1:500, Sigma). Secondary antibodies: HRP-conjugated TrueBlot anti-rabbit IgG (1:10000; Rockland) and HRP-conjugated rabbit anti-mouse (1:10000; Merck). Detection was performed using Western Lightning ECL Substrate (Perkin Elmer). Images have been cropped for presentation.

Cell culture

The human T-ALL cell lines were purchased from the DSMZ repository (Braunschweig, Germany) and cultured in RPMI 1640 medium supplemented with 10% or 20% fetal bovine serum (FBS), 100 U/ml penicillin, 100 µg/ml streptomycin, 100 µg/ml kanamycin sulfate and 2 mM L-glutamine at 37°C with 5% CO2. The mouse T-ALL cell lines were isolated and cultured as described before[4] in RPMI 1640 medium supplemented with 15% heat-inactivated FBS, 100 U/ml penicillin, 100 µg/ml streptomycin, 2 mM L-glutamine and 5 ng/ml recombinant IL-7 (Peprotech) at 37°C with 5% CO2, 95% humidity. The commercially available KDM1A inhibitor GSK2879552 (ActiveBiochem) was dissolved in DMSO at a concentration of 10 mg/ml and diluted further in medium as indicated.

Histone extractions

For each histone preparation, $5x10^6$ cells were harvested by centrifugation (1500 rpm, 4°C, 5 min) and washed twice with ice cold PBS supplemented with 5mM Sodium Butyrate (NaB). Cell pellets were dissolved in 500µl TEB buffer (PBS supplemented with 5mM NaB, 0.5%Triton X-100 and Halt Protease/Phosphatase inhibitor cocktails) and incubated for 10 min on ice for nuclear extraction. Nuclei were collected via centrifugation (2000 rpm, 4°C, 10 min) and washed once in 250µl TEB buffer. Nuclear pellets were resuspended in 25µl of freshly prepared 0.4M HCl and incubated 1 hour at 4^oC. Histone preps were centrifuged (11000 rpm, 4°C, 10 min), supernatant transferred to new tube and neutralized by adding 10 µl neutralizing buffer (0.5M Sodium phosphate dibasic, pH 12.5 NaOH supplemented with 5nM NaB and Halt Protease/Phosphatase inhibitor cocktails). Protein concentration were measured using Bradford assay before further analysis using Western blotting according to standard protocols and as described above, using the following primary antibodies: total Histone 3 (1:1000, mouse mAb clone 1B1-B2, Active motif), H3K4me1 (1:1000, mouse mAb clone MABI0302, Active motif), H3K4me2 (1:1000, mouse mAb clone MABI0303, Active motif), H3K9me2(1:2000, rabbit pAb, Active motif).

Generation of ZEB2 overexpressing KARPAS-45 cells

The ZEB2 open reading frame (ORF) was shuttled using standard Gateway cloning (Life Technologies) from a pDONR207 entry clone into the doxycyclin-inducible lentiviral vector pSIN-TRE-GW-3xHA[5], kindly provided by Prof. dr. Bart Deplancke. Virus production was performed in HEK293TN cells using JetPEI polyplus with pMD2.G (envelope plasmid), psPAX2 (packaging plasmid) and pSIN-TRE-GW-3xHA hZEB2 (target plasmid) in 0.1/0.9/1 ratios. Transduced KARPAS-45 cells were selected by puromycin selection (1µ/ml). Cells were cultured in medium with 20% tetracycline-free FCS. 48h before the start of the KDM1A

inhibition experiment, doxycyclin (1µg/ml) was added to induce ZEB2 expression. Every two or three days, the doxycylin was refreshed.

qRT-PCR

The miRNeasy mini kit (Qiagen) and the RNAse-Free Dnase set (Qiagen) were used to isolate RNA. cDNA synthesis was performed with the iScript Advanced cDNA synthesis kit (Bio-Rad). The SsoAdvanced Universal SYBR Green Supermix (Bio-Rad) was used for the PCR reactions while amplification and detection was done with the LightCycler 480 instrument (Roche, model LC480). Every sample was analyzed in duplicate and the gene expression was normalized against 3 reference genes (B2M, HPRT1, YWHAZ or TBP). ZEB2 primers: (F) 5' ATCAGATGAGCTTCCTACCA 3', (R) 5' GCAATTCTCCCTGAAATCCT 3'; ITGAM (CD11B) primers: (F) 5'- GTGAAGCCAATAACGCAGC-3', (R) 5'-TCTCCATCCGTGATGACAAC-3'; B2M primers: (F) 5' TGCTGTCTCCATGTTTGATGTATCT 3', (R) 5' TCTCTGCTCCCCACCTCTAAGT 3'; HPRT1 primers: (F) 5' TGACACTGGCAAAACAATGCA 3', (R) 5' GGTCCTTTTCACCAGCAAGCT 3'; YWHAZ primers: (F) 5' ACTTTTGGTACATTGTGGCTTCAA 3', (R) 5' CCGCCAGGACAAACCAGTAT 3'; TBP primers: (F) 5'-CACGAACCACGGCACTGATT-3', (R) 5'-TTTTCTTGCTGCCAGTCTGGAC-3'

Xenotransplantations

All animal experimentation was performed according to the regulations and guidelines of the Ethics Committee for care and use of laboratory animals of Monash University and Ghent University. The two *P53/R26-ZEB2^{tg}* mouse T-ALL cell lines were intravenously injected in 6-8 weeks old NOD scid gamma (NSG) mice. 2 X 10^6 cells in 150µl PBS were injected in 10 recipient mice for each of the cell lines. The day after injection the mice were divided into two groups and the treatment was started with 1.5mg GSK2879552/kg body weight or with vehicle via oral gavage for 5 consecutive days. Mice were monitored for illness, leukemia development. NSG mice were injected at 6 weeks of age in the tail vein with 150µl PBS containing 5 X 10^6 LOUCY or PEER cells. At 3 (PEER) and 4 (LOUCY) weeks, the cells were engrafted and the mice were randomly divided into two groups and the treatment was started (day 0). Mice were treated with 1.5 mg GSK2879552/kg body weight or with vehicle via oral gavage for 17 consecutive days. Mice were daily weighted and monitored. The percentage of leukemic cells in the blood was analyzed by staining the cells with an PE-labeled antibody (Miltenyi Biotec) for human CD45 (hCD45), performing red blood cell lysis and measuring the percentage with S3e cell sorter (Bio-Rad). At the end of the experiment, all mice were sacrificed and spleens were collected.

RNA sequencing

Murine tumor cells were counted and seeded at a concentration of 5x10^5 cells/ml and half of the culture was treated with 200 nM of GSK2879552. 24 hours later cells were collected by centrifugation, lysed and RNA was prepared using RNeasy mini Plus kit (Qiagen) with an extra step for gDNA eliminitation. For human cell lines, total RNA was extracted from LOUCY and PEER cells treated with GSK2879552 and DMSO vehicle control using the miRNeasy mini kit (Qiagen) according to the manufacturer's instructions. The RNA quality was evaluated using a RNA Nano chip on a Bioanalyzer (Agilent technologies). Library preparation for human and murine tumor samples was performed using the Illumina TruSeq RNA sample Prep Kit (San Diego, CA, USA) according to the manufacturer's protocol. Library quality was checked using a DNA-1000 chip on a Bioanalyzer (Agilent technologies)

and enriched cDNA libraries were sequenced using an Illumina NextSeq 500 sequencer instrument. RNA sequencing data have been deposited to the GEO repository (GSE8312). Reads were aligned to mm38 reference genome using STAR2.4.2a. Genes were quantified on Ensembl38 GTF. DESeq2 was used to assess differential expression between various groups using a multifactorial design with 2 conditions and 2 genotypes including the interaction term. Functional annotation of differentially expressed genes was performed by DAVID gene ontology analysis using standard settings. Pathway analysis was performed by Reactome and KEGG using standard settings. Finally, pre-ranked GSEA was performed with the c2 MSigDB gene sets collection using the GSEA desktop application (Broad Institute, version v2.2.0). The analysis was run with the default parameters (1000 permutations) and classic enrichment statistic. A ranked list of all the genes detected in our RNA-seq experiment was given as input. As ranking metric, the sign of the fold change multiplied by the inverse of the adjusted p-value was used.

1. Alonso H et al. Structural and mechanistic insights into alkane hydroxylation by Pseudomonas putida AlkB. Biochemical Journal. 2014;460(2):283-293.
2. Cox J and Mann M. MaxQuant enables high peptide identification rates, individualized p.p.b.-range mass accuracies and proteome-wide protein quantification. Nature Biotechnology. 2008;26(12):1367-1372.
3. Hubner NC and Mann M. Extracting gene function from protein-protein interactions using Quantitative BAC InteraCtomics (QUBIC). Methods. 2011;53(4):453-459.
4. Peirs S et al. ABT-199 mediated inhibition of BCL-2 as a novel therapeutic strategy in T-cell acute lymphoblastic leukemia. Blood. 2014;124(25):3738-47.
5. Gubelmann C et al. Identification of the transcription factor ZEB1 as a central component of the adipogenic gene regulatory network. Elife. 2014.

CHAPTER 4
Discussion and Future Perspectives

1. The BCL-2 inhibitor ABT-199 as monotherapy and part of combination therapies for the treatment of T-ALL

In our search for new therapies for the treatment of T-ALL, we noticed that the anti-apoptotic *BCL2* gene is overexpressed in early immature T-ALLs. Inhibition of the BCL-2 protein with the BH3 mimetic ABT-199 proved to be a promising therapeutic strategy in certain T-ALLs. Especially the human T-ALL cell line LOUCY and primary T-ALLs with a developmental arrest at the early stages of T-cell development, were highly sensitive to ABT-199 (**paper 1**). Around the same time, Ni Chonghaile et al.[1] performed BH3 profiling on a panel of human T-ALL cell lines and primary T-ALL samples and demonstrated a dependency on BCL-2 for ETP-ALLs while the more mature T-ALLs depended upon BCL-X_L for their survival. In line with this finding, they also tested the sensitivity to ABT-199 and identified LOUCY and ETP-ALL patient samples to be sensitive, thereby confirming our results. Altogether, this means that T-ALL can be added to the growing list of cancers that could benefit from treatment with ABT-199.

1.1. How to select T-ALL patients that may benefit from ABT-199 treatment

Given the fact that ABT-199 is in clinical trials for several malignancies and already FDA-approved to treat patients with CLL, conducting clinical trials with ABT-199 in T-ALL patients could be feasible in the near future. An important step in the design of such a trial will be the decision about the inclusion criteria. Similar to trials in other malignancies, including T-ALL patients that are refractory or relapsed following standard treatment could be a possibility. However, probably not all these patients will benefit from a treatment with ABT-199. Based on our study (**paper 1**) and the study of Ni Chonghaile et al.[1], one could predict that especially patients with early immature T-ALL will favorably respond to treatment with ABT-199 while patients with typical T-ALL would be better off with small molecules like navitoclax that also target BCL-X_L. Interestingly, some T-ALL patient samples that did not have a very immature immunophenotype were also sensitive to ABT-199 *in vitro*[1] (**paper 1**). As an example, an *MLL*-rearranged (MLLr) primary T-ALL sample showed high sensitivity to ABT-199 in our panel (**paper 1**). With regard to this, two studies[2, 3] recently demonstrated the potent *in vitro* and *in vivo* activity of ABT-199 in MLLr B-cell precursor ALL xenografts. In these MLLr ALLs, *BCL2* expression was shown to be upregulated via DOT1-like histone lysine methyltransferase (DOT1L)-mediated H3K79me2/3 at the *BCL2* locus[3]. In addition, Frismantas et al.[4] performed *ex vivo* drug response profiling of 24 T-ALL patient-derived xenografts and reported high sensitivity to ABT-199 for some cortical and mature T-ALLs. Moreover, the treatment of mice xenografted with a very sensitive cortical T-ALL patient sample resulted in a significant delay of leukemia progression[4]. Altogether, these studies show that response to ABT-199 is not limited to early immature T-ALL.

Having a biomarker that could predict whether a patient may benefit from treatment with ABT-199, would be of enormous value. Several studies, including ours (**paper 1**), found high BCL-2 levels as a potential predictive biomarker for ABT-199 sensitivity in a range of hematological malignancies[2, 5-7]. In contrast, high levels of the anti-apoptotic factors BCL-X_L and MCL-1 can be inversely associated with response to ABT-199[2, 5, 6, 8]. Intrinsic mechanisms of resistance to ABT-199 include the binding of released BIM to stabilized MCL-1 upon ABT-199 administration[9]. Moreover, high levels of phosphorylated BCL-2 can contribute to intrinsic resistance because phosphorylation alters the BH3-binding groove and

impedes ABT-199 binding[10]. These examples illustrate that quantifying individual BCL-2 family members or ratios of selected proteins might not be reliable enough as a clinical biomarker since they do not capture the complex interactions between BCL-2 family members and do not take posttranslational modifications into account[2, 6]. Instead, BH3 profiling could be used to predict ABT-199 response. Indeed, a strong correlation between mitochondrial BCL-2 dependence and ABT-199 sensitivity was observed in primary AML and T-ALL cells[1, 6]. On the other hand, the lack of dependence on BCL-X_L and MCL-1 was a predictor of sustained response to ABT-199 rather than the dependence on BCL-2 in a phase II clinical trial of ABT-199 in AML[11]. BH3 profiling is a rapid and simple method that can be carried out in a couple of hours[12]. Treating a primary sample *in vitro* with ABT-199 is another possibility to predict the ABT-199 sensitivity of a patient. A treatment period of 16 hours was used in our study (**paper 1**) but the fast killing of cells by ABT-199 allows the use of much shorter treatments (two to eight hours) to determine whether a sample is sensitive or not[1, 6].

1.2. Impact of ABT-199 on healthy blood cells

Drugs targeting specific molecular targets are often referred to as “targeted therapies” or “precision medicine”. However, this does not necessarily mean that these drugs will only affect the cancer cells and won’t cause any side effects by inhibiting their target in healthy cells. The main side effects of ABT-199 are neutropenia, nausea, vomiting, diarrhea, hypokalemia and upper respiratory tract infections[11, 13]. Khaw et al.[14] investigated the impact of ABT-199 on normal mature hematopoietic cell lineages and found that human peripheral blood B cells were highly sensitive compared to T cells and granulocytes. The normal B cells had even comparable *in vitro* sensitivities to ABT-199 as primary CLL patient cells[14]. Unlike Khaw et al.[14], the study of Leverson and colleagues[15] detected also an ABT-199-induced reduction in the granulocyte colony formation capacity of human bone marrow cells and a reduced amount of neutrophils in the blood of rats dosed with a selective BCL-2 inhibitor. This corresponds to the neutropenia observed in clinical trials with ABT-199. When ABT-199 sensitivities were studied in isolated murine T cell subsets, DN thymocytes were more susceptible to ABT-199 than DP thymocytes[14]. This is in line with our expression profiles of human thymus subsets in which we noticed high levels of *BCL2* in DN thymocytes and low levels in DP thymocytes (**paper 1**). Interestingly, ABT-199 did not affect $CD34^+$ stem/progenitor cells purified from bone marrow of healthy persons[16].

1.3. Acquired resistance to ABT-199 and how to overcome it

Over time, prolonged treatment with ABT-199 as single agent may result in the emergence of resistance. Indeed, although mice xenografted with the luciferase-positive LOUCY cells initially responded strongly to ABT-199 monotherapy, regrowth of the leukemia occurred already during the second week of treatment indicating the emergence of resistance (**paper 2**). Similarly, Bodo and colleagues[17] observed after 10 days of ABT-199 treatment a recovery of the tumors in a xenograft model of follicular lymphoma. By using resistant cell lines, generated by chronically exposing cells to increasing ABT-199 doses, several research groups studied the mechanisms of acquired resistance to ABT-199 in hematological malignancies. Common observations in cell lines with acquired ABT-199 resistance are reduced expression of the pro-apoptotic factor BIM and/or upregulation of the anti-apoptotic factors MCL-1 and BCL-X_L[17-21]. The increased levels of MCL-1 and BCL-X_L can sequester

the released BIM from BCL-2 upon ABT-199 treatment and therefore prevent apoptosis[19]. The importance of these factors in driving the acquisition of resistance was further demonstrated by the increase in sensitivity to ABT-199 after knockdown of MCL-1 or BCL-XL in resistant cell lines[19, 20]. Moreover, c-Jun N-terminal kinase 1 or 2 (JNK1/2), AKT and/or ERK1/2 can be activated in response to ABT-199 and contribute to the acquired resistance[17, 19]. As described in detail in the introduction of this PhD thesis, the PI3K/AKT/mTOR and RAF/RAS/MEK/ERK pathway can regulate pro- and anti-apoptotic factors. A schematic representation of how these pathways can contribute to the acquired resistance is given in Figure 1. Additionally, acquired selective mutations in BAX and BCL-2 have been described[18, 21]. The BAX mutation detected in an ABT-199-resistant human lymphoma cell line, was located in the transmembrane domain and hampered its anchoring in the mitochondrial membrane and subsequent induction of apoptosis upon ABT-199 treatment[18]. The BAX mutation in a resistant MM cell line resulted in a very short truncated protein[21]. Missense mutations identified in the BH3 domain of BCL-2 made binding of ABT-199 impossible in resistant mouse lymphoma cells[18].

Unfortunately, T-ALL cell lines were not included in the above-mentioned studies. To study the mechanisms of acquired resistance to ABT-199 in the context of T-ALL, our LOUCY xenograft model could be used. Following a two-week treatment with ABT-199, $hCD45^+$ leukemia cells could be isolated and compared to leukemia cells from vehicle-treated mice. Analyzing the mutation status and expression of BCL-2 family members and the activity of the PI3K/AKT/mTOR, IL7R/JAK/STAT and RAF/RAS/MEK/ERK pathway in these cells would provide valuable information. Furthermore, monitoring the acquisition of resistance to ABT-199 during clinical trials via BH3 profiling could be useful to decide when to pause or stop treatment with ABT-199.

Developing strategies to overcome or avoid the emergence of resistance to ABT-199 is very important. ABT-199 can be combined with inhibitors of proteins and pathways whose activation or upregulation is known to be involved in the acquisition of resistance. For example, the dual PI3K/mTOR inhibitor NVP-BEZ235 (dactolisib) is able to (re)sensitize B-cell lymphoma cell lines to ABT-199 treatment via downregulation of MCL-1[19]. Noteworthy, this inhibitor was also in our screen identified as a compound that could synergize with ABT-199 in some T-ALL patient samples (**paper 2**). Another possible strategy is to combine ABT-199 with a CDK inhibitor such as dinaciclib or flavopiridol. Members of the CDK family can regulate cell cycle progression (e.g. CDK1, CDK2 and CDK5) or transcription (e.g. CDK7, CDK8 and CDK9)[22]. Dinaciclib is a potent and selective inhibitor of CDK1, CDK2, CDK5 and CDK9. Since CDK9 phosphorylates RNA polymerase II to promote transcriptional elongation, its inhibition by dinaciclib results in transcriptional repression. Especially the downregulation of MCL-1 is known to be important for dinaciclib's antitumor effects[23, 24]. Furthermore, dinaciclib also affects the protein stability of MCL-1 by inhibiting cyclinE/CDK2-mediated phosphorylation of MCL-1[25]. As a logical consequence of this, dinaciclib synergizes with ABT-199 in DLBCL, a cancer in which BCL-2 and MCL-1 are frequently co-expressed[23, 25]. In T-ALL, a broad sensitivity to the CDK7 inhibitor THZ-1 was found[26]. As CDK7 phosphorylates RNA polymerase II to initiate transcription and activates CDK9 as well[27], this compound could be an alternative to use in combination with ABT-199. Moreover, in T-ALL cell lines treated with THZ1, the expression of the anti-apoptotic proteins MCL-1 and XIAP was reduced[26].

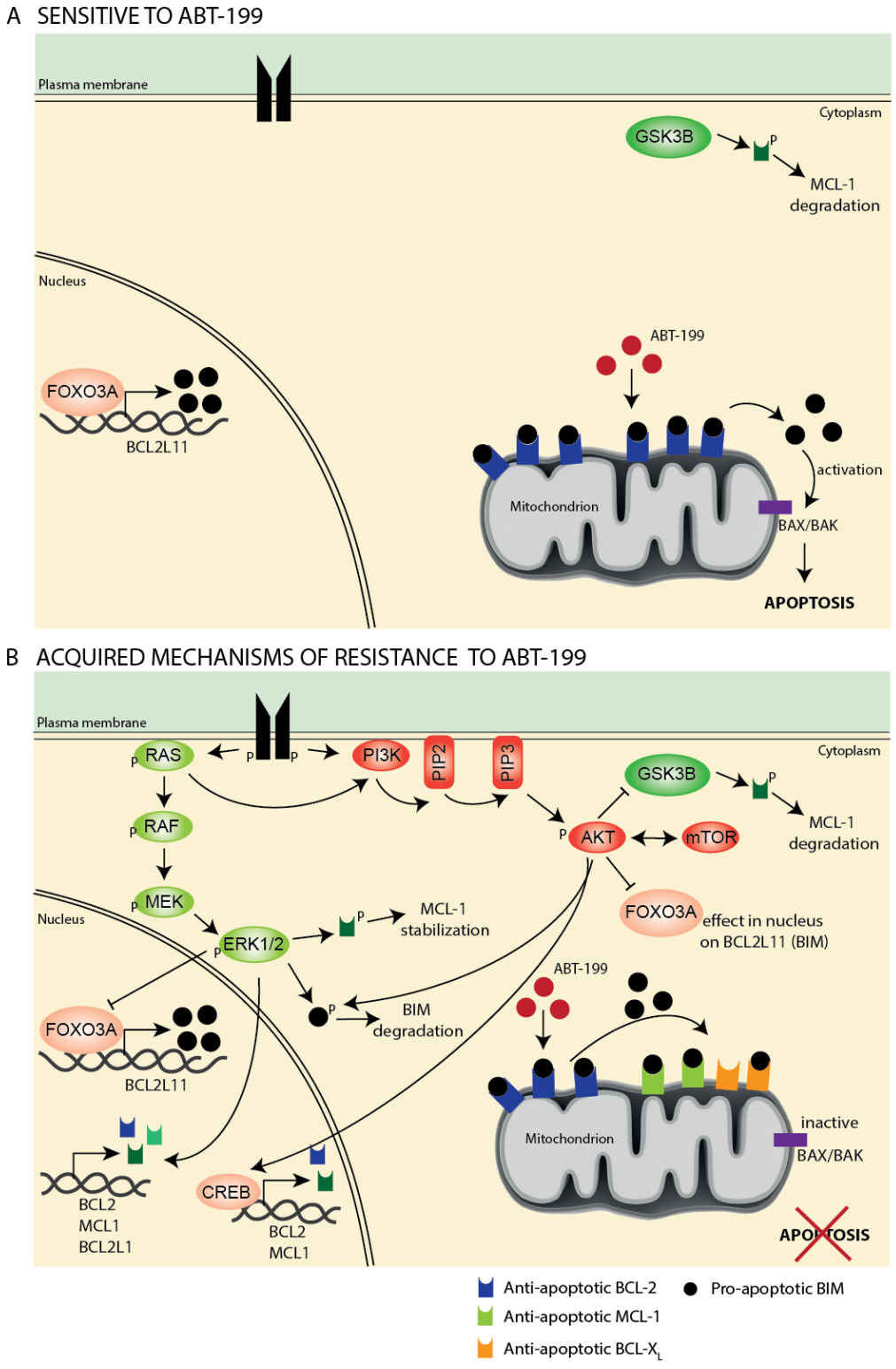

Figure 1. Schematic representation of how the activation of the PI3K/AKT/mTOR and RAF/RAS/MEK/ERK pathway can contribute to the acquisition of resistance to ABT-199. *(A) In cells that are sensitive to ABT-199 treatment, BCL-2 is highly occupied with BIM. ABT-199 competes for the BH3 binding site on BCL-2 which results in the release of BIM. Next, BAX/BAK is activated and apoptosis is induced. (B) Cells that are for a long time continuously exposed to ABT-199 can acquire resistance. Activation of the PI3K/AKT/mTOR and/or RAF/RAS/MEK/ERK pathway results in the upregulation and stabilization of the anti-apoptotic factors MCL-1 and BCL-X_L and in the downregulation and degradation of BIM. The downregulation of BIM will result in a lower occupation of BCL-2 while the high levels of MCL-1 and/or BCL-X_L will sequester the released BIM. Therefore, ABT-199 can't induce apoptosis anymore in these cells.*

1.4. Combination therapies with ABT-199 in T-ALL

Using ABT-199 in combination treatment schedules is not only interesting to avoid the emergence of resistance, it can also enhance the antileukemic effects. Moreover, combining synergistic drugs allows to use lower drug doses and minimize side effects. Above all, ABT-199 could be used to increase the chemosensitivity of T-ALL cells since most conventional chemotherapeutic agents trigger the intrinsic pathway of apoptosis[28]. Anderson et al.[29] were the first to report synergistic activity between ABT-199 and a chemotherapeutic agent, cytarabine, in a T-ALL cell line. Next, we described synergism between ABT-199 and the chemotherapeutic agents doxorubicin, L-asparaginase and dexamethasone in human T-ALL cell lines (**paper 1**). In addition, several chemotherapeutic agents were included in our screen on T-ALL patient samples to identify promising combinations with ABT-199. ABT-199 was able to enhance the effects of etoposide, vincristine, dexamethasone and prednisolone in some samples (**paper 2**). A limitation of our studies is the lack of *in vivo* experiments for these combinations. Ideally, to mimic more closely the clinical situation, where patients receive a cocktail of chemotherapeutic agents, we should evaluate the addition of ABT-199 to the standard combination chemotherapy regimens instead of using only one chemotherapeutic agent in the combination experiments. This is exactly what Benito et al.[3] and Frismantas et al.[4] successfully did in patient-derived xenograft models of BCP-ALL. Adding ABT-199 to a treatment with dexamethasone and vincristine prevented leukemia progression for more than 300 days in some BCP-ALL samples while treatment with ABT-199 or chemotherapy alone resulted in a much shorter delay of disease progression[4].

On the other hand, we also tested combinations with clinically relevant targeted small-molecule inhibitors (**paper 2**). The combination with the BET bromodomain inhibitor JQ1 was the most promising. Strong cell death was induced in cells treated with the combination and the observed response in xenograft models was superior to the response in mice treated with either of the drugs alone. However, bringing the combination of ABT-199 and a BET bromodomain inhibitor into clinical trials for patients with T-ALL might be challenging. Both drugs are not FDA-approved for the treatment of T-ALL and have never been used in T-ALL patients before. Moreover, there is no good biomarker to select patients that will likely respond to the combination of ABT-199 and a BET bromodomain inhibitor. Although the degree of synergism was correlated to the BCL-2 expression levels in human T-ALL cell lines, no correlation was observed in our 6 patient samples. Evaluation of this combination treatment in a larger panel of primary samples and extensive study of parameters that may influence the synergism would be necessary for this. Nevertheless, our study shed light on the working mechanism of BET bromodomain inhibitors and how they may enhance the sensitivity to ABT-199 in the context of T-ALL. In all T-ALL cell lines with clear synergism, JQ1 increased the levels of BIM and decreased the levels of BCL-2. By knocking down and overexpressing BIM in the T-ALL cell line KARPAS-45, we showed that increased BIM levels are important to enhance the antileukemic effect of ABT-199.

2. Pharmacological inhibition of LSD1/KDM1A for the treatment of T-ALL

As the transcription factor ZEB2 can drive the development of early immature T-ALL, targeting ZEB2 could be an interesting strategy to treat this group of patients. However, developing small molecules to directly target transcription factors is at present still very challenging. A more achievable strategy is to indirectly target transcription factors via their protein interactions[30]. We aimed to identify the protein interaction partners of ZEB2 in the context of T-ALL in order to learn more about the oncogenic function of ZEB2 and to find druggable targets (**paper 3**). One of the newly identified interaction partners was the lysine-specific demethylase KDM1A. Noteworthy, previous studies have found the other ZEB family member ZEB1 as part of the CtBP-CoREST-KDM1A co-repressor complex in HeLa cells and pituitary cells[31, 32]. It is possible that the presence of ZEB1 or ZEB2 in this complex is cell-type dependent.

2.1. Limited *in vivo* activity of GSK2879552 in T-ALL xenograft models

Pharmacological inhibition of KDM1A with the small molecule drug GSK2879552 in murine and human T-ALL cell lines demonstrated sensitivity in *ZEB2*-positive T-ALL. The treatment of mice xenografted with a *Zeb2*-overexpressing murine T-ALL cell line caused a significant delay in tumor latency. However, prolonging the survival for only some days is not spectacular. Moreover, when human T-ALL cell line xenografts were treated with GSK2879552, antileukemic effects were only seen in the blood and not in the spleen (**paper 3**).

Yet, Mohammad et al.[33] obtained strong antitumor effects with the same drug in SCLC xenograft models. A substantial difference between both experimental setups was the location of the cancer cells in the body. While we used tail vein injection, allowing the cells to spread throughout the whole body (**paper 3**), Mohammad et al.[33] injected the cancer cells in a matrigel subcutaneously in the flank. To rule out the possibility that GSK2879552 simply does not reach the leukemia cells in the spleen or that the dose is insufficient to treat T-ALL, we analyzed the effects on target genes and histone marks in leukemia cells isolated from the blood and spleen of LOUCY xenografts treated for 5 days (data not shown). The expression of *CD11B*, *VIM* and *GFI1B* was induced in leukemia cells located both in the blood and spleen compared to the expression in leukemia cells from vehicle-treated mice. Moreover, an increase in the H3K4me2 and H3K9me2 mark was detected in the spleen. Besides, higher doses had some added value in inducing the analyzed genes and histone marks. Altogether, daily treatment with 1.5mg GSK2879552/kg body weight was sufficient to provoke *in vivo* changes in transcription and histone marks, but insufficient to achieve strong antileukemic effects in our T-ALL xenograft models.

Strikingly, the *in vivo* experiments carried out by Feng et al.[34] in mice intravenously injected with the AML cell line MV4-11 yielded very nice results. The LSD1 inhibitor ‘Compound 1’ caused 80% less leukemia cells in the bone marrow, 81% less in the spleen and 92% in the blood.

Future experiments will need to sort out whether increasing the dose of GSK2879552 or using another KDM1A inhibitor can enhance the antileukemic effect of KDM1A inhibition in T-ALL xenograft models.

2.2. Combinations with KDM1A inhibitor that are worthwhile to test in the context of T-ALL

Pharmacological inhibition of KDM1A in human T-ALL might be particularly useful as part of a combination therapy. In a first step, one could investigate whether adding a KDM1A inhibitor to standard chemotherapeutic agents would be useful. McGrath et al.[35] reported synergism between the KDM1A inhibitor RN-1 and chemotherapeutic agent cytarabine in AML cell lines. Also chemotherapeutic agents that induce DNA damage might synergize with KDM1A inhibition. KDM1A is namely recruited to sites of DNA damage and promotes the DNA damage response[36].

Furthermore, combinations with some rationally chosen targeted small-molecule inhibitors could be evaluated. In AML, synergistic activity between a KDM1A and pan-HDAC inhibitors has been reported[37]. KDM1A is indeed linked to HDACs since it interacts with the CoREST and NuRD complexes, which contain HDAC1 and HDAC2. Moreover, KDM1A is downregulated by HDAC inhibitors[38]. A pan-HDAC inhibitor such as panobinostat or an HDAC1/2 specific inhibitor like romidepsin could be tested in combination with KDM1A inhibition. There even exists a small molecule named 4SC-202, developed by the company 4SC, that inhibits both KDM1A and HDACs (1,2 and 3) and has been evaluated in a phase I clinical trial in patients with different types of blood cancer (ClinicalTrials.gov identifier: NCT01344707). Another option is the combination with a DNA methyltransferase inhibitor, such as the FDA approved decitabine. The rationale here is that KDM1A demethylates and increases the stability of DNMT1[39] and that synergism between decitabine and a KDM1A inhibitor has already been demonstrated in an AML cell line[40]. T-ALLs belonging to the *HOXA* molecular subgroup often have a *MLL-AF10*, *MLL-AF4*, *MLL-ENL*, *CALM-AF10* or *SET-NUP214* fusion. The resulting fusion proteins recruit the methyltransferase DOT1L, leading to aberrant methylation of H3K79[41]. In this group of T-ALLs, combining KDM1A inhibition with DOT1L inhibition could be a good strategy since strong synergism between the DOT1L inhibitor SYC-522 and the KDM1A inhibitor 'Compound 1' was measured in MLLr AML cell lines[34].

Lastly, we demonstrated that exogenous IL7 decreases the sensitivity to KDM1A inhibition in *Zeb2* transgenic T-ALL cells (**paper 3**). This suggests that paracrine factors, such as interleukin-7, might regulate compensatory pathways that prevent cell death upon KDM1A inhibition *in vivo*. Therefore, combination therapies inhibiting both KDM1A and the IL7R/JAK/STAT signalling pathway, e.g. using the JAK inhibitor Ruxolitinib, or inhibitors of the downstream effector BCL-2, like ABT-199, may *in vivo* be more effective as compared to KDM1A monotherapy.

2.3. Understanding sensitivity towards KDM1A inhibition in *ZEB2*-negative T-ALL

The evaluation of the KDM1A inhibitor GSK2879552 on a panel of human T-ALL cell lines revealed that also some *ZEB2*-negative T-ALL cell lines strongly depend on KDM1A (**paper 3**). Consequently, sensitive T-ALLs are not restricted to one particular T-ALL genetic subtype

or immunophenotype. The molecular mechanisms that drive susceptibility towards KDM1A inhibition in these *ZEB2*-negative T-ALLs are however still unknown. Future experiments will need to clarify which factors determine the sensitivity.

In our study, we looked for protein interaction partners of ZEB2 and identified KDM1A (**paper 3**). Doing the opposite, i.e. determining the interaction partners of KDM1A in both GSK2879552-sensitive and –insensitive cell lines, would be extremely interesting. Since KDM1A has no DNA binding capacity by itself, we hypothesize that KDM1A will bind to essential transcription (co)factors and/or putative oncogenic drivers in order to guide specific histone-modifying activity to their respective target genes. Cell line-specific expression of these essential factors may determine the KDM1A inhibition sensitivity. To confirm that these interaction partners critically mediate sensitivity towards KDM1A inhibition, knockouts of these protein partners could be made and used to check the influence on KDM1A inhibition sensitivity. This type of experiments could also help to identify predictive biomarkers.

In a panel of SCLC cell lines, approximately 30% of the cell lines were sensitive to GSK2879552[33]. In order to identify a predictive biomarker, Mohammad et al.[33] studied the global DNA methylation in sensitive and insensitive SCLC cell lines. DNA hypomethylation correlated with sensitivity to GSK2879552 and a differentially methylated gene signature set was proposed as a predictive biomarker[33]. A similar strategy could be followed to identify a predictive biomarker in T-ALL.

3. General conclusions

T-ALL is an aggressive and rare blood cancer. The chemotherapeutic agents that are commonly used to treat T-ALL patients are often associated with serious acute and long term side effects. Moreover, a significant part of the T-ALL patients can not be cured with the current treatment strategies. Therefore, there is a need for more effective and less toxic therapies. In this doctoral thesis, two new strategies to treat T-ALL were identified and evaluated in *in vitro* and *in vivo* models.

In a first part of this work, high expression levels of the anti-apoptotic factor *BCL2* were found in early immature T-ALL patients. Evaluation of the BCL-2 specific BH3 mimetic ABT-199 in human T-ALL cell lines, tumor cells from the *Lck-Lmo2* mouse model and in primary patient samples indeed revealed high sensitivity to the BCL-2 inhibitor in immature T-ALLs. In mouse xenograft models, ABT-199 showed also promising anti-leukemic effects. In order to increase the efficacy of ABT-199 treatment and to avoid the emergence of resistance, combination strategies were searched for. ABT-199 synergized with standard chemotherapeutic agents. In addition, a screen in a panel of samples coming from patients with medium to very high risk T-ALL identified strong synergistic effects between ABT-199 and the BET bromodomain inhibitors JQ1 and OTX-015. This synergism was also found in human T-ALL cell lines with high BCL-2 levels. Treatment of T-ALL cells with JQ1 resulted in the downregulation of super enhancer-associated genes and in the upregulation of the pro-apoptotic factor BIM. Finally, the treatment of T-ALL xenograft models confirmed the superior effects of a combination treatment with ABT-199 and JQ1 compared to the treatment with each of the agents alone.

Secondly, the lysine specific demethylase KDM1A was discovered as an interaction partner of the oncogenic driver ZEB2, a transcription factor that is often overexpressed in early immature T-ALL. Mouse and human T-ALL cell lines with high *ZEB2* expression levels were sensitive to treatment with the KDM1A inhibitor GSK2879552. In addition, also some *ZEB2*-negative human T-ALL cell lines were sensitive to this inhibitor. This indicates that also other factors than ZEB2 can determine the sensitivity to KDM1A inhibition. The treatment of human T-ALL cell line xenograft models elicited only limited anti-leukemic responses.

Altogether, the studies performed as part of this doctoral thesis generated novel molecular insights and evaluated the use of two novel targeted therapeutics in T-ALL. The importance of combination therapies to increase the efficacy of these targeted agents was also illustrated.

References

1. Chonghaile, T.N., et al., *Maturation stage of T-cell acute lymphoblastic leukemia determines BCL-2 versus BCL-XL dependence and sensitivity to ABT-199.* Cancer Discov, 2014. **4**(9): p. 1074-87.
2. Khaw, S.L., et al., *Venetoclax responses of pediatric ALL xenografts reveal sensitivity of MLL-rearranged leukemia.* Blood, 2016. **128**(10): p. 1382-95.
3. Benito, J.M., et al., *MLL-Rearranged Acute Lymphoblastic Leukemias Activate BCL-2 through H3K79 Methylation and Are Sensitive to the BCL-2-Specific Antagonist ABT-199.* Cell Rep, 2015. **13**(12): p. 2715-27.
4. Frismantas, V., et al., *Ex vivo drug response profiling detects recurrent sensitivity patterns in drug resistant ALL.* Blood, 2017.
5. Touzeau, C., et al., *The Bcl-2 specific BH3 mimetic ABT-199: a promising targeted therapy for t(11;14) multiple myeloma.* Leukemia, 2014. **28**(1): p. 210-2.
6. Pan, R., et al., *Selective BCL-2 Inhibition by ABT-199 Causes On Target Cell Death in Acute Myeloid Leukemia.* Cancer Discov, 2013.
7. Souers, A.J., et al., *ABT-199, a potent and selective BCL-2 inhibitor, achieves antitumor activity while sparing platelets.* Nat Med, 2013. **19**(2): p. 202-8.
8. Punnoose, E.A., et al., *Expression Profile of BCL-2, BCL-XL, and MCL-1 Predicts Pharmacological Response to the BCL-2 Selective Antagonist Venetoclax in Multiple Myeloma Models.* Mol Cancer Ther, 2016. **15**(5): p. 1132-44.
9. Niu, X., et al., *Binding of Released Bim to Mcl-1 is a Mechanism of Intrinsic Resistance to ABT-199 which can be Overcome by Combination with Daunorubicin or Cytarabine in AML Cells.* Clin Cancer Res, 2016. **22**(17): p. 4440-51.
10. Song, T., et al., *Bcl-2 phosphorylation confers resistance on chronic lymphocytic leukaemia cells to the BH3 mimetics ABT-737, ABT-263 and ABT-199 by impeding direct binding.* Br J Pharmacol, 2016. **173**(3): p. 471-83.
11. Konopleva, M., et al., *Efficacy and Biological Correlates of Response in a Phase II Study of Venetoclax Monotherapy in Patients with Acute Myelogenous Leukemia.* Cancer Discov, 2016. **6**(10): p. 1106-1117.
12. Ryan, J. and A. Letai, *BH3 profiling in whole cells by fluorimeter or FACS.* Methods, 2013. **61**(2): p. 156-64.
13. Roberts, A.W., et al., *Targeting BCL2 with Venetoclax in Relapsed Chronic Lymphocytic Leukemia.* N Engl J Med, 2016. **374**(4): p. 311-322.
14. Khaw, S.L., et al., *Both leukaemic and normal peripheral B lymphoid cells are highly sensitive to the selective pharmacological inhibition of prosurvival Bcl-2 with ABT-199.* Leukemia, 2014. **28**(6): p. 1207-15.
15. Leverson, J.D., et al., *Exploiting selective BCL-2 family inhibitors to dissect cell survival dependencies and define improved strategies for cancer therapy.* Sci Transl Med, 2015. **7**(279): p. 279ra40.
16. Jilg, S., et al., *Blockade of BCL-2 proteins efficiently induces apoptosis in progenitor cells of high-risk myelodysplastic syndromes patients.* Leukemia, 2016. **30**(1): p. 112-23.
17. Bodo, J., et al., *Acquired resistance to venetoclax (ABT-199) in t(14;18) positive lymphoma cells.* Oncotarget, 2016. **7**(43): p. 70000-70010.
18. Fresquet, V., et al., *Acquired mutations in BCL2 family proteins conferring resistance to the BH3 mimetic ABT-199 in lymphoma.* Blood, 2014. **123**(26): p. 4111-9.
19. Choudhary, G.S., et al., *MCL-1 and BCL-xL-dependent resistance to the BCL-2 inhibitor ABT-199 can be overcome by preventing PI3K/AKT/mTOR activation in lymphoid malignancies.* Cell Death Dis, 2015. **6**: p. e1593.
20. Lin, K.H., et al., *Targeting MCL-1/BCL-XL Forestalls the Acquisition of Resistance to ABT-199 in Acute Myeloid Leukemia.* Sci Rep, 2016. **6**: p. 27696.
21. Dousset, C., et al., *BH3 profiling as a tool to identify acquired resistance to venetoclax in multiple myeloma.* Br J Haematol, 2016.

22. Malumbres, M., *Cyclin-dependent kinases.* Genome Biol, 2014. **15**(6): p. 122.
23. Li, L., et al., *Synergistic induction of apoptosis in high-risk DLBCL by BCL2 inhibition with ABT-199 combined with pharmacologic loss of MCL1.* Leukemia, 2015. **29**(8): p. 1702-12.
24. Booher, R.N., et al., *MCL1 and BCL-xL levels in solid tumors are predictive of dinaciclib-induced apoptosis.* PLoS One, 2014. **9**(10): p. e108371.
25. Choudhary, G.S., et al., *Cyclin E/Cdk2-dependent phosphorylation of Mcl-1 determines its stability and cellular sensitivity to BH3 mimetics.* Oncotarget, 2015. **6**(19): p. 16912-25.
26. Kwiatkowski, N., et al., *Targeting transcription regulation in cancer with a covalent CDK7 inhibitor.* Nature, 2014. **511**(7511): p. 616-20.
27. Larochelle, S., et al., *Cyclin-dependent kinase control of the initiation-to-elongation switch of RNA polymerase II.* Nat Struct Mol Biol, 2012. **19**(11): p. 1108-15.
28. Davids, M.S. and A. Letai, *Targeting the B-cell lymphoma/leukemia 2 family in cancer.* J Clin Oncol, 2012. **30**(25): p. 3127-35.
29. Anderson, N.M., et al., *BCL2-specific inhibitor ABT-199 synergizes strongly with cytarabine against the early immature LOUCY cell line but not more-differentiated T-ALL cell lines.* Leukemia, 2014. **28**(5): p. 1145-8.
30. Johnston, S.J. and J.S. Carroll, *Transcription factors and chromatin proteins as therapeutic targets in cancer.* Biochim Biophys Acta, 2015. **1855**(2): p. 183-92.
31. Wang, J., et al., *Opposing LSD1 complexes function in developmental gene activation and repression programmes.* Nature, 2007. **446**(7138): p. 882-7.
32. Shi, Y., et al., *Coordinated histone modifications mediated by a CtBP co-repressor complex.* Nature, 2003. **422**(6933): p. 735-8.
33. Mohammad, H.P., et al., *A DNA Hypomethylation Signature Predicts Antitumor Activity of LSD1 Inhibitors in SCLC.* Cancer Cell, 2015. **28**(1): p. 57-69.
34. Feng, Z., et al., *Pharmacological inhibition of LSD1 for the treatment of MLL-rearranged leukemia.* J Hematol Oncol, 2016. **9**: p. 24.
35. McGrath, J.P., et al., *Pharmacological Inhibition of the Histone Lysine Demethylase KDM1A Suppresses the Growth of Multiple Acute Myeloid Leukemia Subtypes.* Cancer Res, 2016. **76**(7): p. 1975-88.
36. Mosammaparast, N., et al., *The histone demethylase LSD1/KDM1A promotes the DNA damage response.* J Cell Biol, 2013. **203**(3): p. 457-70.
37. Fiskus, W., et al., *Highly effective combination of LSD1 (KDM1A) antagonist and pan-histone deacetylase inhibitor against human AML cells.* Leukemia, 2014. **28**(11): p. 2155-64.
38. Huang, P.H., et al., *Histone deacetylase inhibitors stimulate histone H3 lysine 4 methylation in part via transcriptional repression of histone H3 lysine 4 demethylases.* Mol Pharmacol, 2011. **79**(1): p. 197-206.
39. Amente, S., L. Lania, and B. Majello, *The histone LSD1 demethylase in stemness and cancer transcription programs.* Biochim Biophys Acta, 2013. **1829**(10): p. 981-6.
40. Han, H., et al., *Synergistic re-activation of epigenetically silenced genes by combinatorial inhibition of DNMTs and LSD1 in cancer cells.* PLoS One, 2013. **8**(9): p. e75136.
41. Van Vlierberghe, P., et al., *The recurrent SET-NUP214 fusion as a new HOXA activation mechanism in pediatric T-cell acute lymphoblastic leukemia.* Blood, 2008. **111**(9): p. 4668-80.

CHAPTER 5
Summary

Summary

T-cell acute lymphoblastic leukemia (T-ALL) is a rare blood cancer that originates from the malignant transformation of T-cell progenitor cells (lymphoblasts). These malignant cells accumulate in the bone marrow where they hinder the production of normal blood cells. They can also infiltrate other organs such as the spleen, liver and central nervous system. The current treatment of T-ALL patients consists of high-dose multi-agent chemotherapy, potentially followed by hematopoietic stem cell transplantation. Over the past decades, the cure rate for childhood T-ALL has gradually increased and is nowadays approximately 85%. However, still a significant fraction of the children relapses and presents with very dismal survival perspectives. Furthermore, adults diagnosed with T-ALL have a much worse prognosis. On top of that, the chemotherapeutic agents often cause acute and long-term toxicities. Therefore, more effective and less toxic therapies are needed for the treatment of T-ALL.

In this PhD thesis, we aimed to find new treatment strategies for T-ALL by investigating the molecular mechanisms that contribute to the development of T-ALL. The main focus was on early immature T-ALL, a subtype of T-ALL that is characterized by a developmental arrest at a very early stage of T cell development. Nevertheless, our findings appeared to be valuable for other T-ALL subtypes as well.

In a first study (**paper 1**), we used gene expression profiling of a cohort of T-ALL patients to identify genes that are differentially expressed between early immature T-ALL and other T-ALLs. The *BCL2* gene, encoding the anti-apoptotic factor BCL-2, was found to be overexpressed in early immature T-ALL. Moreover, expression analysis of *BCL2* in subsets of normal human thymocytes revealed a high expression in the $CD34^+$ T cell progenitors and a gradual decrease in expression during T cell differentiation. These findings provided a rationale for targeting BCL-2 in immature T-ALL. Indeed, evaluation of the BCL-2 specific inhibitor ABT-199 in tumor cells from the *Lck-Lmo2* mouse model and in a panel of human T-ALL cell lines and primary patient samples, demonstrated especially in the more immature T-ALL samples a high sensitivity to ABT-199. Sensitivity to ABT-199 was significantly correlated with BCL-2 expression in the human T-ALL cell lines. Next, strong antileukemic effects were measured upon ABT-199 treatment of mice xenografted with the immature T-ALL cell line LOUCY. Altogether, our results indicated that T-ALL could be added to the growing list of cancers that may benefit from treatment with ABT-199.

In order to increase the efficacy of the treatment and to lower the risk of developing resistance, combination strategies with ABT-199 were investigated. In a first phase, we tested whether adding ABT-199 to the current treatment schedule could be useful. Synergism between ABT-199 and the chemotherapeutic agents doxorubicin, dexamethasone and L-asparaginase was found in human T-ALL cell lines (**paper 1**). Next, combinations with clinically relevant compounds were tested *in vitro* on a panel of T-ALL patient samples. This screen confirmed that ABT-199 was able to enhance the antileukemic effects of several standard chemotherapeutics. However, the most promising combination was the one with the BET bromodomain inhibitor JQ1. In 5 out of 6 patient samples, this combination was synergistic to even very strong synergistic. Synergistic responses were also found in a panel of human T-ALL cell lines in which the combination treatment induced strong cell death. Moreover, the treatment of cell line- and patient-derived xenografts with the combination of

ABT-199 and JQ1 outperformed the treatment with the single agents. In addition, gene expression profiling of JQ1-treated cells yielded information about the transcriptional effects of JQ1 and provided insights in the mechanism of synergism with ABT-199. The increased expression of the pro-apoptotic factor BIM and its binding to BCL-2 in response to treatment with JQ1 contributed to the enhanced effects of ABT-199 (**paper 2**).

Another important project in this thesis was about the transcription factor ZEB2 (**paper 3**). ZEB2 is an oncogenic driver of early immature T-ALL. Via pull down experiments followed by mass spectrometry, novel protein interaction partners of ZEB2 were identified in the context of T-ALL. We focused on the newly identified interaction with the lysine-specific demethylase KDM1A since inhibitors for this protein are available and in clinical trials for various human cancers. Both murine and human T-ALL cell lines with increased *ZEB2* levels were sensitive to *in vitro* treatment with the KDM1A inhibitor GSK2879552. Interestingly, also several *ZEB2*-negative human T-ALL cell lines were sensitive to KDM1A inhibition. Therefore, we believe that KDM1A could serve as a novel therapeutic target in a broad panel of human T cell leukemias. Surprisingly, the treatment of immunodeficient mice xenografted with GSK2879552-sensitive cell lines elicited only limited antileukemic responses. Hence, inhibition of KDM1A in human T-ALL might be particularly useful as part of a combination therapy.

In conclusion, two new strategies to treat T-ALL were identified and evaluated in *in vitro* and *in vivo* models. First, the BH3 mimetic ABT-199 proved to be a promising drug to treat T-ALLs that depend on the anti-apoptotic factor BCL-2 for their survival. Moreover, its efficacy was further improved in combination with standard chemotherapeutic agents or a BET bromodomain inhibitor. Secondly, KDM1A was found as an interaction partner of the oncogenic driver ZEB2 and T-ALLs with high *ZEB2* expression were sensitive to pharmacological inhibition of KDM1A. However, the *in vivo* results with the KDM1A inhibitor GSK2879552 were not spectacular. Therefore, combination therapies with GSK2879552 should be tested to overcome this problem.

Samenvatting

T-cel acute lymfatische leukemie (T-ALL) is een zeldzame bloedkanker die ontstaat uit de kwaadaardige transformatie van voorloper T-cellen (lymfoblasten). Deze kwaadaardige cellen accumuleren in het beenmerg waar ze de productie van normale bloedcellen hinderen. Ze kunnen ook infiltreren in andere organen zoals de milt en lever en in het centraal zenuwstelsel. De huidige behandeling van T-ALL patiënten bestaat uit hoge dosissen van verschillende chemotherapeutica die eventueel gevolgd worden door een hematopoietische stamceltransplantatie. De voorbije decennia is de genezingskans voor kinderen met T-ALL geleidelijk aan gestegen tot ongeveer 85% momenteel. Desalniettemin zijn er nog steeds kinderen die hervallen en heel slechte overlevingskansen hebben. Volwassenen die de diagnose van T-ALL krijgen, hebben trouwens een veel slechtere prognose. Daarenboven veroorzaakt de chemotherapie vaak acute en lange termijn toxiciteit. Er is dus nood aan doeltreffendere en minder toxische behandelingen voor T-ALL.

In dit doctoraat zochten we naar nieuwe behandelingsstrategieën voor T-ALL door de moleculaire mechanismen die bijdragen aan de ontwikkeling van T-ALL te onderzoeken. De nadruk lag op vroeg immature T-ALL, een subtype van T-ALL dat gekenmerkt wordt door een ontwikkelingsstop in een heel vroeg stadium van T-cel ontwikkeling. Onze bevindingen bleken echter ook waardevol te zijn voor andere T-ALL subtypes.

In een eerste studie (**paper 1**) gebruikten we genexpressie profileringen van T-ALL patiënten om genen te identificeren die differentieel tot expressie komen tussen vroeg immature T-ALL en andere T-ALLs. We vonden dat het gen *BCL2*, dat codeert voor de anti-apoptotische factor BCL-2, hoog tot expressie kwam in vroeg immature T-ALL. Bovendien toonde expressie-analyse van *BCL2* in subsets van normale humane thymocyten een hoge *BCL2* expressie aan in $CD34^+$ voorloper T-cellen en een geleidelijke daling in expressie tijdens T-cel differentiatie. Deze bevindingen leidden tot het idee om BCL-2 te inhiberen in vroeg immature T-ALL. Evaluatie van de BCL-2 specifieke inhibitor ABT-199 in tumorcellen van het *Lck-Lmo2* muismodel en in een panel van humane T-ALL cellijnen en primaire patiëntenstalen liet inderdaad zien dat vooral de meer immature T-ALL cellijnen en primaire patiëntenstalen heel gevoelig waren voor ABT-199. Gevoeligheid voor ABT-199 was significant gecorreleerd met BCL-2 expressie in de humane T-ALL cellijnen. Vervolgens werden sterke anti-leukemische effecten gemeten na behandeling met ABT-199 in een muis xenograft model met de humaan immature T-ALL cellijn LOUCY. Kortom, onze resultaten gaven aan dat T-ALL kon toegevoegd worden aan de groeiende lijst met kankers die voordeel kunnen halen uit een behandeling met ABT-199.

Om de doeltreffendheid van de behandeling te verhogen en om het risico op resistentie te verkleinen, werden combinatiestrategieën met ABT-199 onderzocht. In een eerste fase hebben we getest of het nuttig zou zijn om ABT-199 toe te voegen aan de huidige behandelingsschema's. Er werd synergisme gevonden tussen ABT-199 en de chemotherapeutische agentia doxorubicine, dexamethasone en L-asparaginase in humane T-ALL cellijnen (**paper 1**). In een volgende stap werden combinaties met klinisch relevante compounds *in vitro* getest op een panel van T-ALL patiëntenstalen. Deze screen bevestigde dat ABT-199 in staat was om de anti-leukemische effecten van verschillende standaard chemotherapeutica te versterken. Echter, de meest belovende combinatie was die met de BET bromodomein inhibitor JQ1. In 5 van de 6 patiëntenstalen was deze combinatie

synergistisch tot zelfs sterk synergistisch. Synergistische responsen werden ook gevonden in een panel van humane T-ALL cellijnen waarin de behandeling met de combinatie sterke celdood induceerde. Daarenboven overtrof de behandeling van cellijn- en patiënt- afgeleide xenografts met de combinatie van ABT-199 en JQ1 de behandeling met de afzonderlijke agentia. Verder leverde de genexpressie profilering van JQ1-behandelde cellen informatie op over de transcriptionele effecten van JQ1 en inzichten in het mechanisme van het synergisme met ABT-199. De verhoogde expressie van de pro-apoptotische factor BIM en zijn binding aan BCL-2 als reactie op de behandeling met JQ1, droeg bij aan de versterkte effecten van ABT-199 (**paper 2**).

Een ander belangrijk project in deze thesis ging over de transcriptiefactor ZEB2 (**paper 3**). ZEB2 is een oncogene driver van vroeg immature T-ALL. Via pull down experimenten gevolgd door massaspectrometrie werden nieuwe eiwit interactiepartners van ZEB2 geïdentificeerd in de context van T-ALL. Wij focusten op de nieuw geïdentificeerde interactie met het lysine-specifieke demethylase KDM1A aangezien er inhibitoren beschikbaar zijn voor dit eiwit waarvan sommige in klinische studies geëvalueerd worden voor verschillende humane kankers. Zowel muizen als humane T-ALL cellijnen met verhoogde *ZEB2* niveaus waren gevoelig voor *in vitro* behandeling met de KDM1A inhibitor GSK2879552. Interessant is dat ook meerdere *ZEB2*-negatieve humane T-ALL cellijnen gevoelig waren voor inhibitie van KDM1A. Daarom geloven wij dat KDM1A zou kunnen dienen als een nieuw therapeutisch doelwit in een breed panel van humane T-cel leukemieën. Verrassend genoeg wekte de behandeling van immunodeficiënte muizen met xenograften met GSK2879552-gevoelige cellijnen enkel beperkte anti-leukemische effecten op. Vandaar dat inhibitie van KDM1A in humane T-ALL vooral nuttig kan zijn als onderdeel van een combinatietherapie.

In conclusie kunnen we stellen dat twee nieuwe strategieën om T-ALL te behandelen geïdentificeerd en geëvalueerd werden in *in vitro* en *in vivo* modellen. In de eerste plaats bleek de BH3 mimetic ABT-199 een veelbelovend geneesmiddel om T-ALLs te behandelen die afhankelijk zijn van de anti-apoptotische factor BCL-2 voor hun overleving. De doeltreffendheid van dit geneesmiddel werd verder verbeterd in combinatie met standaard chemotherapeutische agentia of met een BET bromodomein inhibitor. In de tweede plaats werd KDM1A geïdentificeerd als een interactiepartner van de oncogene driver ZEB2 en T-ALLs met hoge *ZEB2* expressie waren gevoelig voor farmacologische inhibitie van KDM1A. De *in vivo* resultaten met de KDM1A inhibitor GSK2879552 waren echter niet spectaculair. Om dit probleem op te lossen zouden combinatietherapieën met GSK2879552 getest moeten worden.

CHAPTER 6

Curriculum Vitae & Word of thanks

Curriculum Vitae Sofie Peirs

Personalia

- Address: Krijgslaan 127, B-9000 Gent
- Date and place of birth: 20/04/1989, Kortrijk
- Nationality: Belgian
- Phone: +32(0)472/69 50 33
- Email: sofie.peirs@ugent.be

Work experience

- **PhD student from October 2012 until now**
  - Institute: Ghent University, Center for Medical Genetics, Ghent, Belgium
  - October 2016 – March 2017: PhD grant 'Emmanuel van der Schueren' of Stand up to Cancer (Kom op tegen Kanker); promotor: Prof. dr. Pieter Van Vlierberghe
  - October 2012 – September 2016: PhD fellowship of FWO-Flanders; promotors: Prof. dr. Bruce Poppe & Prof. dr. Pieter Van Vlierberghe

Diplomas

- **Master of Science in Bioscience Engineering: Cell and Gene Biotechnology**
  - Institute: Ghent University, Faculty of Bioscience Engineering
  - Period: September 2007 – June 2012
  - Master dissertation: "The development of a trachoma DNA vaccine against infectious blindness in humans." Promotor: Prof. dr. Daisy Vanrompay
  - Degree: greatest distinction

- **FELASA C certificate, Laboratory animal science courses I & II**
  - Institute: Ghent University, Faculty of Veterinary Medicine
  - Period: September 2012 – January 2013

Courses

- **Impact and research communication skills workshop**
  - Transferable skills training doctoral schools
  - Period: 22 September 2015

- **Applied Flow Cytometry-Clinical Hematology**
  - Specialist course doctoral schools
  - Period: 22-24 September 2014

- **Personal effectiveness**
  - Transferable skills training doctoral schools
  - Period: January 2014

- **Analysis of Affymetrix microarray data using Bioconductor**
  - Training organised by VIB Bioinformatics Training & Service Facility
  - Period: 30 November and 3 December 2012

- **Statistical computing in R**
  - Course organised by Biostatistics unit of Faculty of medicine and health sciences, Ghent University
  - Period: October 2012

Scientific Achievements

Prizes

- Best oral presentation at 2nd OncoPoint research seminar, 6 February 2014, Ghent, Belgium
- Travel grant winner at 19th Congress of EHA, 12-15 June 2014, Milan, Italy
- Best oral presentation at 4th OncoPoint research seminar, 2 March 2016, Ghent, Belgium

Publications

- **ABT-199 mediated inhibition of BCL-2 as a novel therapeutic strategy in T-cell acute lymphoblastic leukemia.** Peirs S**.**, Matthijssens F., Goossens S., Van de Walle I., Ruggero K., de Bock C., Degryse S., Canté-Barrett K., Briot D., Clappier E., Lammens T., De Moerloose B., Benoit Y., Poppe B., Meijerink J.P., Cools J., Soulier J., Rabbitts TH., Taghon T., Speleman F. & Van Vlierberghe P. **Blood** 2014;124(25):3738-3747. Impact factor 2014: **10.452**.

- **Epigenetics in T-cell acute lymphoblastic leukemia.** Peirs S., Van der Meulen J., Van de Walle I., Taghon T., Speleman F., Poppe B. & Van Vlierberghe P. **Immunological Reviews** 2015;263(1):50-67. Impact factor 2015: **9.542**.

- **ZEB2 drives immature T-cell lymphoblastic leukaemia development via enhanced tumour-initiating potential and IL-7 receptor signalling.** Goossens S., Radaelli E., Blanchet O., Durinck K., Van der Meulen J., Peirs S., Taghon T., Tremblay CS., Costa M., Ghahremani MF., De Medts J., Bartunkova S., Haigh K., Schwab C., Farla N., Pieters T., Matthijssens F., Van Roy N., Best JA., Deswarte K., Bogaert P., Carmichael C., Rickard A., Suryani S., Bracken LS., Alserihi R., Canté-Barrett K., Haenebalcke L., Clappier E., Rondou P., Slowicka K., Huylebroeck D., Goldrath AW., Janzen V., McCormack MP., Lock RB., Curtis DJ., Harrison C., Berx G., Speleman F., Meijerink JPP., Soulier J., Van Vlierberghe P. & Haigh JJ. **Nature Communications** 2015;6. Impact factor 2015: **11.329**.

- **Novel biological insights in T-cell acute lymphoblastic leukemia.** Durinck K., Goossens S., Peirs S., Wallaert A., Van Loocke W., Matthijssens F., Pieters T., Milani G., Lammens T., Rondou P., Van Roy N., De Moerloose B., Benoit Y., Haigh J., Speleman F., Poppe B. & Van Vlierberghe P. **Experimental Hematology** 2015;43(8):625-639. Impact factor 2015: **2.303.**

- **A quantitative proteomics approach identifies ETV6 and IKZF1 as new regulators of an ERG-driven transcriptional network**. Unnikrishnan A., Guan YF., Huang Y., Beck D., Thoms JA., Peirs S., Knezevic K., Ma S. Van de Walle I., de Jong I., Ali Z., Zhong L., Raftery MJ., Taghon T., Larsson J., MacKenzie KL., Van Vlierberghe P., Wong JW. & Pimanda JE. **Nulceic Acids Research** 2016;44(22):10644-10661. Impact factor 2015: 9.202.

- **Targeting BET proteins improves the therapeutic efficacy of BCL-2 inhibition in T-cell acute lymphoblastic leukemia.** Peirs S.*, Frismantas V.*, Matthijssens F., Van Loocke W., Lintermans B., Vandamme N., Pieters T., Berx G., Poppe B., Bourquin JP.**,& Van Vlierberghe P.** **Leukemia** 2017. Epub ahead of print. Impact factor 2015: 12.104. ***co-first authors,** **co-last authors.

- **Oncogenic ZEB2 activation drives sensitivity towards LSD1 inhibition in T-cell acute lymphoblastic leukemia.** Goossens S.*, Peirs S.*, Van Loocke W., Haigh K., Ngyuen T., Sonderegger S., Van Nieuwerburgh F., Deforce D., Costa M., Kleifeld O., Curtis D., Berx G., Van Vlierberghe P.** & Haigh J.** **Blood** 2017;129(8):981-990. Impact factor 2015: 11.847. ***co-first authors,** **co-last authors.

Oral presentations

- **ABT-199 mediated inhibition of BCL-2 as a novel therapeutic strategy in early immature T-cell acute lymphoblastic leukemia.** Peirs S. (speaker), Matthijssens F., Goossens S., Canté-Barrett K., Lammens T., De Moerloose B., Benoit Y., Soulier J., Poppe B., Taghon T., Meijerink J., Speleman F. & Van Vlierberghe P. Second OncoPoint research seminar, 6 February 2014, Ghent, Belgium.

- **ABT-199 mediated inhibition of BCL2 as a novel therapeutic strategy in T-cell acute lymphoblastic leukemia.** Peirs S. (speaker), Matthijssens F., Goossens S., De Bock C., Canté-Barrett K., Lammens T., Van de Walle I., De Moerloose B., Benoit Y., Poppe B., Taghon T., Cools J., Meijerink J., Soulier J., Speleman F. & Van Vlierberghe P. 19th Congress of EHA, 12-15 June 2014, Milan, Italy.

- **Novel targeted therapies in human T-ALL**. Peirs S. (speaker). Course on Molecular Aspects of Hematological Disorders, 9-10 June 2015, Erasmus MC, Rotterdam, The Netherlands.

- **Targeting BET family proteins improves the efficacy of ABT-199 in T-cell acute lymphoblastic leukemia**. Peirs S. (speaker), Matthijssens F., Lintermans B., Pieters T., Vandamme N., Berx G., Poppe B. & Van Vlierberghe P. 4th OncoPoint research seminar, 2 March 2016, Ghent, Belgium.

- **The combination of ABT-199 and JQ1 as a novel therapeutic strategy in T-cell acute lymphoblastic leukemia.** Peirs S. (speaker), Matthijssens F., Pieters T., Vandamme N., Lintermans B., Reunes L., Berx G., Poppe B. & Van Vlierberghe P. Research Day of the Faculty of Medicine and Health Sciences, 16 March 2016, Ghent, Belgium.

Poster presentations

- **BRD4 inhibition improves the efficacy of ABT-199 in T-cell acute lymphoblastic leukemia.** Peirs S., Matthijssens F., Pieters T., Vandamme N., Berx G., Poppe B. & Van Vlierberghe P. AACR Special Conference on Chromatin and Epigenetics in Cancer, 24-27 September 2015, Atlanta, USA.

- **BRD4 inhibition improves the efficacy of ABT-199 in T-cell acute lymphoblastic leukemia.** Peirs S., Matthijssens F., Pieters T., Vandamme N., Berx G., Poppe B. & Van Vlierberghe P. AACR Special Conference on Advances in Pediatric Cancer Research, 9-12 November 2015, Fort Lauderdale, USA.

- **Targeting BET family proteins improves the therapeutic efficacy of BCL-2 inhibition in T-cell acute lymphoblastic leukemia.** Peirs S.[*], Frismantas V.[*], Matthijssens F., Lintermans B., Pieters T., Vandamme N., Van Loocke W., Berx G., Poppe B., Bourquin JP.[**], Van Vlierberghe P.[**] ***co-first authors,** [**]co-last authors. 21th Congress of EHA, 9-12 June 2016, Copenhagen, Denmark.

Conferences attended

- 13th Annual meeting of the Belgian Society of Human Genetics, March 15th, 2013, Brussels, Belgium
- Second ESH-EHA Scientific Workshop on T-cell acute lymphoblastic leukemia, March 22nd-24th, 2013, Lissabon, Portugal
- FASEB SRC on Hematologic Malignancies, August 4th-9th, 2013, Saxtons River, USA
- 55th ASH Annual Meeting and Exposition, October 7th-10th, 2013, New Orleans, USA
- 19th Congress of EHA, June 12th-15th, Milan, Italy
- Second OncoPoint research seminar, February 6th, 2014, Ghent, Belgium
- From Big Data to Bedside: Translational bioinformatics in cancer research, Workshop and Symposium, April 1st-2nd, 2015, Ghent, Belgium
- Course and Master Classes on Molecular Aspects of Hematological Disorders, June 9th-10th, 2015, Rotterdam, The Netherlands

- AACR Special Conference on Chromatin and Epigenetics in Cancer, September 24th-27th, 2015, Atlanta, USA
- AACR Special Conference on Advances in Pediatric Cancer Research, November 9th-12th, 2015, Fort Lauderdale, USA
- 4th OncoPoint research seminar, March 2nd, 2016, Ghent, Belgium
- Research Day of the Faculty of Medicine and Health Sciences, March 16th, 2016, Ghent, Belgium
- Course on Molecular Aspects of Hematological Disorders, June 7th-8th, 2016, Rotterdam, The Netherlands
- 21th Congress of EHA, June 9th-12th, 2016, Copenhagen, Denmark.

Supervision of students

- **Project Biomedical Biotechnology, 1st Master of Biochemistry and Biotechnology 2013-2014:** Jonas Van Damme, DOT1L inhibition in the treatment of SET-NUP214 rearranged leukemias. Supervision: Sofie Peirs, promotor: Bruce Poppe, co-promotor: Pieter Van Vlierberghe

- **Project Biomedical Biotechnology, 1st Master of Biochemistry and Biotechnology 2013-2014:** Robin Vanluchene, DOT1L inhibition in the treatment of SET-NUP214 rearranged leukemias. Supervision: Sofie Peirs, promotor: Bruce Poppe, co-promotor: Pieter Van Vlierberghe

- **Project Biomedical Biotechnology, 1st Master of Biochemistry and Biotechnology 2014-2015:** Wouter Versmessen, Testen van nieuwe compounds voor de behandeling van humane leukemie. Supervision: Sofie Peirs, promotor: Bruce Poppe, co-promotor: Pieter Van Vlierberghe

- **Z-lijn paper, 2nd Bachelor of Medicine 2014-2015:** Hanne Vandevoort, Het anti-apoptotisch eiwit BCL-2 als doelwit voor therapie in kanker. Supervision: Sofie Peirs, promotor: Bruce Poppe

- **Z-lijn paper, 2nd Bachelor of Medicine 2014-2015:** Jesse Demuytere, DNA methylatie inhibitoren in de behandeling van leukemie. Supervision: Sofie Peirs, promotor: Pieter Van Vlierberghe

- **Z-lijn paper, 2nd Bachelor of Medicine 2014-2015:** Cédric De Landsheer, DNA methylatie inhibitoren in de behandeling van leukemie. Supervision: Sofie Peirs, promotor: Pieter Van Vlierberghe

- **Z-lijn paper, 2nd Bachelor of Medicine 2015-2016:** Esthelle Colle, De anti-apoptotische eiwitten BCL-2 en MCL-1 als doelwitten voor de therapie van hematologische maligniteiten. Supervision: Sofie Peirs, promotor: Pieter Van Vlierberghe

- **Z-lijn paper, 2nd Bachelor of Medicine 2015-2016:** Jeroen Dobbelaere, De anti-apoptotische eiwitten BCL-2 en MCL-1 als doelwitten voor de therapie van hematologische maligniteiten. Supervision: Sofie Peirs, promotor: Pieter Van Vlierberghe

Dankwoord (word of thanks)

Mijn doctoraat is een geweldig boeiende periode geweest waarin ik heel veel heb bijgeleerd en fantastische mensen heb leren kennen. Door onderzoek te doen en door veel te lezen, besef ik meer en meer hoe complex maar ook hoe boeiend het menselijk lichaam is. Verder heb ik ook gemerkt dat experimenten soms meer vragen oproepen dan dat ze antwoorden opleveren. Als onderzoeker word je vaak geconfronteerd met tegenslagen en frustraties: ettelijke keren proberen om een techniek te doen werken, een toestel dat plots niet meer wil meewerken of slechte/onverwachte resultaten. Gelukkig zijn er ook veel momenten die grote voldoening geven. Zowel voor de leuke als de iets mindere momenten, is het fijn om die te kunnen delen met geweldige mensen. Ik zou daarom graag een aantal mensen bedanken, zonder wie ik dit onderzoek nooit tot een goed einde had kunnen brengen en zonder wie mijn doctoraatsperiode niet half zo leuk was geweest.

Eerst en vooral moet ik mijn promotoren, prof. Bruce Poppe en prof. Pieter Van Vlierberghe, ontzettend bedanken. Dankzij de inspirerende lessen van Bruce kreeg ik interesse om onderzoek te doen in het Centrum voor Medische Genetica. Bruce, jij hebt me de kans en het vertrouwen gegeven om te komen solliciteren en om samen een FWO mandaat aan te vragen. Ondanks je drukke agenda maakte je steeds tijd en toonde je interesse om de lopende projecten te bespreken. Ik zal nooit vergeten hoe je met me kwam praten toen ik het tijdens mijn eerste jaar moeilijk had. Pieter, van jou heb ik onwaarschijnlijk veel geleerd. Ik bewonder je als onderzoeker: je zit vol ideeën, hebt een enorme kennis en kan als de beste verbanden leggen. Ik ben ook heel dankbaar dat ik aan veel verschillende projecten heb kunnen meewerken en kon samenwerken met internationale onderzoeksgroepen. Daardoor heb ik veel technieken geleerd en heb ik verschillende aspecten van T-ALL kunnen onderzoeken. Wat ik enorm fijn vind, is je positieve ingesteldheid. Als ik wat in de knoop zat met bepaalde experimenten of resultaten, had ik na een gesprek met jou toch altijd terug de volle goesting om het nog eens opnieuw of op een andere manier te proberen.

Steven, jou moet ik ook bedanken om me te betrekken in je ZEB2-verhaal en voor de fijne samenwerking over KDM1A inhibitie in T-ALL. Je hebt zoveel ervaring en kennis waardoor ik al heel veel heb geleerd van jou.

En, wat een geweldige collega's en zelfs vrienden heb ik leren kennen tijdens mijn doctoraat! Eerst in MRB1, waar iedereen altijd bereid was om te helpen of om een babbeltje te slaan in de gang, en nu ook in MRB2. Jullie zijn met veel te veel om allemaal op te sommen, maar weet dat ik ervan genoten heb om samen met jullie in het labo te staan, samen aan de keukentafel te zitten en samen naar feestjes te gaan. Op congres gaan was altijd geweldig met jullie en we hebben samen toch een stukje van de wereld gezien. Vooral het extra weekje vakantie in Florida met Gloria en Renate was een topervaring. Béa, Filip, Gloria, Julie, Juliette, Lindy, Maaike, Morgan, Pieter R., Pieter VV., Renate, Sara, Steven en Tim, oftewel het superfantastische PVV team, bedankt voor de vele afterwork-drinks, -dinners, en –party's, bedankt voor de beforework-breakfasts, bedankt voor de duringwork-breaks en bedankt voor de sfeer en lachmomenten. Béa, jij verdient een speciaal dankwoordje, want hoeveel werk heb jij niet verzet! Zonder jou had ik nooit zoveel goede resultaten gehad en waren de intense dagen op het einde van muizenexperimenten niet te doen geweest. Je bent dan ook niet voor niets verkozen tot beste "Lab Citizen" van de hele wereld!

Wie ik ook niet mag vergeten, zijn mijn familie en vrienden. Jullie hebben voor de nodige afleiding gezorgd en me heel veel ontspannende momenten bezorgd. Mama en papa, dankjewel voor jullie onvoorwaardelijke steun. Tot slot, dankjewel lieve Arun om er altijd voor mij te zijn.